2016-04-18

Effects of Valved Soffit Vents on Low-Rise Buildings with Hip and Gable Roofs

Garth A. Arch
University of Miami, garch@arch-godfrey.com

UNIVERSITY OF MIAMI

EFFECTS OF VALVED SOFFIT VENTS ON LOW-RISE BUILDINGS WITH HIP AND GABLE ROOFS

By

Garth A. Arch

A DISSERTATION

Submitted to the Faculty
of the University of Miami
in partial fulfillment of the requirements for
the degree of Doctor of Philosophy

Coral Gables, Florida

May 2016

UNIVERSITY OF MIAMI

A dissertation submitted in partial fulfillment of
the requirements for the degree of
Doctor of Philosophy

EFFECTS OF VALVED SOFFIT VENTS ON LOW-RISE BUILDINGS WITH HIP AND GABLE ROOFS

Garth A. Arch

Approved:

_____ Wimal Suaris, Ph.D. Associate Professor, Department of Civil, Architectural, and Environmental Engineering	_____ Shihab Asfour, Ph.D. Professor and Associate Dean, Department of Industrial Engineering
_____ Antonio Nanni, Ph.D. Professor, Department of Civil, Architectural, and Environmental Engineering	_____ Guillermo Prado, Ph.D. Dean of the Graduate School
_____ Ali Ghahremaninezhad, Ph.D. Assistant Professor, Department of Civil, Architectural, and Environmental Engineering	

ARCH, GARTH A. (Ph.D., Civil Engineering)
Effects of Valved Soffit Vents on Low-Rise Buildings with Hip and Gable Roofs (May 2016)

Abstract of a dissertation at the University of Miami.

Dissertation supervised by Associate Professor Wimal Suaris.
No. of pages in text. (233)

It is evident from various post-hurricane surveys that soffit failure has been a significant contributor to considerable damage in low-rise buildings. Soffit vents, which are frequently integrated into low-rise buildings in order to provide natural ventilation of the attic space, have been found to be points of particular vulnerability. In high wind events, soffit vents provide a point of entry for wind-induced pressure and wind-driven rain into the attic space. Internal pressurization from wind-induced positive pressure entering the windward soffit vents combined with external suctions on the roof can lead to the potential failure of the roof sheathing. In addition, once water enters the attic space, it accumulates, soaking the insulation and gypsum board, which can cause the full collapse of the ceilings.

This study presents a valved soffit vent technology that has the capability of depressurizing the attic space when strategically positioned in areas of wind-induced negative pressure, i.e. wind separation zones. Valved soffit vents (VSVs) facing the approach flow are activated by wind-induced positive pressure and close for wind speeds greater than 30 mph, thereby preventing air intrusion and wind-driven rain into the building.

Large-scale experimentation was conducted at the Wall of Wind (WOW) facility at Florida International University to investigate the effects of valved soffit vents on internal pressures within the attic space and on net pressures that are often responsible for damage to the roof envelope. In addition, the effectiveness of VSVs in preventing wind-driven rain (WDR) entry into the building was also studied. Four different roof models were tested: a large hip, a large gable, a small hip and a small gable. The large roof models were used to study a patented VSV product, the *BPA Safety Vent*, while the small roof models were used for a 1:6 model scale study.

Results showed that for various wind directions, the net mean pressure coefficients on the gable and hip roofs increased, generating less suction on the roof envelope in the case of soffit openings with VSVs than for soffit openings without VSVs. The hip roofs with VSVs yielded an increase in net mean pressure of more than 90% on the roof sheathing above the windward vents. Furthermore, the mean pressure coefficients on the interior roof surface of the different roof models at any wind direction were reduced when the VSVs were installed.

The net peak pressure coefficients generally remained unchanged for the different roof models, irrespective of wind direction. However, the hip roofs displayed an increase in net peak pressure coefficients at the vent locations. The VSVs also demonstrated their ability to prevent wind-driven rain from entering the attic. Testing was also performed to identify the wind speeds at which the VSVs begin to activate. The valved soffit vents show promise for future applications in the areas of wind-induced pressure and wind-driven rain damage mitigation.

ACKNOWLEDGMENTS

I gratefully acknowledge all those who have made the completion of this work possible. My greatest thanks go to Dr. Wimal Suaris, my advisor and chairman of my dissertation committee, who accepted me as his Ph.D. student. I am extremely grateful to him for his patience, kindness, and guidance along the way. I also extend my sincere gratitude to Dr. Antonio Nanni, Dr. Ali Ghahremaninezhad, and Dr. Shihab Asfour for serving on my committee.

My sincere thanks and appreciation to all faculty and staff members of the Wall of Wind research facility for their support and help during the testing at Florida International University. A special thanks to Walter Conklin, Roy Liu-Marques, Bodhi Hajra, and Mohamed Moravej.

Financial support from Arch and Godfrey (Cayman) Ltd. is acknowledged with sincere thanks. In addition, I would like to express my appreciation to Building Performance Americas Inc. for providing their patented product for use in this research. I am also grateful to CD-adapco for providing an academic license for STAR-CCM+.

I am forever grateful to my father, Heber, for sacrificially postponing his retirement to allow me to complete this work. For her prayers, love and sacrifice, I express my loving gratitude to my wife, Dana, who has been an incredible support during this journey. It is to her, my father and late mother that I dedicate this dissertation. *Soli Deo Gloria.*

TABLE OF CONTENTS

PAGE

LIST OF TABLES……..vi

LIST OF FIGURES……....ix

CHAPTER

I INTRODUCTION……...1

Background Information……..1
Wind Damage……..5
Valved Soffit Vents……8
Research Objectives and Scope……10
Importance of Study……...11
Organization of Document……12

II LITERATURE REVIEW……...13

Model and Full-Scale Testing of Low-Rise Buildings……..13
Aylesbury Experimental Building……16
Texas Tech University (TTU) Building……16
The Silsoe Structures Building……..18
Turbulence Characteristics……20
Mitigation Techniques for Wind-Induced Pressures on Low-Rise Buildings……...24
A Review of Internal Pressures in Low-Rise Buildings……30
Roof Vents and Soffits……...34

III THEORECTICAL BACKGROUND……....38

Wind Flow Characteristics on Low-Rise Buildings……..38
Wind-Induced Pressures on Buildings……...43

IV WALL OF WIND FACILITY…..……..47

Partial Turbulence Simulation…….....52
Velocity and Sampling Time……54
Wall of Wind Scaling Parameters……..…..55

V FULL-SCALE PERFORMANCE EVALUATION OF VALVED SOFFIT VENTS……..60

Overview……...……....60

Experimental Set-Up..……...61

Variable Speed Test……...62
Test Configurations……66
Water Intrusion Testing……67
Wall of Wind Rain Simulation Procedure……..……67
Pressure Measurements……..68
Results and Discussion……..79
Gable Roof Test Results……..……79
Hip Roof Test Results……..……82
Mean and Peak Pressure Coefficient Contours……..…..86
Net Pressure on Roof Envelope……..……...107
Wind Driven Rain Test Results……..…...110
CFD Simulation and Validation of Mean Internal Pressures……...112
CFD Results……...113
Conclusions……..117

VI AN EXPERIMENTAL STUDY OF INTERNAL PRESSURES IN THE ROOF ATTIC SPACE USING VALVED SOFFIT VENTS……120

Background……..120
Experimental Set-Up……121
Test Configurations……..123
Pressure Measurements……124
Results and Discussion……134
Gable Roof Test Results……....134
Hip Roof Test Results……136
Mean and Peak Pressure Coefficient Contours……..……138
Net Pressure on Roof Envelope……..…...153
Comparison of Results: 1:6 Model Scale with Full Scale BPA Safety Vents...157
Immediate Practical Recommendations……..……....161
Conclusions……..164

VII CONCLUSIONS AND RECOMMENDATIONS FOR FUTURE RESEARCH……..…..166

Recommendations for Future Research……...170

APPENDIX

A COMPARISON OF MEAN AND PEAK PRESSURE COEFFICIENTS ……....171

B COMPARISON OF MEAN AND PEAK PRESSURE COEFFICIENTS ……....195

REFERENCES……222

LIST OF TABLES

TABLE PAGE

5-1 Wind speed to activate valved soffit vents (VSVs) on the hip roof model……63

5-2 Wind speed to activate valved soffit vents (VSVs) on the gable roof model……63

5-3 Summary of experimental configurations for the gable roof model……..…66

5-4 Summary of experimental configurations for the hip roof model…….……66

5-5 Summary of wind driven rain (WDR) experimental configurations for the hip roof model…….…….68

5-6 WDR water entry measurements for the hip roof model……..……...110

5-7 CFD and experimental mean C_{pi} comparisons for the gable roof model…….114

5-8 CFD and experimental mean C_{pi} comparisons for the hip roof model……114

6-1 Summary of experimental configurations for the gable roof model……....124

6-2 Summary of experimental configurations for the hip roof model…….……..124

6-3 Pressure taps used for the net pressure analysis……..……154

6-4 Mean and peak net pressure coefficients for the gable roof…….……...154

6-5 Mean and peak net pressure coefficients for the hip roof……..……..155

6-6 Roof type and corresponding soffit vent details, 0° wind direction…….…...158

6-7 Roof type and corresponding soffit vent details, 30° wind direction……..…...158

6-8 Comparison of results between the large gable and large hip roof models…….159

6-9 Comparison of results between the small gable and small hip roof models……159

6-10 Estimated mean internal pressures without and with VSVs for gable roofs……162

6-11 Estimated mean internal pressures without and with VSVs for hip roofs…...…162

6-12 Number of VSVs required per roof side for a 3.5% windward vent porosity….163

6-13 Number of VSVs required per roof side for 4.5% and 9% windward vent porosities……..163

A-1 Comparison of external and internal pressure coefficients without and with VSVs for the large gable roof model at 0° wind direction……..173

A-2 Comparison of external and internal pressure coefficients without and with VSVs for the large gable roof model at 15° wind direction……175

A-3 Comparison of external and internal pressure coefficients without and with VSVs for the large gable roof model at 30° wind direction……177

A-4 Comparison of external and internal pressure coefficients without and with VSVs for the large gable roof model at 45° wind direction……179

A-5 Comparison of external and internal pressure coefficients without and with VSVs for the large gable roof model at 60° wind direction……181

A-6 Comparison of external and internal pressure coefficients without and with VSVs for the large gable roof model at 75° wind direction……183

A-7 Comparison of external and internal pressure coefficients without and with VSVs for the large gable roof model at 90° wind direction……185

A-8 Comparison of external and internal pressure coefficients without and with VSVs for the large hip roof model at 0° wind direction……..187

A-9 Comparison of external and internal pressure coefficients without and with VSVs for the large hip roof model at 15° wind direction……189

A-10 Comparison of external and internal pressure coefficients without and with VSVs for the large hip roof model at 30° wind direction……191

A-11 Comparison of external and internal pressure coefficients without and with VSVs for the large hip roof model at 45° wind direction……193

B-1 Comparison of external and internal pressure coefficients without and with VSVs for the small gable roof model at 0° wind direction……..196

B-2 Comparison of external and internal pressure coefficients without and with VSVs for the small gable roof model at 15° wind direction……198

B-3 Comparison of external and internal pressure coefficients without and with VSVs for the small gable roof model at 30° wind direction……200

B-4 Comparison of external and internal pressure coefficients without and with VSVs for the small gable roof model at 45° wind direction……....202

B-5 Comparison of external and internal pressure coefficients without and with VSVs for the small gable roof model at 60° wind direction……204

B-6 Comparison of external and internal pressure coefficients without and with VSVs for the small gable roof model at 75° wind direction……206

B-7 Comparison of external and internal pressure coefficients without and with VSVs for the small gable roof model at 90° wind direction……208

B-8 Comparison of external and internal pressure coefficients without and with VSVs for the small hip roof model at 0° wind direction……210

B-9 Comparison of external and internal pressure coefficients without and with VSVs for the small hip roof model at 15° wind direction……...213

B-10 Comparison of external and internal pressure coefficients without and with VSVs for the small hip roof model at 30° wind direction……...216

B-11 Comparison of external and internal pressure coefficients without and with VSVs for the small hip roof model at 45° wind direction……...219

LIST OF FIGURES

FIGURE PAGE

1-1 Schematic of roofs with soffits: a) internal pressurization of the attic space without valved soffit vents; b) depressurization of the attic space with valved soffit vents……2

1-2 North Atlantic hurricane tracks since 1848 (Coastal Population Tool, http://coast.noaa.gov/hurricanes/v3.0/#).....2

1-3 Correlation of average sea surface temperatures and total named hurricanes in the North Atlantic (Curry, 2007)…….3

1-4 Damaged soffit due to wind induced suction (FEMA)……...…….6

1-5 Wind effects on a building with valved soffit vents (illustrated by Preiss and Katz)……..9

2-1 a) The WindEEE facility; b) the IBHS facility; and c) The Insurance Research Lab facility (Three Little Pigs project)……...23

3-1 Perspective of the flow field around a cube for: a) θ=0°; b) θ=45° (Borges 1998)……..38

3-2 Overall wind effects on a low-rise building (Minor and Mehta 1979)…….....39

3-3 Separation and reattachment of flow along a short and long building (Liu 1991)……..40

3-4 Conical vortices at the roof corner: a) flow structure; b) pressure distribution (Cook 1985)……....43

3-5 Three regions of the flow field around a building (Aynsley, Melbourne and Vickery 1977)……...…….……..45

3-6 Flow in the wake and rear stagnation point, RS (Cook 1985)…….....45

3-7 Mean pressure distribution for a low-rise building with a flat roof in boundary-layer wind (Liu 1991)……....46

3-8 Hip and gable roofs comparison of peak suctions (Xu and Reardon 1998)….....46

4-1 The 12-fan Wall of Wind (WOW) facility in Miami, Florida……...……....48

4-2 The WOW flow chamber with four spires and floor roughness elements…...…..48

4-3 Wall of Wind configuration (https://wow.fiu.edu/about/technical-aspects - of-the-wall-of-wind)……..49

4-4 Cobra probe and frame set at the roof eave height (1.27 m) to record freestream data……..……..……...50

4-5 Comparison of the measured WOW spectrum with the Von Karman spectrum…….51

5-1 A valved soffit vent (VSV) that was used for this testing: a) front; b) back……60

5-2 Schematics of the test building: a) gable roof model; b) hip roof model…….....62

5-3 Measured mean velocity and turbulence profiles at the WOW: a) comparison of experimental and target mean velocity profile; b) experimental turbulence intensity profile…….…….65

5-4 a) External pressure tap locations on the gable roof……..69

5-4 b) Internal pressure tap locations on the gable roof surface……..70

5-4 c) Internal pressure taps in the attic space of the gable roof; d) internal pressure taps at vents…….71

5-5 a) External pressure tap locations on the hip roof…….72

5-5 b) Internal pressure tap locations on the hip roof surface……..73

5-5 c) Internal pressure taps in the attic space of the hip roof; d) internal pressure taps at vents…….74

5-6 The building models used for the testing: a) gable roof building model ready for testing, 0° wind direction; b) underside of the gable roof with tubing installed; c) hip roof building model ready for testing, 0° wind direction; d) underside of the hip roof with tubing installed; e) soffit vent openings without VSVs, hip roof; f) soffit vent openings with VSVs (*BPA Safety Vents*) installed……..……77

5-7 a) Underside of hip roof with VSVs installed without screen (Test Case 3); b) BPA Safety Vent with taps attached ; c) lifting gable roof in place; d) connecting pressure tap tubing to Scanivalve data acquisition system; e) gable roof without VSVs (Test Case 1); f) gable roof with VSVs (Test Case 2)..78

5-8 Attic space internal pressure distribution due to VSVs: a) mean, gable roof; b) maximum, gable roof; c) mean, hip roof; d) maximum, hip roof…….....84

5-9 Correlation of mean external pressure at each vent and internal pressure: a) gable roof, WD = 0°; b) gable roof, WD = 45°; c) hip roof, WD = 0°; d) hip roof, WD = 45°……....85

5-10 Mean pressure coefficients ($C_{p's}$) on the gable roof model for WD = 0°: a) external roof surface without VSVs; b) external roof surface with VSVs; c) internal roof surface without VSVs; d) internal roof surface with VSVs; e) internal attic surface without VSVs; f) internal attic surface with VSVs……..89

5-11 Peak pressure coefficients ($C_{p's}$) on the gable roof model for WD = 0°: a) external roof surface without VSVs (-ve); b) external roof surface with VSVs (-ve); c) internal roof surface without VSVs (+ve); d) internal roof surface with VSVs (+ve)……....90

5-12 Mean pressure coefficients ($C_{p's}$) on the gable roof model for WD = 15°: a) external roof surface without VSVs; b) external roof surface with VSVs; c) internal roof surface without VSVs; d) internal roof surface with VSVs; e) internal attic surface without VSVs; f) internal attic surface with VSVs……..91

5-13 Peak pressure coefficients ($C_{p's}$) on the gable roof model for WD = 15°: a) external roof surface without VSVs (-ve); b) external roof surface with VSVs (-ve); c) internal roof surface without VSVs (+ve); d) internal roof surface with VSVs (+ve)……....92

5-14 Mean pressure coefficients ($C_{p's}$) on the gable roof model for WD = 30°: a) external roof surface without VSVs; b) external roof surface with VSVs; c) internal roof surface without VSVs; d) internal roof surface with VSVs; e) internal attic surface without VSVs; f) internal attic surface with VSVs……..93

5-15 Peak pressure coefficients ($C_{p's}$) on the gable roof model for WD = 30°: a) external roof surface without VSVs (-ve); b) external roof surface with VSVs (-ve); c) internal roof surface without VSVs (+ve); d) internal roof surface with VSVs (+ve)……....94

5-16 Mean pressure coefficients ($C_{p's}$) on the gable roof model for WD = 45°: a) external roof surface without VSVs; b) external roof surface with VSVs; c) internal roof surface without VSVs; d) internal roof surface with VSVs; e) internal attic surface without VSVs; f) internal attic surface with VSVs……..95

5-17 Peak pressure coefficients ($C_{p's}$) on the gable roof model for WD = 45°: a) external roof surface without VSVs (-ve); b) external roof surface with VSVs (-ve); c) internal roof surface without VSVs (+ve); d) internal roof surface with VSVs (+ve)……....96

5-18 Mean pressure coefficients ($C_{p's}$) on the gable roof model for WD = 60°: a) external roof surface without VSVs; b) external roof surface with VSVs; c) internal roof surface without VSVs; d) internal roof surface with VSVs; e) internal attic surface without VSVs; f) internal attic surface with VSVs……..97

5-19 Peak pressure coefficients ($C_{p's}$) on the gable roof model for WD = 60°: a) external roof surface without VSVs (-ve); b) external roof surface with VSVs (-ve); c) internal roof surface without VSVs (+ve); d) internal roof surface with VSVs (+ve)……....98

5-20 Mean pressure coefficients ($C_{p's}$) on the hip roof model for WD = 0°: a) external roof surface without VSVs; b) external roof surface with VSVs; c) internal roof surface without VSVs; d) internal roof surface with VSVs; e) internal attic surface without VSVs; f) internal attic surface with VSVs……..…99

5-21 Peak pressure coefficients ($C_{p's}$) on the hip roof model for WD = 0°: a) external roof surface without VSVs (-ve); b) external roof surface with VSVs (-ve); c) internal roof surface without VSVs (+ve); d) internal roof surface with VSVs (+ve)……..100

5-22 Mean pressure coefficients ($C_{p's}$) on the hip roof model for WD = 15°: a) external roof surface without VSVs; b) external roof surface with VSVs; c) internal roof surface without VSVs; d) internal roof surface with VSVs; e) internal attic surface without VSVs; f) internal attic surface with VSVs……101

5-23 Peak pressure coefficients ($C_{p's}$) on the hip roof model for WD = 15°: a) external roof surface without VSVs (-ve); b) external roof surface with VSVs (-ve); c) internal roof surface without VSVs (+ve); d) internal roof surface with VSVs (+ve)……..102

5-24 Mean pressure coefficients ($C_{p's}$) on the hip roof model for WD = 30°: a) external roof surface without VSVs; b) external roof surface with VSVs; c) internal roof surface without VSVs; d) internal roof surface with VSVs; e) internal attic surface without VSVs; f) internal attic surface with VSVs……....103

5-25 Peak pressure coefficients ($C_{p's}$) on the hip roof model for WD = 30°: a) external roof surface without VSVs (-ve); b) external roof surface with VSVs (-ve); c) internal roof surface without VSVs (+ve); d) internal roof surface with VSVs (+ve)……..104

5-26 Mean pressure coefficients ($C_{p's}$) on the hip roof model for WD = 45°: a) external roof surface without VSVs; b) external roof surface with VSVs; c) internal roof surface without VSVs; d) internal roof surface with VSVs; e) internal attic surface without VSVs; f) internal attic surface with VSVs…...…105

5-27 Peak pressure coefficients ($C_{p's}$) on the hip roof model for WD = 45°: a) external roof surface without VSVs (-ve); b) external roof surface with VSVs (-ve); c) internal roof surface without VSVs (+ve); d) internal roof surface with VSVs (+ve)……106

5-28 Net mean and peak pressure coefficients: a) gable roof (mean); b) gable roof (peak); c) hip roof (mean); d) hip roof (peak)……108

5-29 Net averaged mean pressure coefficients for the complete roof area: a) hip roof b) gable roof……109

5-30 a) Plastic membrane used to collect water; b) WOW spray nozzles, pre-test check; c) test specimen with access door removed to check water entry; d) water captured for the 0° wind direction, without VSVs ; e) weighing dry container; f) measured volume of water that entered the attic for the 0° wind direction, without VSVs……111

5-31 CFD models with polyhedral mesh: a) gable roof; b) hip roof……113

5-32 The velocity flow field: vertical plane at centerline for the gable roof model for 0° and 45° wind directions……115

5-33 The velocity flow field: vertical plane at centerline for the hip roof model for 0° and 45° wind directions……115

5-34 The velocity flow field: horizontal plane at 1.2 m for the gable roof model for 0° and 45° wind directions……115

5-35 The velocity flow field: horizontal plane at 1.2 m for the hip roof model for 0° and 45° wind directions……116

5-36 Mean external pressure coefficients for the gable and hip roofs, 45° wind direction……116

6-1 a) External pressure tap locations on the gable roof……126

6-1 b) Internal pressure tap locations on the gable roof surface……127

6-1 c) Internal pressure taps in the attic space of the gable roof; d) internal pressure taps at vents……128

6-2 a) External pressure tap locations on the hip roof……129

6-2 b) Internal pressure tap locations on the hip roof surface……130

6-2 c) Internal pressure taps in the attic space of the hip roof; d) internal pressure taps at vents……131

6-3 The building models used for the testing: a) gable roof building model ready for testing, 0° wind direction; b) underside of the gable roof with tubing installed; c) hip roof building model ready for testing, 0° wind direction; d) underside of the hip roof with tubing installed……..……..132

6-4 a) Installing the hip roof to the model base; b) location of the vents on the hip roof; c) location of the vents on the gable roof; d) the attic floor layout…...133

6-5 Mean pressure coefficients ($C_{p's}$) on the gable roof model for WD = 0°: a) external roof surface without VSVs; b) external roof surface with VSVs; c) internal roof surface without VSVs; d) internal roof surface with VSVs; e) internal attic surface without VSVs; f) internal attic surface with VSVs…..…..141

6-6 Peak pressure coefficients ($C_{p's}$) on the gable roof model for WD = 0°: a) external roof surface without VSVs (-ve); b) external roof surface with VSVs (-ve); c) internal roof surface without VSVs (-ve); d) internal roof surface with VSVs (-ve); e) internal roof surface without VSVs (+ve); f) internal roof surface with VSVs (+ve)……142

6-7 Mean pressure coefficients ($C_{p's}$) on the gable roof model for WD = 15°: a) external roof surface without VSVs; b) external roof surface with VSVs; c) internal roof surface without VSVs; d) internal roof surface with VSVs; e) internal attic surface without VSVs; f) internal attic surface with VSVs……...143

6-8 Peak pressure coefficients ($C_{p's}$) on the gable roof model for WD = 15°: a) external roof surface without VSVs (-ve); b) external roof surface with VSVs (-ve); c) internal roof surface without VSVs (-ve); d) internal roof surface with VSVs (-ve); e) internal roof surface without VSVs (+ve); f) internal roof surface with VSVs (+ve)……144

6-9 Mean pressure coefficients ($C_{p's}$) on the gable roof model for WD = 30°: a) external roof surface without VSVs; b) external roof surface with VSVs; c) internal roof surface without VSVs; d) internal roof surface with VSVs; e) internal attic surface without VSVs; f) internal attic surface with VSVs……...145

6-10 Peak pressure coefficients ($C_{p's}$) on the gable roof model for WD = 30°: a) external roof surface without VSVs (-ve); b) external roof surface with VSVs (-ve); c) internal roof surface without VSVs (-ve); d) internal roof surface with VSVs (-ve); e) internal roof surface without VSVs (+ve); f) internal roof surface with VSVs (+ve)……...146

6-11 Mean pressure coefficients ($C_{p's}$) on the gable roof model for WD = 45°: a) external roof surface without VSVs; b) external roof surface with VSVs; c) internal roof surface without VSVs; d) internal roof surface with VSVs; e) internal attic surface without VSVs; f) internal attic surface with VSVs…..…..147

6-12 Peak pressure coefficients ($C_{p's}$) on the gable roof model for WD = 45°: a) external roof surface without VSVs (-ve); b) external roof surface with VSVs (-ve); c) internal roof surface without VSVs (-ve); d) internal roof surface with VSVs (-ve); e) internal roof surface without VSVs (+ve); f) internal roof surface with VSVs (+ve)……..……...148

6-13 Mean pressure coefficients ($C_{p's}$) on the hip roof model for WD = 30°: a) external roof surface without VSVs; b) external roof surface with VSVs; c) internal roof surface without VSVs; d) internal roof surface with VSVs; e) internal attic surface without VSVs; f) internal attic surface with VSVs…..…..149

6-14 Peak pressure coefficients ($C_{p's}$) on the hip roof model for WD = 30°: a) external roof surface without VSVs (-ve); b) external roof surface with VSVs (-ve); c) internal roof surface without VSVs (-ve); d) internal roof surface with VSVs (-ve); e) internal roof surface without VSVs (+ve); f) internal roof surface with VSVs (+ve)…...……..150

6-15 Mean pressure coefficients ($C_{p's}$) on the hip roof model for WD = 45°: a) external roof surface without VSVs; b) external roof surface with VSVs; c) internal roof surface without VSVs; d) internal roof surface with VSVs; e) internal attic surface without VSVs; f) internal attic surface with VSVs…...….151

6-16 Peak pressure coefficients ($C_{p's}$) on the hip roof model for WD = 45°: a) external roof surface without VSVs (-ve); b) external roof surface with VSVs (-ve); c) internal roof surface without VSVs (-ve); d) internal roof surface with VSVs (-ve); e) internal roof surface without VSVs (+ve); f) internal roof surface with VSVs (+ve)……..……...152

6-17 Net mean pressure coefficients: a) gable roof; b) hip roof…….……157

6-18 Regression lines and equations to estimate the change in mean $C_{pi's}$ with VSVs installed.....161

A-1 Atmospheric boundary layer (ABL) velocity profiles at various throttle percentages for the WOW variable speed testing……172

CHAPTER I

INTRODUCTION

The primary focus of this dissertation is the study of a new concept to mitigate wind-induced pressures and wind-driven rain into the roof attic space of low-rise buildings. The roof soffit has proven to be an area of weakness in many low-rise buildings, most notably in residential structures that have been damaged by high velocity wind events, namely hurricanes. As shown in Figure 1-1, soffit vents provide a point of entry for wind-induced pressure and wind-driven rain into the attic space. Internal pressurization from wind-induced positive pressure entering the windward soffit vents combined with external suctions on the roof can produce large uplift forces, which can lead to the potential failure of the roof sheathing. Even if the roof structure remains intact, the wind can drive rain into the attic through the soffit vents, which alone can cause significant loss, albeit non-structural. In fact, soffit failure has resulted in extensive damage to homes as reported in various post-hurricane surveys (Leatherman 2008). However, the soffit vents can be valved to prevent air flow into the attic space; thereby, allowing for the relief of positive pressure within the attic space while mitigating wind-driven rain entry, a concept which this dissertation investigates.

Background Information

As illustrated in Figure 1-2, hurricanes in the North Atlantic region have been a real threat. Since the 1970s, the Sea Surface Temperatures (SST) have increased, as shown in Figure 1-3. Should this trend continue, models and predictions agree that

hurricane intensity will likely increase and the number of hurricanes developing in the North Atlantic region will also increase (Curry 2007).

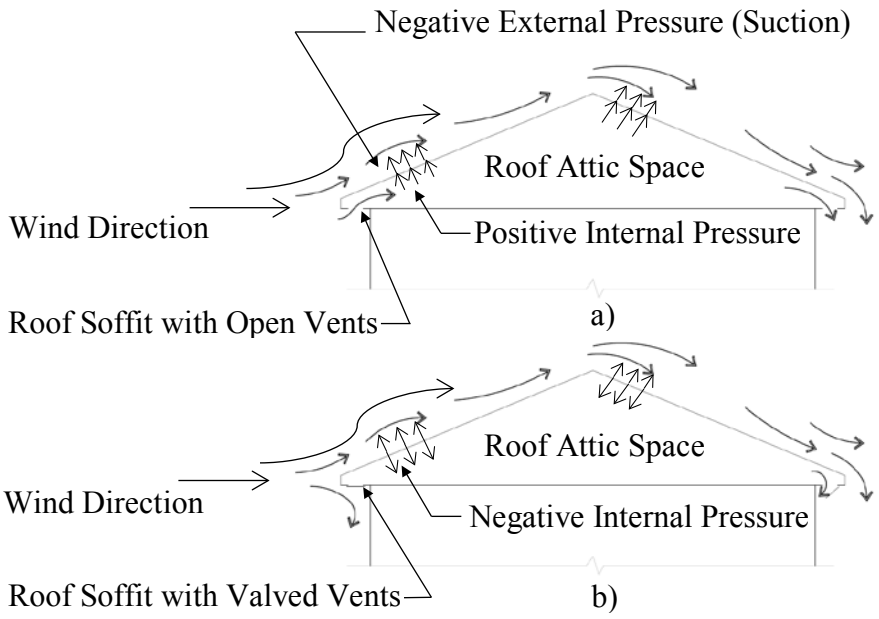

Figure 1-1. Schematic of roofs with soffits: a) internal pressurization of the attic space without valved soffit vents; b) depressurization of the attic space with valved soffit vents

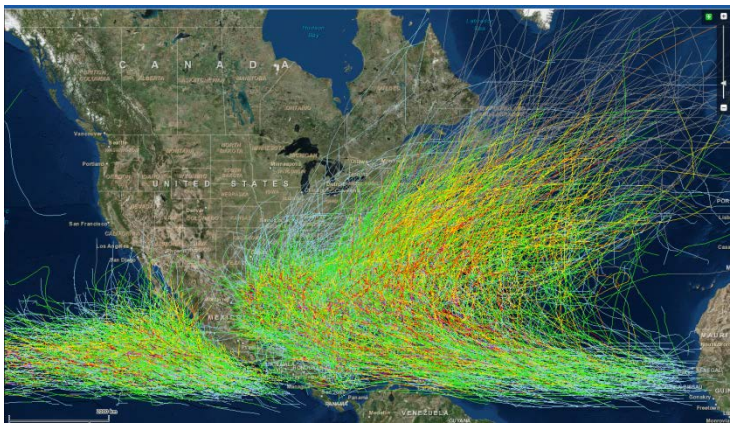

Figure 1-2. North Atlantic hurricane tracks since 1848 (Coastal Population Tool, http://coast.noaa.gov/hurricanes/v3.0/#)

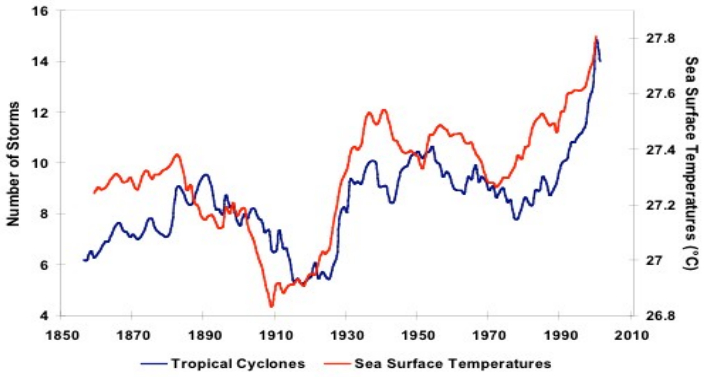

Figure 1-3. Correlation of average sea surface temperatures and total named hurricanes in the North Atlantic (Curry, 2007)

According to Smith and Katz (2013), the frequency and distribution of damage from U.S. billion-dollar weather/climate disasters between 1980 and 2011 has been dominated by tropical cyclone losses. Moreover, 2015 was the warmest year that has been recorded since 1880 (NOAA 2015). In addition to the likelihood of increased hurricane intensity and occurrence, another risk factor that must be highlighted is the increased migration towards the coasts. In Florida alone, 80% of the residents live within 35 km (20 miles) of the coast. In fact, approximately half of the U.S. population lives near the coastline. Therefore, it can be argued that the risk of potential hurricane activity in the United States should be one of the chief concerns to the public (BND 1999).

In 2005, Hurricanes Katrina, Wilma and Rita together were responsible for estimated property damages of around USD 158 billion. Additionally, during the past ten years, there have been other major hurricane events affecting the United States including: Hurricanes Ike (2008), Irene (2011) and Sandy (2012), which resulted in the region of USD 110 billion in losses. The State of Florida, which is the most hurricane-prone state, has experienced more than USD 60 billion in losses due to hurricane damages over the

past twelve years. Florida suffered four hurricanes (Charley, Frances, Ivan, and Jeanne) alone in 2004. In fact, Hurricane Charley was the second costliest hurricane to hit Florida since Hurricane Andrew in 1992 (Lott and Ross 2006, Meloy et al. 2007, Leatherman, 2008, NOAA 2014).

Hurricanes are a global hazard that have inflicted extreme destruction not only in the United States, but also in the regions of the Pacific, Indian and Atlantic oceans, encompassing the Caribbean, Australia, the South Pacific, India, China, Japan, Taiwan and the Philippines. In 2004 alone, an unprecedented ten tropical cyclones hit Japan (Trenberth 2005). Hurricanes in the South Sea and Pacific Northwest are known as typhoons and those in the region of Australia and the Indian Ocean are termed cyclones. Hurricanes, typhoons and cyclones can all be categorized as tropical cyclones. During the past decade, typhoons and cyclones have caused severe destruction in various countries around the world, such as: Cyclone Nargis (2008), which accounted for USD 10 billion in losses, 85,500 deaths, 53,800 people missing and 1.5 million people homeless; Cyclone Phalin (2013), Typhoon Fitow (2013) and Typhoon Haiyan (2013), one of the strongest tropical cyclones ever recorded, which together caused over 7,500 deaths and resulted in close to USD 26.5 billion in damages; Cyclone Hudhud (2014) and Cyclone Rammasun (2014), which together caused over USD 12 billion of destruction and 270 deaths; and Tropical Cyclone Winston, which in February 2016 was responsible for major damages, leaving over 8,000 people homeless and causing at least 21 deaths when it passed over the island nation of Fiji. Cyclone Winston was the first Category 5 storm to make landfall in Fiji and was the second most powerful storm to hit the South Pacific (Weather 2016). In summary, since 2005 tropical cyclones worldwide have caused over USD 300 billion

in damages and have taken more than 148,000 lives (SwissRe 2015). Thus, the strengthening of buildings to withstand these major storms should take global priority. The engineering industry has an opportunity to play a major role by responding to the need to develop methods and techniques to assist with natural disaster mitigation.

Wind Damage

Tropical cyclones are the costliest natural catastrophes in the U.S. (Emmanuel 2005). Furthermore, the most significant losses due to natural disasters in the United States are attributed to high winds (Liu 1989, Fu 2012). Wind storms, which primarily include hurricanes, tornadoes, thunderstorms and downbursts, account for 70% of the total insured losses, with hurricanes being the largest contributor (Simiu and Scanlan 1996, Holmes 2007). Pielke et al. (2008) reported that the decade between 1996 and 2005 suffered the second most damage in the history of the United States. Intense hurricanes of Saffir-Simpson Categories 3, 4 and 5 were responsible for about 85% of the total damage.

The majority of the global building stock is low-rise buildings, which are comprised mainly of residential, commercial and industrial structures. In the U.S., over 70% of the buildings are low-rise buildings, where "low-rise" is typically considered to be 18 m (60 ft) or less in height (ASCE 7-10, Fu 2012). Low-rise buildings account for the majority of losses due to hurricanes. Unfortunately, in times past low-rise buildings, in particular houses, were often constructed with minimal (or even without) sound engineering input. Preliminary estimates indicate that there are over 12 million houses located in the hurricane belt that were built prior to the adoption of modern building

codes. These homes were likely built according to practices by builders and architects that would not have included proper methods to adequately resist wind loads. Since Hurricane Andrew in 1992, field investigations have shown similar and predictable damage by different hurricanes. A consistent finding is that roofs and roofing systems are the most vulnerable areas to fail in these high velocity wind events (Liu 1989, Platts et al. 2003, Meloy et al. 2007).

Minor (2005) reported that the hundreds of damage assessments that he has participated in during the past 33 years have revealed that the building envelope is crucial to the performance of buildings in windstorms. The part of the building envelope that is usually overlooked is the roof soffits. At the conclusion of an overview of wind damage caused by Hurricane Katrina, Graettinger (2006) recorded that the attic vents were a typical point of entry for wind-induced pressure, resulting in pressurization of the attic space and failure of the roof sheathing and interior ceiling drywall. Moreover, damaged soffits were regularly observed, as shown in Figure 1-4. According to Vickery (2008), there is a soffit loading deficiency in *ASCE-7*.

Figure 1-4. Damaged soffit due to wind-induced suction (FEMA)

In addition to structural damage that can occur to roofs, wind-driven rain can penetrate openings in residential roof systems causing substantial damage to the interior space. Numerous post-hurricane evaluations have reported that water entry through roof vents or damaged soffits caused ceiling damage and water damage to building contents. Water infiltration, which can be expected when rain occurs with wind speeds over 30 m/s (67 mph), can cause damage to interior finishes, mold growth, and even total loss of amenity (Reardon et al. 1999, Ginger et al. 2010, Dixon and Prevatt 2010).

Damage surveys that were conducted by Wyndham Partners (2004 and 2005) of Hurricanes Charley and Katrina reported the following: soffit failure problems may have increased uplift forces from the underside of the roof, possibly compounding vulnerability of poorly attached roof sheathing; buildings displayed significant construction deficiencies in the weakness of soffit installations; large and poorly detailed vinyl soffits were significant contributors to progressive roof failures and internal ceiling damage; common progressive failure was due to internal pressurization from positive pressure acting on soffits; and the pressurization on the windward soffits led to a massive progressive failure of leeward sheathing and gable ends.

It is evident from various post-hurricane surveys that soffit failure has significantly contributed to considerable damage to houses. In fact, it is estimated that improved soffit design would have led to an $8.4 billion savings in hurricane damage in Florida in 2004 alone (Leatherman, 2008).

One solution to reduce the risk of soffit damage by major wind events such as hurricanes is to develop novel mitigation technologies to strengthen homes to resist high velocity winds. One such technology is the valved soffit vent (VSV).

Valved Soffit Vents

The valved soffit vent concept was first introduced by a team of Canadian engineers and scientists: Robert Platts (inventor), the late Tony Woods and Dr. Alan G. Davenport, as part of Hurricane Resistance Technologies (HRT) solutions. One of the main objectives of the VSVs is to upgrade the performance of roofs on the current building stock of houses by influencing the internal pressure effects in the roof attic space to reduce the net pressure experienced on the roof components and cladding such as the sheathing. The VSVs also provide a mechanism to protect the building from wind-driven rain. In addition, the VSV technology allows for a less disruptive upgrade procedure compared with more conventional methods (Platts 2003).

The novel VSV technology works as a system to enhance the performance of the roof envelope. The valved vents are installed in the roof soffits and positioned in the regions that produce high suctions, i.e. the wind separation zones at the building corner edges.

Figure 1-5 illustrates the valved vent theory. The one-way valved vents on the windward side of the building shut tight to stop positive wind pressure from entering the roof attic space. Concurrently, the other valved vents, which are in the negative pressure areas, remain open, thereby reducing the internal pressures in the attic space. Therefore,

VSV technology provides three major advantages: the vents keep the soffits intact, stop wind-driven rain from entering the attic space and help keep the roof sheathing on.

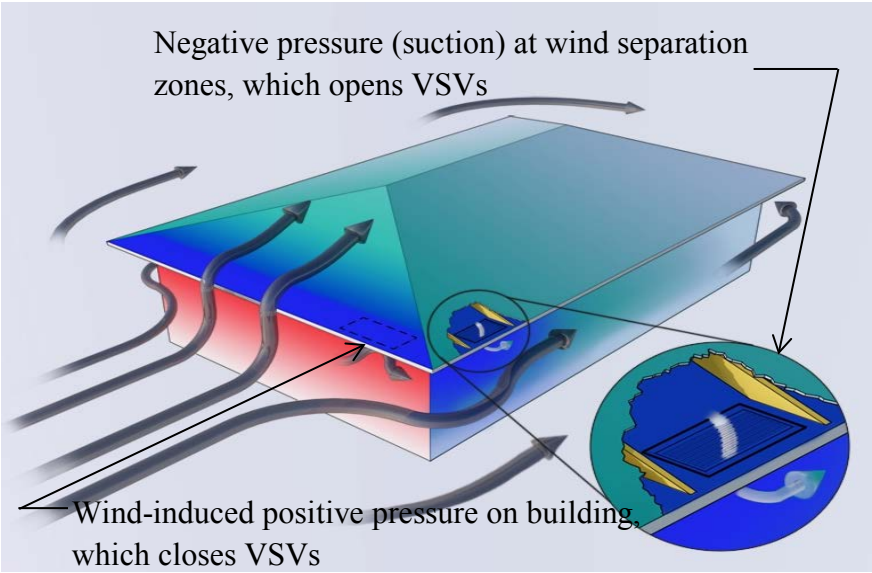

Figure 1-5. Wind effects on a building with valved soffit vents (illustrated by Preiss and Katz)

The valved soffit ventilation system consists of rectangular soffit vents fitted with louvers, which act as one-way valves. The VSVs are installed on the soffits around the building. The louvers hang open for natural ventilation but quickly close whenever wind and rain press inward. Therefore, only those VSVs facing the negative pressure areas stay open to depressurize the roof attic space.

Research Objectives and Scope

The objective of this study was to investigate the valved soffit vent concept, including the performance of the Building Performance Americas' (BPA) valved soffit vent design using the International Hurricane Research Center's 12-fan Wall of Wind (WOW) at Florida International University in Miami, Florida. To date, limited research has been conducted on soffits in general and only a few studies exist on soffit vents. More importantly, to the best of the author's knowledge there has been no previous study on valved soffits vents other than preliminary investigations by the inventor of the BPA vent. However, valved vent theory was suggested by Surry et al. (2005) as follows:

"A particularly interesting possibility is the suggested use of valved vents at strategic areas of high negative pressure to ensure that the net loads on the roof are downwards (at the cost of higher loads on the windward wall."

More recently, Gan Chowdhury et. al (2010) performed a study on roof vents subjected to simulated hurricane effects. They concluded:

"…further research is needed for developing methods for reducing water infiltration through soffit vents…Active controls could also be designed to close various vents automatically as differential pressure increases with the wind speed and wind angle of attack."

In addition, the study that was conducted at the Insurance Institute for Business & Home Safety (IBHS) on water entry through attic vents reported the following:

"As a preliminary study, this work suggests that more investigation is needed to quantify how much water entry is likely to be reduced with various water entry prevention measures."

The scope of this present research was to:

1. Clarify the influence of VSVs on wind-induced pressures within the roof attic space;

2. Document the performance characteristics of the *BPA Safety Vent* with regard to opening and closing with positive and negative pressures at different wind speeds and wind angles of attack. In addition, the extent to which the VSVs prevent wind-driven rain from entering the roof attic space was examined; and
3. Validate that the VSV concept is an effective mitigation technique to reduce wind-induced pressures on roofs.

Importance of Study

First and foremost, this experimental study sought to advance the knowledge base for establishing valved soffit vent technology as a viable mitigation technique for reducing wind-induced pressures on roofs of low-rise buildings. Implementation of the VSV strategy could ultimately have a significant benefit to society as there are millions of houses in the United States and around the world in need of strengthening to resist hurricane winds. In addition, the VSVs are able to provide natural ventilation for homes while acting as a barrier to water entry when required.

The valved soffit vent concept could provide the construction and engineering industry with a retrofit option that is less intrusive to install and consequently more cost effective. The validation of the VSVs has the ability to reduce the inherent risk of roof and interior damage caused by high velocity winds and wind-driven rain from storm events such as hurricanes.

Organization of Document

Chapter 2 offers a review of available literature on full and model-scale testing of in particular low-rise buildings, as well as a review of reported mitigation techniques for wind-induced pressures on low-rise buildings. In addition, a review of previous literature on roof vents and soffits is included. Chapter 3 provides a theoretical background related to wind flow around low-rise buildings. A description of the Wall of Wind facility is summarized in Chapter 4. In Chapter 5, the performance testing of the full-scale BPA valved soffit vents is documented. Chapter 6 describes the experimental configuration developed to evaluate the internal pressures in the roof attic space using the valved soffit vent concept. Finally, Chapter 7 presents conclusions resulting from this study and recommendations for future research.

CHAPTER II

LITERATURE REVIEW

Model and Full-Scale Testing of Low-Rise Buildings

There has been a considerable amount of research and studies performed on wind-induced pressures and loading on low-rise buildings and structures. One of the first wind tunnel tests on a model low-rise residential building dates as far back as the late 19th century. In 1891, Irminger conducted a study of wind pressures on a small model of a house. Then in Russia, in the late 1920s, there was a thorough study of pressures on roof and walls of various types of houses performed by Bounkin and Tcheremoukhin. A short time later, Irminger and Nokkentved performed extensive wind tunnel studies in Denmark. These tests involved the measurement of internal and external pressures. In addition, they examined the wind flow around models of buildings of different shapes and sizes. During this period, the wind tunnel testing techniques were quite basic. The approach flow that was developed in the wind tunnel was typically uniform, generating steady pressures that could be measured using manometers. One of the important aerodynamic factors, which was discovered with the use of steady flow wind tunnels, was that the sharp edged models of the buildings did not show any significant sensitivity to Reynolds Number (Stathopoulos, 1979, Davenport, 1982, and Holmes, 1983).

Around the same time, there was a burgeoning interest in understanding the natural wind boundary layer. To this end, Bailey (1933) compared wind tunnel tests with measurements from full scale experiments on a roof of a railway car shed at the

Metropolitan-Vickers Electrical Manufacturing Co. Ltd., in Manchester, England. Bailey noted:

"Before these results of model tests can be applied with confidence to full-scale conditions, it is necessary to know whether there is any scale effect, and whether the effects of the natural wind are the same as those of the artificial wind in the wind-tunnel".

The uniform steady flow wind tunnel test produced slightly larger pressures and lower suctions than those that were measured in full-scale. More progress was made by Bailey and Vincent (1943) at the National Physical Laboratory (NPL) in Great Britain. They endeavored to determine the relationship between wind speed and pressure distribution over buildings of various forms. The tests were performed on seven model buildings in a wind tunnel, under fully exposed conditions and in close proximity to other buildings. They concluded that the model test only provided an approximate guide for preliminary calculations.

However, a major development was credited to Jensen (1958) at the Technical University of Denmark, where Jensen proposed his Model Law:

"The correct model test for phenomena in the wind must be carried out in a turbulent boundary layer to be scaled as regards the velocity profile."

Jensen's experiments of comparing mean pressures on wind tunnel models with full-scale small buildings adequately explained the differences between wind tunnel and full-scale pressure measurements by identifying the similarity parameter h/z_o (building height/roughness length), the Jensen Number. He determined that when h/z_o was the same, the full-scale and model-scale measurements were in agreement. Thus, equality of h/z_o is required for wind tunnel mean pressure measurements on the model to match the full-scale values (Holmes 2007). Then in the 1960s, Jensen and Frank conducted an extensive wind tunnel study on low-rise buildings. This work, along with contributions

from J.E. Cermak and A.G. Davenport, assisted in advancing boundary layer wind tunnel testing on low-rise buildings as a major tool for engineering.

The first meteorological wind tunnel (MWT) was designed by Cermak to meet the requirements for simulation of the natural wind (Cermak 1975). Stathopoulos (1979) conducted a comprehensive wind tunnel study on low-rise buildings at the University of Western Ontario's (UWO) Boundary Layer Wind Tunnel Laboratory, which is the basis for the current ASCE/SEI-7 wind load provisions. The study included a variety of low-rise building geometries, two terrain types, a number of wind directions, ranges in roof slope, three wall heights, various building lengths, and the presence of eaves or parapets. He determined that both roof slope and height influence the loads significantly; however, there is little effect for building length. There were increased loads near the roof corners with the addition of low parapets, and the eaves extend the roof area, exposing them to high edge and corner loads.

Vickery and Surry (1983) pointed out the importance of wind tunnel test data compared with full-scale experiments, stating that the comparisons are essential to the reliability of wind tunnel testing. In an effort to obtain high quality data on wind and building surface pressures and to confirm and improve upon the wind-tunnel procedure, a number of full-scale experiments were developed. The three most noteworthy are: the Aylesbury Experiment, the Wind Engineering Research Field Laboratory (WERFL) at Texas Tech University (TTU), and the Silsoe Structures Building (SSB).

Aylesbury Experimental Building

In the 1980s, the Aylesbury experiments produced some of the most comprehensive full- scale data available at that time. As outlined by Sill et al. (1989, 1992), the Aylesbury experimental building was a two-story house that was constructed in Aylesbury, England, with dimensions of 7 m x 13.3 m x 5 m (23 ft x 43'-7" x 16'-5"), $W \, x \, L \, x \, h_{eave}$. One of the unique features of this building was the gable roof of changing roof pitch from 5° to 45°. The main purpose of the experiment was to validate wind tunnel testing techniques for low-rise buildings. A total of 17 laboratories worldwide used the identical 1:100 model of the experimental building and comparative wind tunnel experiments were conducted. The comparison between the full-scale and wind tunnel measurements concluded that the variation in pressure coefficients was due to the differences in the data acquisition methods and in the measuring point of the reference pressures. The Aylesbury experiment pointed out the differences associated with different wind tunnel studies; thereby, identifying the need to continue further studies.

Texas Tech University (TTU) Building

The TTU building has been an important research facility that was constructed at Texas Tech University in Lubbock, Texas, in the late 1980s. The facility is also known as the Texas Tech Field Experiment and consists of a prefabricated metal test building with dimensions, *B x L x h* of 9.1 m x 13.7 m x 4.0 m (30 x 45 x 13 ft) and a 49 m (160 ft) meteorological tower. The roof of the building is almost flat and it has the capability of being rotated, thus providing control of the wind angle of attack. The TTU experiment has facilitated a variety of research on low-rise buildings, including; wind loads on

building surfaces, internal pressures, wind flow around buildings, and performance of roofing materials. A significant amount of data has been collected at the TTU facility, which has been available for various analyses. In addition, wind tunnel simulations have been conducted at facilities around the world. The comparisons of the wind tunnel studies with the full-scale TTU measurements have contributed to advancing the wind tunnel simulation technique (Levitan and Mehta, 1992a,b, Yeatts and Mehta, 1993, Uematsu and Isyumov, 1999, Holmes, 2007). The TTU data has allowed for extensive wind-tunnel simulations of approach flow and wind-induced loading on the TTU test building. Surry (1991), Okada and Ha (1992), Cochran and Cermak (1992), and Tieleman et.al. (1996), all found good agreement between the wind-tunnel and field data. However, discrepancies in the peak and root-mean-square point pressure were recognized at the roof corner regions. The difference between the compared data was due to the lateral turbulence intensity, small and large-scale spectra content of the approach flow fluctuations, frequency response of the pressure measurement system, sampling frequency of the acquired data, and Reynolds Number effects. Cheung et al. (1997) performed wind tunnel tests on a 1/10 scale model of the TTU building. He concluded that the mean and root-mean-square pressure coefficients from the model are in excellent agreement with the corresponding values from the full-scale building. In addition, Cheung claimed that the increased Reynolds Number contributed to the improved agreement of the pressure coefficients that were obtained. Ham and Bienkiewicz (1998) studied the approach wind flow and wind-induced pressure on a 1:50 geometric scale model of the TTU building in the boundary layer wind tunnel at Colorado State University. They observed very good agreement with the field data and attributed this

agreement to improved modeling of the approach flow and relatively high frequency response of the pressure measurement system.

The Silsoe Structures Building

The Silsoe Structures Building (SSB) is an experimental building that was constructed during 1986/87 in Silsoe, England, with dimensions of 24.13 m long x 12.93 m wide x 4 m to the eaves (79'-2" x 42'-5" x 13'-1"). The Silsoe building was built specifically to carry out full-scale wind pressure measurements. The building had optional eaves geometry of either curved eaves or conventional sharp roof edges. It was located on a flat, open country site at the Silsoe Research Institute (SRI). The SSB had a 10° gable roof pitch and the building structure consisted of steel portal frames at 4 m (13'-1") on center.

The Silsoe experimental building has made possible extensive measurements of the wind pressures at various locations on the building surface. The research also found that the curved eaves give lower mean negative pressures downwind of the windward wall, compared to those developed by the sharp eaves (Holmes, 2007). Hoxey and Robertson (1994) revealed that the quasi-steady approach for determining pressure coefficients was justified by the measurements obtained from the full-scale experiments. One of the main objectives of the SSB work was to make available reliable full-scale data for comparison with wind tunnel measurements. Comparison wind tunnel studies were conducted at the University of Western Ontario (UWO) and at the Building Research Establishment (BRE). The results showed that there was good agreement for the mean

pressure coefficients between the full-scale and wind tunnel measurements (Hoxey and Robertson, 1994, Richardson and Surry, 1991, and Richardson, et al. 1997).

In addition, a 6 m (19'-8") cube structure was also constructed at the SRI location. Richards et al. (2001) reported that the mean pressure coefficient data for the 6 m cube was compared with published wind tunnel data. The wind perpendicular to one face provides a general agreement for the windward wall pressures; however, the roof and leeward wall pressures were underestimated. This is apparently due to Reynolds Number sensitivity and/or relative roughness effects.

There were other full-scale studies being conducted as well. Marshall (1975) compared wind pressures on a single family house with wind tunnel results for a 1:50 scale model. The study was carried out at the Malmstrom Air Force Base in Montana. He suggested that the simulation of the lowest 30 m (98'-5") of the atmospheric boundary layer is achievable using a scale of 1:50. There was a general agreement between the model and full-scale pressure fluctuations. However, the experiment revealed peak pressure coefficients that were deficient in the model studies, which was attributed to the improper simulation of the turbulence. In addition, full-scale testing on three single family homes in Quezon City, Philippines, in the 1970s also confirmed that the key factor in generating realistic surface pressure fluctuations on the wind tunnel model is proper modeling of turbulence intensity. In Australia, a major study for testing wind loads on tropical houses commenced at James Cook University (JCU) following the severe damage to those structures during Cyclone Tracy in 1974 (Holmes 1983). And Milford (1992), performed a comparison between full-scale and wind-tunnel results on a 1:300 scale model for the Jan Smuts full-scale experiment, which is a large aircraft hangar at

Jan Smuts Airport. He found that the comparison between the mean and root-mean-square pressure coefficients is satisfactory; however, a shift between the full-scale and wind-tunnel mean pressure coefficients was observed.

The various full-scale experiments around the world have been essential for developing wind-tunnel simulation techniques for buildings and structures. These experiments revealed the importance of proper simulation of the approach flow characteristics on small-scale models in wind tunnels.

Turbulence Characteristics

The experiment performed by Bailey (1933) was one of the first to attribute the discrepancies with the pressure measurements to much lower turbulence in the flow used in the model tests. Jensen (1958) also noticed that the pressure distribution over the roof was affected by the increase in turbulence at eaves height. Then it was the work of Gartshore in the early 1970s who provided the first insightful description of effects of turbulence on flow around bluff bodies. He observed that increasing turbulence caused the radius of curvature of the separated shear layer to reduce, thus causing earlier reattachment of the flow. Soon after, Melbourne advanced Gartshore's conclusions by showing that an increase in small-scale turbulence within flows with the same large-scale turbulence increases the magnitude of low pressures under reattaching shear layers (Melbourne, 1993).

Hillier and Cherry (1981) described the effects of freestream turbulence on two-dimensional separating and reattaching flows in order to develop how accurately the properties of the atmospheric wind must be developed. They explained that the mean

flow field responds strongly to turbulence intensity but only slightly by the integral scale; however, fluctuating pressures depend strongly on both. They also showed that mean pressures were dependent on turbulence intensity. Saathoff and Melbourne (1989) investigated the occurrence of large negative pressures near the leading edge of sharp-edged bluff bodies. They reported that the large negative peak pressures in separated and reattaching flows are related to the intermittent roll-up of separated shear layers. In addition, the experiment emphasized the need to accurately model turbulence levels when conducting wind tunnel experiments.

Tieleman and Akins (1990) analyzed mean and fluctuating pressures on three-dimensional rectangular prisms for a number of geometries and incident flows. They emphasized that proper scaling of the atmospheric boundary layer should account for turbulent intensity and longitudinal integral scale. In addition, some measure of the small-scale turbulence should be accounted for. Tieleman (1992) discussed new criteria for the simulation of the lowest part of the atmospheric boundary layer (ABL), where low-rise buildings are located. He claimed that the high suction pressures at the edges and corners of roofs could not be correctly measured from wind tunnels using conventional methods. Tieleman reported that the duplication of small-scale turbulence is more important than simulating the velocity profile or the integral length scale. Throughout the 1990s, Tieleman extensively studied the comparison of full-scale and wind tunnel model test results for wind-induced pressures on low-rise buildings. Tieleman (1996), Tieleman et al. (1994, 1996, 1997, and 1998) explained the importance of wind tunnel simulation, which produces the turbulence intensities and the small-scale turbulence in the incident flow for predicting pressures on low-rise buildings.

During the past twenty years there has been progress in proper simulation of natural wind characteristics, including the simulation of hurricane winds. Yu, Gan Chowdhury, and Masters (2008) performed analyses of wind speeds obtained from five towers in four hurricanes based on data acquired by the Florida Coastal Monitoring Program (FCMP). They concluded that turbulent energy at lower frequencies is higher in hurricane winds when compared to non-hurricane winds. In addition, estimates of turbulence spectra, cospectra, and integral turbulence scales are suggested that can be used in experimental facilities of hurricane wind flows. The Florida Coastal Monitoring Program is a collaborative, multi-university experimental program that has been ongoing since 1998. This field research program was initiated to study the intensity and structure of surface wind and rain characteristics of Atlantic hurricanes (Balderrama et al. 2011).

There has also been recent progress with the development of full and large-scale testing facilities. Wind tunnel testing of low-rise buildings presents many challenges with particular need for relatively large models, which is very difficult to achieve in standard atmospheric boundary layer (ABL) wind tunnel testing facilities. The full-scale wind tunnel studies can provide valuable data between full-scale field studies and model-scale wind tunnel studies. In addition, investigations can be carried out on a full range of structural systems and building components (Kopp et al. 2012).

In 2003, the International Hurricane Research Center (IHRC) began planning to build a full-scale wind testing facility to generate experimental data for a better understanding of the effects of extreme winds on low-rise residential structures (Leatherman et al. 2008). The facility is known as the Wall of Wind (WOW). The IHRC initially conducted testing with a 2-fan system, then a 6-fan WOW was commissioned

and now the 12-fan WOW is operational. In addition to the Wall of Wind facility there are other notable facilities which can provide full- scale or large-scale testing. These include: the Wind Engineering, Energy and Environment (WindEEE) Dome at the University of Western Ontario and the Institute of Business and Home Safety facility in South Carolina (Figure 2-1 (a, b)).

a) b) c)

Figure 2-1. a) The WindEEE facility; b) the IBHS facility; and c) the Insurance Research Lab facility (Three Little Pigs project)

Surry, Kopp, and Bartlett (2005) introduced the "Three Little Pigs" project around the same time as the WOW, a full-scale test facility for entire, small, low-rise buildings (Figure 2-1 (c)). They recognized that achieving the behavior and failure of all the building components at model scale is extremely difficult, if not impossible to do. Soon after, the testing facility for the Insurance Institute for Business & Home Safety (IBHS) was developed in 2010 in Chester County, South Carolina. The facility can accommodate full-scale testing of one and two-story buildings in a simulated hurricane environment. The test chamber is 44.2 m long x 44.2 m wide x 18.3 m in height (145 ft x 145 ft x 60 ft).

Mitigation Techniques for Wind-Induced Pressures on Low-Rise Buildings

The majority of previous studies on mitigation techniques for alleviating wind-induced pressures on low-rise buildings were mainly aerodynamic modifications on low buildings with flat roofs. Both full and model-scale studies have confirmed that extremely high suctions are found near the roof corners. Consequently, these corner suctions are responsible for wind-induced damages on many low-rise buildings. As reported by Lin and Surry (1993):

"The high suctions on the roof are caused by the vortices which are generated near the corner by adjacent straight sharp edges and sweep the upper surface in a similar mechanism to the delta wing vortices creating high lift on airplanes."

There has been a number of well documented studies on conical vortices and the high suction pressures observed on flat low-rise buildings, including the following: Kind 1986, Mehta and Levitan 1992, Cochran and Cermak 1992, Milford et al. 1991, Tieleman et al. 1994, Lin et al. 1995, Kawai and Nishimura 1996, Lin and Surry 1998, Banks 2000, and Wu 2000.

Earlier investigations by several researchers have examined various techniques for roof pressure mitigation, such as: solid, partial and porous parapets, fences and spoilers, and curving or chamfering the roof edges. Surry and Lin (1995) suggested four categories of aerodynamic mechanisms for reducing high roof-corner suction pressures, which are as follows:

1. Full parapets to displace the vortices;
2. Partial or porous parapets to disrupt the formation of the vortices;
3. Porous fence, rooftop cylinders and splitters to disturb the vortices on the rooftop; and
4. Curved and rounded edges to eliminate the sharp edges that create the vortices.

The parapet can be used to lift the separated shear layers away from the roof surface.

Stathopoulos (1979) observed in his wind tunnel study of a low-rise building with 1.22 m (4 ft) high solid parapets around the perimeter that the mean pressure coefficients are higher than without the parapet, particularly at the corner areas. However, there was little change to the peak and root-mean-squared values. He also noted that previous studies by both Columbus in 1972 and Davenport and Surry in 1974 generally showed similar results. Melbourne (1980) measured pressure coefficients on the streamwise surface of a 114 x 57 x 57 mm (4.5 x 2.2 x 2.2 in) rectangular prism with and without an eave (sealed and slotted). He recognized that using devices such as a slotted eave have beneficial applications with regard to reducing loads on low pitched roofs of houses and other low-rise buildings. Lythe and Surry (1983), Stathopoulos and Baskaran (1987), Kind (1988) and Kareem and Lu (1992) investigated the effects of parapets and building height on wind-induced pressures on roofs. They found that low parapets on low buildings increase the magnitude of both peak and mean pressures in the corner regions. However, parapets generally can be used to reduce local high wind suctions, and therefore, parapets of a minimum height of 1.0 m (3.28 ft) are recommended.

Baskaran and Stathopoulos (1988) also performed a wind tunnel study on the influence of parapet configurations on roof suctions on flat roofs. The experiment determined that roof edge wind loads are generally reduced in the presence of parapets. In addition, they revealed that parapet configurations with cuts and slots may decrease the high suction loads. Following this, Stathopoulos et al. (1999) measured mean pressure coefficients on the flat roof corner of a full-scale low-rise building with and without parapets. Then a wind tunnel study was carried out, which showed that roof suction increases for a parapet height to building ratio of $0.01 < h/L < 0.02$.

Surry and Lin (2005) examined the effects of different parapet configurations on roof pressures on low-rise buildings; i.e., sawtooth partial parapets, porous parapets, and rooftop solid and porous splitters. They used a 1:50 scale model of the TTU experimental buildings and conducted the wind tunnel study at the Boundary Layer Wind Tunnel Laboratory, University of Western Ontario. They reported that all of the configurations adopted in the study reduced the high roof suctions at the corner and edges. However, the porous parapets resulted in the most significant reduction of up to 70% near the roof corner. Around the same time, Kopp et al. (2005) performed a study on alternative parapet geometries to alleviate area-averaged loads as a result of corner vortices. A summary of their conclusions is as follows:

1. A continuous solid parapet for small areas is better than keeping the corner open;
2. It is better to raise a solid parapet at the corner than to have a solid continuous parapet;
3. Using porous perimetric parapets or spoilers will reduce roof corner suctions; and
4. The least effective configuration is the single, isolated parapet.

More recently, Suaris and Irwin (2010) conducted a study on the effect of roof-edge parapets on a 1:20 model of a typical single-story home with a 3:12 roof slope. This study is significant as most of the previous mitigation studies were conducted on flat roofs. Moreover, using a 1:20 scale allowed for modeling of the roof eave conditions. It should also be noted that the previous studies were based on scaled models usually between 1:50 and 1:400. Another important detail of their study was that the height of the parapets was 0.2 m (8 in) in full scale. This parapet height is lower and more practical than was previously suggested. They concluded that the peak pressure coefficients in the corner region decreased over 50% with parapets along the perimeter. In addition, the perforated

parapets located at the roof corners and at the ridge generated about a 60% reduction in peak roof corner pressure coefficients.

Other techniques that have been studied to reduce roof suction pressures include modifying the roof edge and corner geometry and/or adding architectural elements to the building. Blackmore (1988) demonstrated the effects of chamfered roof edges on wind-induced loads on flat roofs. He found that chamfers effectively reduce the wind loads on flat roofs, with the 30° chamfer providing a 34% reduction of the overall design roof load. Robertson (1991) described the results of full-scale wind pressure measurements on the Silsoe Structures Building with a curved roof edge compared to the traditional sharp roof edge. The study showed that the curved roof edge reduced the high suctions at the lower region of the windward roof slope. However, the curved edge produced higher suctions over the roof ridge. As a precursor to their study in 1995, Lin and Surry (1993) explored the effects of different roof corner configurations; i.e., installing rooftop cylinders at a corner, placing partial parapets around the edge of the roof, and rounding the roof edge by attaching an edge plate. They determined that the round roof configuration provided the most reduction in high suctions on the roof. Wu (2000) and Banks (2000) introduced a conical vortex disrupter or spoiler as an effective mitigation device for reducing high suctions at the roof corner edges. The spoiler was 0.1 m (4.0 in) wide and 0.086 m (3.375 in) high with an 11° pitch. The spoiler was found to reduce mean pressure coefficients on the roof by up to nearly 50%.

Taher (2007) reported a “cyclone home” being studied by French wind engineering researchers at the Centre Scientifique et Technique du Bâtiment (Center for Building Science and Technology), CSTB, in Nantes, France. The home was designed with

specific aerodynamic features to reduce wind loads. The CSTB researchers recommended a maximum roof overhang of 50 cm (20 in), which should have a separate structural connection from the main roof structure. In addition, the home was designed for a "notched vertical frieze" at the roof eaves, which was installed along the roof edge. One other feature of the home was the central shaft, which provided a connection between the roof ridge and the interior space. As noted by Taher:

"This connection helps balance pressures between the home's exterior and interior leading to significant reductions in the roof's wind loads. The central shaft also creates a strong internal depression thus minimizing the risk of damage from suction forces."

Blessing et al. (2009) used the 6-fan Wall of Wind (WOW) to study the effectiveness of aerodynamic edge devices at full-scale and under hurricane force winds in reducing vortex-induced roof pressures at the corners and edges. Two different tests were conducted: a gravel scour test and pressure testing. The test building had dimensions of 3.05 m x 3.05 m x 3.05 m (10 ft x 10 ft x 10 ft). The results showed that no gravel scour occurred with the aerodynamic edge shapes. Furthermore, it was suggested that the tested aerodynamic edge shape products could provide a cost-effective method for wind damage mitigation on low-rise buildings. Most recently, Bitsuamlak et al. (2013) also utilized the 6-fan WOW to examine simple architectural devices that can be used to mitigate roof and wall corner suctions. The devices include: trellises or pergolas, gable end ribs (roof extensions to the gable ends), wall ribs (extensions to the walls), and ridge rib, a roof ridgeline extension. The testing was performed using a small-scale model of a residential villa with gable and hip roof geometries. The study concluded that the peak suction can be significantly reduced by the architectural devices.

In addition to the many studies done on mitigation techniques for wind-induced pressures on low-rise buildings, a number of investigations have been conducted on the effects of building length and height, roof slope and type, terrain roughness, and nearby structures on wind pressures on low-rise buildings. The following studies (Stathopolous 1979, Holmes 1983, 1994, Meecham et al. 1991, Meecham 1992, Gerhardt and Kramer 1992, Xu and Reardon 1998, Case and Isyumov, 1998, and Ginger and Homes 2003) reported that: wind loads increase with building height; length effects become significant for low-rise buildings with steep roofs and length-to-width ratios of greater than 3; roof type and slope have a considerable effect on the magnitude and distribution of wind loads; rougher terrain generally produces lower wind loads than smoother terrain; and nearby structures provide a shielding effect that is dependent on the ratio of building spacing to height. Further details of the effects of wind loads on low-rise buildings are reported in three available reviews of the state-of- the-art of wind loads on low-rise buildings; Holmes (1983), Stathopoulos (1984), and Krishna (1995).

Meecham et al. (1991) compared the aerodynamic performance of similar hip and gable roofs with a 4:12 pitch. They determined that the local peak negative pressures on gable roofs are almost 50% higher than on hip roofs with the same wind speed and similar geometry. Additionally, Xu and Reardon (1998) found that for a roof pitch of 30°, both gable and hip roofs have similar peak suction coefficients. More recently, Gavanski et al. (2013) conducted a study on wind loads on roof sheathing of typical low-rise houses. A number of parameters were considered, which included; roof shape (hip and gable), roof slope (4:12 to 7:12, 9:12 and 12:12), building height (1-story, 2-story, and 3-story), upstream terrain (open and suburban), wind direction and the presence of

surrounding structures. The experiments were performed in the boundary layer wind tunnel II at the University of Western Ontario. The study concluded that roof shape and upstream terrain have the most significant effect on wind loads acting on roof sheathing. Moreover, lower roof sheathing loads were observed for the houses with hip roofs in suburban terrain.

A Review of Internal Pressures in Low-Rise Buildings

A detailed review of internal pressures in low-rise buildings was provided by Oh et al. (2007). In addition, a study was also conducted by Oh et al. (2007) on wind-induced internal pressures in a low-rise building. This study was Part 3 of a series of wind tunnel tests involving low-rise buildings that were performed at the University of Western Ontario (UWO) for contribution to the National Institute on Standards and Technology (NIST) aerodynamic database. The model building was constructed with one rectangular opening, which was the "large" opening representing 3.3% of the single wall area, and there were two circular openings used for the smaller openings, which represented 0.3% of the single wall area. Uniform background leakage was also provided by 80 small holes. Only one dominant opening was open at a time; however, the background leakage was always open. Additionally, measurements were taken for open country and suburban terrain conditions. The study concluded that external pressure fluctuations are dramatically attenuated for buildings with leakage only. The suburban terrain produced higher peak and root-mean-square internal pressure coefficients for all opening cases. Peak internal pressures occured for the wind direction normal to the wall

with the dominant opening. Helmholtz resonance (response of small volumes to the fluctuating external pressures) occurs for a single centrally located opening with background leakage (Holmes 2007). It was also found that the peak internal pressure coefficients exceed the values which are provided in ASCE 7-02 and other standards.

Shortly thereafter, Kopp et al. (2008) further studied wind-induced pressures in a 1:50 model-scale two-story, gable-roofed house using the Boundary Layer Wind Tunnel II at UWO. The effects of ten different opening configurations were investigated including: the size and locations of dominant openings, wall leakage, horizontal compartmentalization of the attic space from the living space, and ridge and soffit vents. The total uniform background leakage area was 0.1% of the total area of the four walls. This was the same value that was used by Oh et al. (2007), which is consistent with typical values of well-built wood frame houses. The investigation concluded that horizontal compartmentalization such as a ceiling can be used to reduce loads on roof sheathing. A ceiling with an opening of only 0.4% of the attic floor area transmitted 80% of the peak pressures into the attic space from the living space. In addition, they found a strong correlation between the peak external roof pressures and the internal pressures. When the dominant open area is larger than 2 m^2 for an internal volume of around 700 m^3, Helmholtz resonance will begin. The experiment also showed that reducing the ratio of the internal volume to the area of the dominant opening increased the peak internal pressures by enhancing Helmholtz resonance for wind directions normal to the opening. Kopp et al. (2008) also revealed that when the internal pressure is due exclusively to the venting provided at the soffit and ridge vents, the maximum pressures range from -0.2 to 0.1. In addition, it was evident that the roof vents allowed relief of the positive pressures.

More recently, Tecle et al. (2012) studied how building envelope openings and compartmentalization affect the wind pressure in low-rise buildings with hip and gable roofs. The 6-fan Wall of Wind was used to examine wind-induced internal and external pressures on a test building with two interchangeable roofs. The model building had the following features: doors and windows (multiple dominant openings), soffit vents, roof turbine ventilators, a gooseneck roof vent, and horizontal and vertical compartmentalization (ceiling and wall). The study assessed internal pressures due to size and location of dominant openings, background leakage, and compartmentalization. The experiment showed that peak positive internal pressures occurred when the dominant opening was perpendicular to the direction of the wind and peak negative internal pressures occurred when the opening was parallel to the wind approach flow. Thus, internal pressure intensity is due to the amount, size, and location of openings with respect to the direction of the wind flow. There were increases in negative and positive pressures due to the presence of the roof vents. In addition, compartmentalization had a significant effect on the intensity of internal pressures. Moreover, the peak internal pressure for the gable attic was 190% higher than the values recorded for the hip attic.

A number of earlier studies on internal pressures were performed as well. Holmes (1979) investigated mean and fluctuating internal pressures in low-rise buildings using a boundary layer wind tunnel. The measurements were observed on a 1:50 scale model of a two-story house with a single dominant opening on the windward wall. The experiment showed that mean and root-mean-square fluctuating internal pressures increased with an increase to the ratio of windward open area to the leeward open area. In addition, Holmes reported that resonance effects on the fluctuating internal pressures were present for the

single dominant opening.. Stathopoulos et al. (1979) performed a wind tunnel study on three 1:250 scale models with uniform porosities of 0, 0.5% and 3.0% of the total surface area to examine wind-induced internal pressure characteristics of low-rise buildings. The models had wall openings that ranged from 0 to 100% of the wall's area. The study concluded that there was a strong correlation between external and internal pressures and that the largest internal pressures occurred when dominant openings are perpendicular to the wind direction. Moreover, internal pressure fluctuations showed very little spatial variation. In their evaluation of internal pressures of multi-room buildings, Saathoff and Liu (1983) stated that peak internal pressure resulting from a sudden opening will increase with the increase in opening area and reduction in internal volume. Furthermore, as the area of the dominant opening increases and the internal volume decreases, the frequency of oscillation of internal pressure will also increase. Stathopoulos and Luchian (1989) conducted a wind tunnel experiment to examine the transient response of wind-induced internal pressures in buildings. They concluded that under steady-state conditions higher internal pressure peaks have been measured compared to the transient peaks that were recorded in their experiment. Vickery and Bloxham (1992) also examined the transient and steady-state conditions of internal pressure following a sudden breach in a building. The effect of background leakage was found to be of little consequence for buildings with a single dominant opening and a leakage area of less than 10% of the main opening. A study on internal pressures and the significance of dynamic action on peak loads across a building envelope was conducted by Vickery (1994). He investigated a building with a dominant opening and no background leakage and another that was sealed with background leakage. Vickery reported that a dominant opening can

increase the differential load on elements in the leeward area of the building by a significant amount. Another study on the effect of dominant openings and porosity on internal pressures was performed by Woods and Blackmore (1995). They found that the mean internal pressure is similar to the external pressure at the single dominant opening. Womble et al. (1995) performed a comparative study on internal pressures using a wind tunnel test on a model-scale of the Texas Tech University (TTU) building. Building porosity, internal volume, turbulence intensity, building height, and dominant openings were all found to be important factors for internal pressure effects in low-rise buildings. Ginger et al. (1997) and Ginger and Letchford (1999) studied internal and net pressures on the low-rise full-scale building at TTU. Sharma and Richards (2003) examined the effects of Helmholtz resonance on internal pressures for oblique wind directions on a 1:50 scale model of the TTU building. In addition, Sharma and Richards (2005) investigated net pressures on the roof of a low-rise building with dominant openings.

Roof Vents and Soffits

Roof vents are commonly found on residential structures to provide natural ventilation of the attic space, allowing air to flow into and out of the attic. There are a number of devices that can provide roof attic ventilation, including: soffit vents, ridge vents, gable end vents, and turbine ventilators. In warm climates or on hot summer days, heat and moisture can build up in the attic space, which can contribute to the deterioration of the building materials. In addition, the heat in the attic space can be transferred to the living space below. Therefore, proper ventilation of attics can: 1) promote the health and longevity of the structural timber framing and other materials, and 2) maintain

comfortable temperatures inside the building, while increasing energy efficiency and sustaining indoor air quality (Gan Chowdhury et al. 2010).

The typical attic natural ventilation process for low-rise residential buildings is simply the changing of air in the attic space. The ridge vent which is installed at the roof ridge is for the benefit of the stack effect. When the temperature in the attic is greater than the outside temperature, the warm indoor air will rise and exit through the ridge vent, and cooler, denser air through the soffit vents will replace the escaping warmer air. Wind-driven ventilation will enhance this process, providing a continuous air exchange.

Boulard and Bailey (1995) conducted a study for predicting natural ventilation with continuous vents. They derived several models of air exchange rates in a greenhouse and found that the wind was the main driving force of ventilation and the air exchange rate appeared to be mainly dependent on the wind turbulence. Breeze (2003) performed experiments at the British Research Establishment (BRE) to investigate the aerodynamic performance and water-tightness of pitched roof vents (PRVs). The PRVs can be used to draw in fresh air and extract the air inside the building back into the atmosphere. Katsoulas et al. (2006) experimentally investigated the effect of vent openings and insect screens on greenhouse ventilation. They determined that the use of the anti-aphid screen (55 x 27 mesh size and 50% porosity) reduced the greenhouse ventilation rate by 33%. Grant et al. (2007) tested the performance of a new omnidirectional roof vent using a wind tunnel. The vent has no moving parts; however, it uses the wind flow to create a low pressure zone inside the vent base.

Vickery (2008) studied the component and cladding wind loads for soffits. Wind tunnel tests were conducted on 1:50 scale models of one, two, and three-story buildings with hip and gable roofs. The experiments measured wind induced pressures on the soffits, walls and roof surfaces for the buildings in both open and suburban terrains. It was concluded that wall and soffit pressures are highly correlated, thereby suggesting that both the positive and negative pressures used for the component and cladding loading should be identical for the design of soffits.

Roof soffit vents generally respond poorly to hurricane winds, which can drive large amounts of water through the vents. Once the water enters the attic space, it accumulates, soaking the insulation and gypsum board. Water entry by wind-driven rain can lead to mold growth and even full collapse of the ceilings. In addition, vinyl and aluminum soffit panels are usually blown off during a hurricane, increasing the potential for water intrusion (FEMA 2010). If the soffit material is not properly connected to the roof framing, it can be removed by the high suctions generated around the building corners during a hurricane.

Jesteadt et al. (2007) conducted a preliminary investigation into wind-driven rain (WDR) intrusion through six soffit systems. The six systems included: a hidden vent vinyl soffit, a perforated vinyl soffit, a perforated aluminum soffit, two hybrid perforated soffits, and a custom soffit. The portable 2-fan Wall of Wind was used as the wind-driven simulator. They found that the perforated vinyl soffit supplemented by an insect screen outperformed the other soffit systems. Gan Chowdhury et al. (2010) studied roof vents subjected to simulated hurricane effects using the 6-fan WOW. They examined the vent performance with wind-driven rain and recorded pressure differentials. The study

demonstrated that the increase in water intrusion with higher positive differential pressure across the vent appears to be affected by the vent mechanism and different wind angles of attack.

Quarles et al. (2012) performed a full-scale study at the Insurance Institute for Business & Home Safety (IBHS) Research Center to evaluate water entry into the attic through gable end and soffit vents and through a sealed and unsealed roof deck. The water intrusion through the vents was evaluated using up to three wind exposures and a target rain deposition rate of 8 inches per hour. A perforated vinyl soffit was used in the study. The experiment compared the vinyl soffit performance with an open soffit. The results showed that a wind speed of 31.3 m/s (70 mph) produced a water intrusion rate of 18.5 mm/hr (0.73 in/hr) for the vinyl soffit. This was compared to a water intrusion rate of 74 mm/hr (2.9 in/hr) for the open soffit at the same wind speed.

Masters and Kiesling (2012) investigated the wind load resistance, air permeability and wind-driven rain resistance of aluminum, vinyl, fiber cement board, oriented strand board (OSB) and stucco vented soffits. However, the main focus of the study was the structural resistance of the panel system as soffit blow out/in is a major concern for water entry into the attic space. There were both straight and corner sections with two overhang lengths of 12 in and 24 in. They reported that the OSB and stucco soffits performed best, followed by the fiber cement board soffit. The vinyl and aluminum soffits generally performed poorly. In addition, they found that the corner sections are more susceptible to wind loading than the straight sections and that the 24 in overhang soffits fail at lower pressures compared to the 12 in soffits.

CHAPTER III

THEORETICAL BACKGROUND

Wind Flow Characteristics on Low-Rise Buildings

Since the majority of low-rise buildings are not streamlined, they are considered "bluff bodies" in traditional aerodynamics. The term 'bluff' is an aerodynamic term which is used to describe blunt or sharp-edged obstacles, such as buildings, whereas an airfoil is an example of a streamlined body. The flow around a bluff body, such as a cube type building forms complex three-dimensional flow phenomena. There is flow separation from the building surface, possible reattachment downwind from the sharp edges, and horseshoe vortex formation as the downward flow interacts with the separated flow. In addition, the flow separation produces a wake on the leeward section of the building, which will reattach downstream (ASCE 2012). The perspective of the flow field around a cubic-like building is illustrated in Figure 3-1.

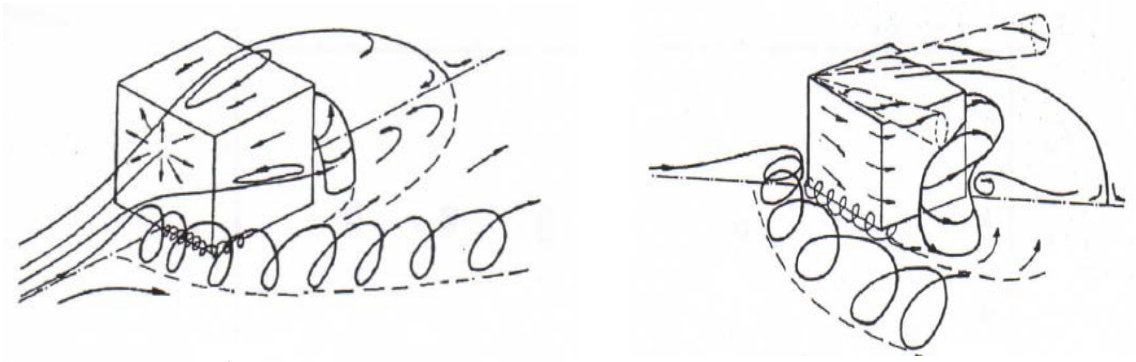

a) b)

Figure 3-1. Perspective of the flow field around a cube for: a) θ=0°; b) θ=45° (Borges 1998)

Peterka et al. (1985) reported that the flow separation location is dependent on the building's height-to-width ratio, height-to-boundary-layer-height ratio and the upstream surface roughness. In addition, flow reattachment depends on the building's length-to-width ratio, height-to-length ratio and upstream roughness. The upstream roughness, which determines the turbulence intensity in the approaching wind, is a significant factor with regard to distance to reattachment. If reattachment does not occur, a separation cavity forms at the top, sides and rear of the building as shown in Figures 3-2 and 3-3. It will require a good distance downstream for the flow to recover to the approach flow characteristics and for disrupting effects of the building to diminish.

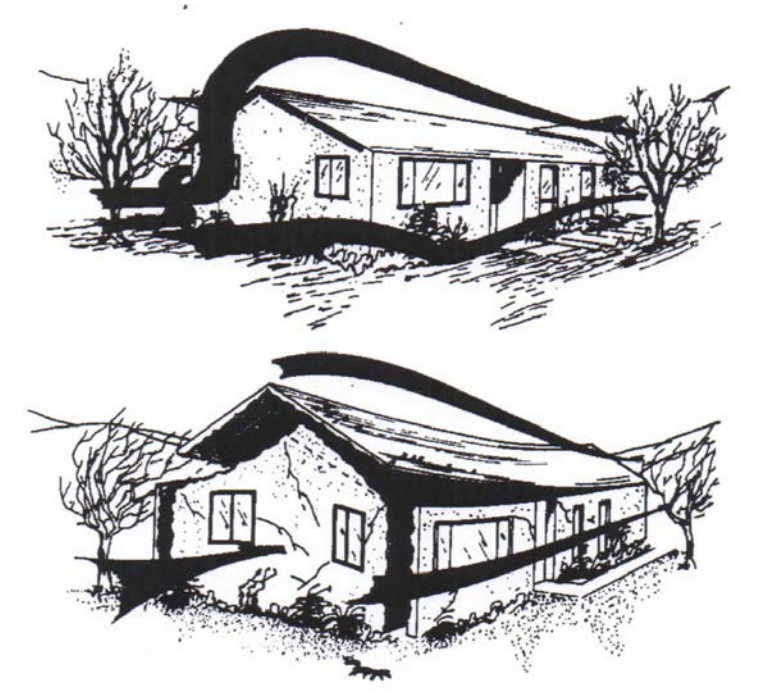

Figure 3-2. Overall wind effects on a low-rise building (Minor and Mehta 1979)

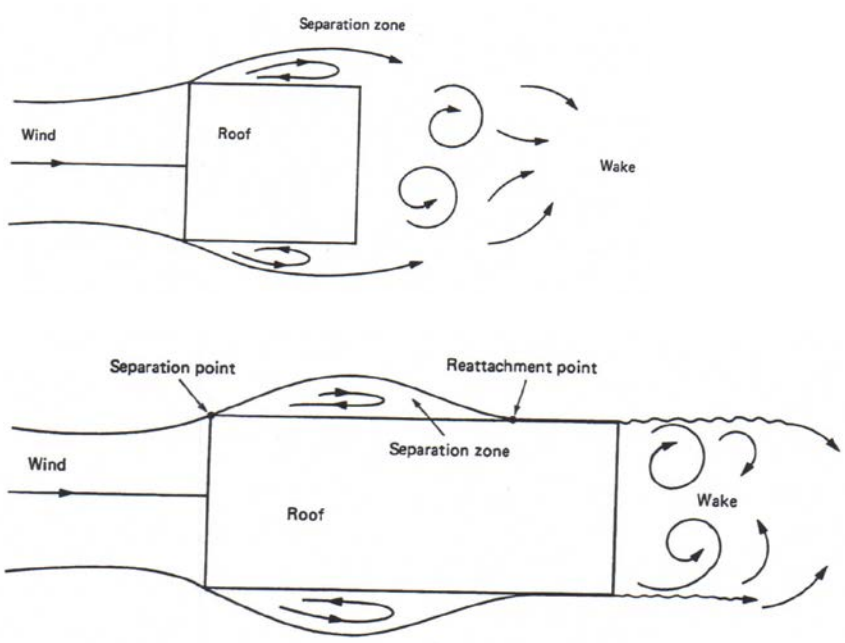

Figure 3-3. Separation and reattachment of flow along a short and long building (Liu 1991)

The wind flow field can be divided into three flow regions: the freestream flow, shear layers, and wake flow. The freestream flow is the flow immediately ahead of and outside of the bluff body. In this region, the Bernoulli equation is valid. When there is boundary layer separation at a sharp edge, it becomes a free shear layer which separates the freesteam flow from a wake. The wake flow region develops behind a separating shear layer and contains vortices that have a lower velocity compared to the freestream flow (Aynsley, Melbourne and Vickery 1977).

There are two important factors that must be considered for the assessment of wind flow characteristics for low-rise buildings. The first is that low-rise buildings are usually immersed within the layer of aerodynamic roughness on the earth's surface, the Atmospheric Surface Layer (ASL), which is the lower part of the Atmospheric Boundary

Layer (ABL). Here turbulence effects are significant, which will affect the wind loadings. Secondly, the roof loadings are most important for low-rise buildings with the amount of variations and changes in geometry. The most severe loadings generated on the surface of low-rise buildings are typically the separation zones, specifically high suctions on the roof. However, one of the major benefits of low-rise buildings is that inertia loading (i.e. dynamic effects) due to wind can usually be neglected (Holmes 1983, 2007).

The atmospheric turbulence or 'gustiness' has a major influence on the wind-structure interaction. In particular, the wind flow around low-rise buildings. The Longitudinal (x-direction) turbulence is described as fluctuations in wind velocity in the wind field (mean wind) direction. The main descriptors of atmospheric turbulence are (Holmes 2007, Gan Chowdhury et al. 2009 and ASCE 49-12):

- *Integral (Macro) Length Scale*, a measure of the average size of eddies or gusts present in the atmospheric boundary layer;
- *Longitudinal Turbulence Intensity,* the ratio of the standard deviation of the longitudinal fluctuating component to the longitudinal mean wind speed at elevation, z;
- *Turbulence spectra,* estimates the frequency content of the wind speed fluctuations; and
- *Cospectra,* an indication of the level coherence of wind fluctuations with various frequencies at different points in space.

It has been well documented that the high frequency or small scale turbulence production is important for aerodynamic testing of low-rise buildings. Typical bluff body aerodynamic phenomena such as, flow separation at wall and roof edges, and the

formation of conical vortices at roof corners, which cause negative pressures, are affected by the small scale turbulence. Large-scale turbulence, however, does not have a significant impact on the aerodynamic phenomena for low rise buildings, except for enhancing the sustained wind speed (Fu 2013).

Wind-induced loads on the roof and walls of a low-rise building depend mainly on the interaction of the wind flow with the building's envelope. The wind flow characteristics and the building's geometry are the two main factors to consider in the wind and building interaction. When the wind approaches and collides with a low-rise building square-on, the freestream path is blocked, forming a stagnation region. There is a consequent build-up of positive pressure against that face of the building and the wind has to change its path to accommodate the building's geometry. The flow then moves outward to all the edges on the windward wall. The deflected flow accelerates around the side walls and over the roof, producing separation zones, resulting in a reduction of pressure, thereby, exerting suction on these areas. In addition, a suction force is produced on the rear face of the building as a result of the low pressure region formed by the wake.

The roof pitch also has an effect on wind-induced pressures on low-rise buildings. The pressure exerted on the roof facing the direction of the wind field is dependent on the roof pitch. A roof pitch less than 30° will be subject to suction, whereas steeper roofs having an angle greater than 35° will develop positive pressure on the windward slopes. However, there is the separation zone near the roof ridge where suction develops. When the wind direction is parallel to the roof's ridge, the roof pitch will have no major impact on the wind behavior. The roofs are affected by suction at their windward edges and at the leeward slopes. The roof soffits (eaves) will be affected by the upward deflection of

the wind field by the windward wall. Thus, additional positive pressure will be exerted on the underside of the roof overhang, whereas the soffits will experience suctions in the separation zones, which often results in soffit failure during hurricanes.

Wind-Induced Pressures on Buildings

The flow around low-rise buildings produces pressure distributions on the surface of the building. In order to mitigate wind damage on low-rise buildings, it is very important to know the wind-induced pressure distributions. The distribution of positive and negative external pressures is generally not uniform. The pressure at the center of the windward wall is typically the largest and will then decrease towards the windward wall edges. The greatest negative pressure is generated at the separation zones. When the wind is at a 45° angle of attack to the building, a pair of strong conical vortices will form. These vortices will develop at the roof corner and travel along the concurrent edges at shown in Figure 3-4. The conical vortices will produce very high suctions at the roof corners.

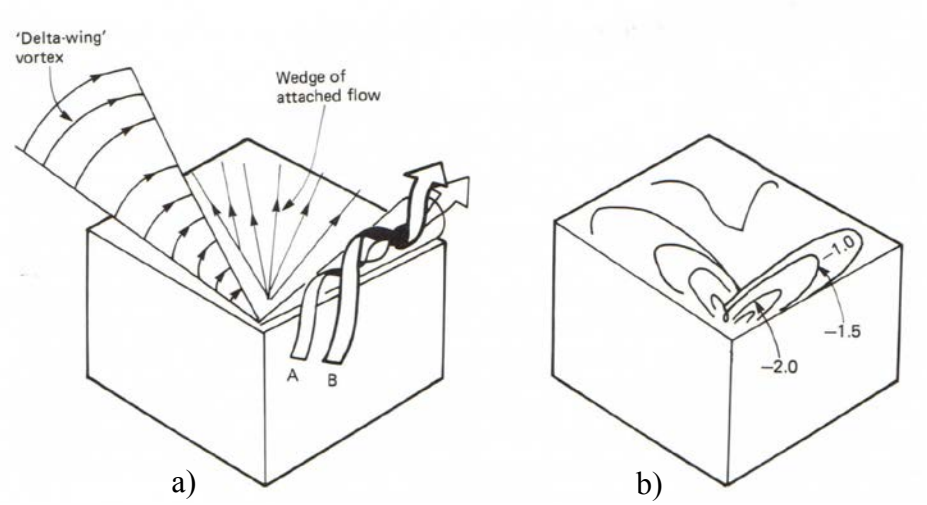

Figure 3-4. Conical vortices at the roof corner: a) flow structure; b) pressure distribution (Cook 1985)

Figure 3-5 shows the basic characteristics of steady flow around a rectangular building. As previously mentioned, the flow separates and forms an outer flow where there is no viscosity effect and an inner flow, the wake region. The shear layer separates the outer and inner flow regions. It is only in the outer region of the bluff-body flow where Bernoulli's equation is valid, where ideal conditions of steady, inviscid (zero viscosity) and irrotational (zero vorticity) flow exist. The flow velocity, *V* produces a pressure, *P* and for a horizontal flow Bernoulli's equation is as follows:

$$P + \frac{1}{2}\rho V^2 = \text{a constant} \tag{3.1}$$

where ρ is the air density. The second term is known as the dynamic pressure.

The surface pressure on a bluff-body is typically expressed in the form of a non-dimensional pressure coefficient to be independent of velocities. The pressure coefficient, C_p is stated as:

$$C_p = \frac{\Delta P}{\frac{1}{2}\rho Vo^2} \tag{3.2}$$

where ΔP is the wind induced pressure that is either above or below the ambient atmospheric pressure. Equation 3.2 can be rewritten as follows:

$$C_p = \frac{\Delta P}{\frac{1}{2}\rho Vo^2} = \left[1 - \left(\frac{V}{Vo}\right)^2\right] \tag{3.3}$$

where *Vo* is the velocity in the region outside the influence of the body.

Therefore, at the stagnation point where V=0, Equation 3.3 gives a pressure coefficient of +1. Moreover, on the windward sides of the building, C_p will have positive values, close to one and negative values when V > Vo (roofs and sides of buildings). When V=Vo in the freestream, C_p=0 (Holmes, 2007, Stathopoulos, 2007). Figure 3-6 shows the flow in the wake of a building and Figures 3-7 and 3-8 illustrate the pressure distribution on a low-rise building and on hip and gable roofs respectively.

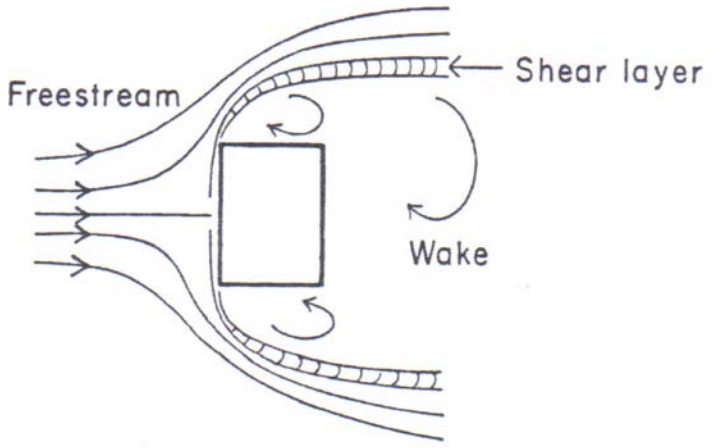

Figure 3-5. Three regions of the flow field around a building (Aynsley, Melbourne and Vickery 1977)

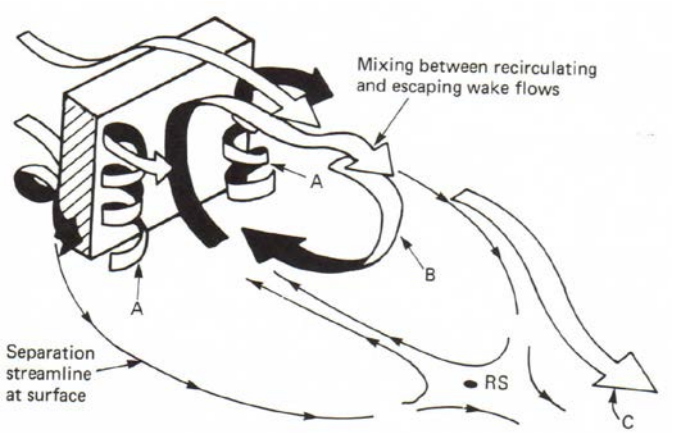

Figure 3-6. Flow in the wake and rear stagnation point, RS (Cook 1985)

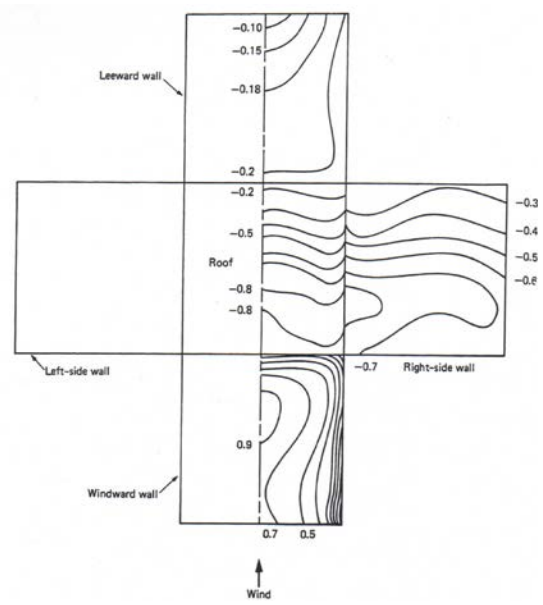

Figure 3-7. Mean pressure distribution for a low-rise building with a flat roof in boundary-layer wind (Liu 1991)

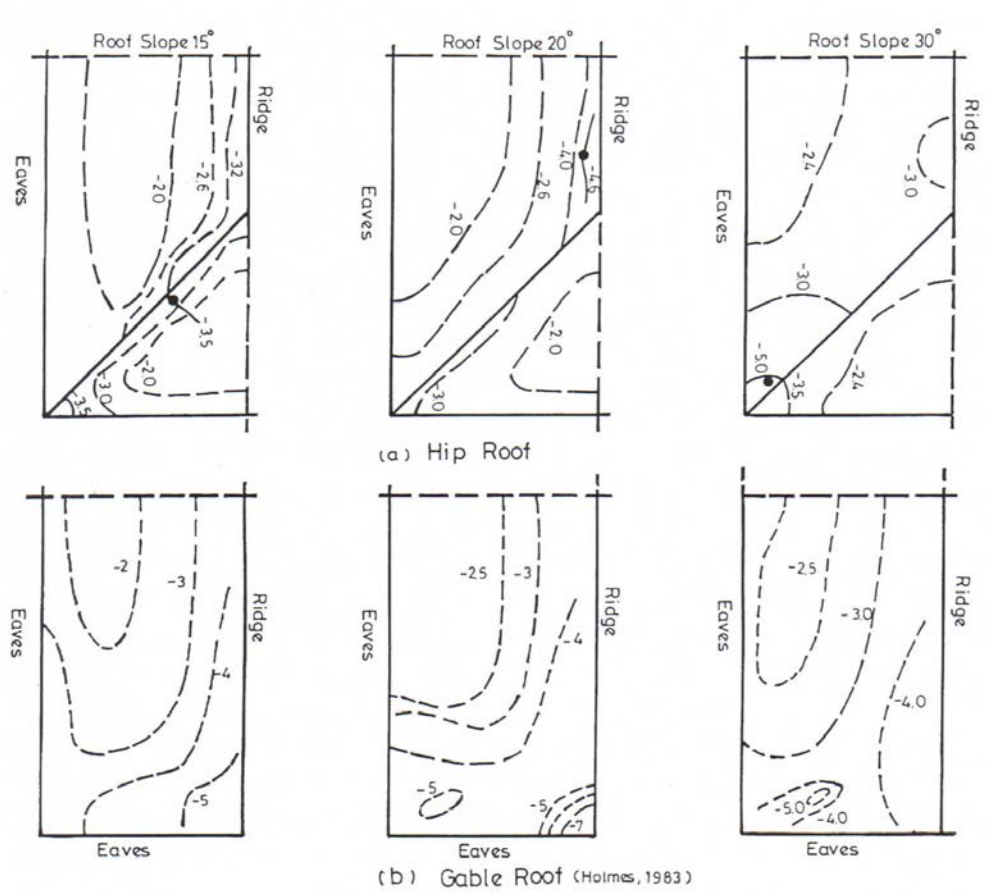

Figure 3-8. Hip and gable roofs comparison of peak suctions (Xu and Reardon 1998)

CHAPTER IV

WALL OF WIND FACILITY

The Wall of Wind (WOW) facility can produce a wind field which is approximately 6.1 m wide by 4.3 m tall (20 ft x 14 ft), with variable wind speeds from 6.7 m/s (15 mph) up to Category 5 hurricane wind speeds (over 155 mph). The 12 fans are arranged in a two-row by six-column array as shown in Figure 4-1. The fans are driven by 3-phase electric motors, 700 hp each (8400 hp combined), and their rotation speeds are controlled by variable frequency drives. Each fan has a maximum flow rate of 240,000 cubic feet/minute with a total pressure head of 15 in. H_2O. The contraction section maintains a uniform flow field, achieving the mean wind speed up to 72 m/s (161 mph) at approximately 2.6 m (8.5 ft) above the ground. In addition, a set of vertical flow directing vanes located at the exit of the contraction section guides the air flow in the longitudinal direction.

The desired atmospheric boundary layer is developed in the 9.75 m (32 ft) long flow simulation box, which is positioned downwind of the contraction zone (Figures 4-2 and 4-3). This region provides the required fetch length and consists of triangular spires and blocks representing floor roughness elements. A small-scale (1:15) version of the 12-fan Wall of Wind was used to establish the appropriate shape and size of the spires and floor roughness for both suburban and open terrain wind profiles (Baheru et al. 2014, Aly et al. 2011).

Figure 4-1. The 12-fan Wall of Wind (WOW) facility in Miami, Florida

Figure 4-2. The WOW flow chamber with four spires and floor roughness elements

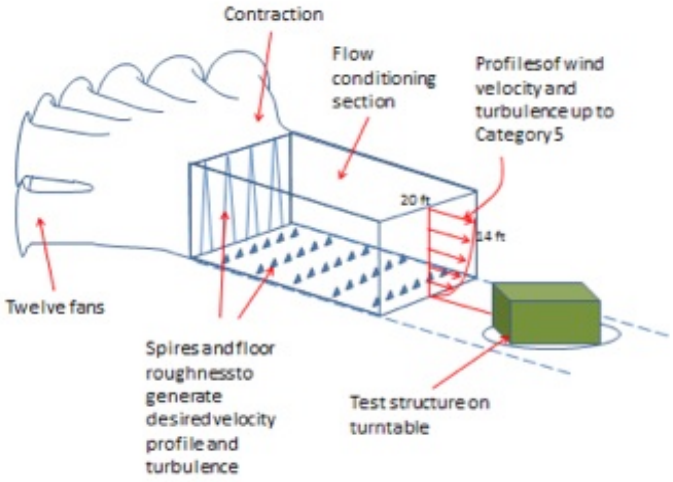

Figure 4-3. Wall of Wind configuration (https://wow.fiu.edu/about/technical-aspects-of-the-wall-of-wind)

For all of the studies conducted in this dissertation, the Wall of Wind was configured for an open terrain mean wind profile. In order to obtain the velocity profile measurements of the flow field, a movable frame was constructed over the area where the test structure would be mounted. Cobra probes were arranged vertically at various heights above the WOW floor on the frame capturing the flow velocity components in the three major (x, y and z) directions. The corresponding turbulence intensities were also determined from the velocity measurements. The Cobra probes measured the flow field characteristics using a sampling frequency of 100 Hz. In addition, wind speeds and their corresponding WOW throttle setting were measured specifically at the proposed roof eave height of 1.27 m (50 in) for the test structure (Figure 4-4). The non-dimensional spectrum of longitudinal turbulence was measured at the roof eave height for the 1:6

model scale test building in the WOW and normalized with respect to the mean velocity (Figure 4-5).

Figure 4-4. Cobra probe and frame, set at the roof eave height (1.27 m) to record freestream data

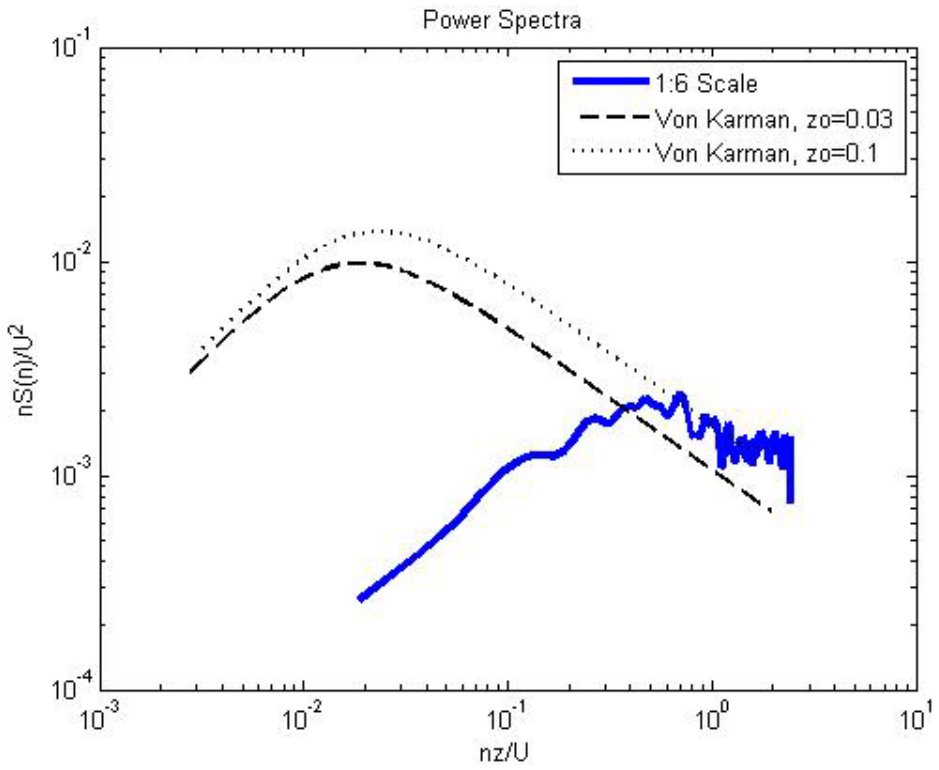

Figure 4-5. Comparison of the measured WOW spectrum with the Von Karman spectrum

Figure 4-5 illustrates that the higher end of the spectrum, i.e. components with non-dimensional frequencies nZ/U greater than 10^{-1} (n = frequency, Z = height above the surface, and U = mean wind speed of turbulent flow averaged over 10 min or 1 hour) compared well with the Von Karman Spectrum. However, there is a clear discrepancy in the lower frequency part of the spectrum as one issue with large-scale model testing is the difficulty of appropriately simulating the low-frequency content of the turbulence spectrum.

For small structures, such as low-rise residential buildings, it is more appropriate to use large model scales, i.e. 1:6, in order to obtain suitable geometric accuracy, maintain resolution of pressure measurements, and minimize Reynolds number effects.

The small turbulence eddies, which correspond to the high frequency end of the turbulence spectrum, can be well simulated in the WOW facility for large model scales, as shown in the plotted spectrum (Figure 4-5), although it is not possible to simulate the large scale turbulence eddies, which correspond to the low frequency end of the turbulence spectrum (Irwin 2015).

It is the small scale turbulence that influences the local aerodynamics of shear layers and vortices around the structure; therefore, suitable data can still be obtained despite the deficiency of large scale turbulence eddies. Moreover, the accurate simulation of high frequency turbulence is necessary for properly modeling flow separation and reattachment (Mooneghi et. al., 2015). The large scale, low frequency turbulence will typically affect variations in mean wind speed and direction only. Thus, for this type of study it is reasonable to match the turbulence spectrum at the high frequencies only. Furthermore, the role of the large scale turbulence can be incorporated into the wind loads using the quasi-steady assumptions, whereby peak pressures are predicted by using mean pressure coefficients with a peak gust wind speed. This is the 'Partial Turbulence Simulation' approach (Mooneghi et. al., 2015, Irwin 2015, Holmes 2007).

Partial Turbulence Simulation

As outlined in *ASCE 7-10, 31.2*, there are seven conditions that are required for wind tunnel or similar tests for determining mean and fluctuating forces and pressures for buildings or structures. Kopp and Banks (2013) divided these seven requirements into four groups, which include: the correct modeling of the approach flow (mean wind speed and turbulence profiles and the longitudinal turbulence spectrum), modeling the test

building and surroundings correctly, ensuring that the wind tunnel walls are accounted for, and the use of proper instrumentation. For the WOW, special attention is given to the second requirement in *ASCE 7-10, "The relevant macro- (integral) length and micro-length scales of the longitudinal component of atmospheric turbulence are modeled to approximately the same scale as that used to model the building or structure."* However, as previously mentioned, one of the difficulties associated with large-scale testing is effectively simulating the low frequency content of the turbulence spectrum; in particular, the integral length scale parameter. To alleviate this limitation, a partial turbulence simulation method has been developed for the WOW. This method ensures that the high frequency portion of the WOW turbulence spectrum matches the high frequency portion in the atmospheric boundary layer (ABL) spectrum.

In addition, it is also important to note in the ASCE Standard, *ASCE/SEI 49-12*, *"If the partial ABL simulation is deficient in similarity, (for example, missing spectral content at the low frequency end of the spectrum), then any additional interpretation of the data shall refer to recognized literature for methods to make corrections."* Therefore, the code recognizes that there will be scenarios when it is necessary to modify the macro-(integral) length scale requirements; however, an appropriate method of correction must be used. Thus, the partial turbulence simulation method developed for the WOW works within the guidelines of the above-mentioned standard.

The Partial Turbulence Simulation (PTS) has been used for the testing in this dissertation. According to Mooneghi et al. (2015), "*In the PTS method, the wind tunnel tests focus on achieving a good match of the high frequency part of power spectrum. The effects of the missing low frequency turbulence (including the longitudinal, lateral and*

vertical components) are then included in post-test analysis using the quasi-steady approximation." The guidelines for a PTS study at the Wall of Wind are outlined by Irwin (2015).

Velocity and Sampling Time

In order to simulate an open terrain condition in Miami, the 3-second gust wind speed for Miami-Dade County of 78.2 m/s (175 mph) would be used for open terrain at 10 m (32.8 ft) above the ground. Residential low-rise structures would fall under Risk Category II, which corresponds to a Mean Recurrence Interval (MRI) of 700 years. For Risk Category II structures, the probability of being exceeded in an average 50-year period is around 7%. Therefore, the probability of being exceeded in any one year would be 0.07/50 = 0.0014 (0.14%). This gives a 1/0.0014 or 700-year MRI (Simiu 2011, ASCE 7-10).

The WOW velocity scaling is based on the mean hourly wind speed, U. Therefore, converting the 3-second gust wind speed to the corresponding mean hourly wind speed over open terrain is accomplished by dividing the 3-second gust by a factor of 1.52. Thus, the mean hourly wind speed would be 78.2 /1.52 = 51.4 m/s (115 mph). The power law can be used to calculate the corresponding wind speed at the roof eave height at full scale, 7.62 m (25 ft). Using the power law exponent of 0.154, the wind speed is calculated to be 49.3 m/s (110 mph) at Z=7.62 m, the prototype roof eave height.

All tests were run at 25.67 m/s (57.44 mph) wind speed at roof eave height, with a model scale of 1:6. Therefore, the corresponding wind speed is 33.8 m/s (75.6 mph) at

the prototype roof eave height. The equivalent 3-second gust wind speed is 39 m/s (87 mph) at the model scale roof eave height and 51.4 m/s (115 mph) at the prototype roof eave height, which are classified as Category 1 and Category 2 hurricanes respectively in the Saffir/Simpson Hurricane Scale (*ASCE 7-10, Table C26.5-2*).

Wall of Wind Scaling Parameters

From Engineering Science Data Unit (ESDU) 85020, it can be estimated that at full scale at roof eave height, the longitudinal integral length scale of turbulence is 95 m (312 ft) and the turbulence intensity is 0.17. The test building is at 1:6 model-scale and the mean wind speed at roof eave height used for testing is 25.67 m/s (57.44 mph). The integral length scale of turbulence in the WOW is 0.4 m (1.31 ft) at roof eave height.

Equations 4.1 to 4.14 are set out by Irwin (2014). When the low frequency turbulence is missing from a wind simulation, the aim is to ensure that the kinetic energy of the high frequency turbulence per unit frequency is in the correct ratio to the kinetic energy of the mean wind. This is possible if the non-dimensional power spectra, $nS_u(n)/U^2$ is the same for high frequencies in the scale model tests as in the full scale wind (Irwin 2014). Therefore, at high frequencies,

$$\frac{n_m S_u(n)_m}{U_m^2} = \frac{n_p S_u(n)_p}{U_p^2} \tag{4.1}$$

where n is the frequency, $S_u(n)$ is the spectral density of the u-velocity component and U is the mean wind velocity. The subscripts m and p represent model scale and prototype values respectively. The Von Karman spectrum can be described by:

$$\frac{nS_u(n)}{\sigma_u^2} = \frac{4\frac{n^x L_u}{U}}{\left(1+70.78\left(\frac{n^x L_u}{U}\right)^2\right)^{5/6}} \tag{4.2}$$

where σ_u^2 is the variance of turbulence and ${}^xL_u$ is the longitudinal integral scale of turbulence. At high frequencies, the Von Karman spectrum can be written as follows:

$$\frac{nS_u}{U^2} = \frac{4I_u^2}{70.78^{5/6}\left(\frac{n^x L_u}{U}\right)^{2/3}} \tag{4.3}$$

where I_u is the total turbulence intensity.

The non-dimensional frequency, nb/U must also match at the model and prototype scale. Therefore,

$$\frac{n_m b_m}{U_m} = \frac{n_p b_p}{U_p} \tag{4.4}$$

where b is the reference dimension, such as the building width for the model and prototype.

Equations 4.1, 4.3 and 4.4 are combined to produce,

$$\frac{I_{um}}{\left(\frac{xL_{um}}{b_m}\right)^{1/3}} = \frac{I_{up}}{\left(\frac{xL_{up}}{b_p}\right)^{1/3}} \tag{4.5}$$

which can be arranged as follows:

$$\frac{I_{um}}{I_{up}} = \left(\frac{xL_{um}}{xL_{up}}\right)^{1/3}\left(\frac{b_p}{b_m}\right)^{1/3} \tag{4.6}$$

Equation 4.6 can be used to determine the desired turbulence intensity on the model. Thus, for this WOW testing, the ratio of model turbulence intensity to prototype turbulence intensity is:

$$I_{um} = 0.17\left(\frac{0.4}{95}\right)^{\frac{1}{3}}(6)^{\frac{1}{3}} = 0.05$$

The value calculated in Equation 4.6 can be added to Equation 4.7 as I_{um} is assumed to match $I_{uH,}$ the turbulence intensity of the partial turbulence simulation (high frequency intensity):

$$I_{uL} = \sqrt{I_u^2 - I_{uH}^2} = \sqrt{0.17^2 - 0.05^2} = 0.162 \tag{4.7}$$

where I_{uL} is the missing low frequency turbulence intensity. However, the turbulence intensity of the WOW partial turbulence simulation was measured as 0.074 at roof eave height. Therefore,

$$I_{uL} = \sqrt{0.17^2 - 0.074^2} = 0.153$$

According to Irwin (2015), *"time scaling can be based on*

$$\frac{T_m}{T_p} = \frac{U_p(1 + gI_{uL})}{U_m}\frac{b_m}{b_p} \tag{4.8}$$

where g = a peak factor representative for the missing low frequency turbulence. A suggested value for g is 3.4. This time scaling is based on treating the mean velocity in the wind tunnel as equivalent to a typical low frequency peak gust, the justification being that the most probable situation where a peak load occurs is during a peak low frequency gust."

Therefore, using the peak factor of 3.4 and U_p = 49.3 m/s for Miami-Dade conditions, the full scale gust due to the missing low frequency turbulence is:

$$\widehat{U}_{LP} = U_p(1 + gI_{uL}) = 49.3x(1 + 3.4x0.153) = 74.9\ m/s$$

This value is equal to the 3-second gust of 74.9 m/s at the prototype roof eave height, which indicates that the WOW mean wind speed corresponds to a gust duration of 3 seconds at full scale.

The Wall of Wind testing was performed using a mean wind speed of 25.67 m/s (57.44 mph). Thus, the model wind speed scaling for Miami- Dade conditions is:

$$\frac{U_m}{\widehat{U}_{LP}} = \frac{25.67}{74.9} = 0.343 \tag{4.9}$$

With the length scale being 1:6, the frequency scale is calculated using:

$$\frac{n_m}{n_p} = \frac{b_p}{b_m}\frac{U_m}{U_p} = 0.343x6 = 2.06 \tag{4.10}$$

The time scale is:

$$\frac{t_m}{t_p} = \frac{n_p}{n_m} = 0.485 \tag{4.11}$$

For the sampling time, 1 hour at full scale will be the target, as T_s = 1 hour is considered sufficient in order to achieve stable statistics when measuring fluctuating wind loads, Irwin (2015). The representative characteristic time for the turbulence at full scale is:

$$\frac{xL_u}{U} = \frac{95}{51.4} = 1.85\ sec. \tag{4.12}$$

The ratio of sample time, T_s, to turbulence characteristic time is:

$$T_s \times U/^xL_u = 3600/1.85 = 1946 \quad (4.13)$$

By determining the same ratio of sample time to turbulence characteristic time on the model, stable statistics should be achieved. Thus,

$$T_{sm} = (T_s \times U/^xL_u)(^xL_{um}/U_m) = 1946 \times 0.4/25.67 = 30.3 \text{ sec.} \quad (4.14)$$

Therefore, a sample time of at least 30.3 seconds is required on the model.

As a result of the above analysis, a sample time of 60 seconds was used for the testing of this research.

CHAPTER V

FULL-SCALE PERFORMANCE EVALUATION OF VALVED SOFFIT VENTS

Overview

The primary objective of this study was to investigate the wind performance of a new valved soffit venting system in a large-scale wind tunnel environment. External and internal pressure measurements were recorded on a gable and a hip roof for various wind directions in an open terrain. The testing also investigated potential water entry mitigation into the attic space using valved soffit vents (VSVs) under wind-driven rain (WDR) simulation. The testing was conducted at the International Hurricane Research Center's (IHRC) Wall of Wind (WOW) facility at Florida International University (FIU) in Miami, Florida. Two test cases were evaluated; soffit openings without VSVs and soffit openings with VSVs. The valved soffit vents were invented by Robert Platts, P.Eng and are patented (Publication number, US6484459 B1) by Building Performance Americas (BPA). The product is termed *BPA Safety Vent* (Figure 5-1).

a) b)

Figure 5-1. A valved soffit vent (VSV) that was used for this testing: (a) front; (b) back

Experimental Set-Up

A building with dimensions of length 1.44 m by width 1.44 m and an eave height of 1.27 m (4'-8 1/2" x 4'-8 1/2" x 4'-2") was constructed for the testing. The dimensions selected fit appropriately within the blockage requirements of the WOW, thereby allowing the test building to be fully immersed in the wind field. It was concluded during the blockage assessment of the WOW that roof heights of 33% to 50% of the wind field height and a tunnel blockage ratio of 7% to 16% provide roof pressure measurements that compare well to the values reported in previous studies (Aly et al. 2011). The dimensions of the test specimen provided a blockage ratio of approximately 8%.

The test building was constructed using traditional wood framing and plywood sheathing. In addition, there were interchangeable roofs, a gable and a hip roof, both with a 4:12 pitch roof slope. The building's eaves/soffits were 0.36 m (14") all around. Internal compartmentalization was provided by a ceiling at a height of 1.27 m (4'-2") from the ground, which separated the attic space from the base of the building. The attic was fully sealed. Figure 5-2 (a, b) shows schematics of the test specimen with each roof.

Four soffit vent openings were installed on the gable roof (V1 to V4) and eight openings were installed on the hip roof (V1 to V8). The net area of each opening is 0.07 m^2 (0.72 ft^2), which corresponds to the *BPA Safety Vent* dimensions. Each opening provided an 8.8% under soffit open area ratio per vent location.

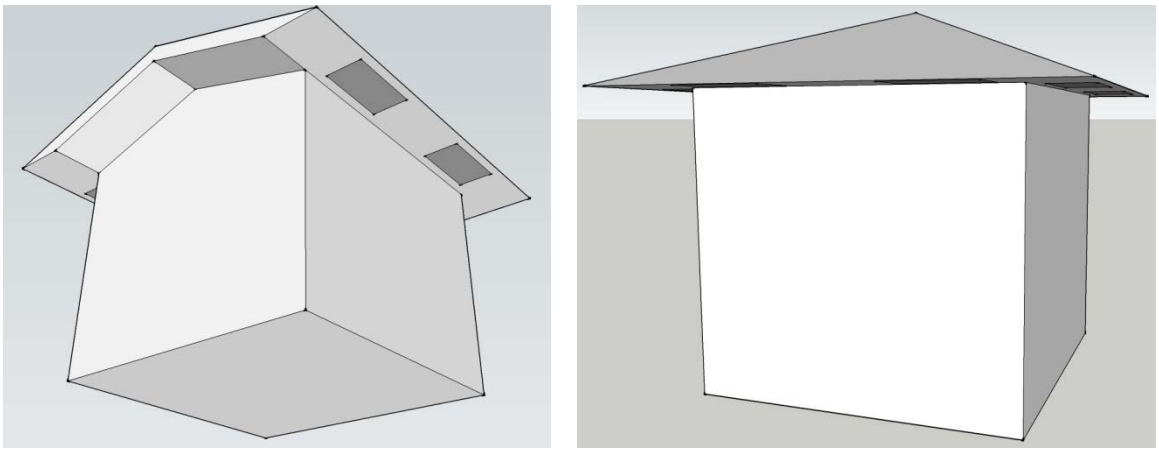

a) b)

Figure 5-2. Schematics of the test building: a) gable roof model; b) hip roof model

Variable Speed Test

Prior to conducting wind pressure tests, a variable wind speed study was performed to obtain the wind speed required to activate the valved soffit vents at various wind directions for the gable and hip roof models. At each wind direction, throttle was slowly applied to the 12 WOW fans, gradually increasing the wind velocity from 0% throttle. High definition cameras were used to record the VSVs and the video was monitored in the WOW control room. The activation speed was established once the louvers on the the VSVs shut and remained closed due to the wind induced positive pressure acting on the louvers. The valved soffit vents located in the wind separation zones were also monitored. The louvers in the vents at these locations remained open. In order to clearly see the movement of the louvers, the outer screen/mesh was removed. It was observed from this part of the study that the operational mechanism of the VSVs performed as anticipated. The results of the variable speed test are shown in Tables 5-1 and 5-2.

Table 5-1. Wind speed to activate valved soffit vents (VSVs) on the hip roof model

Wind Direction	VSVs Activated	Throttle (%)	Wind Speed, m/s (mph)
0°	V1 & V2	16	10.4 (23.2)
15°	V1 & V2	18	11.8 (26.3)
30°	V1, V2 & V8	32	21.4 (47.8)
45°	V1, V2, V7 & V8	38	25.7 (57.4)

Table 5-2. Wind speed to activate valved soffit vents (VSVs) on the gable roof model

Wind Direction	VSVs Activated	Throttle (%)	Wind Speed, m/s (mph)
0°	V1 & V2	16	10.4 (23.2)
15°	V1 & V2	18	11.8 (26.3)
30°	V1 & V2	32	21.4 (47.8)
45°	V1 & V2	38	25.7 (57.4)
60°	V1 & V2	38	25.7 (57.4)
75°	V2*	38	25.7 (57.4)
90°	NONE	N/A	N/A

* V2 flutters for this wind direction only

The VSVs all remained open for the 90° wind direction for the gable roof model as they were all in the wind separation zones.

Based on the results of the VSV activation testing, it was determined that a throttle percentage of 38% would be used as the testing speed for all remaining tests. The atmospheric boundary layer (ABL) profiles for the different throttle percentages are included in Figure A-1 in Appendix A.

The velocity and turbulence intensities were measured using Cobra probes at various heights above the WOW floor with a sampling frequency of 100 Hz. Figure 5-3 (a) shows the measured WOW and targeted mean velocity profiles corresponding to open terrain Exposure C in *ASCE-7-10*. The tests were carried out using a full-scale roughness length, z_0=0.02-0.03 m as recommended in *ASCE 7-10 (Table C26.7-1)* for Exposure Category C. The exposure C velocity profile is determined using the 'power law' equation, which is:

$$\frac{V}{V_{ref}} = \left(\frac{Z}{Z_{ref}}\right)^{\bar{\alpha}} \tag{5.1}$$

where V is the mean wind speed at height, Z; V_{ref} is the reference wind speed; Z_{ref} is the reference height for the power law boundary layer approximation; and $\bar{\alpha}$=1/6.5. The mean wind speed profile fits well with the *ASCE 7* target profile. The measured turbulence profile in WOW is shown in Figure 5-3 (b). The target turbulence intensity profile, which is given by $1/\ln(z/z_o)$, Holmes (2007), is not shown as the turbulence intensity in the WOW will be much lower due to the partial turbulence simulation which is explained further in Chapter 4. The turbulence intensity at 1.27 m was 7.4%.

A mean velocity of 25.67 m/s (57.44 mph) at roof eave height (1.27 m) was used for the tests, which corresponds to a 38% WOW throttle setting. The equivalent 3-second gust wind speed being 39 m/s (87.3 mph). The Reynolds number based on the roof eave height and velocity at that height was calculated to be 2.18 x 10^6.

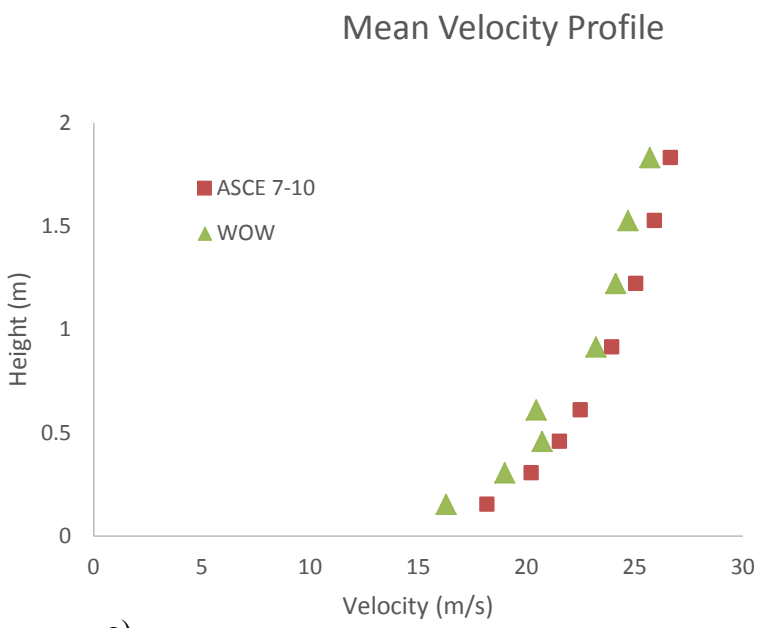

a)

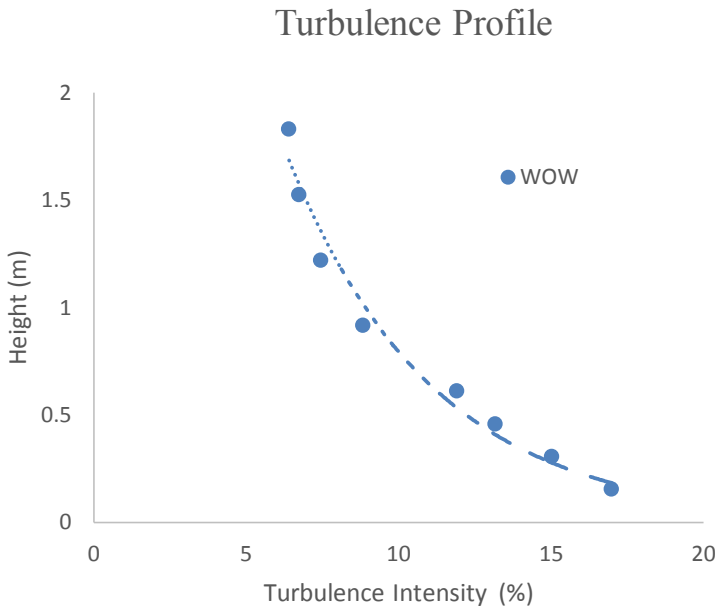

b)

Figure 5-3. Measured mean velocity and turbulence profiles at the WOW: a) comparison of experimental and target mean velocity profiles; b) experimental turbulence intensity profile.

Test Configurations

The building was tested for wind directions from 0° to 45° at 15° intervals for the hip roof model and 0° to 90° at 15° intervals for the gable roof model. There were three test configurations. Test Case 1 investigated pressure measurements for soffit openings without valved soffit vents (control test). To achieve this configuration, openings with dimensions 171 mm x 389 mm (6 ¾" x 15 5/16") were placed in the soffits at the vent locations. Each opening represented the net open area of a valved vent. Test Case 2 examined the pressure measurements for the hip and gable roof configurations with valved soffit vents (*BPA Safety Vents*) installed. Test Case 3 was the same as test Case 2; however, the outside screen that covers the exterior face of the valved vents was removed to determine the effect, if any, that the screen would have on mean internal pressure coefficients.

Table 5-3. Summary of experimental configurations for the gable roof model

Test Case ID	Soffit Vents	Ceiling	Comments
1	All open (w/out VSVs)	Yes	None
2	With VSVs	Yes	None
3	With VSVs	Yes	Screen removed

Wind direction: 0°, 15°, 30°, 45°, 60°, 75° and 90°

Table 5-4. Summary of experimental configurations for the hip roof model

Test Case ID	Soffit Vents	Ceiling	Comments
1	All open (w/out VSVs)	Yes	None
2	With VSVs	Yes	None
3	With VSVs	Yes	Screen removed

Wind direction: 0°, 15°, 30° and 45°

Water Intrusion Testing

Wind-driven rain tests were performed on the hip roof model for 0 and 45 degree wind directions. The open soffit area was 0.13 m^2 (1.44 ft^2) for the 0° wind direction and 0.27 m^2 (2.88 ft^2) for the 45° wind direction. Water intrusion through the soffit openings was measured and the total volume of water entering the test building was quantified. A plastic membrane was attached inside the attic space, which created a collection area between the attic and living space. At the completion of each test, the captured water was drained into dry plastic containers, which was then measured and recorded.

A wind-driven rain deposition rate of 203 mm/hr (8 in/hr) was used for the WDR tests. The selected rain deposition rate is based on the rate specified for wind-driven rain in ASTM E 331-00 (Quarles 2014). Water entry through the soffit openings without VSVs and with VSVs was evaluated. The tests were conducted at a wind speed of 25.67 m/s (57.44 mph) for a duration of 300 seconds (5 min). Table 5-5 illustrates the WDR experimental configurations for the hip roof.

Wall of Wind Rain Simulation Procedure

The Wall of Wind procedure for simulating wind-driven rain is as outlined by Baheru et al. (2014). The WOW uses equally spaced *TeeJet* full cone spray nozzles, which are installed on four vertical lines attached to the frame of the spires to generate the target rain deposition rate at the test building. The plumbing system is supplied by a 50.8 mm (2.0 in) diameter main water supply line. Water can be supplied at a rate of 5 m^3 per hour.

Table 5-5. Summary of wind-driven rain (WDR) experimental configurations for the hip roof model

Test Case ID	Soffit Vents	Ceiling	Comments
1	All open (w/out VSVs)	Yes	None
2	With VSVs	Yes	None

Wind direction: 0° and 45°

Pressure Measurements

For the gable roof, there were a total of 61 pressure taps installed on the model building, which measured the external and internal pressures. To measure the external pressures distribution, 26 pressure taps were evenly placed over the roof. There was also an external pressure tap at the periphery of each vent location. The internal pressures were measured by 35 pressure taps, which were uniformly positioned on the interior surface of the roof, in the attic space and at the soffit vent locations. There was a similar pressure tap layout for the hip roof model. A total of 97 pressure taps (44 taps externally and 53 taps internally) were used on the hip roof model. The internal and external pressures at the soffit vents were measured as well. The pressure tap layouts and soffit vent locations for the gable and hip roofs are shown in Figure 5-4 and Figure 5-5 respectively.

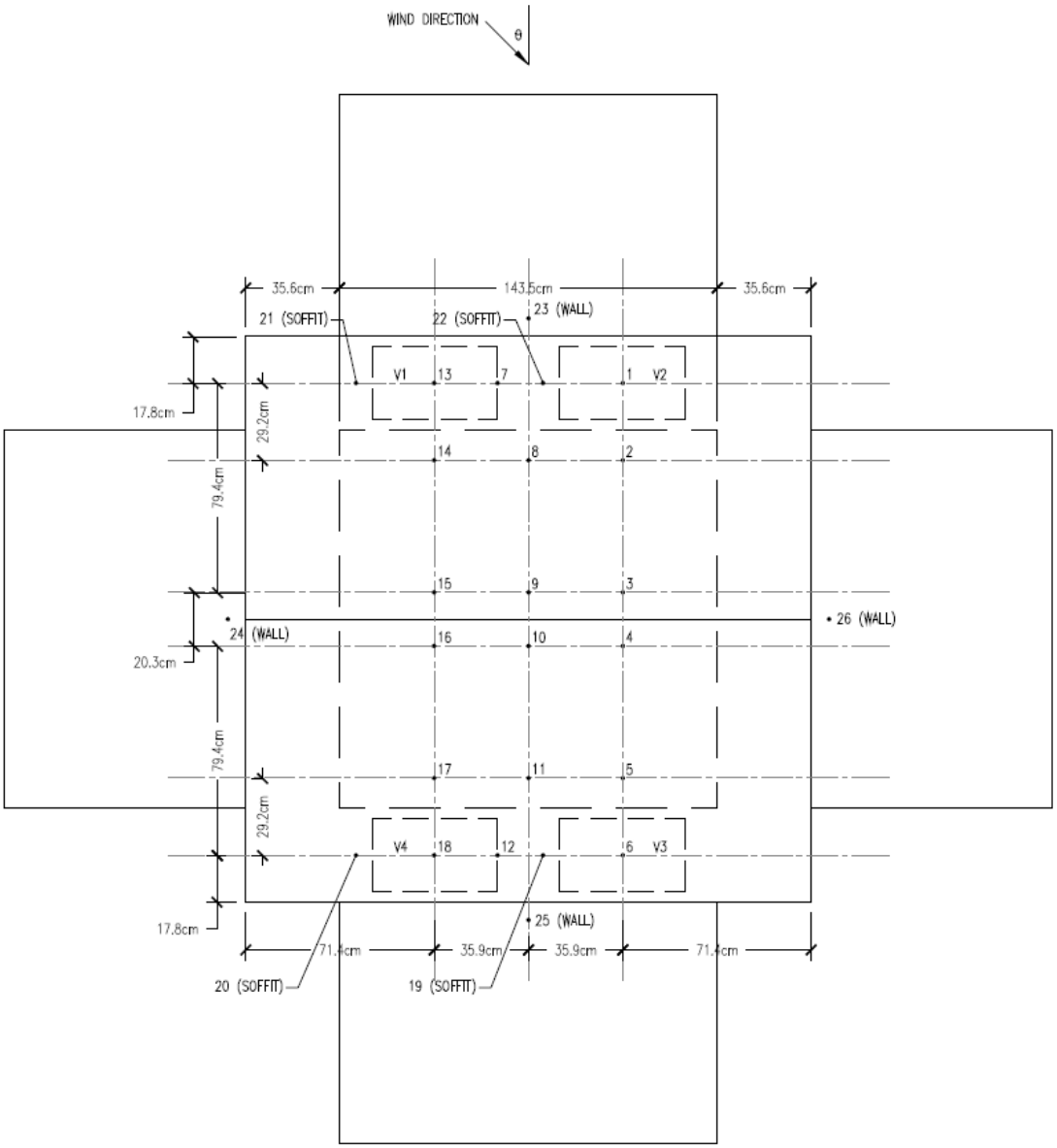

a)

Figure 5-4. a) External pressure tap locations on the gable roof

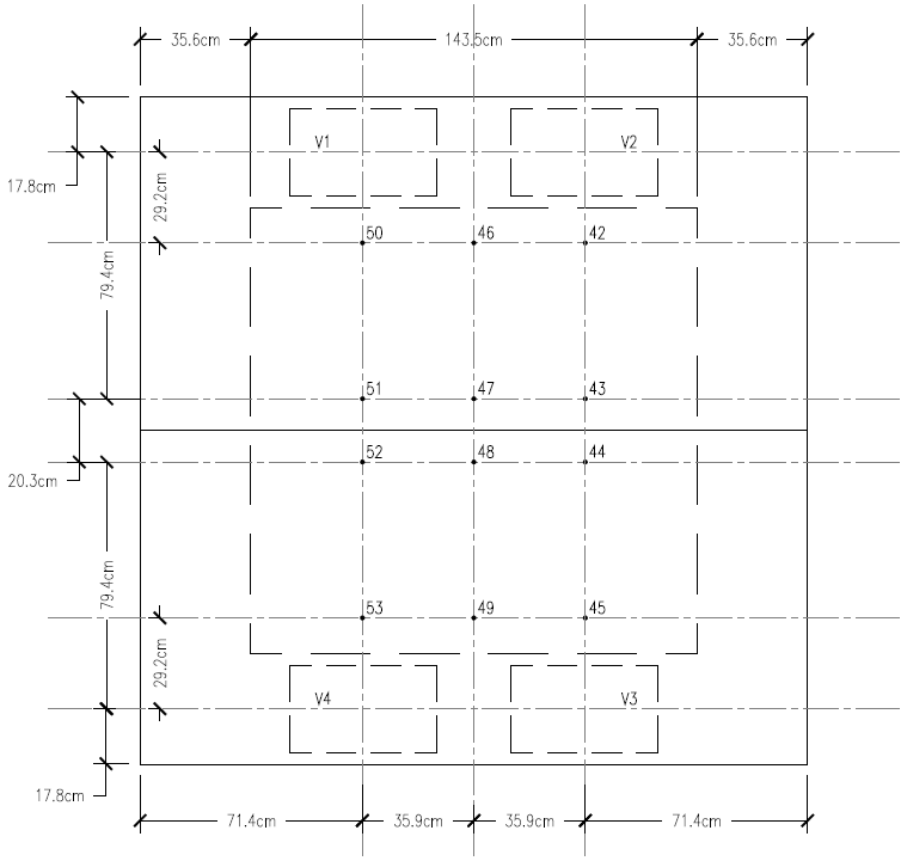

b)

Figure 5-4. b) Internal pressure tap locations on the gable roof surface

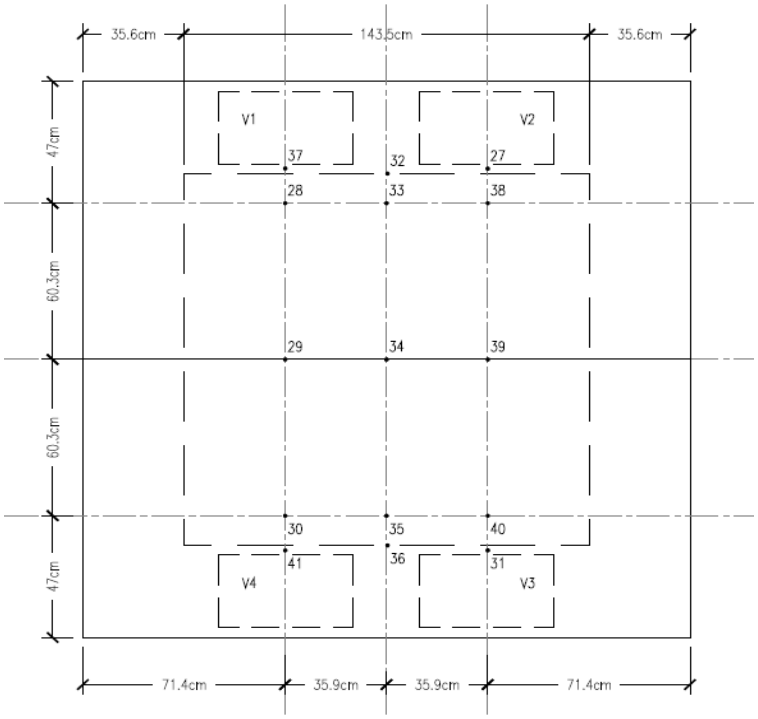

c)

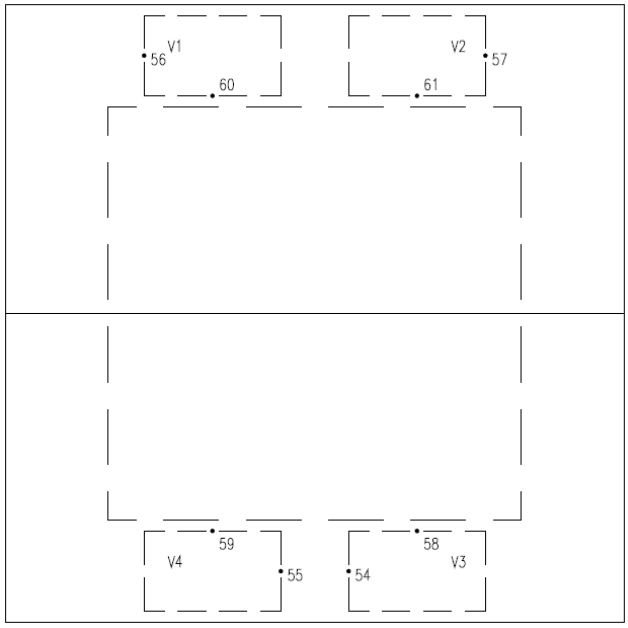

d)

Figure 5-4. c) Internal pressure taps in the attic space of the gable roof; d) internal pressure taps at vents

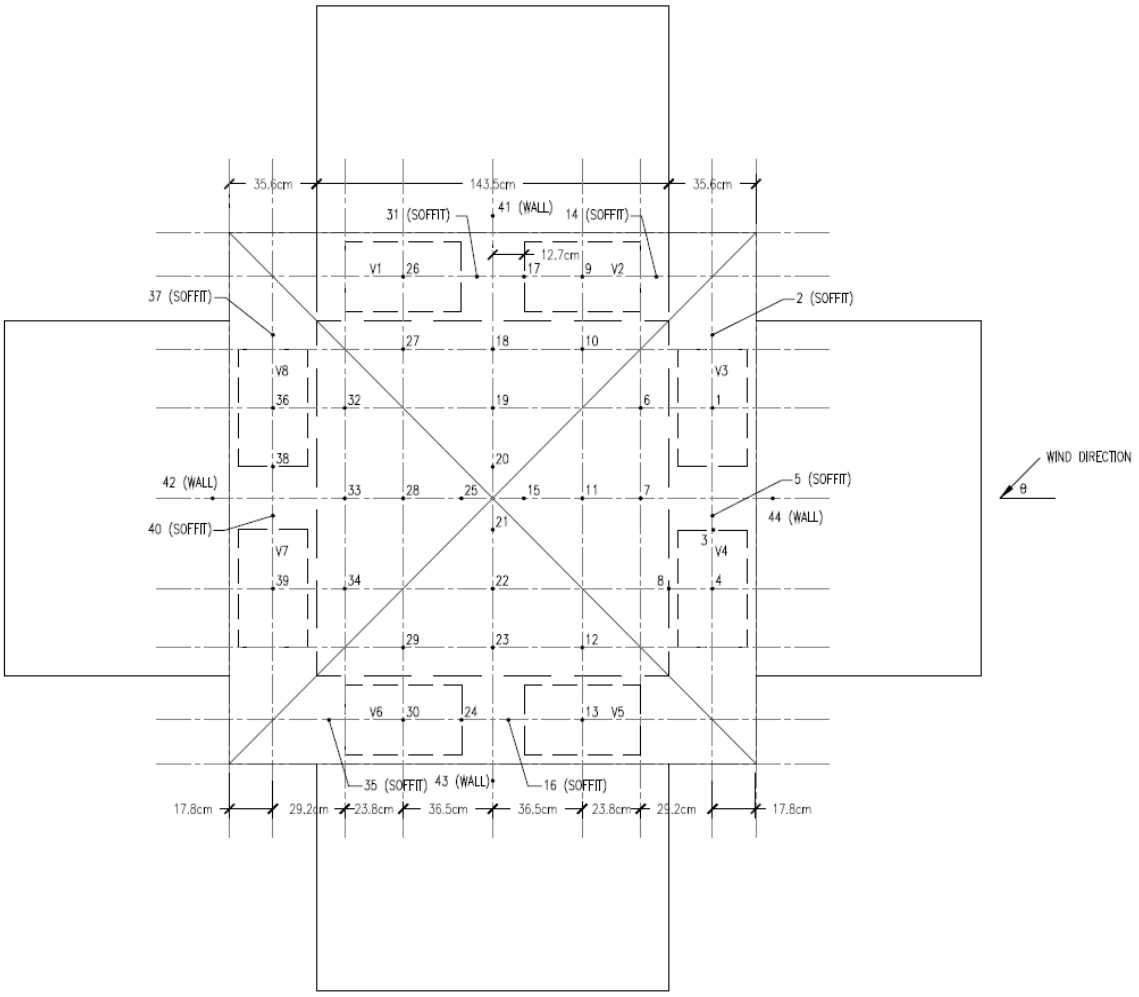

a)

Figure 5-5. a) External pressure tap locations on the hip roof

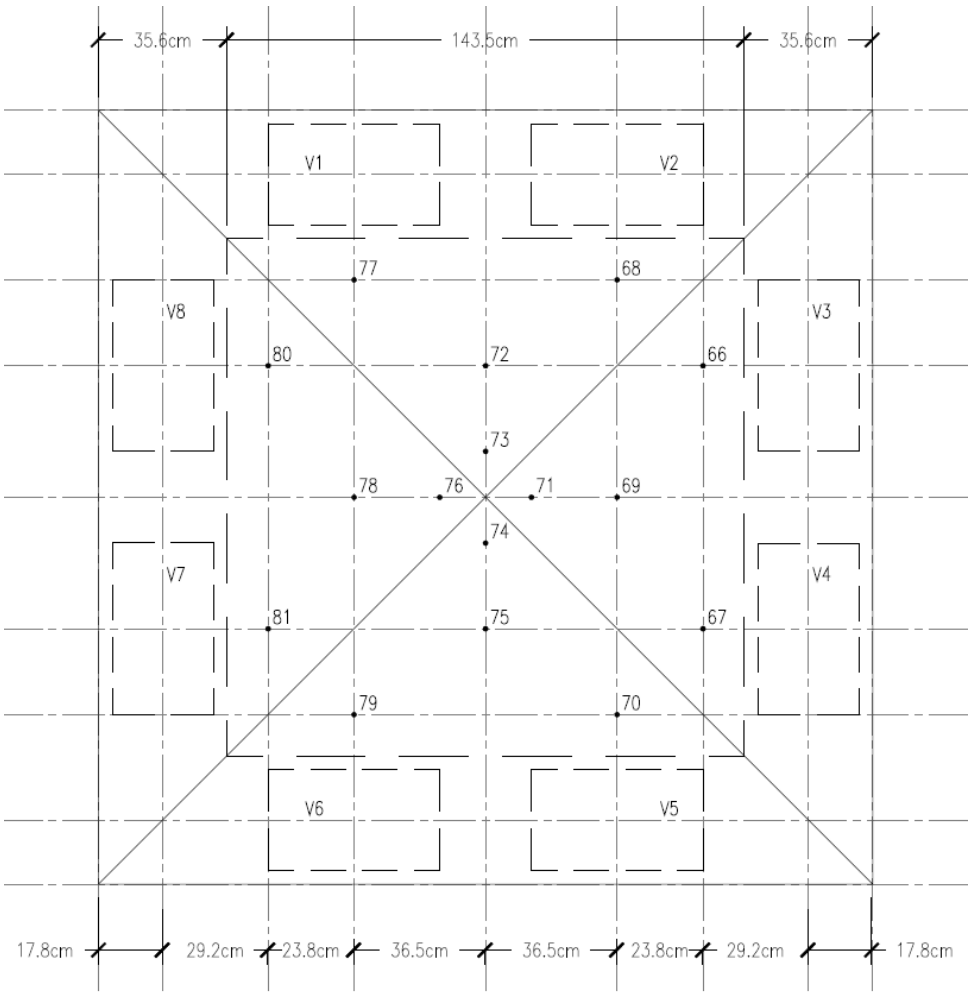

b)

Figure 5-5. b) Internal pressure tap locations on the hip roof surface

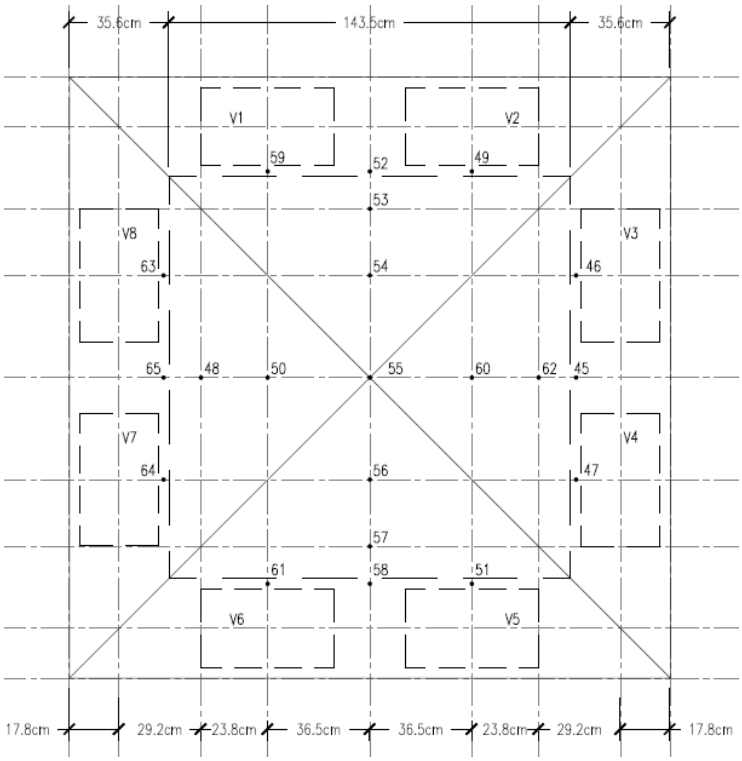

c)

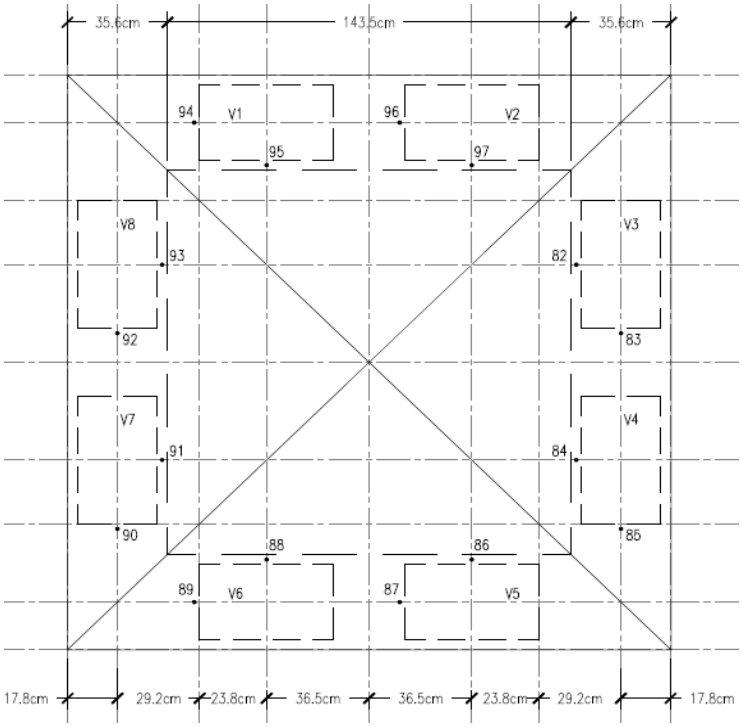

d)

Figure 5-5. c) Internal pressure taps in the attic space of the hip roof; d) internal pressure taps at vents

The pressure time history data was captured using a Scanivalve pressure acquisition system. A Scanivalve ZOC 33 scanner was used with a 520 Hz sampling rate. Each test was performed for 1 minute once a stable flow was achieved. The pressure taps on the roof and inside the attic were connected to the Scanivalve pressure scanner using 1.34 mm (1/16") diameter PVC tubes that were 1.52 m (5'-0") long. A transfer function designed for the tubing system was applied to the raw pressure data to correct the distortion effects. The correction for tube transfer was achieved by the method outlined by Irwin et al. (1979), which involved digital correction to the pressure signals using the inverse of the tubing system transfer function.

From the pressure time history data, the mean and peak (maximum and minimum) non-dimensional pressure coefficients ($C_{p's}$) were estimated by using Equations 5.2 and 5.3:

$$Cp_{\_Mean} = \frac{P_{mean}}{\frac{1}{2}\rho V_{eave}^2} \tag{5.2}$$

$$Cp_{\_Peak} = \frac{P_{peak}}{\frac{1}{2}\rho V_{eave}^2} \tag{5.3}$$

where C_{p_Mean} and C_{p_Peak} are the mean and peak non-dimensional pressure coefficients respectively; P_{mean} and P_{peak} are the mean and peak pressures measured at the tap location; V_{eave} is the mean wind speed at the reference height (roof eave) for estimating C_{p_Mean} and the 3- second gust wind speed at the model eave height (1.27 m) for

obtaining the peak pressure coefficients; and ρ is the air density, which for Miami is 1.225 Kg/m^3. The pressure measurements were for both external (C_{pe}) and internal (C_{pi}) pressure coefficients.

The C_{p_Peak} values were estimated using the Partial Turbulence Simulation (PTS) method as outlined by Mooneghi et al. (2015). To obtain more statistically stable peak pressure values, the sample time was divided into 50 sub-intervals to carry out an extreme-value, Fisher-Tippet Type 1 (FT1) analysis on the measured peak pressures. As outlined by Cook (1985), the extreme (peak) values from each segment are sorted into ascending order of magnitude. The peak pressure values can be fitted within a FT1 distribution and the resulting mode and dispersion of the FT1 distribution can be found. A MATLAB program was used to conduct the PTS method, which included the FT1 analysis on the measured peak pressures. The dispersion and mode parameters of the FT1 distribution were used to estimate the peak C_p values with an 80% probability of not being exceeded in one hour of wind.

a) b)

c) d)

e) f)

Figure 5-6. The building models used for the testing: a) gable roof building model ready for testing, 0° wind direction; b) underside of the gable roof with tubing installed; c) hip roof building model ready for testing, 0° wind direction; d) underside of the hip roof with tubing installed; e) soffit vent openings without VSVs, hip roof; f) soffit vent openings with VSVs (*BPA Safety Vents*) installed

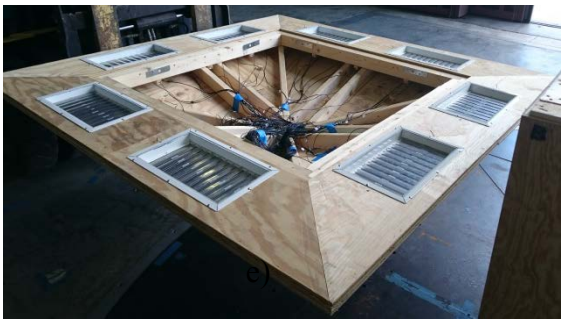

a)

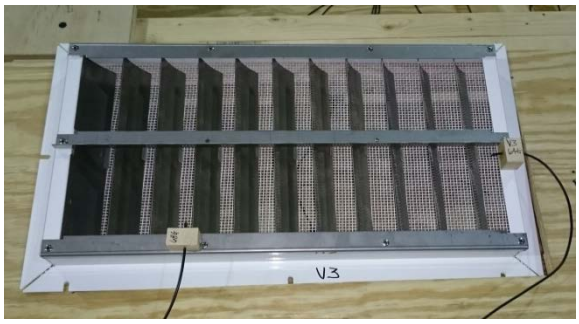

b)

c)

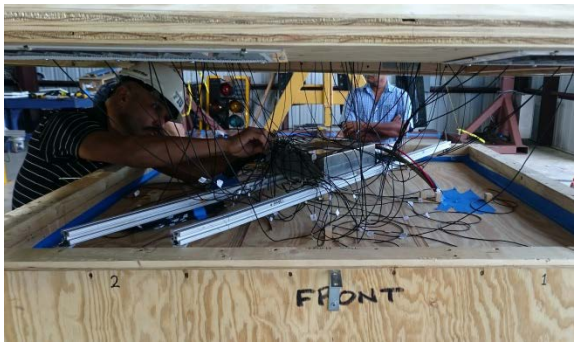

d)

e)

f)

Figure 5-7. a) Underside of the hip roof with VSVs installed, without screen (Test Case 3); b) BPA Safety Vent with taps attached; c) lifting gable roof into place; d) connecting pressure tap tubing to Scanivalve data acquisition system; e) gable roof without VSVs (Test Case 1); f) Gable roof with VSVs (Test Case 2)

Results and Discussion

The valved soffit vents (*BPA Safety Vents*) performed well. As claimed, the windward facing VSVs shut with positive wind-induced pressure and remained open at the negative pressure (suction) areas, i.e. the separation zones. The variable speed test demonstrated that the *BPA Safety Vents* started to activate normal to the wind at 10.4 m/s (23 mph). In addition, the wind-driven rain test verified that the VSVs can be used to prevent wind driven rain from entering the attic space.

Pressure testing of the gable and hip roofs without and with VSVs confirmed that the use of VSVs had a notable impact on the internal pressure distribution within the roof attic space. Moreover, the VSVs proved consistent in reducing the positive mean pressure entering the attic space at the vent locations and allowed for the relief of positive pressure within the attic space.

Gable Roof Test Results

Tables A-2 to A-8 show the comparative results of the mean and peak pressure coefficients for the gable roof model for the various wind directions. The tap numbers listed in the tables correspond to the tap layout in Figure 5-4. The tables show the mean and peak C_p values for Test Case 1 (without VSVs), Test Case 2 (with VSVs) and Test Case 3 (with VSVs, but exterior screen removed). Taps 1 to 18 were located on the external roof surface, while taps 19 to 26 were located on the building (soffit and walls). The remaining taps were placed inside the attic space. Taps 27 to 41 were located on the attic floor, while taps 42 to 53 were placed on the underside of the roof. In addition, taps 54 to 61 were positioned at the soffit vent/VSV locations. Taps 54, 55, 56 and 57 were

covered over once the VSVs were installed; however, they were replaced with equivalent taps on the VSVs.

The mean external C_{pe} values did not show any significant changes for each test case for any given wind direction, which is the expected trend as the air flow on the external surfaces of the model would not be influenced by the vents on the soffits. However, the mean internal C_{pi} values showed a different result. Overall, the trend of the mean internal pressure coefficients was that the C_{pi} values changed from positive to negative when the valved soffit vents were utilized for the 0, 15, and 30 degree wind directions. This was because the VSVs automatically shut to prevent air flow into the attic space. The mean values were mostly negative for both test cases for the 45° and 60° wind directions, but were reduced by 87.5% and 40% respectively with VSVs installed. However, the mean values did not change for the 75 and 90 degree wind directions, which was due to the fact that all the VSVs were mostly operating in the wind separation zones for these wind directions. Therefore, the vents remained open acting as a normal soffit opening.

For the 0° wind direction, the mean internal C_{pi} values changed from 0.22 for Test Case 1 (without VSVs) to -0.09 for Test Case 2 (with VSVs). In addition, at the windward vent locations (V1 and V2), the mean values were reduced from 0.73 without VSVs to -0.06 with VSVs. Similarly, for the 15° wind direction, the mean internal C_{pi} values changed from 0.15 for Test Case 1 to -0.16 for Test Case 2. Moreover, at the windward vent locations, the mean values were reduced from 0.70 without VSVs to -0.13 with VSVs. Positive mean C_{pi} values of 0.1 were obtained inside the attic space for the 30° wind direction for Test Case 1. This value changed to -0.17 for Test Case 2. The

mean values at the windward vent locations were 0.65 without VSVs and -0.18 with VSVs. For the 45° wind direction, the mean internal C_{pi} values changed from -0.03 for Test Case 1 to -0.24 for Test Case 2. At the windward vent locations, the mean values were 0.72 without VSVs, but changed to -0.24 with VSVs. Lastly, for the 60° wind direction, the mean internal C_{pi} values changed from -0.15 for Test Case 1 (without VSVs) to -0.25 for Test Case 2 (with VSVs). In addition, at the windward vent locations, the mean values were reduced from 0.65 without VSVs to -0.25 with VSVs. The mean values were reduced as a result of the windward facing VSVs closing and disallowing air intrusion into the attic, while the VSVs located in the wind separation zones around the building remained open, allowing airflow out of the attic space. Therefore, the roof experiences a suction (negative internal pressure), thereby validating the valved soffit vent theory, which can mitigate the roof from lifting off in high winds. The results also show that removing the screen on the outside of the VSVs has no effect on the mean C_{pi} values with VSVs.

Overall, changes in the C_{p_Peak} values were much less consistent as compared with the C_{p_Mean} results, where some taps reflected an increase in C_{p_Peak}, while others reflected a decrease in C_{p_Peak}. The peak positive internal pressure coefficients within the attic space did not change in any meaningful way between Test Case 1 and Test Case 2. At localized areas, such as the windward vent locations, there were some reductions, but also increases to the internal peak positive C_{pi} values for various angles of attack. For example, for the 45° wind direction, $C_{pi\_Peak\ (+ve)}$, increased by 10% at V1; however, decreased by 25% at V2. Figure 5-8 (a,b) shows the internal mean and peak $C_{pi's}$ for the gable roof model for the various wind directions.

Hip Roof Test Results

Tables A-9 to A-12 in Appendix A show the comparative results of the mean and peak pressure coefficients for the hip roof model for the various wind directions. The tap numbers listed on the tables correspond to the tap layout in Figure 5-5. The tables show the mean and peak C_p values for Test Case 1 (without VSVs), Test Case 2 (with VSVs) and Test Case 3 (with VSVs, but exterior screen removed). Taps 1 to 40 were located on the external roof surface, while taps 41 to 44 were located on the building walls. The remaining taps were placed inside the attic space. Taps 45 to 65 were located on the attic floor, while taps 66 to 81 were placed on the underside of the roof. In addition, taps 82 to 97 were positioned at the soffit vent/VSV locations. Taps 83, 85, 87, 89, 90, 92, 94 and 96 were covered over once the VSVs were installed; however, they were replaced with equivalent taps on the VSVs.

Similar to the gable roof results, the mean external C_{pe} values for the hip roof did not change considerably for each test case for any given wind direction. However, the mean internal C_{pi} values consistently decreased for all wind directions (0° to 45°). For the 0° wind direction, the mean internal C_{pi} values decreased by 58%, from -0.11 for Test Case 1 (without VSVs) to -0.26 for Test Case 2 (with VSVs). In addition, at the windward vent locations, the mean value was reduced from 0.48 without VSVs to -0.22 with VSVs. Similarly, for the 15° wind direction, the mean internal C_{pi} values decreased from -0.07 for Test Case 1 to -0.2 for Test Case 2. Moreover, at the windward vent locations, the mean values were reduced from 0.6 without VSVs to -0.17 with VSVs. Positive mean C_{pi} values of 0.03 were obtained inside the attic space for the 30° wind direction for Test Case 1. This value reduced to -0.16 for Test Case 2. The mean value at

the windward vent locations was 0.69 without VSVs and -0.12 with VSVs. For the 45° wind direction, the overall mean internal C_{pi} values changed from 0.06 for Test Case 1 to -0.15 for Test Case 2. At the windward vent locations, the mean value was 0.72 without VSVs, but became -0.13 with VSVs. The results also showed that removing the screen on the outside of the VSVs had no effect on the mean C_{pi} values with VSVs. These results clearly demonstrate the efficacy of the VSVs in reducing mean internal pressures.

As with the gable roof model, the peak positive internal pressure coefficients within the attic space did not change in any significant way between Test Case 1 and Test Case 2. The C_{pi_Peak} values were much less consistent as compared with the C_{pi_Mean} results, where some taps reflected an increase in C_{pi_Peak}, while others reflected a decrease in C_{pi_Peak}. However, at the windward vent locations, the peak C_{pi} values were more consistent with the mean C_{pi} values. For example, at Tap 85 (V4), the maximum C_{pi_Peak} and C_{pi_Mean} values all decreased for wind directions 0° to 45°. The 15° wind direction was the most critical, yielding reductions in the positive internal roof peak C_{pi} values by 51%. Figure 5-8 (c, d) shows the internal mean and peak $C_{pi's}$ for the hip roof model for the various wind directions.

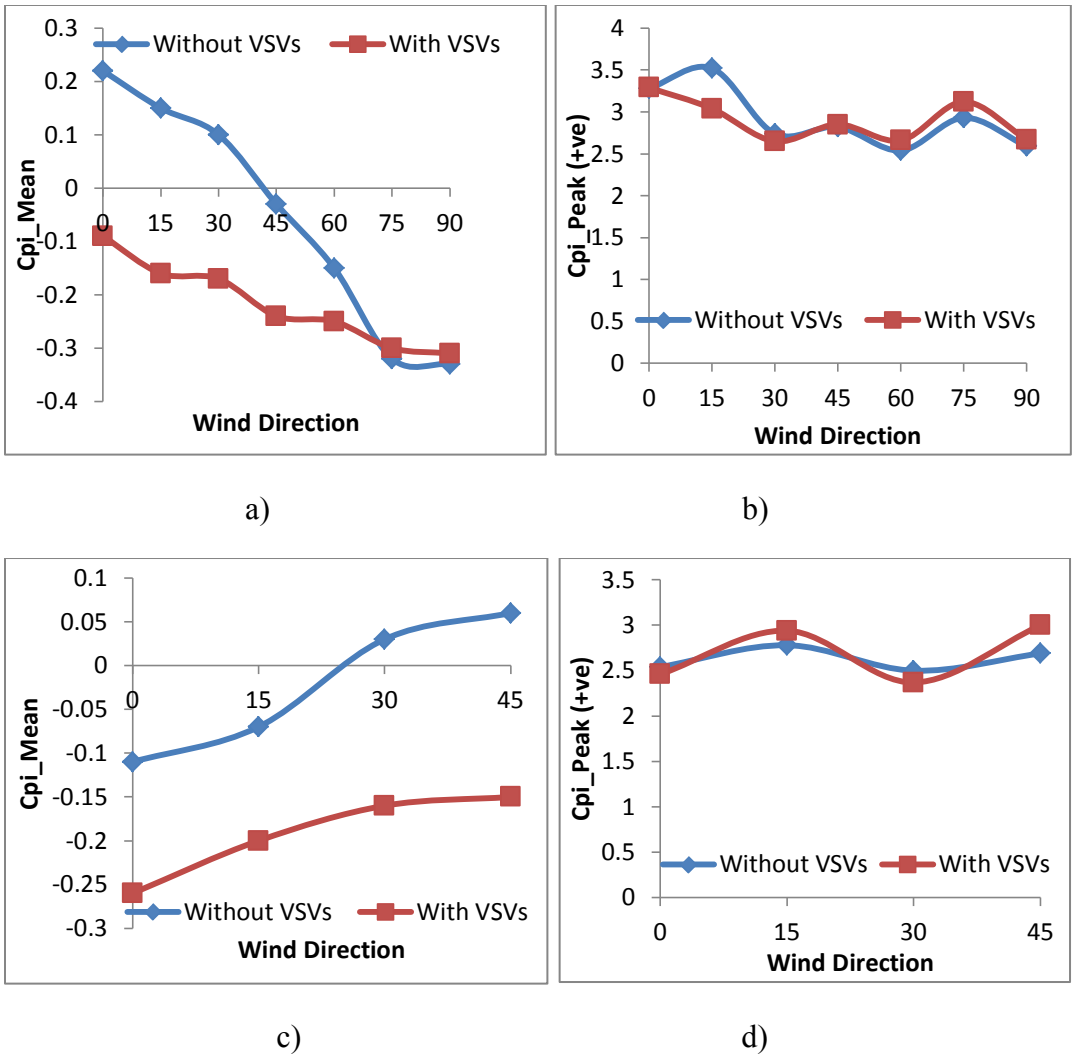

Figure 5-8. Attic space internal pressure distribution due to VSVs: a) mean, gable roof; b) maximum, gable roof; c) mean, hip roof; d) maximum, hip roof

Figure 5-8 (a, c) shows that the hip roof generated greater internal suction for the 0 and 15 degree wind directions. There was a 65% decrease in the mean C_{pi} value for the 0° wind direction for the hip roof model. The mean internal pressure in the attic space was similar for both roofs for the 30° degree wind direction; however, the gable roof produced more internal suction at the 45° wind direction when compared to the hip roof.

An examination of the mean external pressure coefficient that was measured at the periphery of each vent location was conducted for the 0 and 45 degree wind directions. The mean external $C_{pe's}$ were compared to the mean internal pressure coefficients at the vent locations, where it was found that there was a correlation between the mean internal pressure coefficients and the mean external pressure coefficients for roofs without VSVs. However, as shown in Figure 5-9, this correlation changed with VSVs installed. At the windward vent locations with VSVs, the mean $C_{pi's}$ were found to be correlated with the mean $C_{pe's}$ at the VSVs located in the wind separation zones. Correlation coefficients ranged from 0.1 to 0.7.

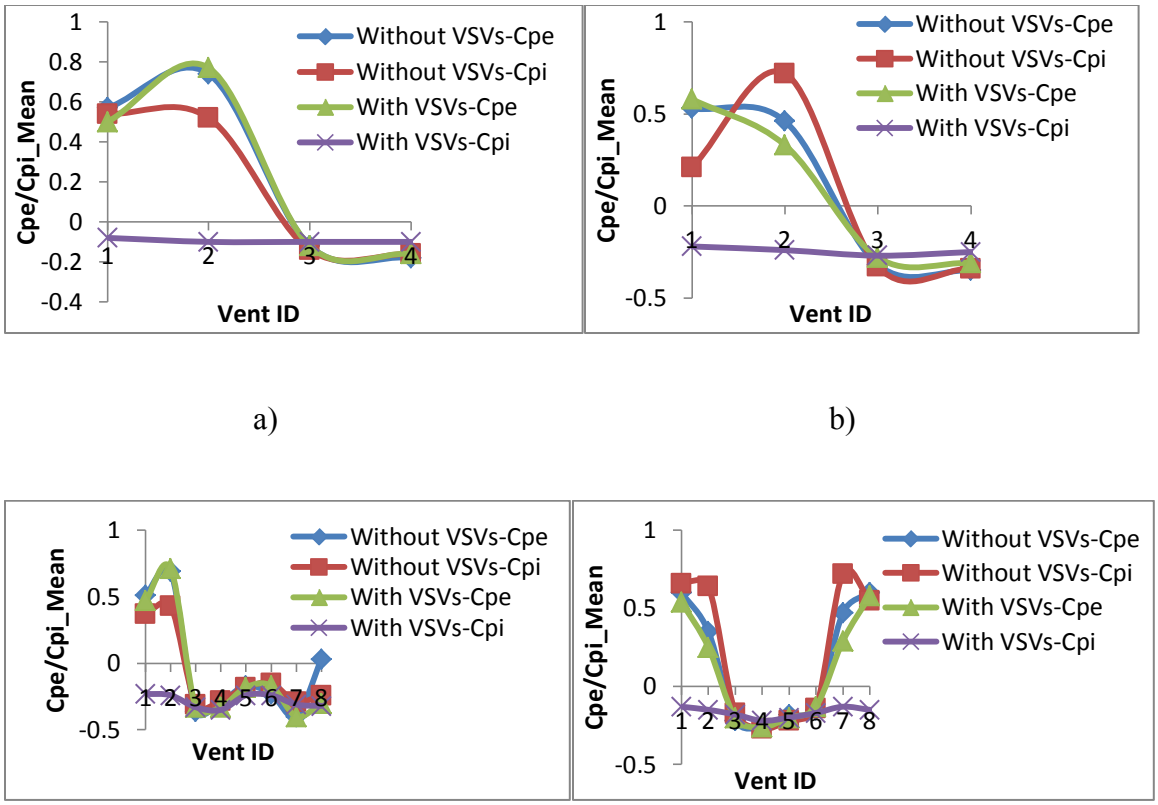

Figure 5-9. Correlation of mean external pressure at each vent and internal pressure: a) gable roof, WD = 0°; b) gable roof, WD = 45°; c) hip roof, WD = 0°; d) hip roof, WD = 45°.

Mean and Peak Pressure Coefficient Contours

The mean and peak pressure coefficients for the gable and hip roof models for selected wind directions are presented in this section. Figures 5-10 to 5-19 show the mean and peak C_p values on the external and internal roof surfaces and the mean C_{pi} values on the attic floor of the gable roof building for wind directions of 0, 15, 30, 45 and 60 degrees. In addition, Figures 5-20 to 5-27 show the mean and peak C_p values for the hip roof building for wind directions of 0, 15, 30 and 45 degrees. There are two figures associated with each wind direction of each roof. The first figure presents the mean C_p values for the following conditions: a) external roof surface without VSVs; b) external roof surface with VSVs; c) internal roof surface without VSVs; d) internal roof surface with VSVs; e) internal attic surface without VSVs; f) internal attic surface with VSVs. The second figure for each wind direction shows the peak C_p values for the following conditions: a) external roof surface without VSVs ($C_{p\_Peak\ (-ve)}$); b) external roof surface with VSVs ($C_{p\_Peak\ (-ve)}$); c) internal roof surface without VSVs ($C_{p\_Peak\ (+ve)}$); d) internal roof surface with VSVs ($C_{p\_Peak\ (+ve)}$).

The figures show that the mean C_{pe} values did not change for Test Case 1 (without VSVs) and Test Case 2 (with VSVs) on the external surface as shown in Figures 5-10, 5-12, 5-14, 5-16, 5-18, 5-20, 5-22, and 5-24 (a, b). The values were similar for both test cases. However, the mean C_{pi} distributions were different in the interior locations (roof surface and attic floor) for Test Cases 1 and 2 (Figures 5-10, 5-12, 5-14, 5-16, 5-18, 5-20, 5-22, and 5-24 (c, d and e, f)).The mean C_{pi} values were consistently positive within the windward facing region of the attic in the absence of the valved soffit vents, however, they changed to negative with the installed VSVs. For internal C_{pi_Mean} values

on the underside of the roof, the 0 and 15 degree wind directions yielded the critical cases for the gable roof. Figure 5-10 (c) shows positive values (0.73 to 0) without VSVs, while the values are negative (-0.06 to -0.10) with the installed VSVs (Figure 5-10 (d)). Similarly, in Figure 5-12 (c), the mean internal pressure coefficients were positive (0.7 to 0) without VSVs, but changed to negative (-0.13 to -0.19) with VSVs (Figure 5-12 (d)). The 30 and 45 degree wind directions produced mean C_{pi} values of 0.65 to 0 and 0.48 to 0 respectively for Test Case 1. However, these values decreased to -0.21 to -0.27 and -0.20 to -0.29 for Test Case 2 (Figures 5-14 and 5-16 (c,d)). This trend was repeated for the 0 to 45 degree wind directions for the hip roof model (Figures 5-20, 5-22, 5-24 and 5-26 (c,d)). For example, the case without VSVs for the 15° wind direction produced positive mean $C_{pi's}$ (0.60 to 0), which changed to negative values (-0.13 to -0.40) with VSVs. These results show that the VSVs effectively depressurize the attic space producing a suction on the underside of the roof.

In the absence of VSVs for the interior attic regions of the hip and gable roof buildings, the attic area was directly exposed to the wind at various wind directions, which generated a positive mean C_{pi} in the range of 0.12 to 0.54 for the gable roof and 0.18 to 0.30 for the hip roof (0° to 45° wind directions). However, with the VSVs installed, the wind-induced positive pressure shut the VSVs, thereby providing a negative mean pressure coefficient throughout the attic space in the range of -0.08 to -0.27 for the gable roof and -0.14 to -0.33 for the hip roof. The critical case for the mean C_{pi} values on the the attic floor was for the 15 degree wind direction for the hip roof (Figure 5-22 (e, f)). The values changed from 0.30 to 0 for Test Case 1 to -0.17 to -0.33 for Test Case 2.

The mean C_{pi} values for the gable roof changed from 0.44 to 0 for Test Case 1 to -0.14 to -0.19 for Test Case 2 for the 15 degree wind direction.

Figures 5-11, 5-13, 5-15, 5-17, 5-19, 5-21, 5-23, 5-25 and 5-27 (c, d) show contours for the internal peak (+ve) C_{pi} values on the underside of the roof surface for both the gable and hip roof buildings. The interior peak (+ve) C_{pi} values were reduced in certain areas by 14-44% (gable roof) and 16-37.5% (hip roof) on the leading edge of the internal roof locations depending on the wind direction. The 15° wind direction for both the gable and hip roofs yielded the highest reductions in interior peak (+ve) C_p values at specific locations along the leading edge of the roof. Figure 5-13 (c, d) shows that for the gable roof, the $C_{pi\_Peak\ (+ve)}$ was 4.0 without VSVs, but reduced to 2.5 with VSVs installed. Likewise, Figure 5-23 (c, d) shows that for the hip roof, the $C_{pi\_Peak\ (+ve)}$ was 3.2 without VSVs, but reduced to 2.0 with VSVs installed.

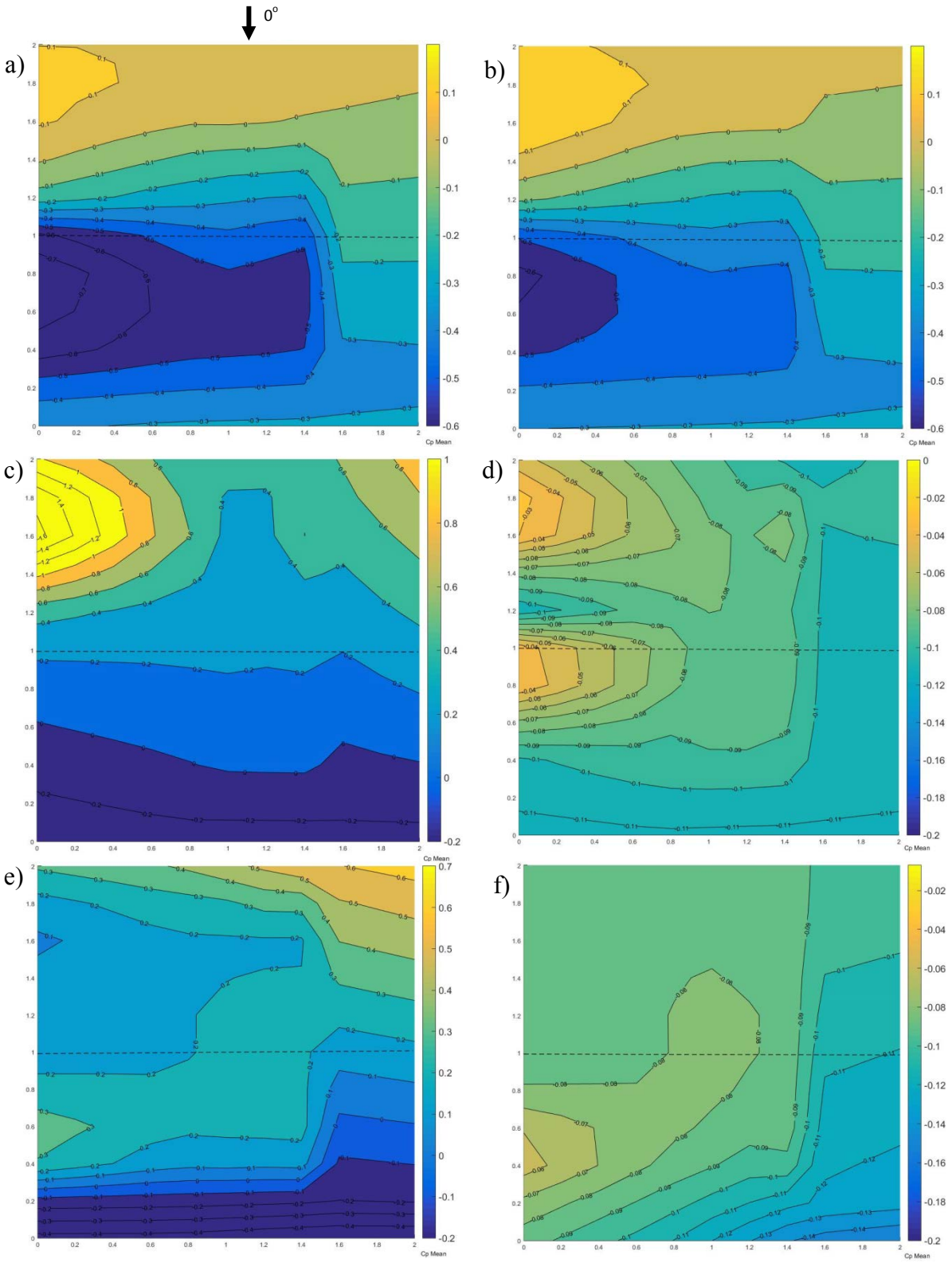

Figure 5-10. Mean pressure coefficients ($C_{p's}$) on the gable roof model for WD = 0°: a) external roof surface without VSVs; b) external roof surface with VSVs; c) internal roof surface without VSVs; d) internal roof surface with VSVs; e) internal attic surface without VSVs; f) internal attic surface with VSVs

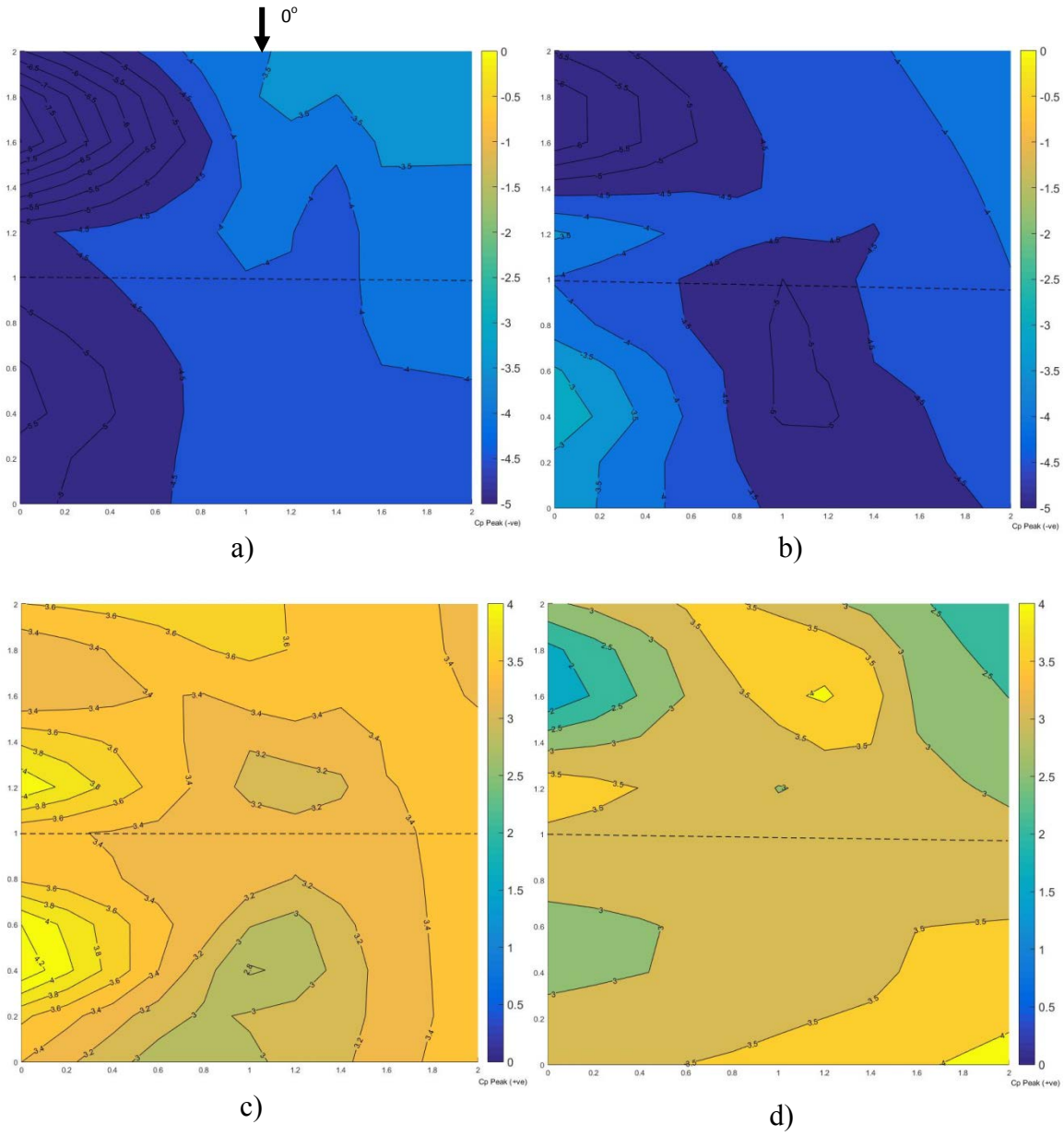

a) b)

c) d)

Figure 5-11. Peak pressure coefficients ($C_{p's}$) on the gable roof model for WD = 0°: a) external roof surface without VSVs (-ve); b) external roof surface with VSVs (-ve); c) internal roof surface without VSVs (+ve); d) internal roof surface with VSVs (+ve)

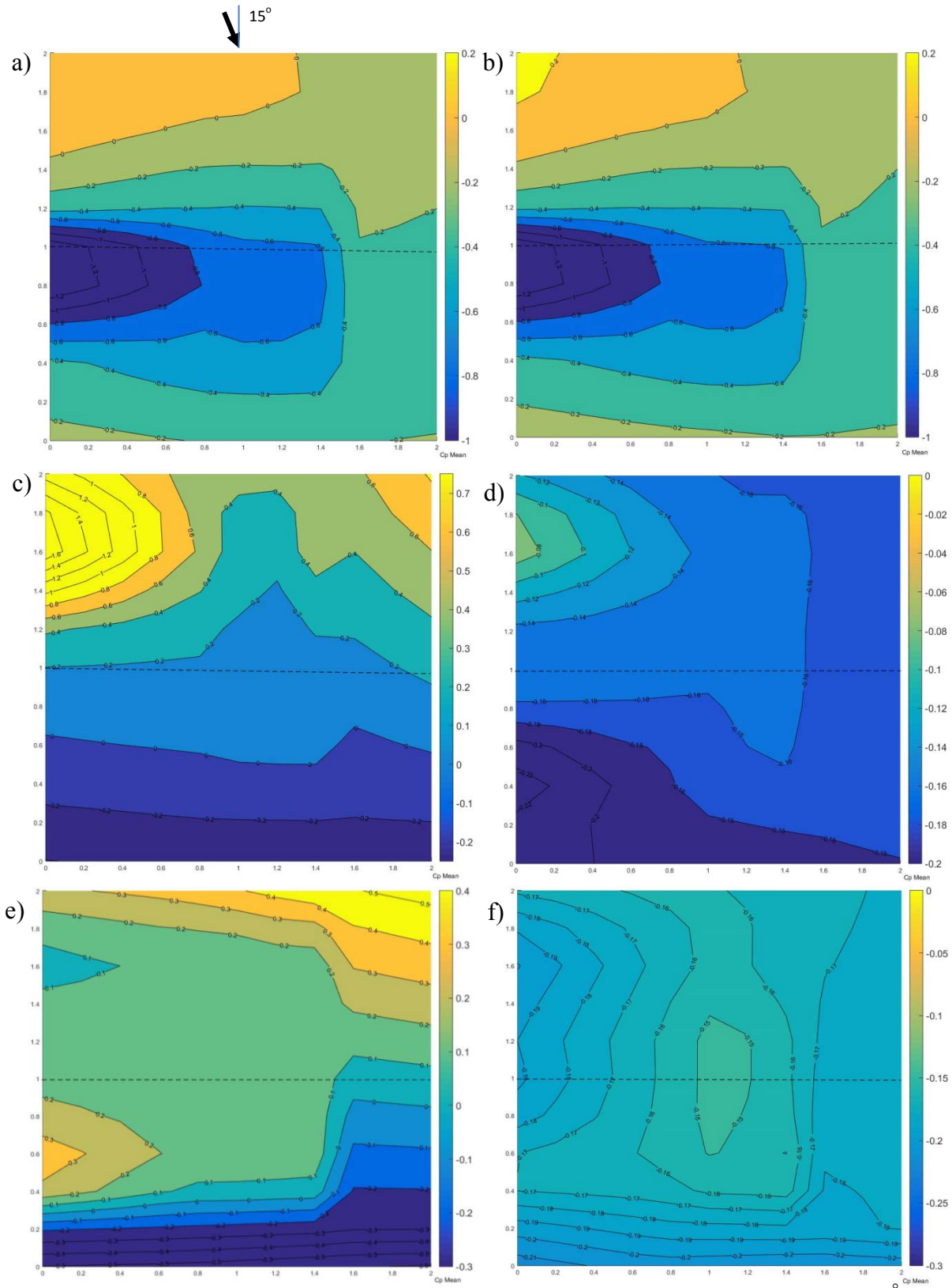

Figure 5-12. Mean pressure coefficients ($C_{p's}$) on the gable roof model for WD = 15°: a) external roof surface without VSVs; b) external roof surface with VSVs; c) internal roof surface without VSVs; d) internal roof surface with VSVs; e) internal attic surface without VSVs; f) internal attic surface with VSVs

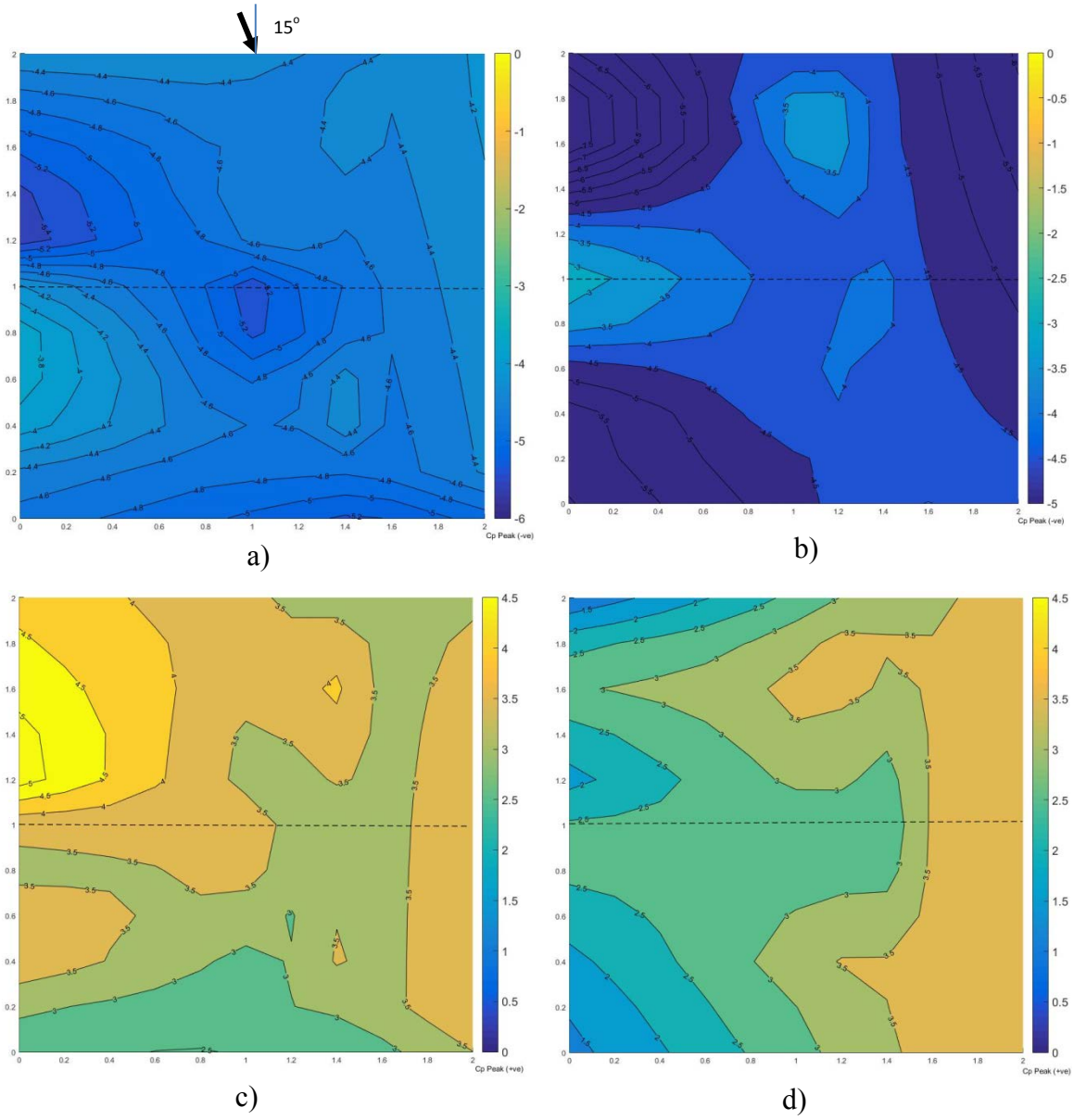

Figure 5-13. Peak pressure coefficients ($C_{p's}$) on the gable roof model for WD = 15°: a) external roof surface without VSVs (-ve); b) external roof surface with VSVs (-ve); c) internal roof surface without VSVs (+ve); d) internal roof surface with VSVs (+ve)

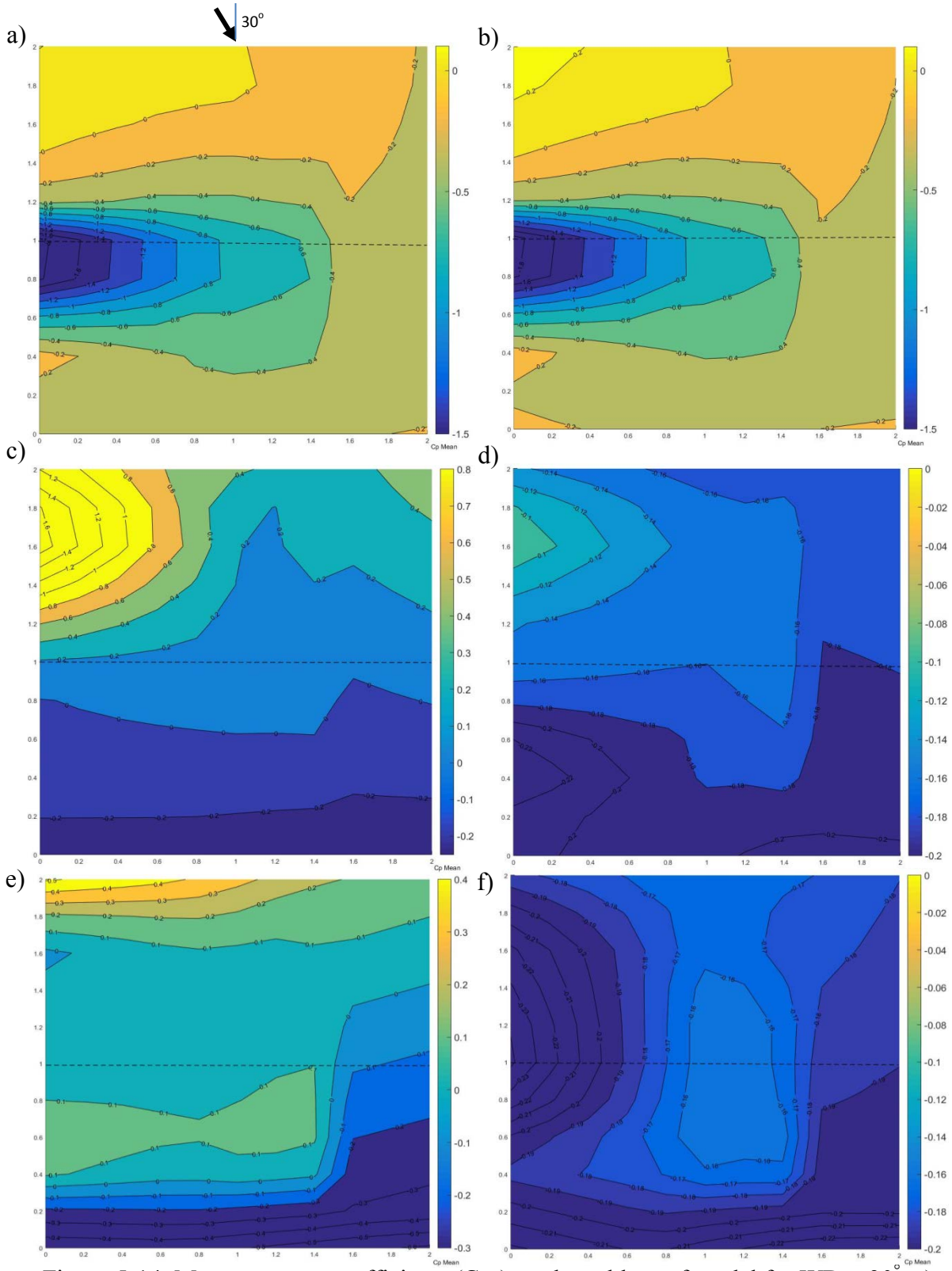

Figure 5-14. Mean pressure coefficients ($C_{p's}$) on the gable roof model for WD = 30°: a) external roof surface without VSVs; b) external roof surface with VSVs; c) internal roof surface without VSVs; d) internal roof surface with VSVs; e) internal attic surface without VSVs; f) internal attic surface with VSVs

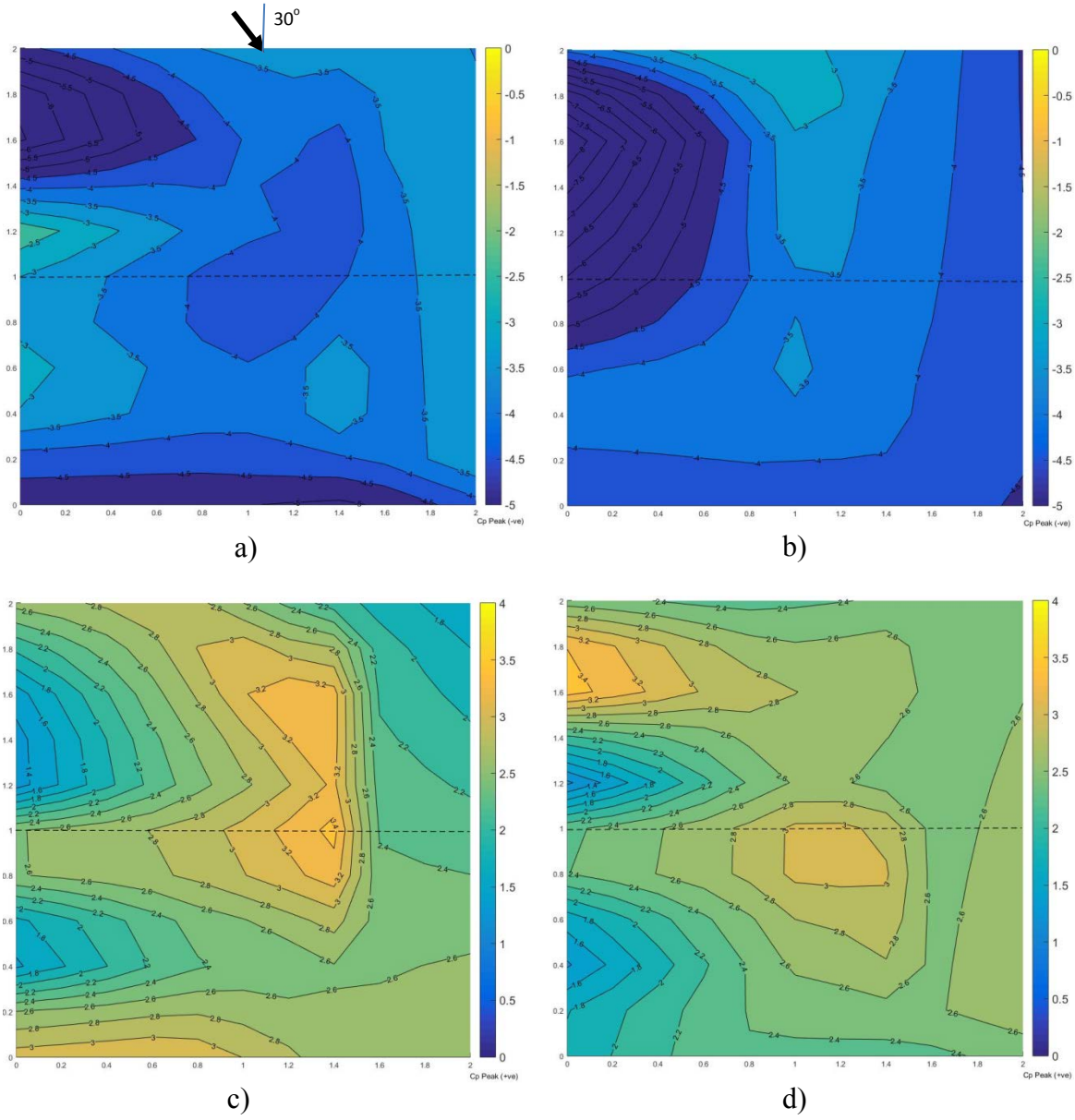

a) b)

c) d)

Figure 5-15. Peak pressure coefficients ($C_{p's}$) on the gable roof model for WD = 30°: a) external roof surface without VSVs (-ve); b) external roof surface with VSVs (-ve); c) internal roof surface without VSVs (+ve); d) internal roof surface with VSVs (+ve)

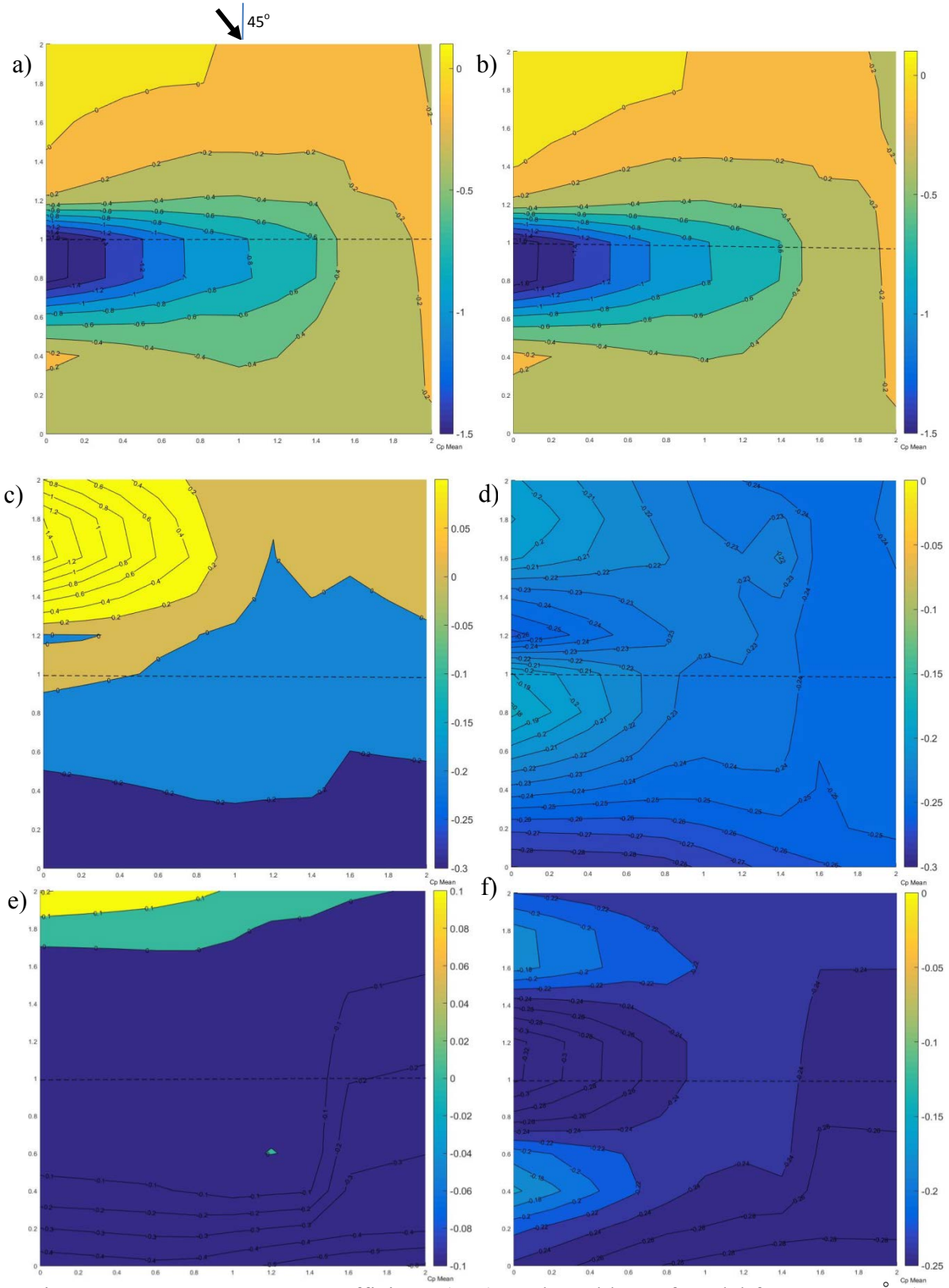

Figure 5-16. Mean pressure coefficients ($C_{p's}$) on the gable roof model for WD = 45°: a) external roof surface without VSVs; b) external roof surface with VSVs; c) internal roof surface without VSVs; d) internal roof surface with VSVs; e) internal attic surface without VSVs; f) internal attic surface with VSVs

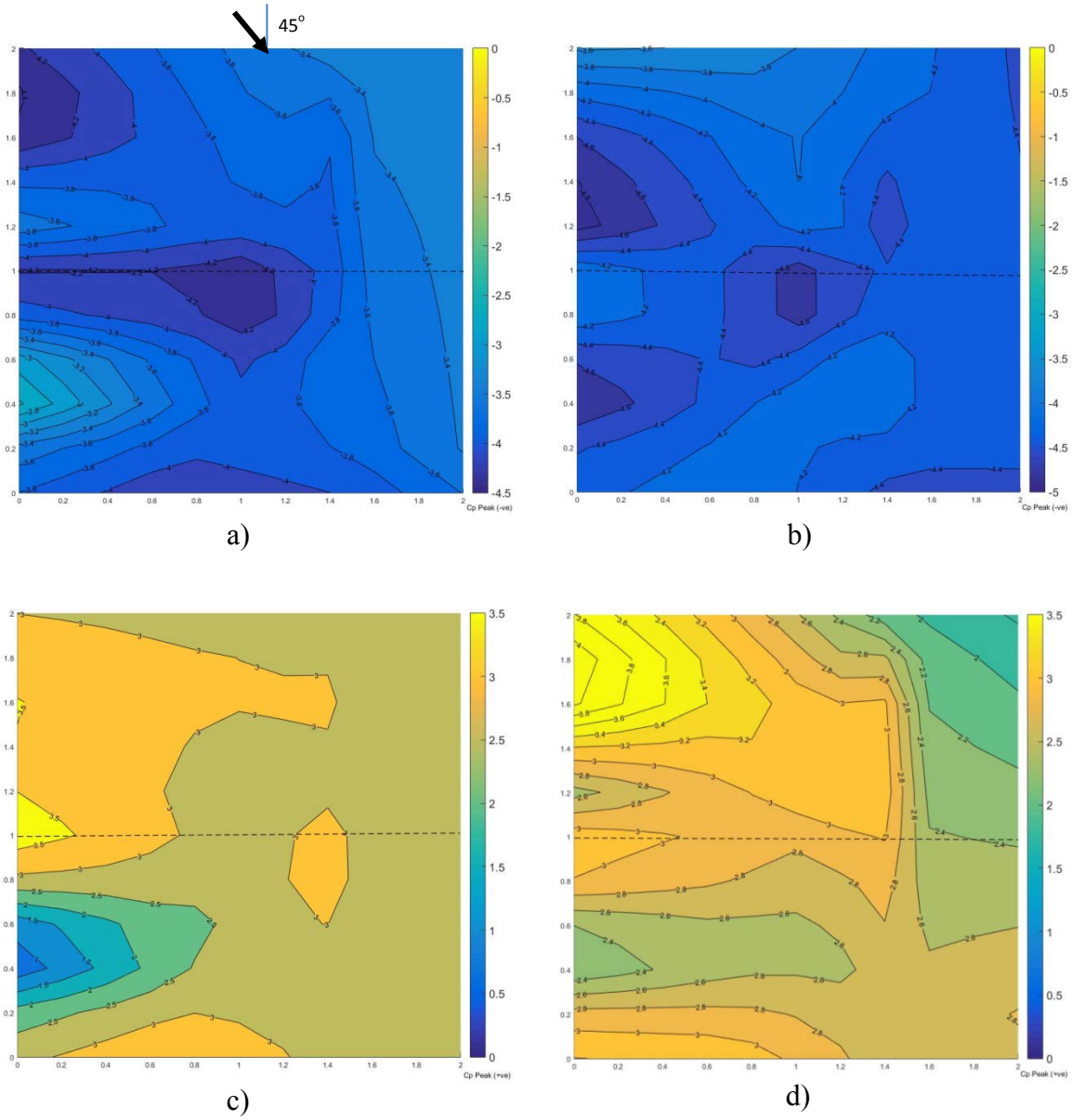

Figure 5-17. Peak pressure coefficients ($C_{p's}$) on the gable roof model for WD = 45°: a) external roof surface without VSVs (-ve); b) external roof surface with VSVs (-ve); c) internal roof surface without VSVs (+ve); d) internal roof surface with VSVs (+ve)

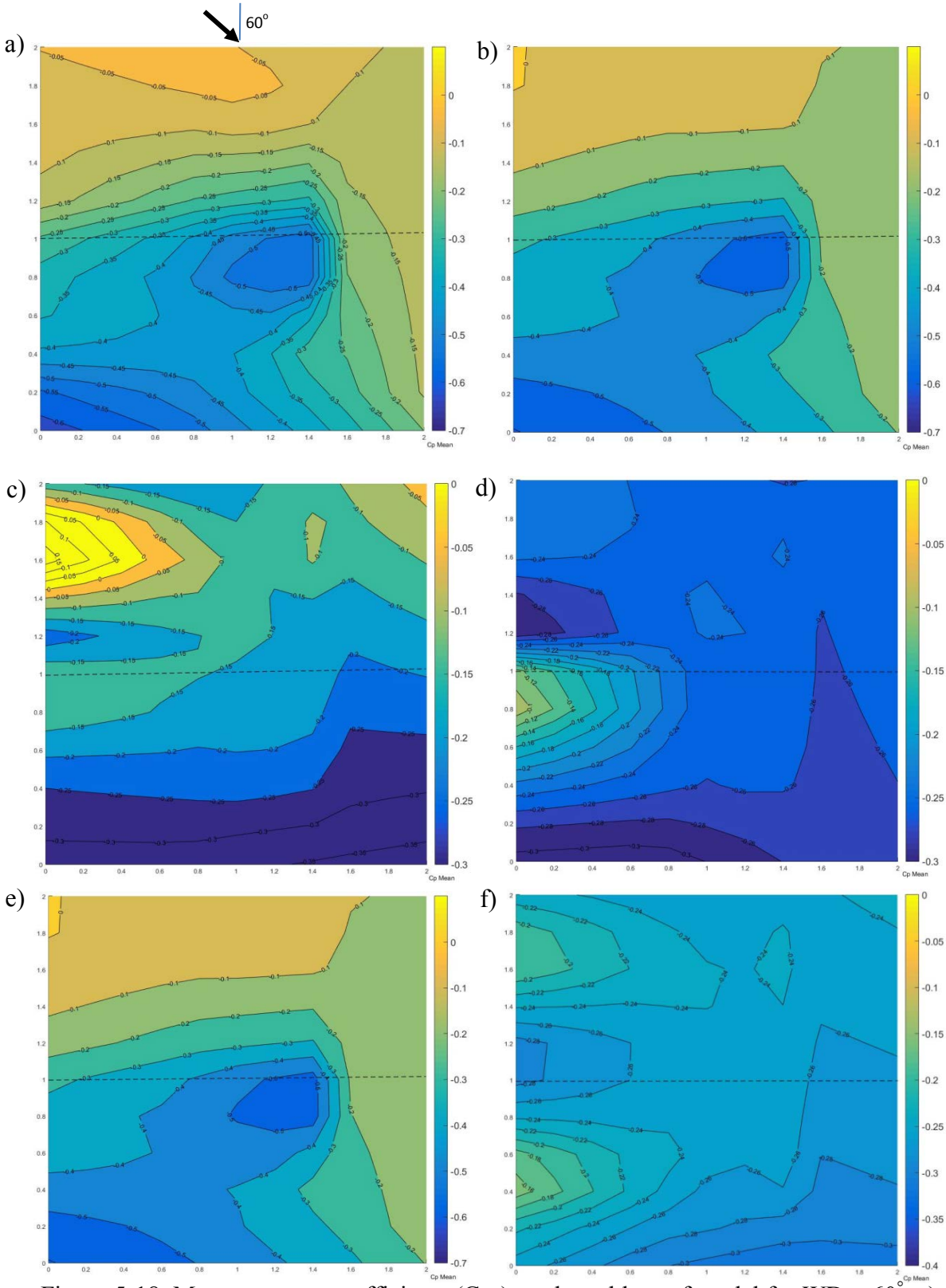

Figure 5-18. Mean pressure coefficients ($C_{p's}$) on the gable roof model for WD = 60°: a) external roof surface without VSVs; b) external roof surface with VSVs; c) internal roof surface without VSVs; d) internal roof surface with VSVs; e) internal attic surface without VSVs; f) internal attic surface with VSVs

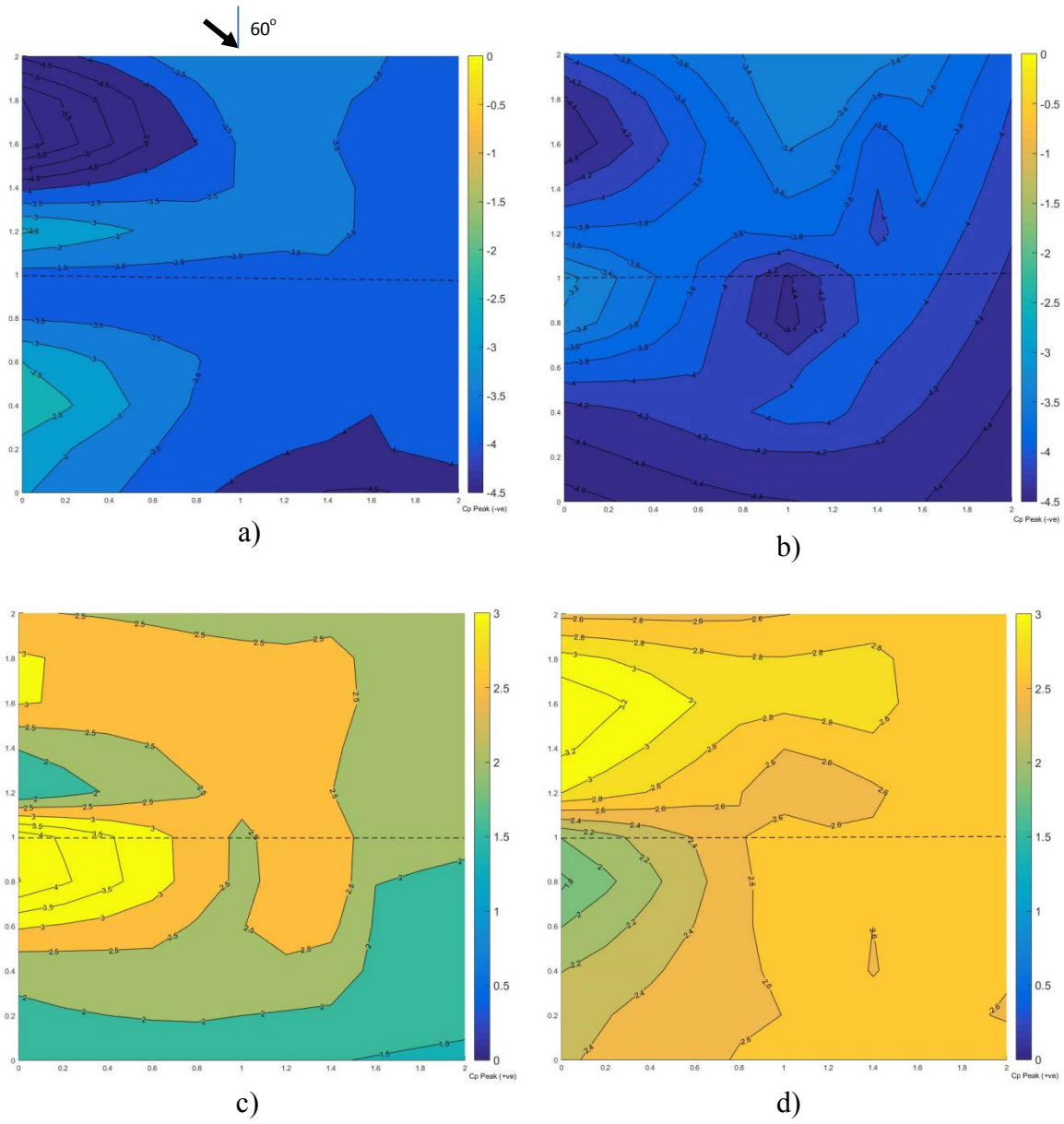

a) b)

c) d)

Figure 5-19. Peak pressure coefficients ($C_{p's}$) on the gable roof model for WD = 60°: a) external roof surface without VSVs (-ve); b) external roof surface with VSVs (-ve); c) internal roof surface without VSVs (+ve); d) internal roof surface with VSVs (+ve)

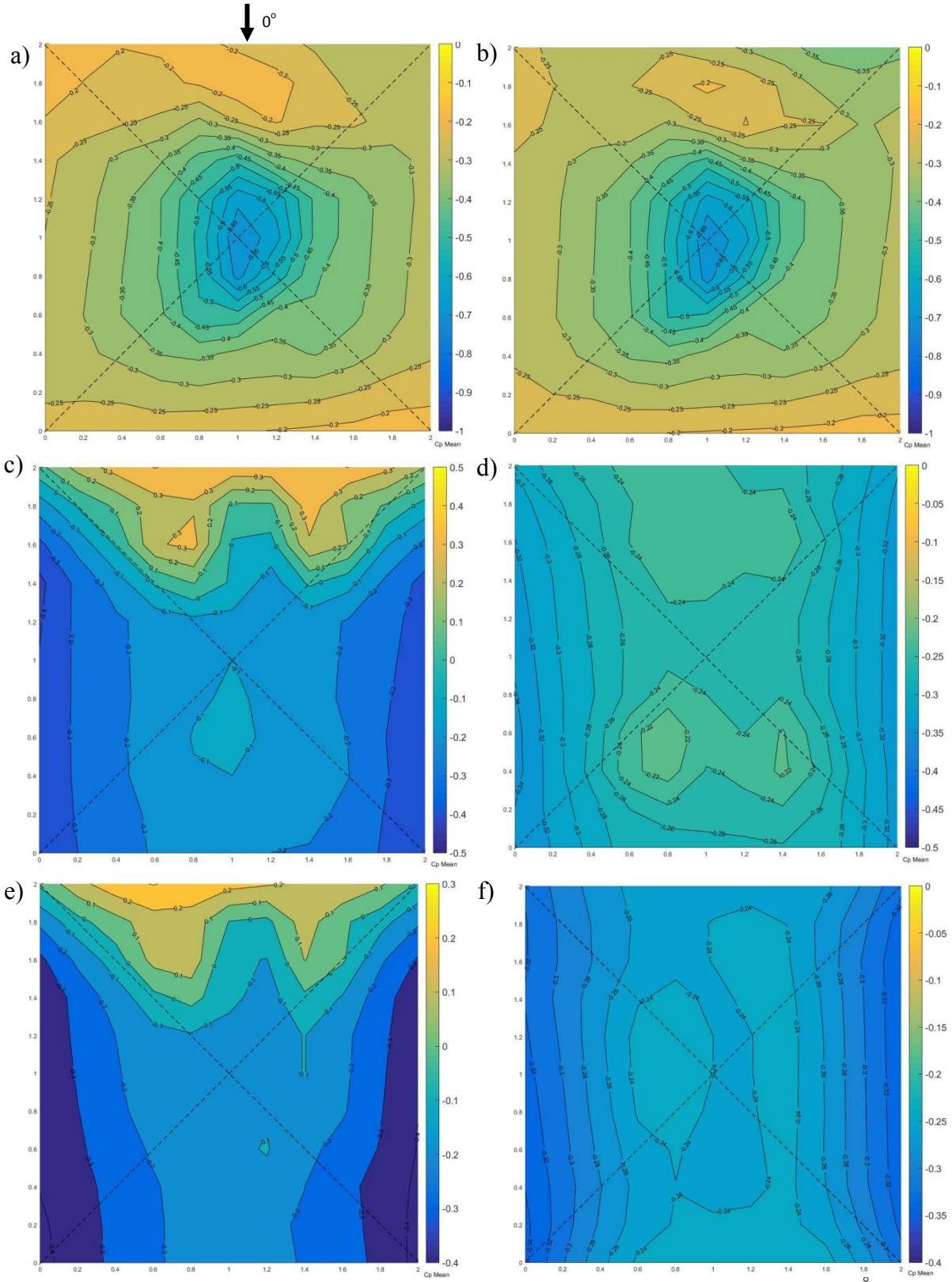

Figure 5-20. Mean pressure coefficients ($C_{p's}$) on the hip roof model for WD = 0°: a) external roof surface without VSVs; b) external roof surface with VSVs; c) internal roof surface without VSVs; d) internal roof surface with VSVs; e) internal attic surface without VSVs; f) internal attic surface with VSVs

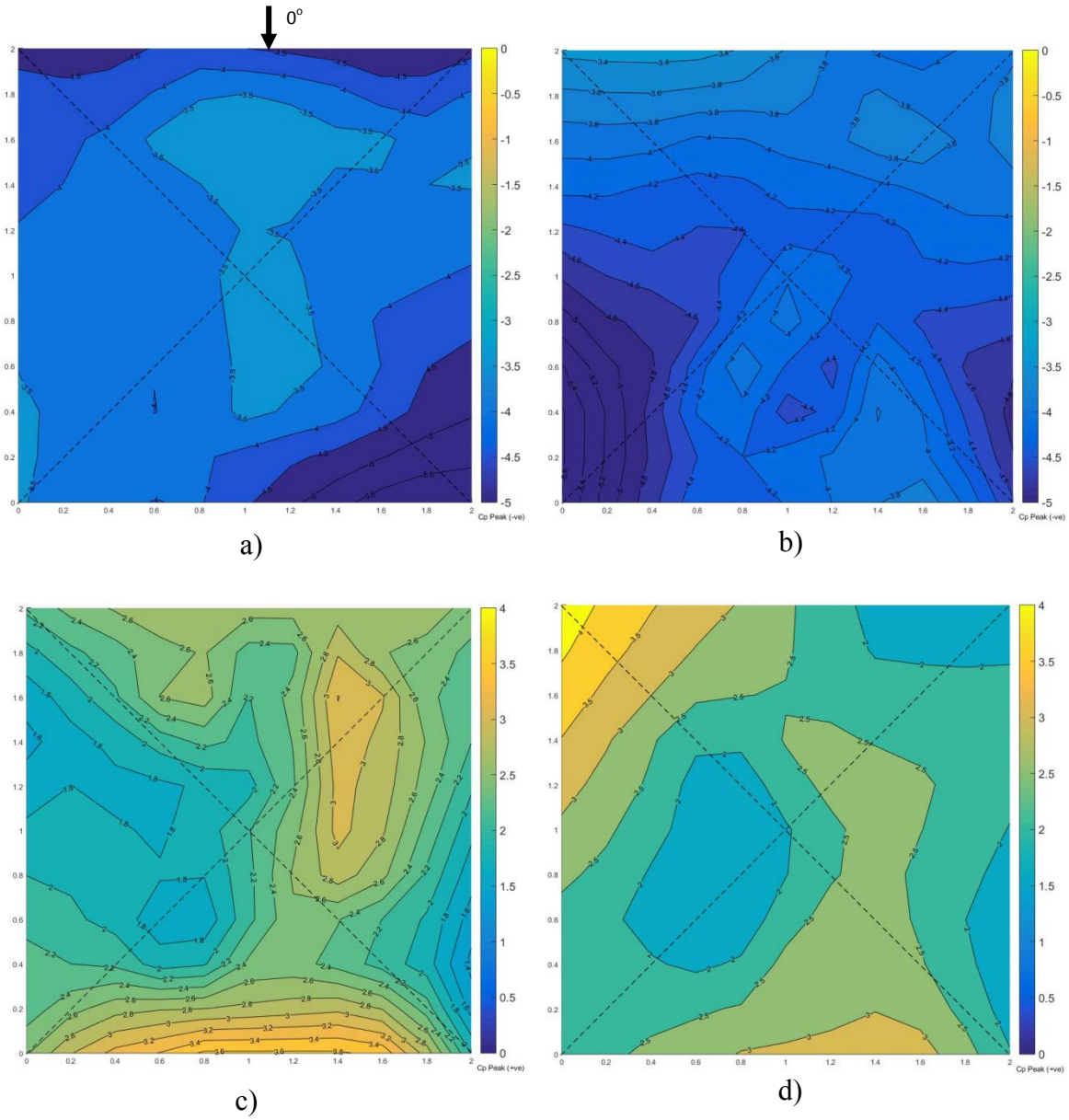

Figure 5-21. Peak pressure coefficients ($C_{p's}$) on the hip roof model for WD = 0°: a) external roof surface without VSVs (-ve); b) external roof surface with VSVs (-ve); c) internal roof surface without VSVs (+ve); d) internal roof surface with VSVs (+ve)

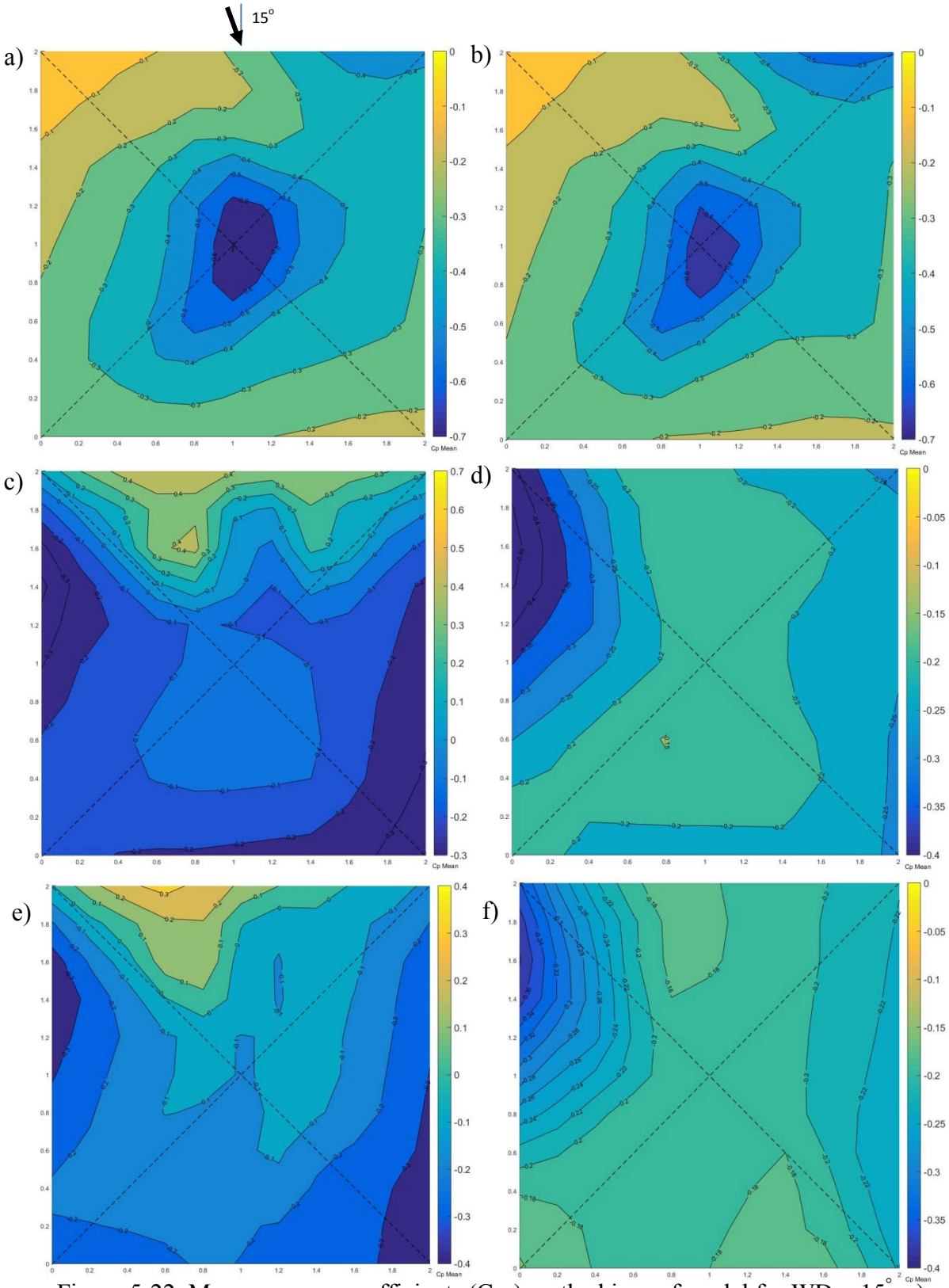

Figure 5-22. Mean pressure coefficients ($C_{p's}$) on the hip roof model for WD = 15° : a) external roof surface without VSVs; b) external roof surface with VSVs; c) internal roof surface without VSVs; d) internal roof surface with VSVs; e) internal attic surface without VSVs; f) internal attic surface with VSVs

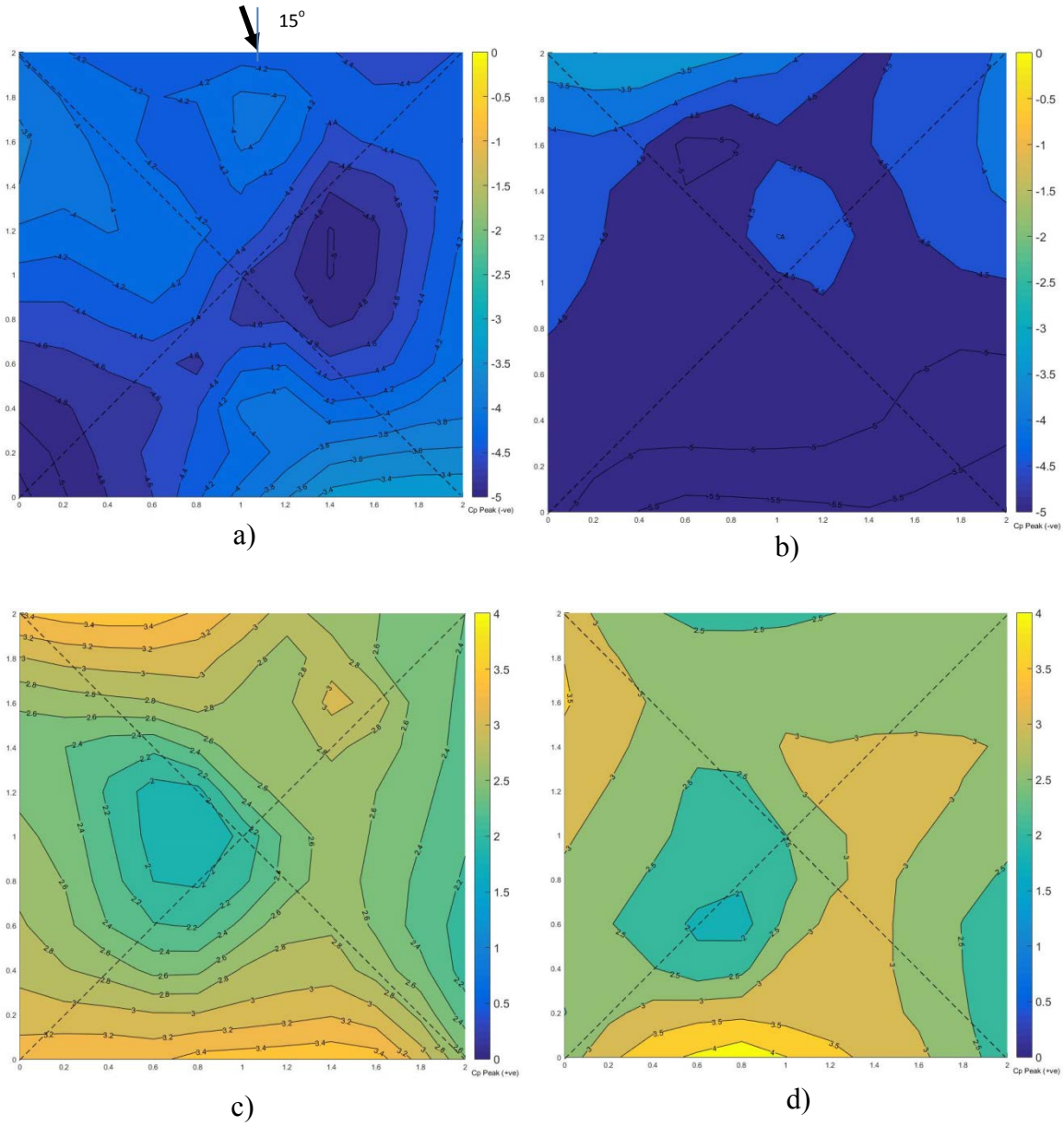

a) b)

c) d)

Figure 5-23. Peak pressure coefficients ($C_{p's}$) on the hip roof model for WD = 15°: a) external roof surface without VSVs (-ve); b) external roof surface with VSVs (-ve); c) internal roof surface without VSVs (+ve); d) internal roof surface with VSVs (+ve)

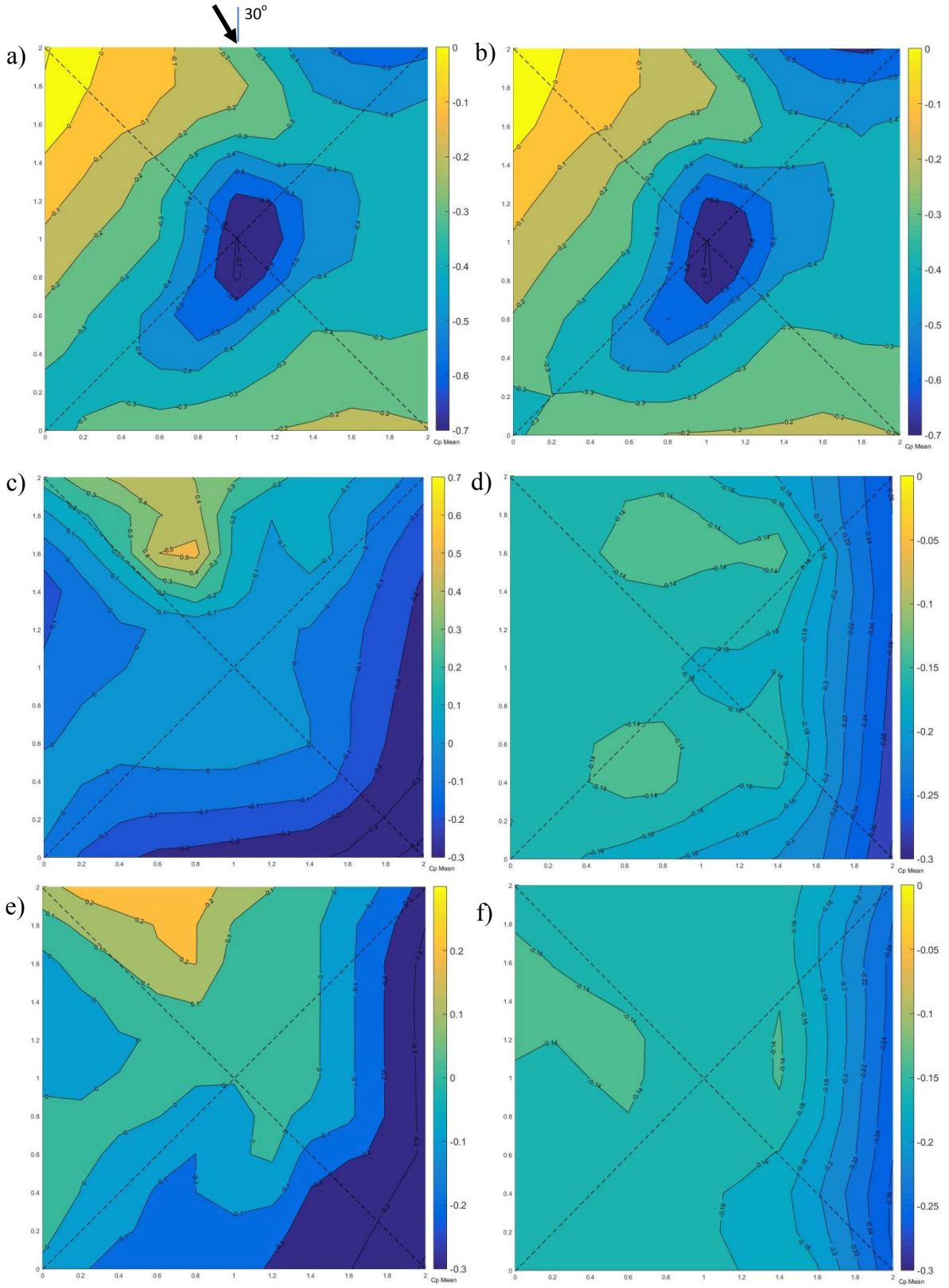

Figure 5-24. Mean pressure coefficients ($C_{p's}$) on the hip roof model for WD = 30°: a) external roof surface without VSVs; b) external roof surface with VSVs; c) internal roof surface without VSVs; d) internal roof surface with VSVs; e) internal attic surface without VSVs; f) internal attic surface with VSVs

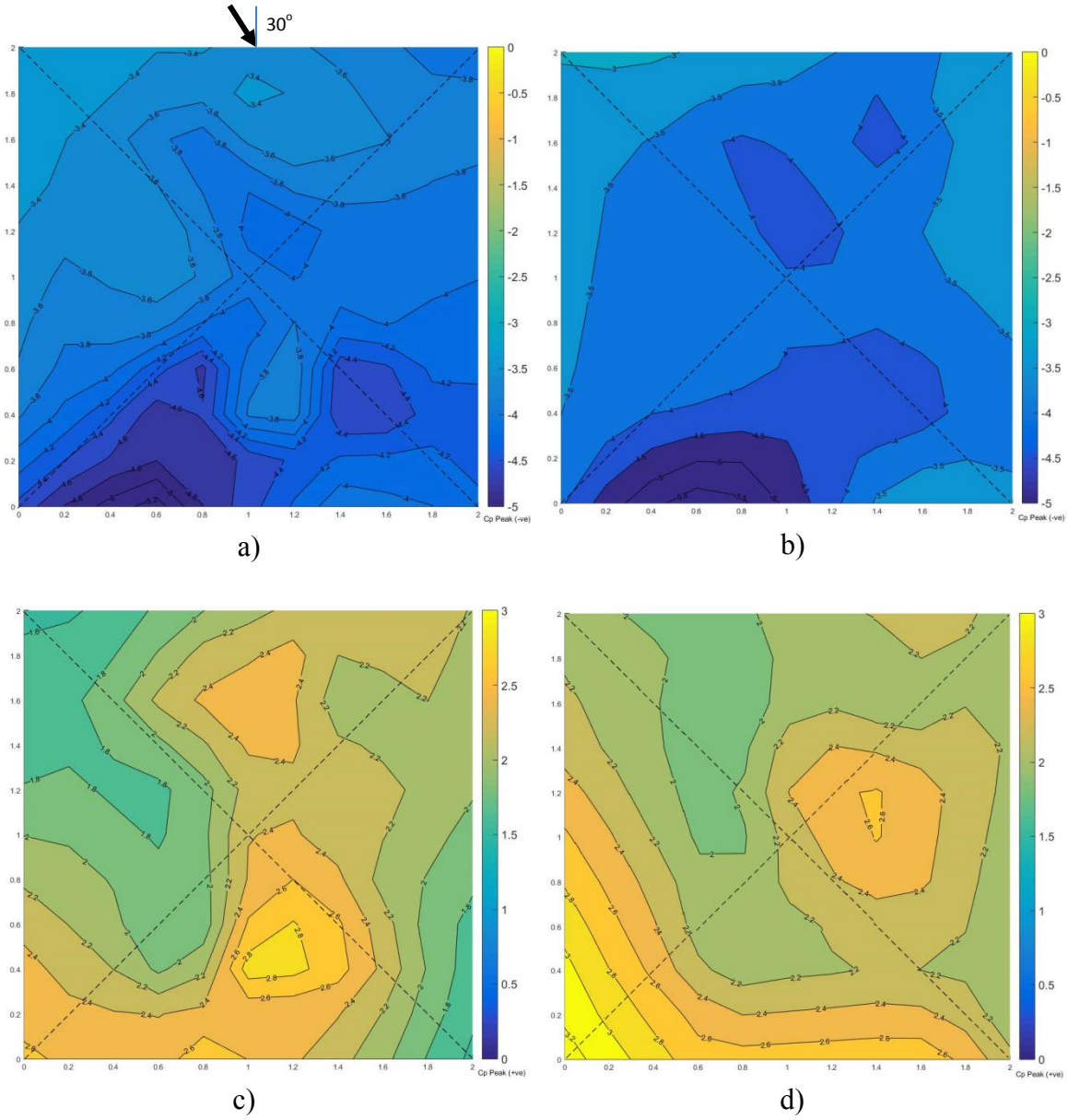

Figure 5-25. Peak pressure coefficients ($C_{p's}$) on the hip roof model for WD = 30°: a) external roof surface without VSVs (-ve); b) external roof surface with VSVs (-ve); c) internal roof surface without VSVs (+ve); d) internal roof surface with VSVs (+ve)

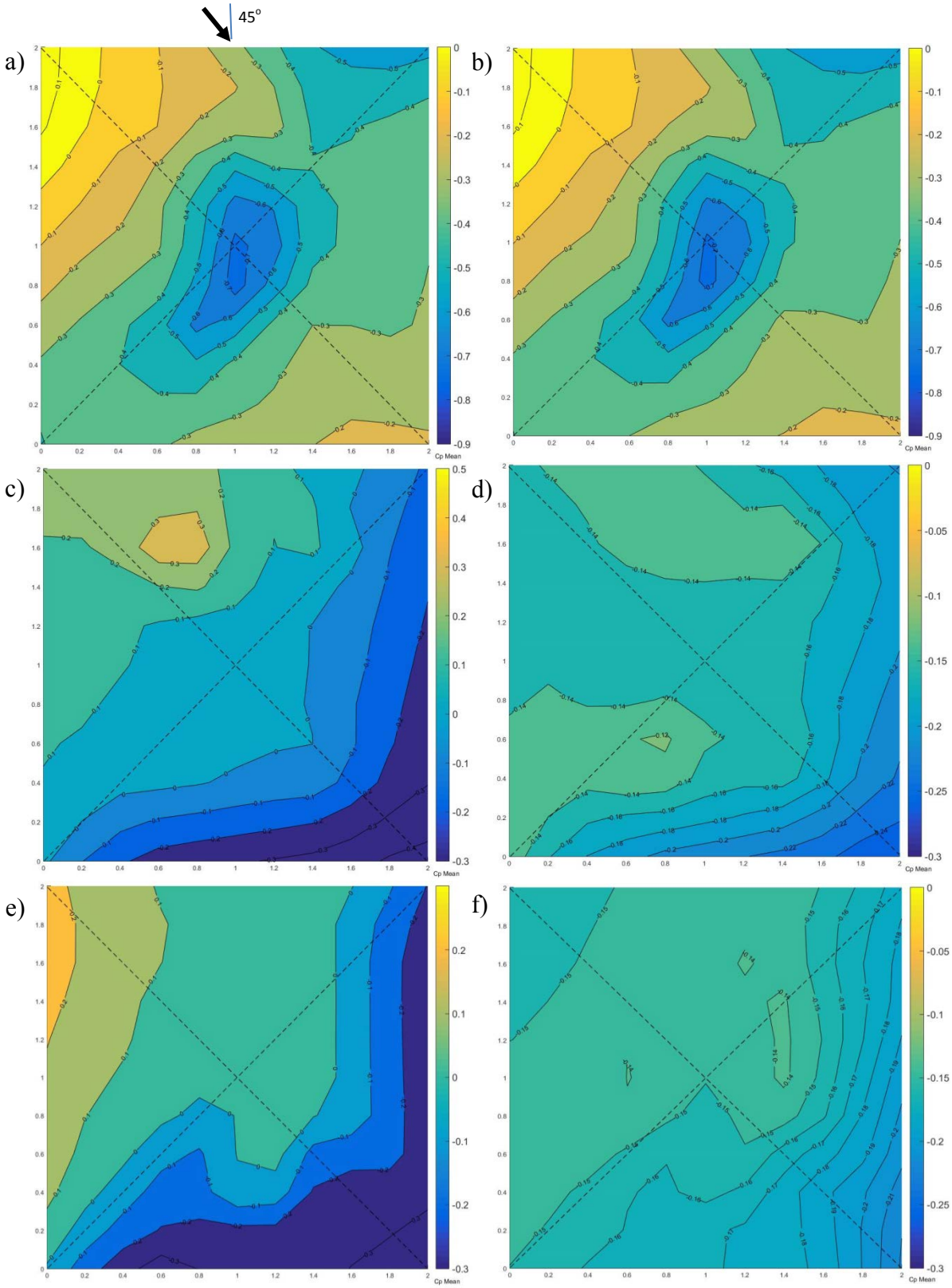

Figure 5-26. Mean pressure coefficients ($C_{p's}$) on the hip roof model for WD = 45°: a) external roof surface without VSVs; b) external roof surface with VSVs; c) internal roof surface without VSVs; d) internal roof surface with VSVs; e) internal attic surface without VSVs; f) internal attic surface with VSVs

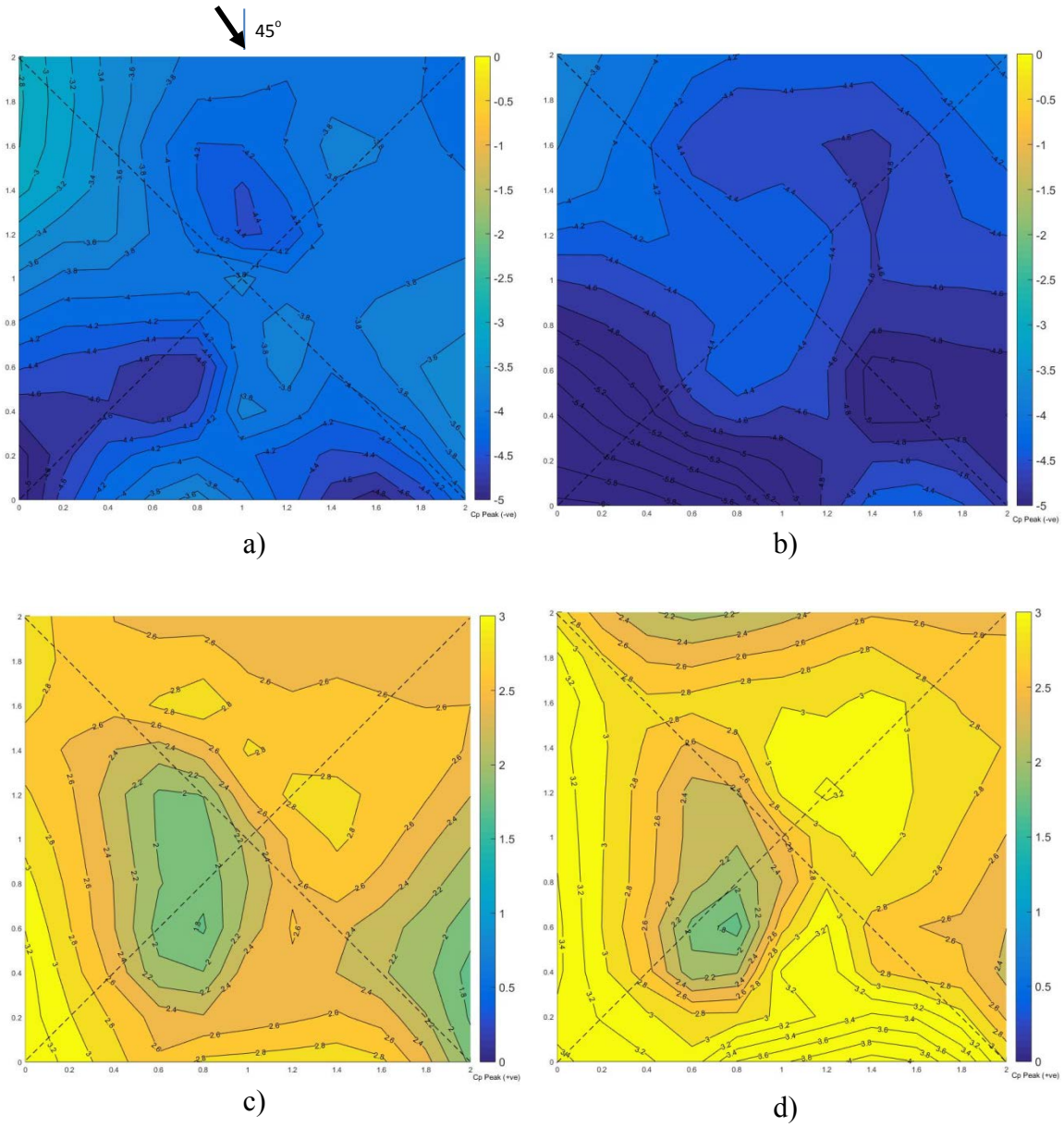

a) b)

c) d)

Figure 5-27. Peak pressure coefficients ($C_{p's}$) on the hip roof model for WD = 45°: a) external roof surface without VSVs (-ve); b) external roof surface with VSVs (-ve); c) internal roof surface without VSVs (+ve); d) internal roof surface with VSVs (+ve)

Net Pressure on Roof Envelope

The internal pressures in the absence of valved soffit vents can contribute to the overall wind induced loading on the roof. For a typical windward soffit opening, the internal pressure will combine with the external suctions on the roof, thereby increasing the loading. Therefore, the characteristics of the internal pressure induced through the soffit openings (without and with VSVs) and the extent to which it combines with suction on the roof envelope are important.

The mean and peak C_p values of the net pressure on the roof envelope are obtained by a summation of the external and internal pressures acting upon the surface. Thus, the net pressure coefficients are determined by the following equation:

C_{p_Net} = exterior roof surface $C_{pe(Mean/Peak\ (-ve)}$-interior roof surface $C_{pi(Mean/Peak\ (+ve)}$ (5.4)

Two cases were considered in the analysis of the net pressure on the roof, Case 1 (without VSVs) and Case 2 (with VSVs). The area averaged external and internal pressure coefficients at the windward vent locations were examined, which would be equivalent to Zone 2 in *ASCE 7-10* for components and cladding. For the gable and hip roofs, this included Vent #1 (V1) and Vent #2 (V2). The vent locations are shown on Figures 5-4 and 5-5. Figure 5-28 illustrates the net mean and peak pressure coefficients for both roofs. In addition, Figure 5-29 shows the net mean pressure coefficients for the complete roof area for both roofs (hip and gable). With the VSVs installed, the net mean $C_{p's}$ increase by 56.5-65% for the hip roof and by 66.7-91% for the gable roof for the 0 to 45 and 60 degree wind directions.

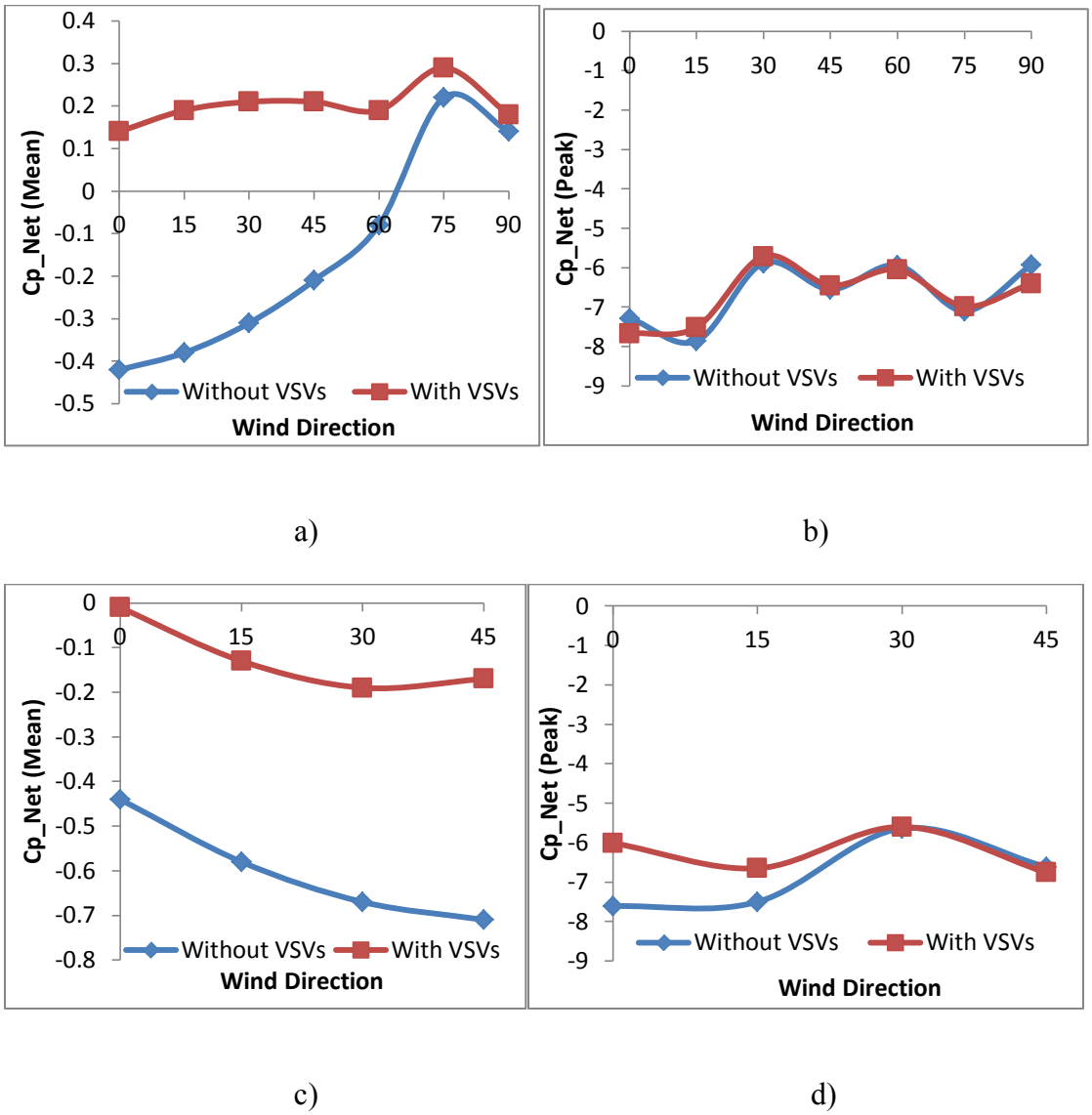

a) b)

c) d)

Figure 5-28. Net mean and peak pressure coefficients: a) gable roof (mean); b) gable roof (peak); c) hip roof (mean); d) hip roof (peak)

The results showed that for the gable and hip roofs, the net mean pressure coefficients consistently increased when the VSVs were installed, thus confirming the hypothesis that the VSVs can be utilized to reduce suction on the roof. For the gable roof, the net mean $C_{p's}$ changed from negative (suction) to positive on the roof envelope with VSVs

installed for wind directions of 0 to 60 degrees (Figure 5-28 (a)). However, the net peak $C_{p's}$ did not change markedly. For the hip roof, the net mean $C_{p's}$ increased by over 70% for all wind directions, thereby reducing suction on the roof. The highest increase to the net mean values was at the 0° wind direction (Figure 5-28 (c)). The VSVs clearly have an effect on the differential pressure acting on the roof envelope, which help reduce suctions on the external roof sheathing, thereby preventing possible roof fly-off due to the wind.

The hip roof results also demonstrated that the net peak pressure coefficients increased by 21% and 11.3% for the 0 and 15 degree wind directions respectively, assuming that the peak external and internal pressure coefficients are simultaneous in time. Thus, suggesting that the VSVs can provide a reduction in roof loading at the windward leading edge of the roof.

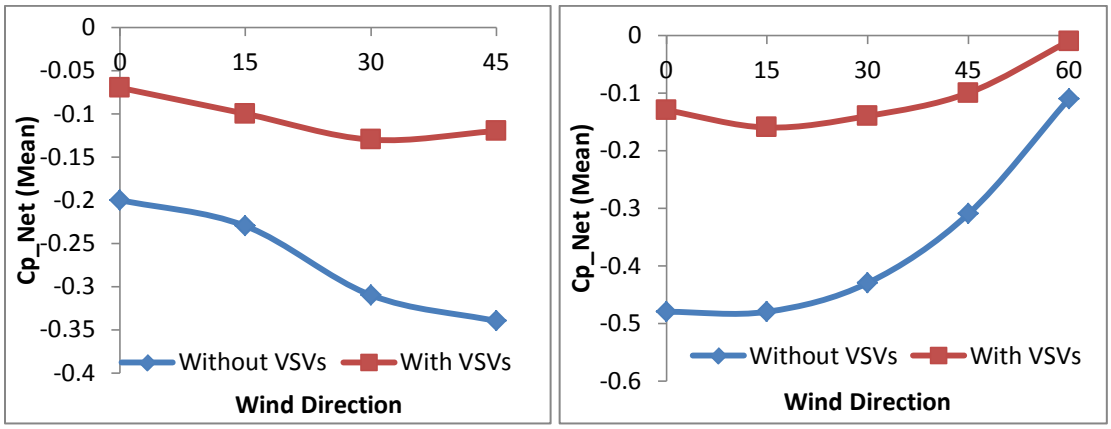

a) b)

Figure 5-29. Net averaged mean pressure coefficients for the complete roof area: a) hip roof b) gable roof

Wind-Driven Rain Test Results

The water entry through the soffit openings without and with valved soffit vents (VSVs) was evaluated by comparing the volume of water entering the attic space. For both wind directions (0° and 45°), the test case with VSVs prevented water entry into the attic. At the completion of the test with VSVs, there were only very small traces of water entry, which could not be measured. However, the tests without VSVs showed that significant amounts of water entered the attic. For the 0° wind direction, the total volume of water that entered the attic was 0.154 gal (583 ml), which is equivalent to 1.85 gal (7 liters) of water entering during a one hour period. There was less water entry recorded for the 45° wind direction without VSVs (0.011 gal (41.26 ml)). A summary of the WDR test results are shown in Table 5-6.

Table 5-6. WDR water entry measurements for the hip roof model

Test No.	Wind Direction	Soffit Opening Condition	Measured Accumulation
1	0°	Without VSVs	0.154 gal (583 ml)
2	0°	With VSVs	Small traces (unmeasurable)
3	45°	Without VSVs	0.011 gal (41.26 ml)
4	45°	With VSVs	Small traces (unmeasurable)

The results of the wind-driven rain testing determined that only small traces of water entered the attic space when the VSVs were installed, demonstrating the effectiveness of the VSVs in preventing water entry.

a)

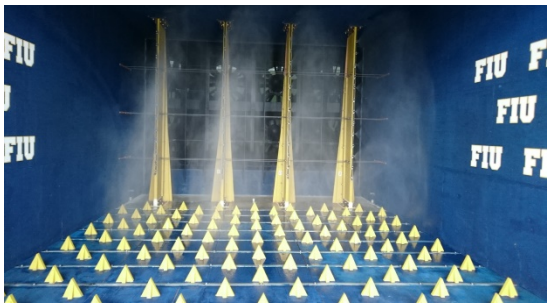

b)

c)

d)

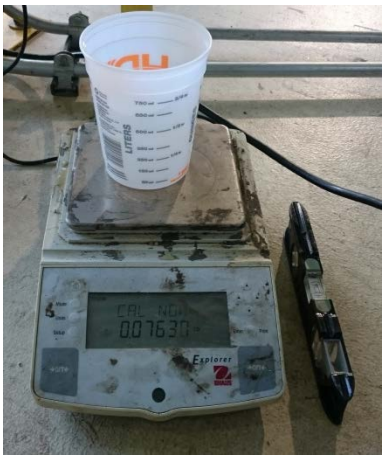

e)

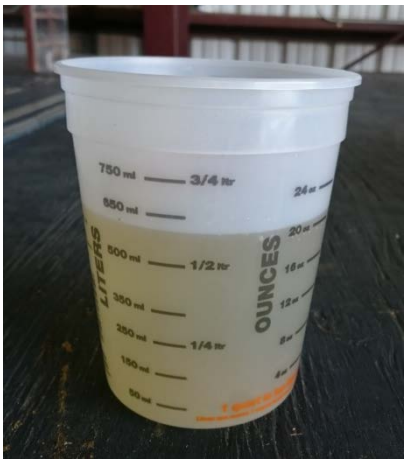

f)

Figure 5-30. a) Plastic membrane used to collect water; b) WOW spray nozzles, pre-test check; c) test specimen with access door removed to check water entry; d) water captured for the 0° wind direction, without VSVs ; e) weighing dry container; f) measured volume of water that entered the attic for the 0° wind direction, without VSVs

CFD Simulation and Validation of Mean Internal Pressures

Computational Fluid Dynamics (CFD) simulations were conducted using the commercial software STAR-CCM+ v. 9.06.009 to validate the mean internal pressure experiments performed at the WOW. The geometrical modeling for the CFD simulations was based on the dimensions of the gable and hip test models used for this study. The CFD evaluation was performed on both the gable and hip roofs for the 0 and 45 degree wind directions for the test cases without VSVs and with VSVs.

A 3D steady (time-averaged) Reynolds Averaged Navier-Stokes (RANS) together with the Realizable K-Epsilon model with two-layer wall treatment was adopted as the governing turbulence model of the flow field. As recommended by COST Action 732 (COST732, 2007), the computational domain (CD) was established using the height (H) of the test model as a reference. The CD was extended vertically and laterally by 5H from the model building. However, the outflow boundary was extended 15H from the back wall to allow for flow re-development.

The mean velocity of the approach flow was the same as the mean wind speed used in the WOW (57.4 mph at roof eave height). However, a turbulence intensity of 0.17 was selected to represent the total turbulence intensity. The surface and volume mesh was automatically generated by STAR-CCM+ using the Polyhedral Mesher option. The mesh consisted of 1.1 million cells (Figure 5-31).

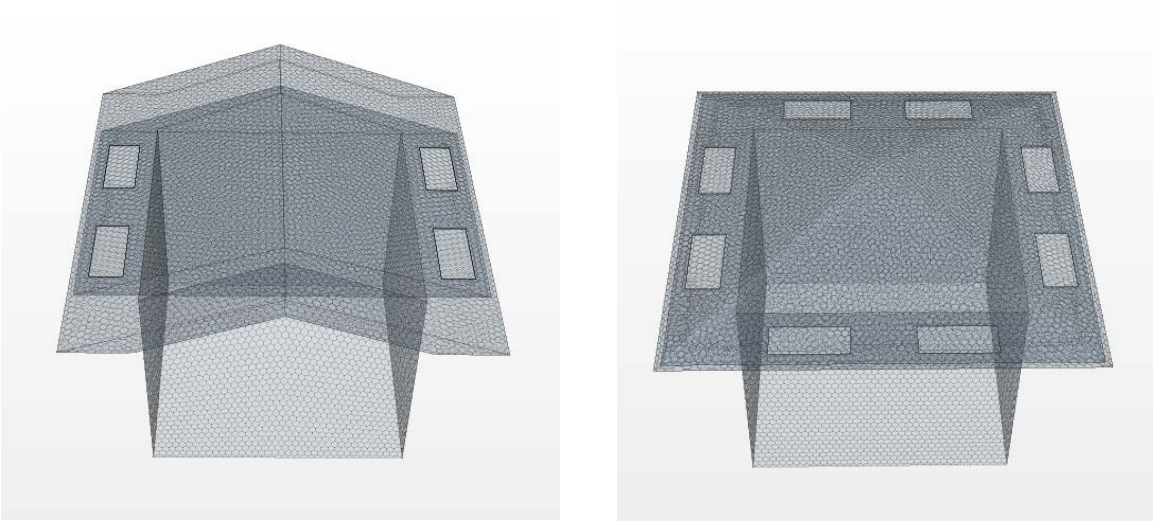

a) b)

Figure 5-31. CFD models with polyhedral mesh: a) gable roof; b) hip roof

The velocity flow fields are illustrated in Figures 5-32 to 5-35 for the gable and hip roofs for 0° and 45° wind directions. The RANS Realizable K-Epsilon model captured the wake circulation behind the building, in addition to the flow separation at the sides. Except for the gable roof at the 45° wind direction, the vortices and recirculating flow were all symmetrical, forming a horseshoe vortex. The gable roof formed a small and large recirculating vortex for the 45° wind direction. Figure 5-36 shows the mean external pressure distribution for the gable and hip roofs for the 45° wind direction.

CFD Results

Tables 5-7 and 5-8 show the measured and CFD predicted mean internal pressure values. The mean C_{pi} values were measured at each individual pressure tap on the attic floor between Vents 1 and 4 (V1 and V4) for the gable roof and between Vents 1 and 6 (V1 and V6) for the hip roof. The values were then numerically averaged to obtain the

mean C_{pi} for each roof. The mean internal pressure values from the CFD simulations were obtained by using a line probe which matched the experimental pressure tap layouts.

Table 5-7. CFD and experimental mean C_{pi} comparisons for the gable roof model

Wind Direction	Soffit Opening	Mean Cpi CFD	Mean Cpi WOW
0°	Without VSVs	0.09	0.17
0°	With VSVs	-0.44	-0.09
45°	Without VSVs	-0.26	-0.04
45°	With VSVs	-0.61	-0.23

Table 5-8. CFD and experimental mean C_{pi} comparisons for the hip roof model

Wind Direction	Soffit Opening	Mean Cpi CFD	Mean Cpi WOW
0°	Without VSVs	-0.35	-0.30
0°	With VSVs	-0.46	-0.31
45°	Without VSVs	-0.17	-0.07
45°	With VSVs	-0.44	-0.17

The results demonstrated that the mean internal pressure coefficients obtained through CFD modeling also decreased when the VSVs were installed. However, the CFD simulation appears to under-predict the mean $C_{pi's.}$ This can be attributed to the limitation of the turbulence model in capturing some of the complex three-dimensional flow phenomena around the building. A more sophisticated and advanced turbulence model, such as a large eddy simulation (LES), should improve the CFD predicted mean internal pressure coefficients. Generally, it can be concluded that CFD simulations can be used as an alternative tool for preliminary investigations in predicting mean internal pressures within the attic space for roofs without and with VSVs.

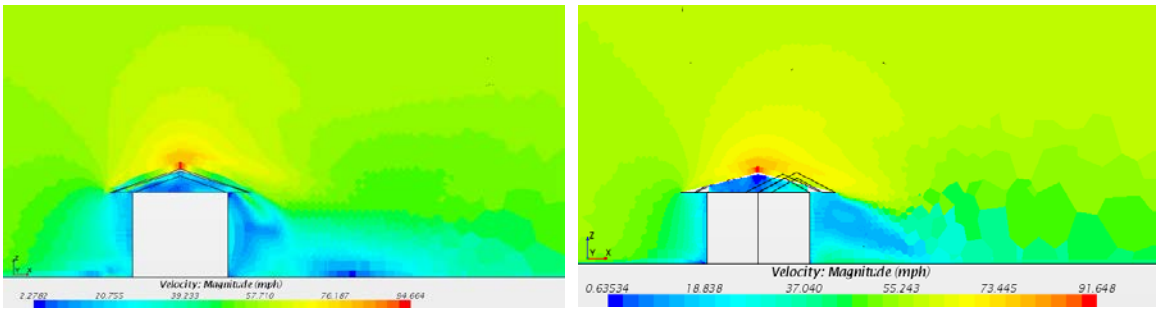

Figure 5-32. The velocity flow field: vertical plane at centerline for the gable roof model for 0° and 45° wind directions

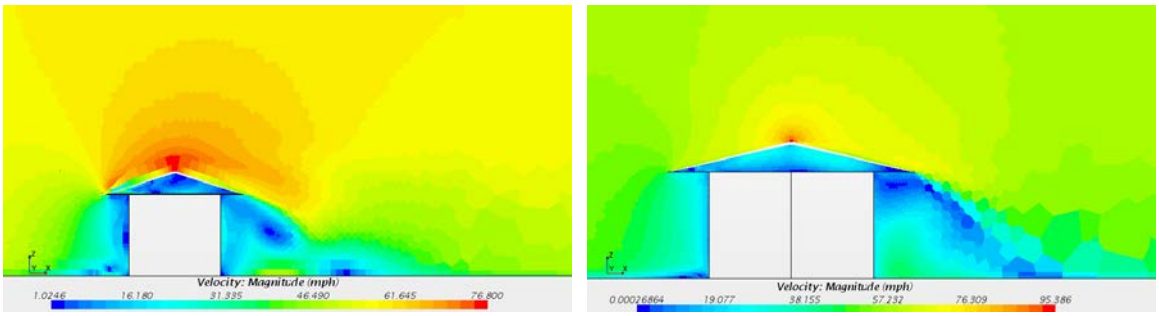

Figure 5-33. The velocity flow field: vertical plane at centerline for the hip roof model for 0° and 45° wind directions

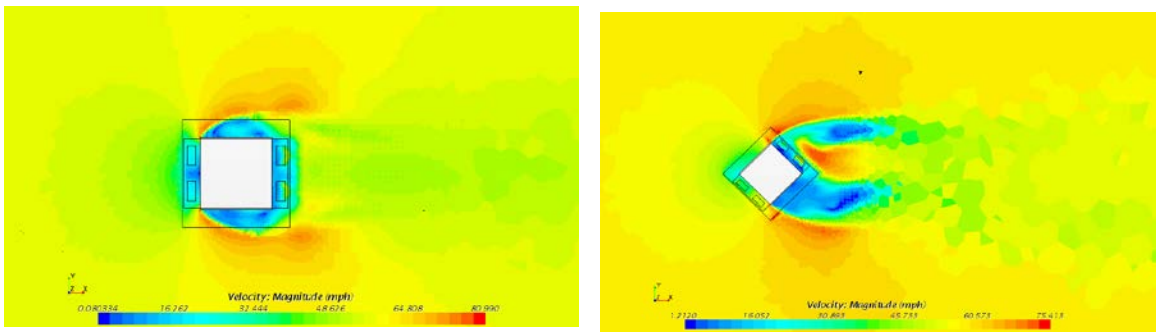

Figure 5-34. The velocity flow field: horizontal plane at 1.2 m for the gable roof model for 0° and 45° wind directions

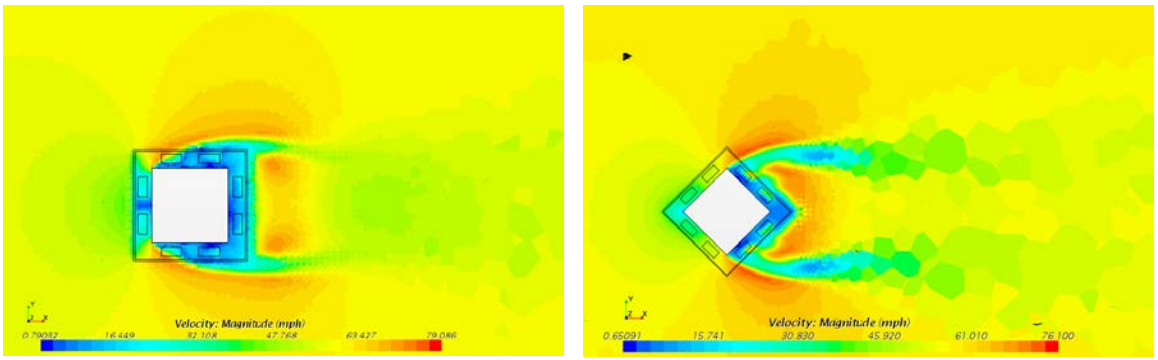

Figure 5-35. The velocity flow field: horizontal plane at 1.2 m for the hip roof model for 0° and 45° wind directions

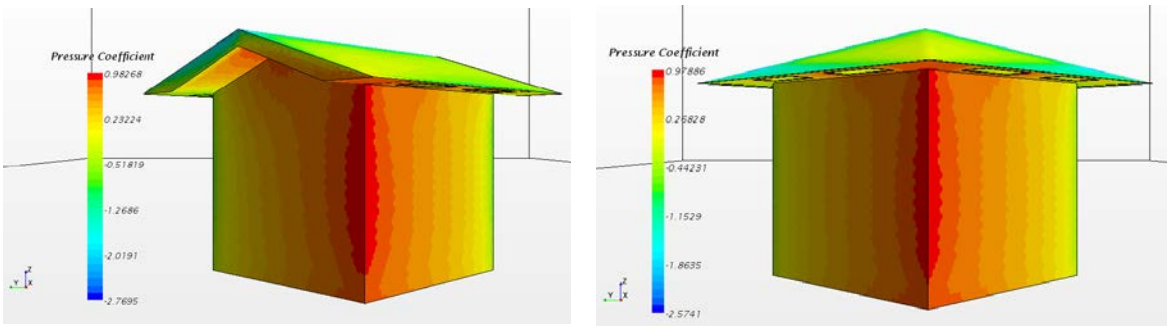

Figure 5-36. Mean external pressure coefficients for the gable and hip roofs, 45° wind direction

Conclusions

This study evaluated the performance of valved soffit vents (VSVs) installed on a gable and a hip roof in a large-scale wind tunnel environment. External and internal pressure measurements were recorded on each roof for various wind directions in an open terrain. Prior to conducting wind pressure tests, a variable speed examination was performed to establish the wind speed that fully activated the VSVs at all wind directions. The testing also investigated potential water entry mitigation into the attic space using valved soffit vents (VSVs) under wind-driven rain (WDR) simulation. The experimental study was conducted at the International Hurricane Research Center's (IHRC) Wall of Wind (WOW) facility at Florida International University (FIU) in Miami, Florida. Two main test cases were evaluated: soffit openings without VSVs and soffit openings with VSVs. The valved soffit vents used for the testing are patented by Building Performance Americas, USA (BPA) and are termed, *BPA Safety Vents.*

It was determined from the variable wind speed evaluation that the VSVs prevent air entry into the attic space at wind speeds greater than 10 m/s (23 mph) by allowing the wind induced positive pressure to shut the vent, thereby closing the opening. A wind speed of 25.7 m/s (57.4 mph), referenced at the roof eave height 4'-2" (1.27 m), was found to activate the VSVs at all wind directions. This wind speed was selected as the testing speed for this study, which is equivalent to a 3-second gust wind speed of 39 m/s (87 mph) at roof eave height.

The mean and peak pressure coefficients were measured on the external and internal roof surfaces, including on the floor of the building attic. Results revealed that the mean

external pressure coefficients did not change markedly for both of the cases on the exterior roof locations. However, the mean pressure coefficients were consistently reduced in magnitude (greater suction) in the interior locations with the VSVs installed.

The net mean $C_{p's}$ increased for the gable and hip roofs for the 0 to 45 and 60 degree wind directions. For the gable roof, the greatest increase was 91% for the 60° wind direction and for the hip roof, the 0° and 45° wind directions produced the highest increase of around 65%. In addition, net mean $C_{p's}$ increased for both roofs at the windward vent locations and leading edge of the roof for the case with VSVs, thereby, producing less suction on the roof sheathing. The net mean values increased as much as 98% for the hip roof for the 0° wind direction. The net mean values for the gable roof changed from negative to positive for the 0 to 60 degree wind directions.

The study also included an investigation of the mean internal pressures with VSVs installed without the exterior screen (Test Case 3). The effect of removing the screen was found to be of little consequence on the mean internal pressures for the roofs with VSVs.

The internal peak positive pressure coefficients were reduced by as much as 44% for the gable roof and 37.5% for the hip roof at localized areas, specifically at the roofs' leading edges and the windward vent locations with VSVs. Moreover, the net peak $C_{p's}$ on the leading edge of the hip roof were increased by 21% and 11.3% for the 0 and 15 degree wind directions respectively, thereby demonstrating the value in using VSVs to mitigate wind induced damage to roofs by effectively reducing suction on the roof envelope. For the gable roof, net peak C_p values increased for the 15, 30 and 45 degree

wind directions by 1.5-4.5% with VSVs installed. The hip roof model with VSVs performed better than its gable counterpart for the 0 and 15 degree wind directions.

The study also revealed that there is a correlation between the mean external and internal pressure coefficients at the vent locations. This correlation is clearly disrupted at the windward vent locations with the VSVs installed. However, the correlation was maintained at the VSVs located in the wind separation zones. This is because the windward VSVs shut under-wind induced external positive pressure, and the VSVs located in the areas of external negative pressure remained open.

The wind-driven rain (WDR) investigation concluded that the VSVs successfully prevented water entry into the attic space.

The results of the steady Reynolds Averaged Navier-Stokes (RANS) CFD evaluation demonstrated that the mean internal pressure coefficients obtained through CFD modeling also decreased when the VSVs were installed.

The results of this study show the efficacy of the installed VSVs (*BPA Safety Vents*) in reducing mean pressure within the attic space, increasing mean and peak net pressure on the roof envelope at the leading edge of the roof, and disallowing wind-driven rain from entering the building. Therefore, it can be concluded that installing VSVs into the soffits of low-rise buildings with gable and hip roofs is a valuable and effective method for mitigating the possibility of wind-induced pressure damage to the roof and wind-driven rain damage to the inside of the building.

CHAPTER VI

AN EXPERIMENTAL STUDY OF INTERNAL PRESSURES IN THE ROOF ATTIC SPACE USING VALVED SOFFIT VENTS

The primary objective of this study was to investigate the wind-induced internal pressure characteristics of a typical residential attic space which is vented with the valved soffit vents (VSVs) in a large-scale wind tunnel environment. The testing was conducted at the Wall of Wind (WOW) facility at Florida International University (FIU) in Miami, Florida.

Background

Wind-induced internal pressures in a low-rise building are influenced by the external pressure distribution and the size, shape and position of the openings on the building envelope, i.e. soffit vents, which connect the inside of the building to the outside. The external pressures generated by the approach flow are affected by the shape of the building, the approach wind characteristics, terrain and surroundings, and wind direction. However, the internal pressures also depend on background leakage, interior compartmentalization, the internal volume, and flexibility of the building "skin" and structure. One of the main considerations of internal pressures is their contribution to the total wind load effects on low-rise buildings, in particular, the roof sheathing. The difference between the external pressure and the internal pressure determines the net pressure and wind loading on the building elements (Irwin and Sifton 1998, Ginger and Letchford 1999, Oh et al. 2005).

Experimental Set-Up

The wind tunnel tests in this study were carried out on a 1:6 scale model in flow conditions equivalent to standard open country terrain (Exposure C in *ASCE 7-10*). The full-scale plan dimensions of the test building were 8.61 m x 8.61 m (28'-3" x 28'-3") with an eave height of 7.62 m (25 ft). The eaves (soffits) overhang was 0.6 m (2 ft) on all sides. The model building represented a full-scale two-story residential building, common to North America and the Caribbean region. There were two interchangeable roofs, a gable and a hip, both modeled with a 4:12 roof slope. The model was fabricated using wood framing and plywood sheathing. The building model was symmetrical; therefore, the tests were conducted for wind directions of 0° to 45° at 15° intervals for the hip roof and 0° to 90° for the gable. The model building dimensions for length, width, and eave height were 1.44 m x 1.44 m x 1.27 m (4'-8 1/2" x 4'-8 1/2" x 4'-2"). The gable and hip roofs' dimensions were a square plan of 1.64 m x 1.64 m (5'-4 ½" x 5'-4 ½"). The dimensions selected fit appropriately within the blockage requirements of the WOW.

The International Code Council's (ICC) International Residential Code (IRC 2009) allows for ventilation of attic spaces. The ventilation opening area is to be a minimum of 1/150 of the attic area to be ventilated (5.25 ft^2). In addition, an attic access opening is required when the attic area is greater than 2.8 m^2 (30 ft^2) and has a minimum height of 762 mm (30"). The minimum attic access opening allowed is 559 mm x 762 mm (22" x 30") (2009 IRC). Each of the roofs in this experiment had a 93 mm x 127 mm (3.69" x 5") attic access opening, which could be sealed with a covering. In addition, there were openings to represent the full-scale valved soffit vents. The VSVs had dimensions of 279 mm x 475 mm (11" x 18.69"), with a net opening area of 0.07 m^2

(0.72 ft^2); therefore, a total of eight valved vents satisfied the code requirements (5.76 ft^2). The scaled dimensions for the valved soffit vent were 47 mm x 79 mm (1.83" x 3.12"), with a net opening area of 29 mm x 65 mm (1.125" x 2.55"). The location of the attic access opening and the valved soffit vent arrangements is shown in Figure 6-1 for the gable roof and Figure 6-2 for the hip roof. There were four soffit vent openings on the gable roof and eight openings on the hip roof. The soffit vent openings were strategically positioned at the corner of the roofs to benefit from the wind-induced negative pressure at the wind separation zones.

It was not feasible to scale the valved soffit vents; however, openings were cut into the soffit to represent the net scaled area of two vents per location, which was 3770 mm^2 (5.74 in^2), thereby providing a 2.2% open area ratio per vent for the windward soffit. The soffit openings were sealed at the windward locations; however, they remained open at the wind separation zones for the various wind directions.

There was a ceiling at 1.27 m (4'-2") from the ground on the test model which provided horizontal compartmentalization. The model building was sealed as tight as possible. However, uniform background leakage was produced in the attic space by distributing 6 small holes of 19 mm (¾") diameter in the ceiling of the test building. This provided a background leakage opening ratio of 0.1%. This ratio corresponded to previous studies performed by Oh et al. (2007) and Kopp et al. (2008). The background leakage was only considered for Test Case 3 and 4.

The approach flow characteristics used in this study were the same as those used for the full-scale VSV study documented in Chapter 5 (refer to pages 63-64). A mean

velocity of 25.67 m/s (57.44 mph) at roof eave height (1.27 m) was used for the tests, with the equivalent 3-second gust wind speed being 39 m/s (87.3 mph). The Reynolds number based on the roof eave height and velocity at that height was calculated to be 2.18×10^6.

Test Configurations

There were four test cases for each roof type which were tested for wind directions of 0° to 45° at 15° intervals for the hip roof and 0° to 90° at 15° intervals for the gable roof, which are listed in Tables 6-1 and 6-2. Test Case 1 (without VSVs) was the control test where the attic space was separated from the living space and sealed off with no leakage in the ceiling or walls. The vents were all fixed open for Test Case 1, representing normal soffit vent openings. Test Case 2 (with VSVs) was the same as Test Case 1; however, the soffit vent openings in the direct path of the approaching wind were sealed off to represent the valved soffit vents (VSVs) closing under wind-induced positive pressure. Test Case 3 and 4 investigated the effects of a uniform ceiling leakage. However, Test Case 4 examined the effects of having the attic access open in addition to the background leakage.

Table 6-1. Summary of experimental configurations for the gable roof model

Test Case ID	Soffit Vents	Attic Access Hatch	Ceiling Leakage	Wall Leakage
1	All open (w/out VSVs)	Closed	None	None
2	With VSVs	Closed	None	None
3	With VSVs	Closed	Yes	Yes
4	With VSVs	Open	Yes	Yes

Wind direction: 0°, 15°, 30°, 45°, 60°, 75° and 90°

Table 6-2. Summary of experimental configurations for the hip roof model

Test Case ID	Soffit Vents	Attic Access Hatch	Ceiling Leakage	Wall Leakage
1	All open (w/out VSVs)	Closed	None	None
2	With VSVs	Closed	None	None
3	With VSVs	Closed	Yes	Yes
4	With VSVs	Open	Yes	Yes

Wind direction: 0°, 15°, 30° and 45°

Pressure Measurements

For the gable roof, there were a total of 81 pressure taps installed on the model building which measured the external and internal pressures. To measure the distribution of external pressures, 37 pressure taps were placed evenly over the roof. The internal pressures were measured by 44 pressure taps which were positioned uniformly on the interior surface of the roof, in the attic space and at the soffit vent locations. The hip roof model had a similar pressure tap layout. A total of 117 pressure taps (50 external taps and

67 internal taps) were used on the hip roof. The internal and external pressures at the soffit vents were measured as well. The pressure tap layouts for the gable and hip roofs are shown in Figures 6-1 and 6-2 respectively.

The instrumentation and process used to capture the time history data were the same as those used for the full-scale VSV testing which is outlined in Chapter 5 (refer to pages 67-69). The mean and peak non-dimensional pressure coefficients ($C_{p's}$) at the tap locations were obtained by using Equations 6.1 and 6.2:

$$Cp_{\_Mean} = \frac{P_{mean}}{\frac{1}{2}\rho V_{eave}^2} \tag{6.1}$$

$$Cp_{\_Peak} = \frac{P_{peak}}{\frac{1}{2}\rho V_{eave}^2} \tag{6.2}$$

where the variables have also been previously defined in Chapter 5. A MATLAB program was used to perform the Partial Turbulence Simulation (PTS) method to obtain the C_{p_Peak} values.

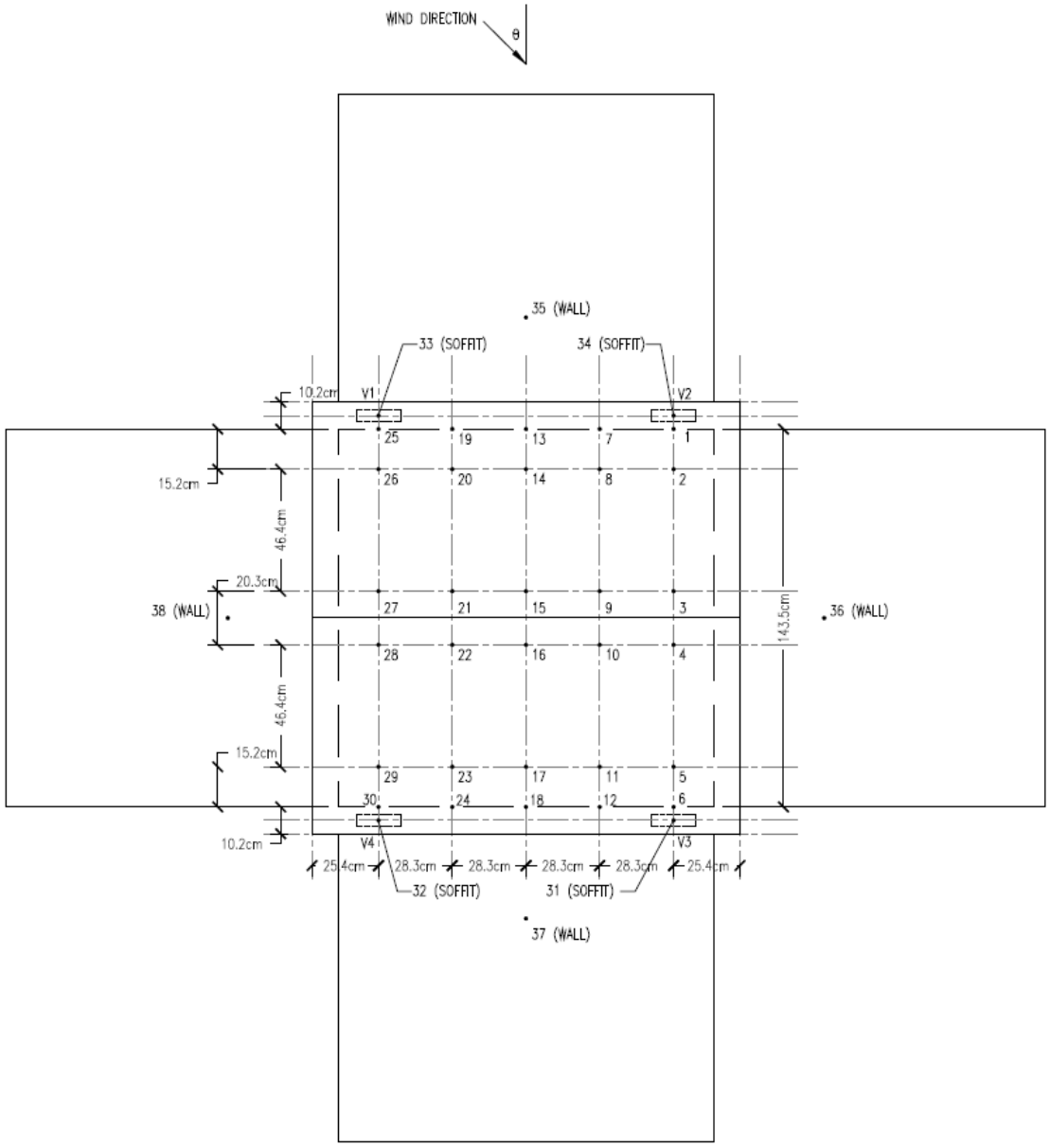

a)

Figure 6-1. a) External pressure tap locations on the gable roof

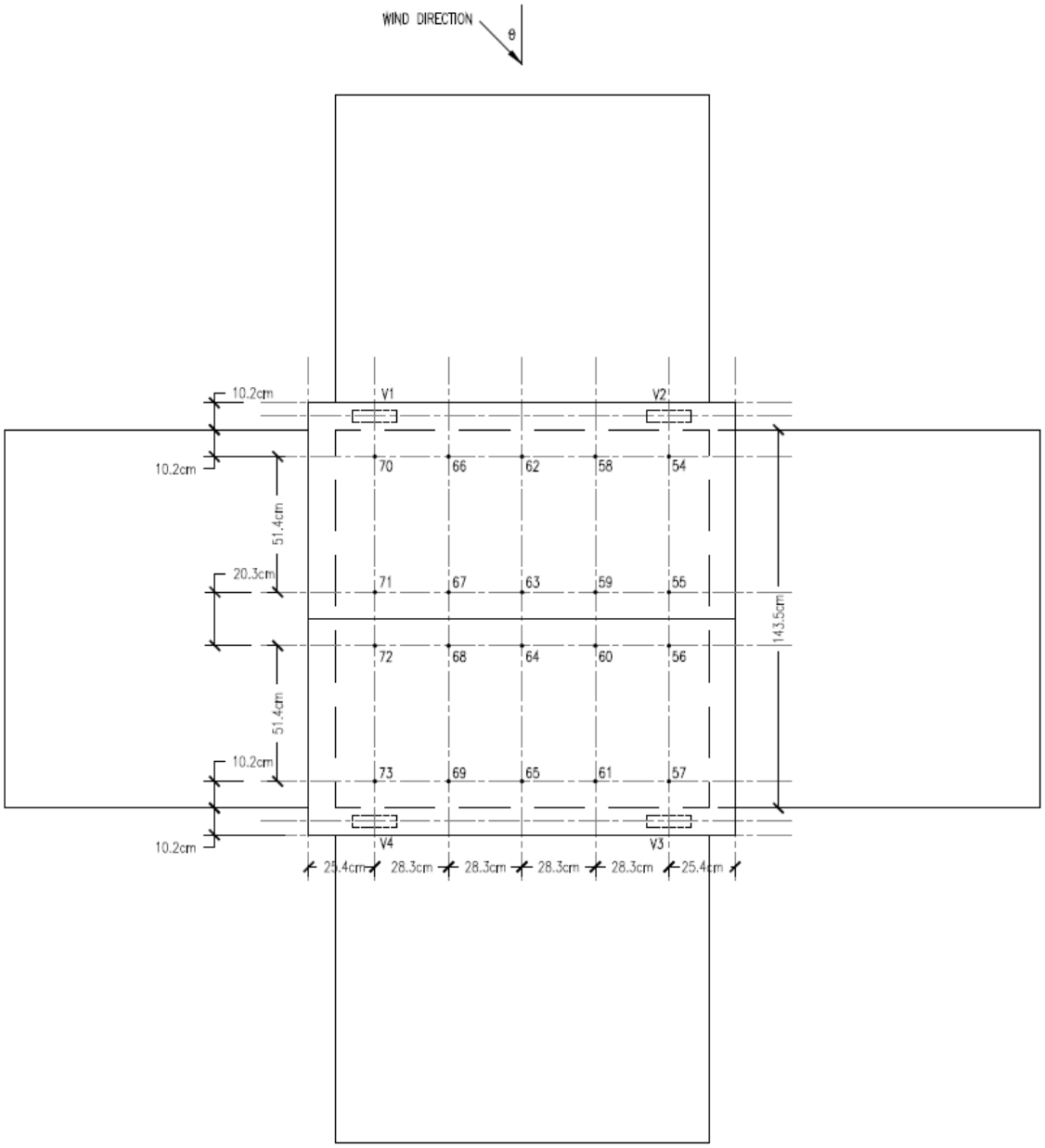

b)

Figure 6-1. b) Internal pressure tap locations on the gable roof surface

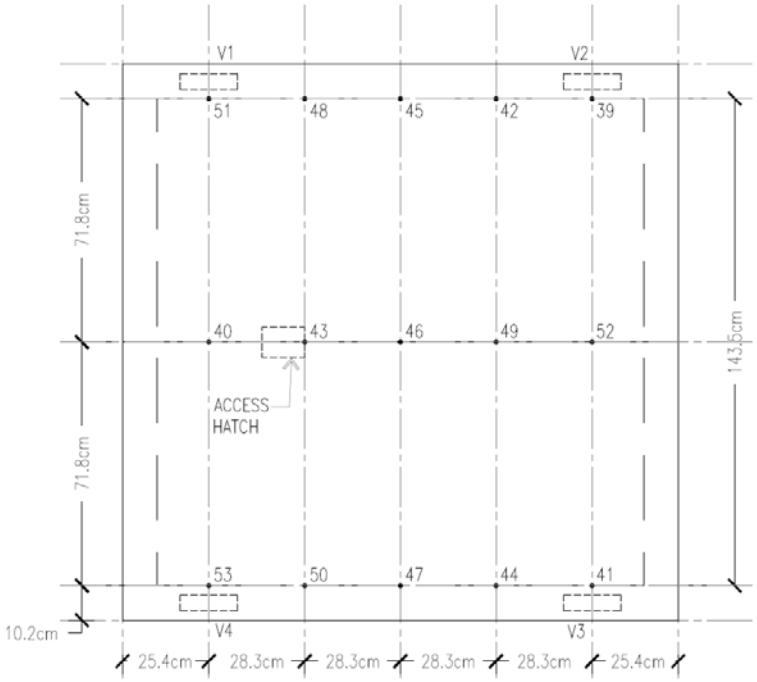

c)

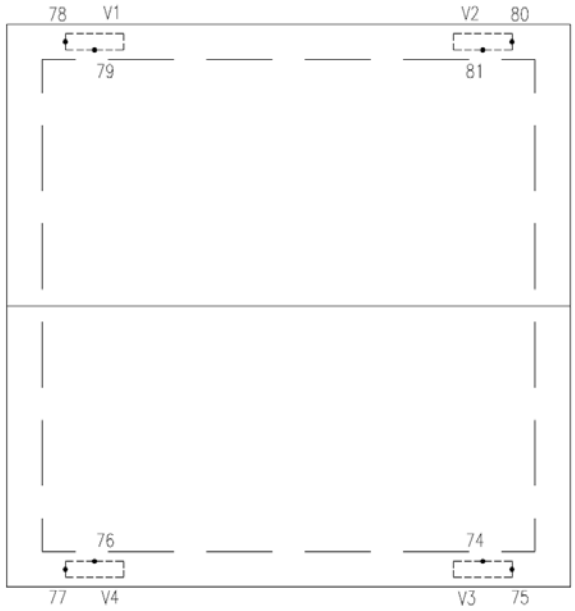

d)

Figure 6-1. c) Internal pressure taps in the attic space of the gable roof; d) internal pressure taps at vents

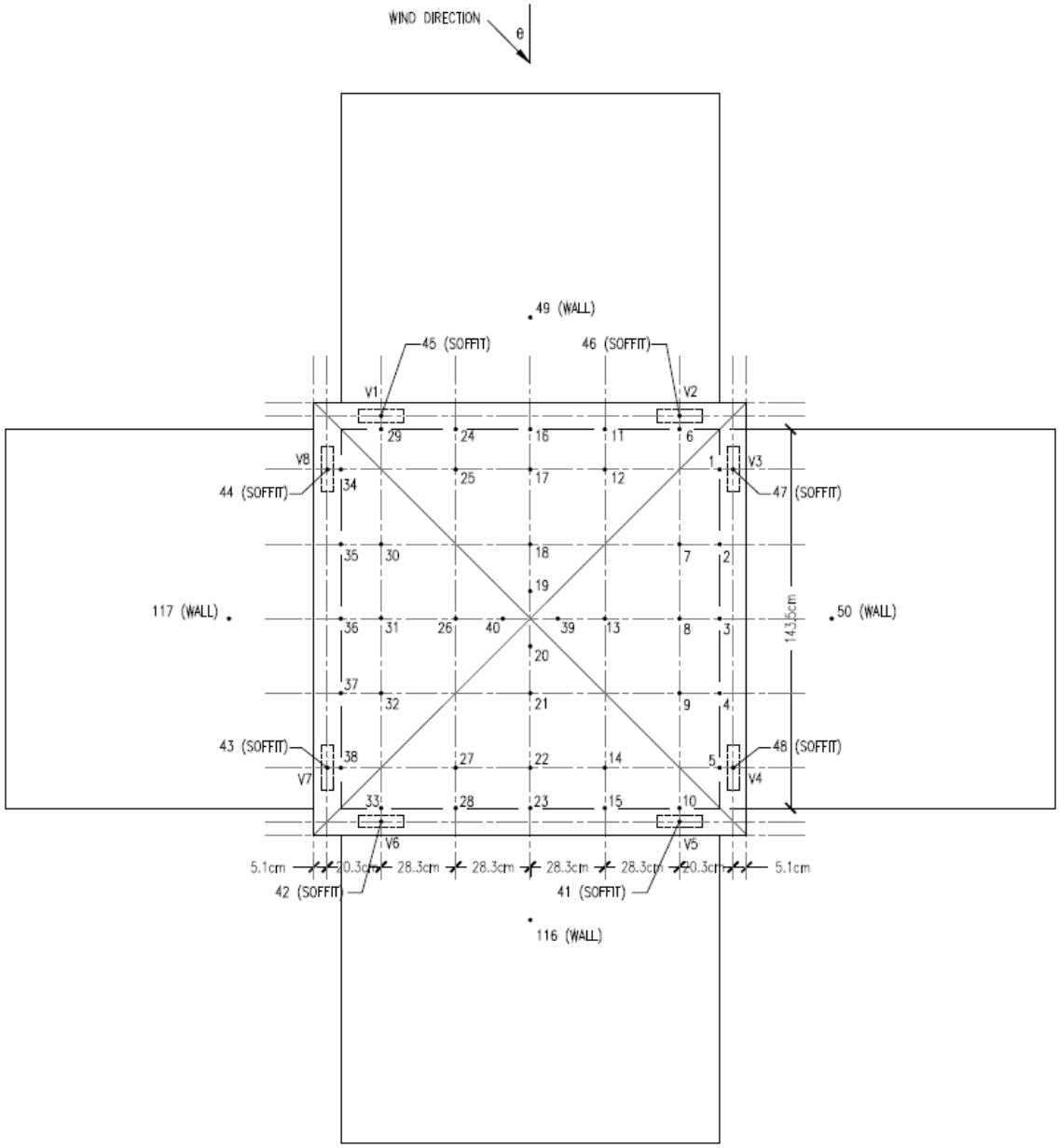

a)

Figure 6-2. a) External pressure tap locations on the hip roof

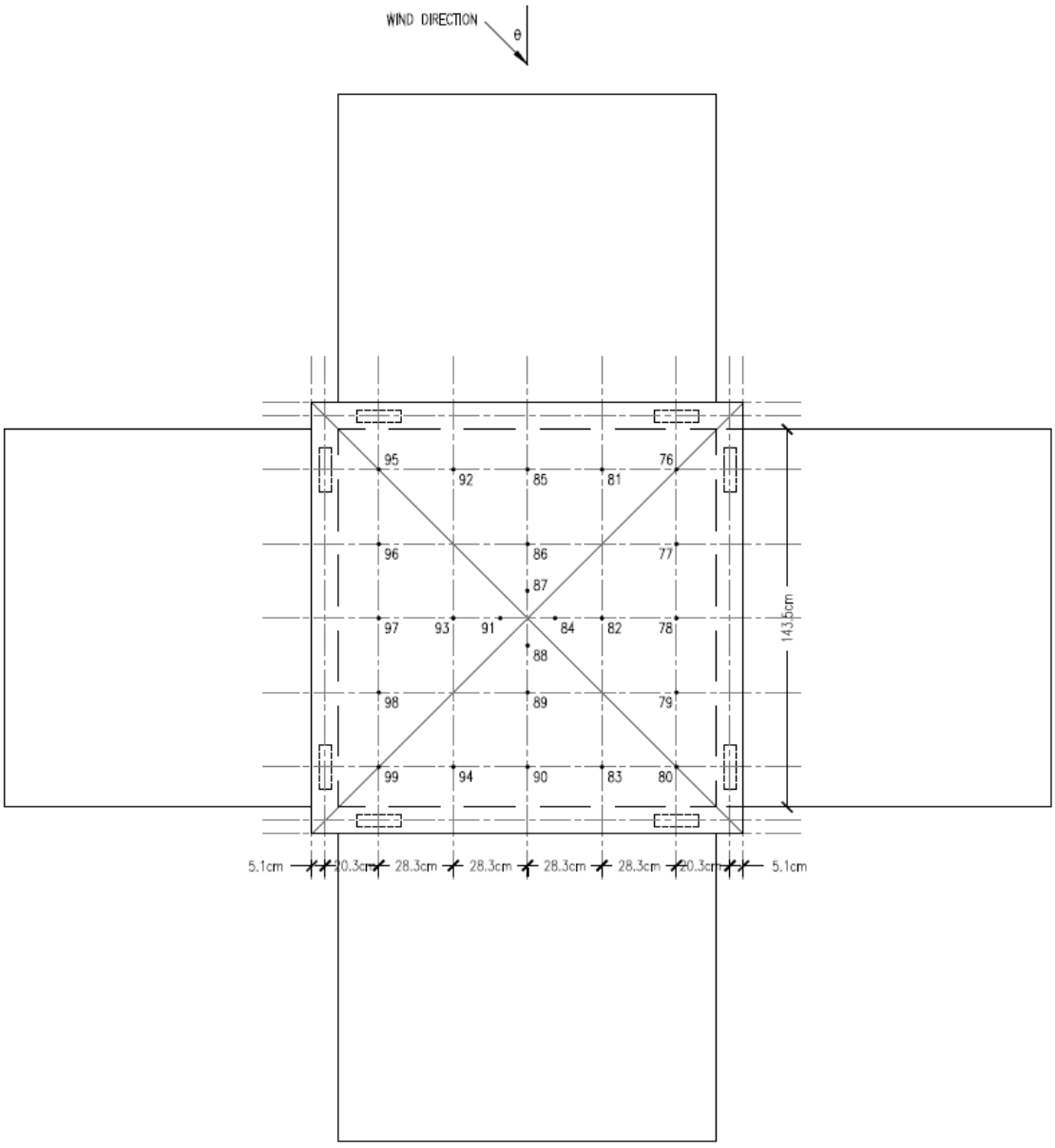

b)

Figure 6-2. b) Internal pressure tap locations on the hip roof surface

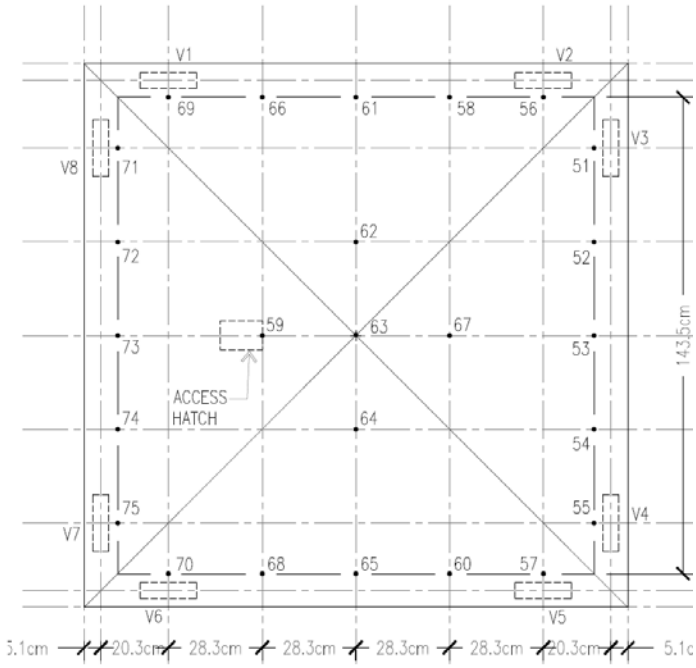

c)

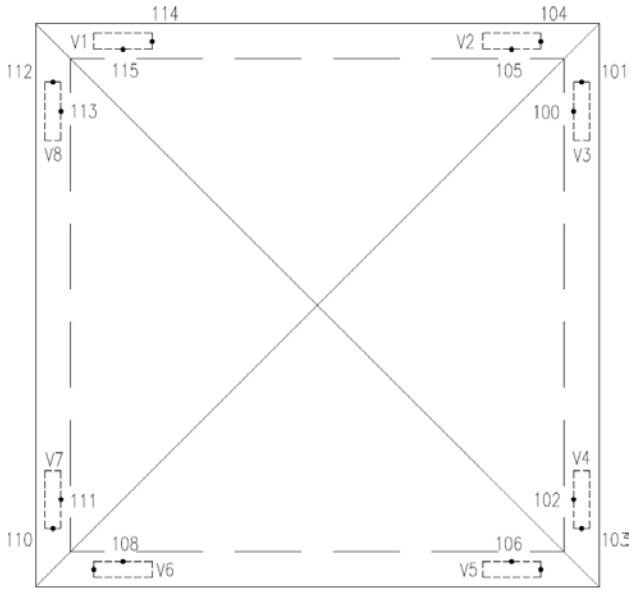

d)

Figure 6-2. c) Internal pressure taps in the attic space of the hip roof; d) internal pressure taps at vents

a)

b)

c)

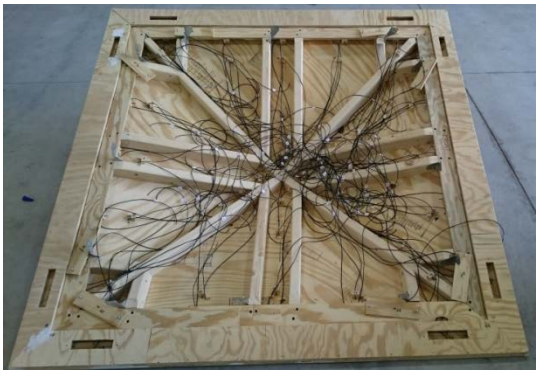

d)

Figure 6-3. The building models used for the testing: a) gable roof building model ready for testing, 0° wind direction; b) underside of the gable roof with tubing installed; c) hip roof building model ready for testing, 0° wind direction; d) underside of the hip roof with tubing installed

a)

b)

c)

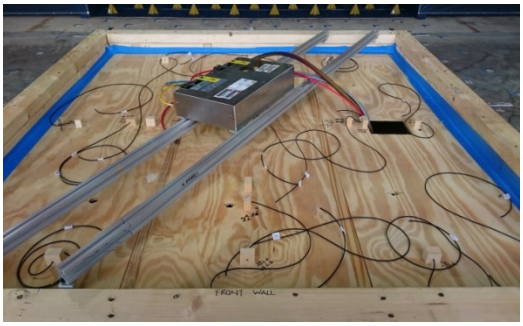

d)

Figure 6-4. a) Installing the hip roof on the model base; b) location of the vents on the hip roof; c) location of the vents on the gable roof; d) the attic floor layout

Results and Discussion

Pressure testing of the gable and hip roofs without and with valved soffit vents (VSVs) demonstrated that the use of VSVs had a notable impact on the internal pressure distribution within the roof attic space. In addition, the VSVs proved consistent in reducing the positive mean pressure entering the attic space at the vent locations and allowed for the relief of positive pressure within the attic space.

Gable Roof Test Results

Tables B-1 to B-7 in Appendix B show the comparative results of the mean and peak pressure coefficients for the gable roof model for the various wind directions. The tap numbers listed in the tables correspond to the tap layout in Figure 6-1. The tables show the mean and peak C_p values for Test Case 1 (without VSVs), Test Case 2 (with VSVs), Test Case 3 (with VSVs and background leakage) and Test Case 4 (with VSVs, background leakage and an opening in the attic ceiling). Taps 1 to 38 are located on the external roof and building surface, with the remaining taps placed inside the attic space. Taps 39 to 53 are located on the attic floor, while Taps 54 to 73 are placed on the underside of the roof. In addition, Taps 74 to 81 are positioned at the soffit vent/VSV locations.

The mean external C_{pe} values did not change considerably for each test case for any given wind direction, which is the expected trend as the air flow on the external surfaces of the model would not be influenced by the vents on the soffits. However, the mean internal C_{pi} values displayed a different result. Overall, the trend of the mean internal pressure coefficients was that the C_{pi} values changed from positive to negative

when the valved soffit vents are utilized for 0, 15, 30 and 45 degree wind directions. This is because the VSVs automatically shut to prevent air flow into the attic space. However, the mean values did not change significantly for the 60, 75 and 90 degrees wind directions, which is due to the fact that the VSVs were mostly operating in the wind separation zones for these wind directions. Therefore, the vents remained open acting as a normal soffit opening.

For the 0° wind direction, the mean internal C_{pi} values changed from 0.11 for Test Case 1 (without VSVs) to -0.1 for Test Case 2 (with VSVs). In addition, at the windward vent locations, the mean values were reduced from 0.25 without VSVs to -0.1 with VSVs. Similarly, for the 15° wind direction, the mean internal C_{pi} values changed from 0.09 for Test Case 1 to -0.11 for Test Case 2. Moreover, at the windward vent locations, the mean values were reduced from 0.34 without VSVs to -0.1 with VSVs. Positive mean C_{pi} values of 0.07 were obtained inside the attic space for the 30° wind direction for Test Case 1. This value changed to -0.07 for Test Case 2. The mean values at the windward vent locations were 0.48 without VSVs and -0.14 with VSVs. For the 45° wind direction, the mean internal C_{pi} values changed from 0 for Test Case 1 to -0.1 for Test Case 2. At the windward vent locations, the mean values were 0.52 without VSVs, but became negative (-0.16) with VSVs. The mean values are reduced as a result of the VSVs closing and disallowing air intrusion into the attic. Therefore, the roof experiences a suction (negative internal pressure), which can mitigate the roof from lifting off in high winds.

The mean internal C_{pi} values were all negative for the three remaining wind directions (60°, 75°, and 90°). Moreover, the values did not change considerably.

However, for the 60° wind direction the mean value at the windward vent location changed from 0.37 without VSVs to -0.11 with VSVs.

The results also showed that neither the background leakage nor the opening in the attic floor had any significant effect on the mean C_{pi} values with VSVs. Although, for wind directions 75° and 90° where the attic space is fully in suction, Test Case 3 and 4 showed slightly higher mean C_{pi} values compared with the other test cases.

In general, changes in the C_{p_Peak} values were much less consistent compared with the C_{p_Mean} results, as some taps reflected an increase in C_{p_Peak}, while others reflected a decrease in C_{p_Peak}. Typically, the internal peak C_{pi} values change with dominant openings; however, the vent openings were small compared to the windward soffit area. However, at localized areas, such as at the windward vent locations, the peak C_{pi} values were more consistent with the mean C_{pi} values. For example, at Tap 80, the maximum C_{pi_Peak} and C_{pi_Mean} values all decreased for wind directions 0° to 75°. The 30° and 60° wind directions were the most critical, yielding reductions in the maximum internal roof peak C_{pi} values by 30.6% and 35.2% respectively.

Hip Roof Test Results

Tables B-8 to B-11 in Appendix B show the comparative results of the mean and peak pressure coefficients for the hip roof model for the various wind directions. The tap numbers listed in the tables correspond to the tap layout in Figure 6-2. The tables show the mean and peak C_p values for Test Case 1 (without VSVs), Test Case 2 (with VSVs), Test Case 3 (with VSVs and background leakage) and Test Case 4 (with VSVs, background leakage and an opening in the attic ceiling). Taps 1 to 50 are located on the

external roof and building surface, with the remaining taps placed inside the attic space. Taps 51 to 75 are located on the attic floor, while Taps 76 to 99 are placed on the underside of the roof. In addition, Taps 100 to 115 are positioned at the soffit vent/VSV locations.

Similar to the gable roof results, the mean external C_{pe} values for the hip roof did not change markedly for each test case for any given wind direction. However, the mean internal C_{pi} values consistently decreased for all wind directions (0° to 45°). For the 0° wind direction, the mean internal C_{pi} values decreased by 35%, from -0.15 for Test Case 1 (without VSVs) to -0.23 for Test Case 2 (with VSVs). In addition, at the windward vent locations, the mean value was reduced from 0.02 without VSVs to -0.2 with VSVs. Similarly, for the 15° wind direction, the mean internal C_{pi} values decreased from -0.14 for Test Case 1 to -0.2 for Test Case 2. Moreover, at the windward vent locations, the mean values were reduced from 0.3 without VSVs to -0.17 with VSVs. Negative mean C_{pi} values of -0.04 were obtained inside the attic space for the 30° wind direction for Test Case 1. This value was reduced by 71% to -0.14 for Test Case 2. The mean value at the windward vent locations was 0.45 without VSVs and -0.13 with VSVs. For the 45° wind direction, many of the taps recorded positive C_{pi_Mean} values; however, the overall mean internal C_{pi} values changed from -0.01 for Test Case 1 to -0.16 for Test Case 2, which is a 93% reduction. At the windward vent locations, the mean value was 0.32 without VSVs, but became negative (-0.15) with VSVs. These results demonstrated the efficacy of the VSVs in reducing mean internal pressures. The results also showed that neither the background leakage nor the opening in the attic floor had any significant effect on the mean C_{pi} values with VSVs.

The C_{p_Peak} values were much less consistent compared with the C_{p_Mean} results, where some taps reflected an increase in C_{p_Peak}, while others reflected a decrease in C_{p_Peak}. However, at the windward vent locations, the peak C_{pi} values were more consistent with the mean C_{pi} values. For example, at Tap 104, the maximum C_{pi_Peak} and C_{pi_Mean} values all decreased for wind directions 0° to 45°. The 30° wind direction was the most critical, yielding reductions in the maximum internal roof peak C_{pi} values by 26%.

Mean and Peak Pressure Coefficient Contours

The mean and peak pressure coefficients for the gable and hip roof models for selected wind directions are presented in this section. Figures 6-5 to 6-12 show the mean and peak C_p values on the external and internal roof surfaces, and the mean C_{pi} values on the attic floor of the gable roof building for wind directions of 0, 15, 30 and 45 degrees. In addition, Figures 6-13 to 6-16 show the mean and peak C_p values for the hip roof building for wind directions 30 and 45 degrees. There are two figures associated with each wind direction of each roof. The first figure presents the mean C_p values for the following conditions: a) external roof surface without VSVs; b) external roof surface with VSVs; c) internal roof surface without VSVs; d) internal roof surface with VSVs; e) internal attic surface without VSVs; f) internal attic surface with VSVs. The second figure for each wind direction shows the peak C_p values for the following conditions: a) external roof surface without VSVs ($C_{pe\_Peak\ (-ve)}$); b) external roof surface with VSVs ($C_{pe\_Peak\ (-ve)}$); c) internal roof surface without VSVs ($C_{pi\_Peak\ (-ve)}$); d) internal roof surface with VSVs ($C_{pi\_Peak\ (-ve)}$); e) internal roof surface without VSVs ($C_{pi\_Peak\ (+ve)}$); f) internal roof surface with VSVs ($C_{pi\_Peak\ (+ve)}$).

The figures show that the mean C_{pe} values did not change for Test Case 1 (without VSVs) and Test Case 2 (with VSVs) on the external surface as shown on Figures 6-5, 6-7, 6-9, 6-11, 6-13, 6-15 (a, b). The values were similar for both cases. However, the mean C_{pi} distributions were different in the interior locations (roof surface and attic floor) for Test Cases 1 and 2 (Figures 6-5, 6-7, 6-9, 6-11, 6-13, 6-15 (c, d and e, f)).The mean C_{pi} values were consistently positive in the absence of the valved soffit vents; however, they changed to negative with the installed VSVs. For internal C_{pi_Mean} values on the underside of the roof, the 30 and 45 degree wind directions yielded the critical cases for the gable roof. Figure 6-9 (c) shows positive values (0.5 to 0) without VSVs, while the values were negative (-0.1 to -0.15) with the installed VSVs (Figure 6-9 (d)). Similarly, in Figure 6-11 (c), the mean internal pressure coefficients were positive (0.5 to 0) without VSVs, but changed to negative (-0.1 to -0.15) with VSVs (Figure 6-11 (d). There were comparable trends for the 30 and 45 degree wind directions for the hip roof building (Figures 6-13 and 6-15 (c, d)). This shows that the introduction of the VSVs increases internal suction on the roof, thereby, mitigating potential uplift.

In the absence of VSVs for the interior attic regions of the gable and hip roof buildings, the attic area was directly exposed to the wind at various wind directions which generated a positive mean C_{pi} in the range of 0 to 0.16. However, with the VSVs installed the wind- induced positive pressure shut the VSVs, which discontinued the infiltration of air into the attic. At the same time, the leeward VSVs remained open, thus providing a negative mean pressure coefficient throughout the attic space in the range of -0.08 to -0.24. The critical case for the mean C_{pi} values on the the attic floor was for the 15 degree wind direction for the gable roof (Figure 6-7 (e, f)). The values changed from

0.16 to 0 for Test Case 1 to -0.08 to -0.16 for Test Case 2. Moreover, with the VSVs the internal pressures at the sides of the attic floor, where Vents 3 and 4 were installed, produced the lowest mean C_p value (-0.16). This indicates that the leeward VSVs induce a suction internally, thereby reducing the mean internal pressures of the attic space. A similar trend was also observed for the other wind directions for both the gable and hip roofs.

Figures 6-6, 6-8, 6-10, 6-12, 6-14 and 6-16 (e, f) show contours for the internal peak (+ve) C_{pi} values on the underside of the roof surface for both the gable and hip roof buildings. The interior peak (+ve) C_{pi} values were reduced anywhere from 7-33% on the leading edge of the internal roof locations depending on the wind direction. The 30° wind direction for both the gable and hip roofs yielded the highest reductions in interior peak (+ve) C_{pi} values. Figure 6-10 (e, f) shows that for the gable roof, the $C_{pi\_Peak\ (+ve)}$ was 2.1 without VSVs, but reduced to 1.4 with VSVs installed. Likewise, Figure 6-14 (e, f) shows that for the hip roof, the $C_{pi\_Peak\ (+ve)}$ was 2.2 without VSVs, but reduced to 1.6 with VSVs installed.

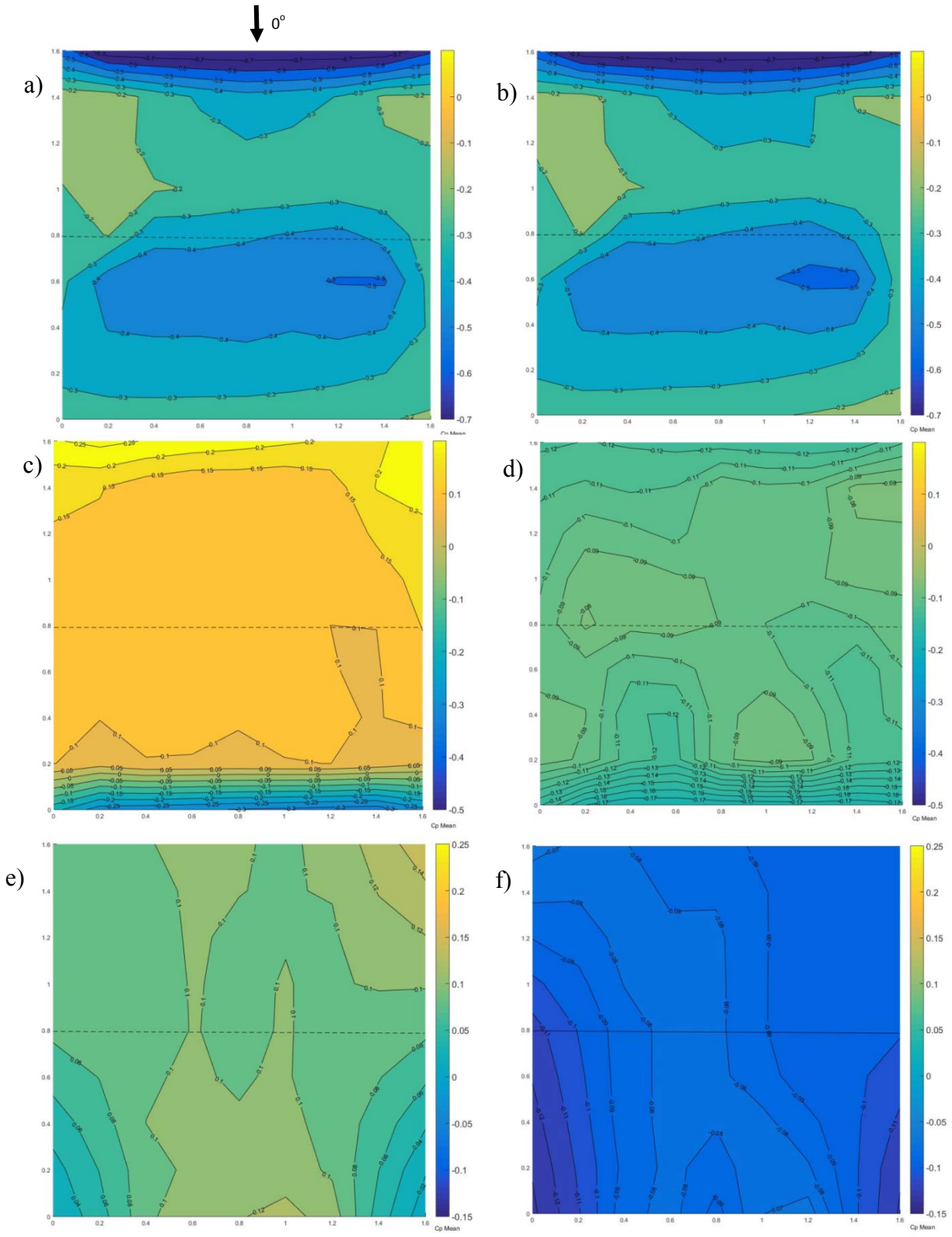

Figure 6-5. Mean pressure coefficients ($C_{p's}$) on the gable roof model for WD = 0°: a) external roof surface without VSVs; b) external roof surface with VSVs; c) internal roof surface without VSVs; d) internal roof surface with VSVs; e) internal attic surface without VSVs; f) internal attic surface with VSVs

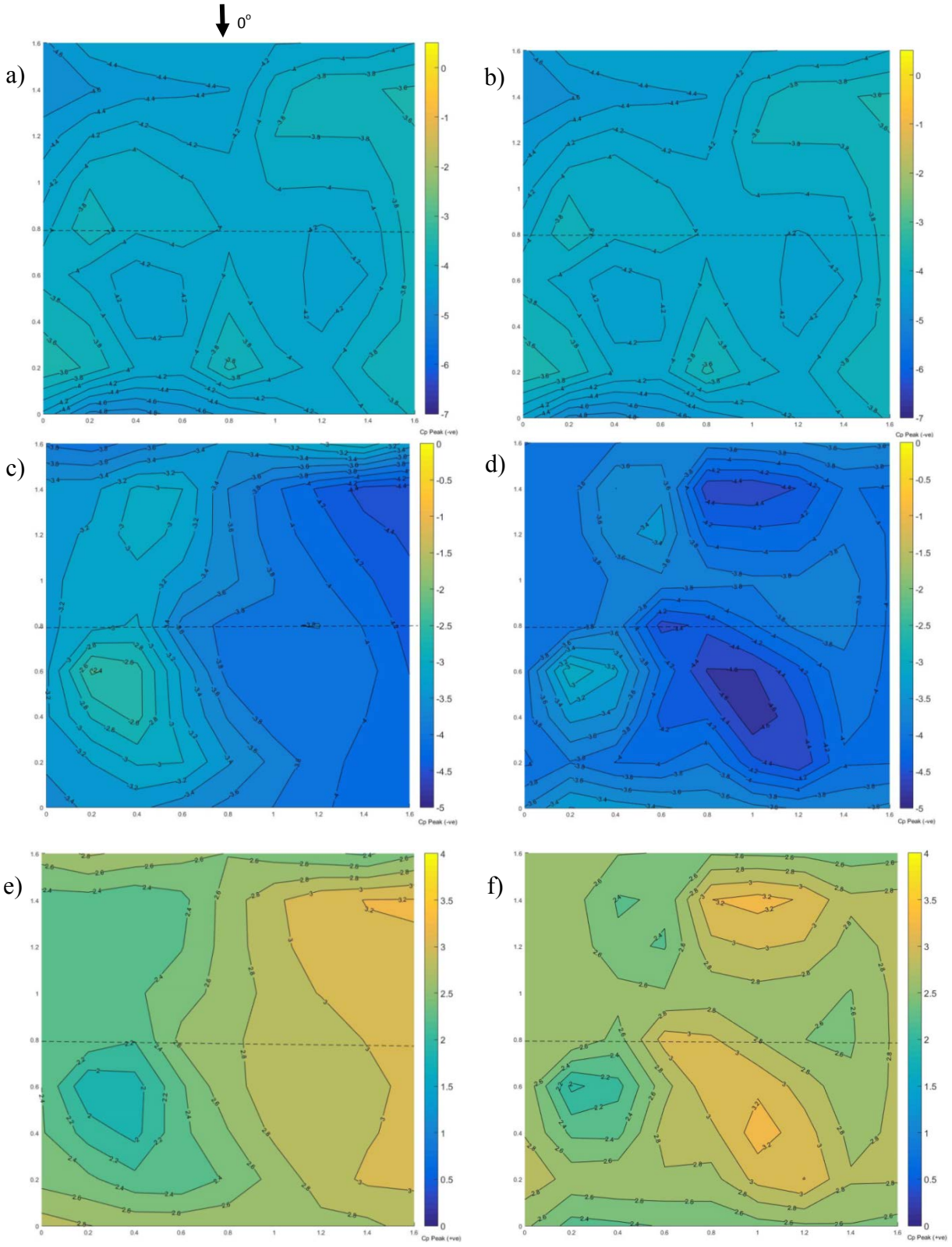

Figure 6-6. Peak pressure coefficients ($C_{p's}$) on the gable roof model for WD = 0°: a) external roof surface without VSVs (-ve); b) external roof surface with VSVs (-ve); c) internal roof surface without VSVs (-ve); d) internal roof surface with VSVs (-ve); e) internal roof surface without VSVs (+ve); f) internal roof surface with VSVs (+ve).

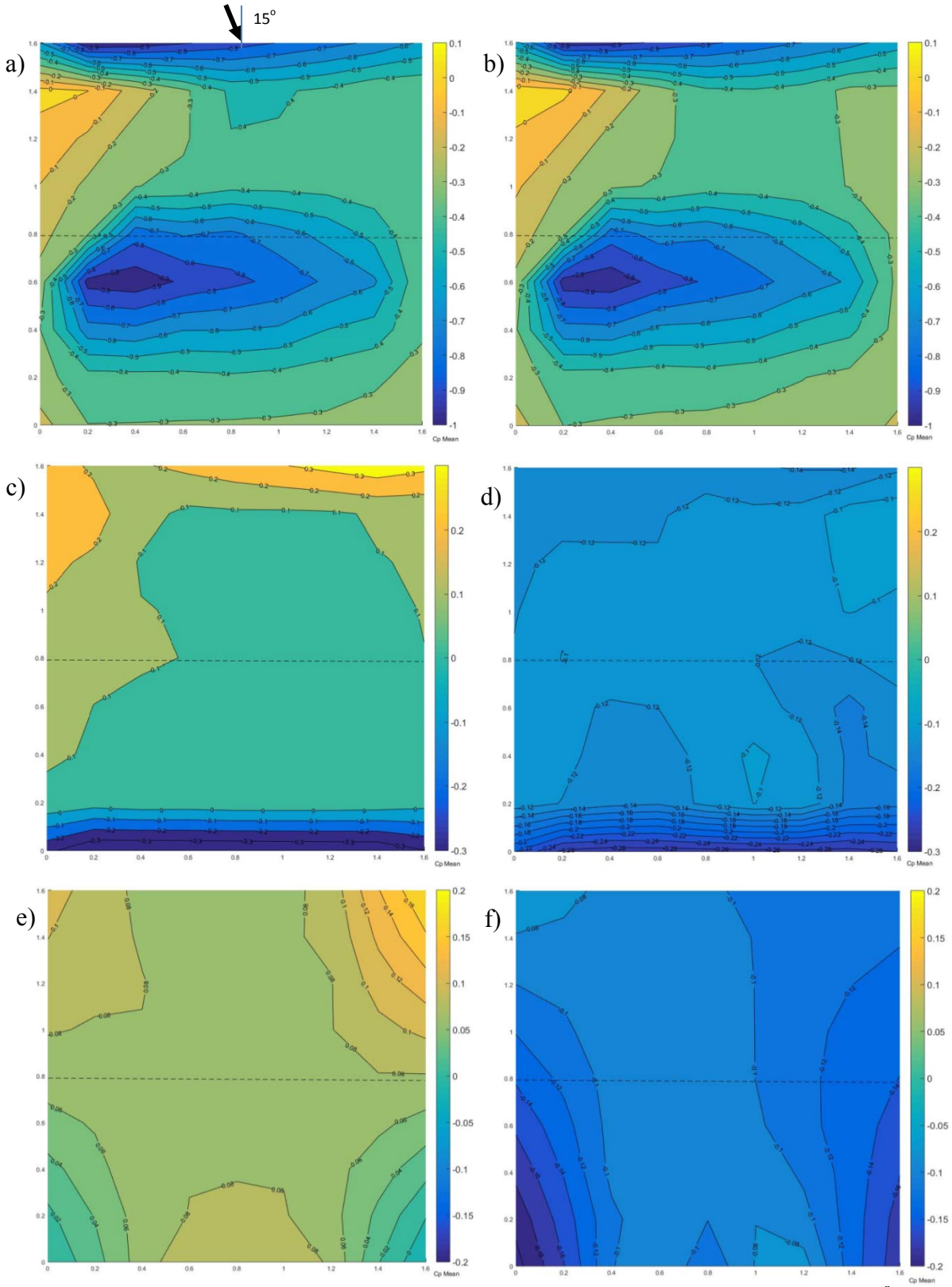

Figure 6-7. Mean pressure coefficients ($C_{p's}$) on the gable roof model for WD = 15°: a) external roof surface without VSVs; b) external roof surface with VSVs; c) internal roof surface without VSVs; d) internal roof surface with VSVs; e) internal attic surface without VSVs; f) internal attic surface with VSVs

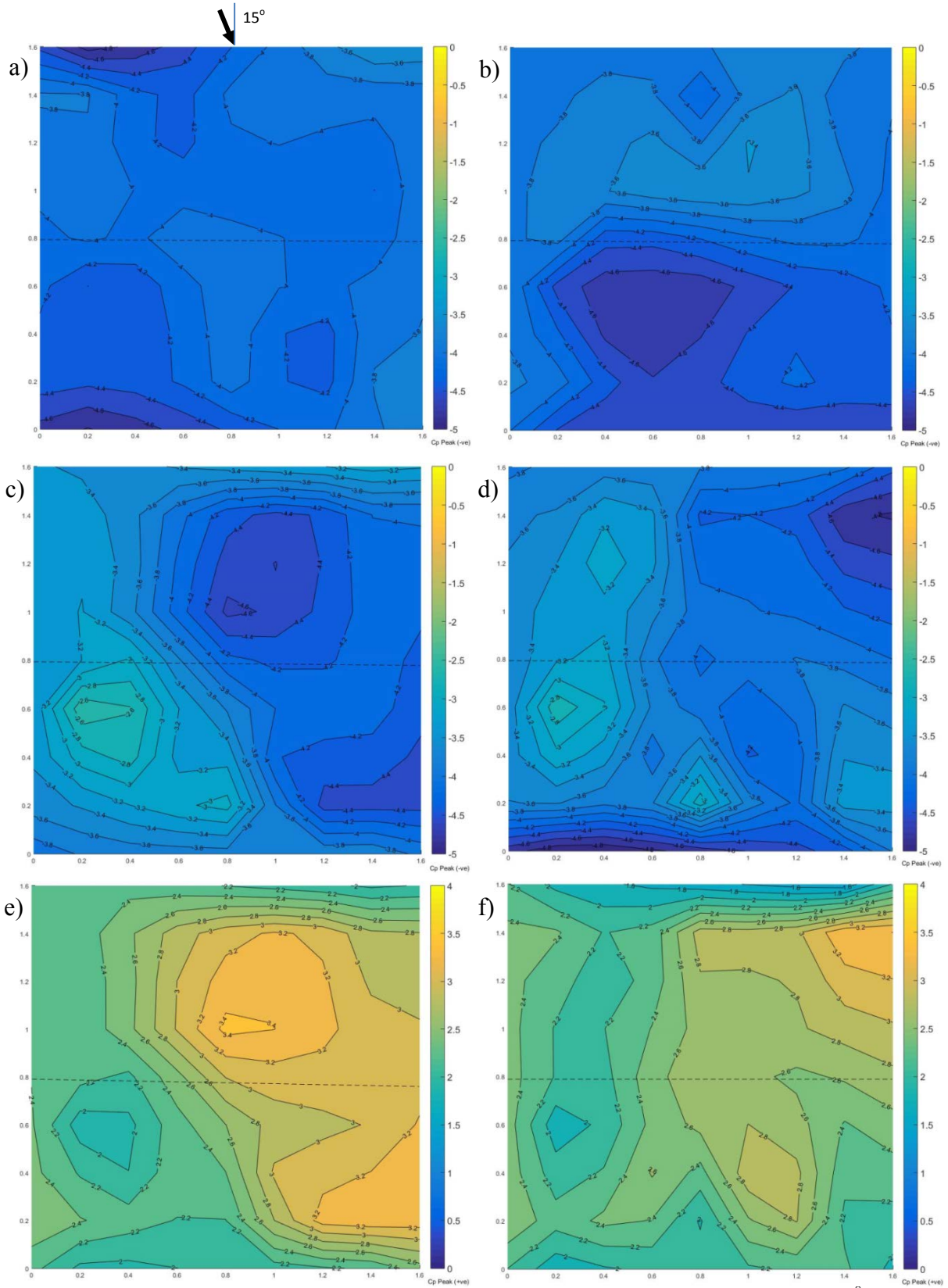

Figure 6-8. Peak pressure coefficients ($C_{p's}$) on the gable roof model for WD = 15°: a) external roof surface without VSVs (-ve); b) external roof surface with VSVs (-ve); c) internal roof surface without VSVs (-ve); d) internal roof surface with VSVs (-ve); e) internal roof surface without VSVs (+ve); f) internal roof surface with VSVs (+ve)

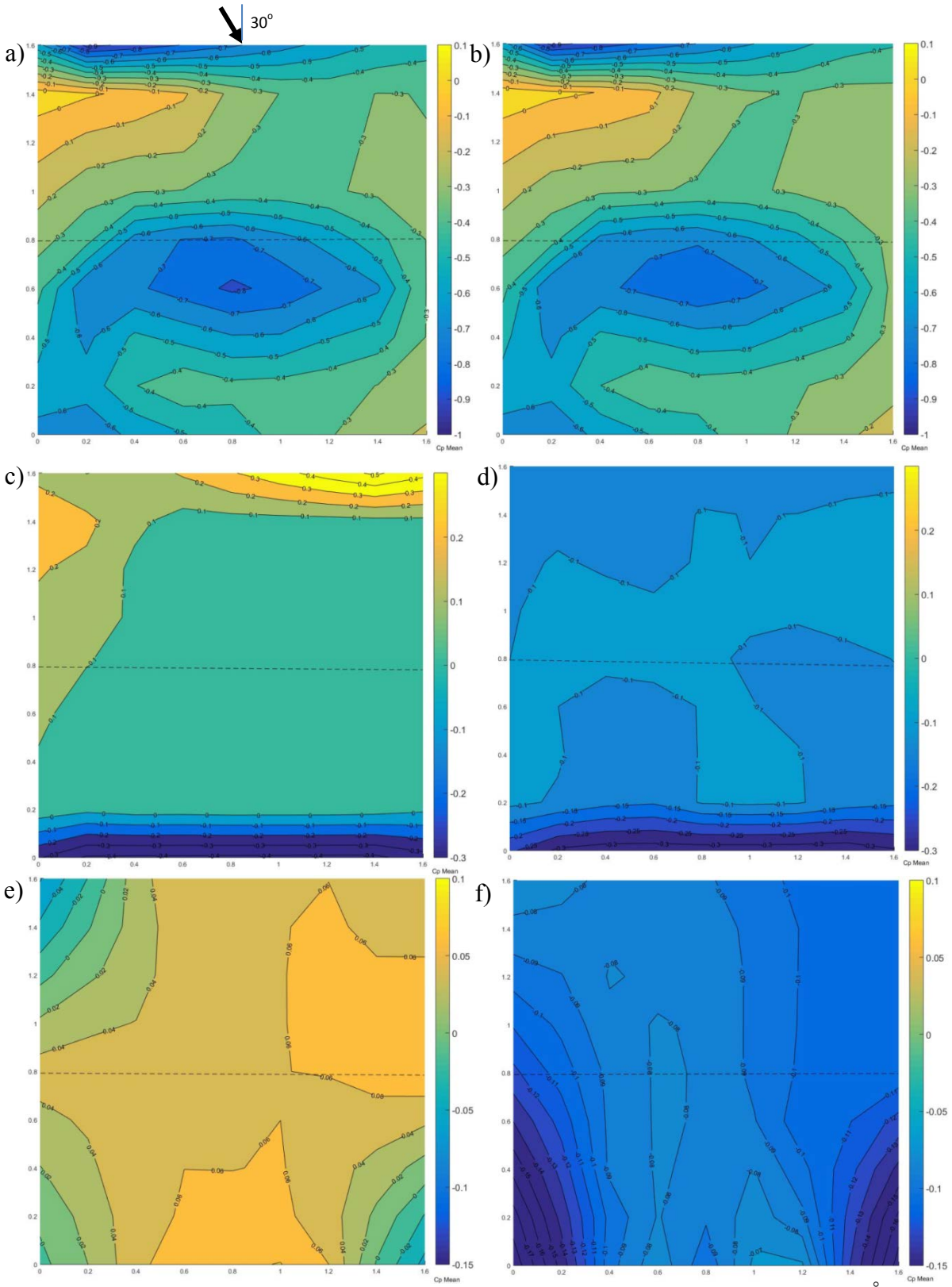

Figure 6-9. Mean pressure coefficients ($C_{p's}$) on the gable roof model for WD = 30°: a) external roof surface without VSVs; b) external roof surface with VSVs; c) internal roof surface without VSVs; d) internal roof surface with VSVs; e) internal attic surface without VSVs; f) internal attic surface with VSVs

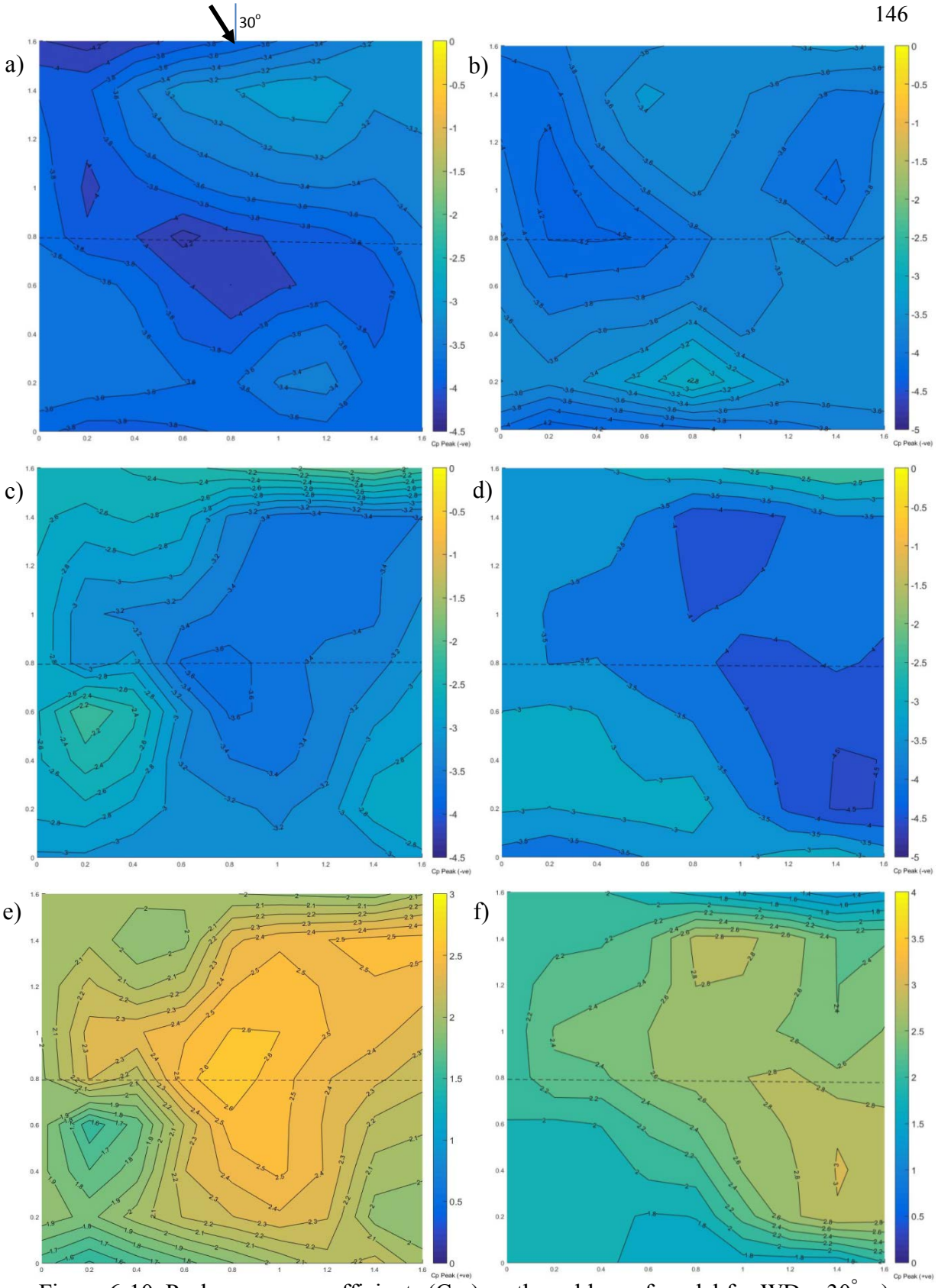

Figure 6-10. Peak pressure coefficients ($C_{p's}$) on the gable roof model for WD = 30°: a) external roof surface without VSVs (-ve); b) external roof surface with VSVs (-ve); c) internal roof surface without VSVs (-ve); d) internal roof surface with VSVs (-ve); e) internal roof surface without VSVs (+ve); f) internal roof surface with VSVs (+ve)

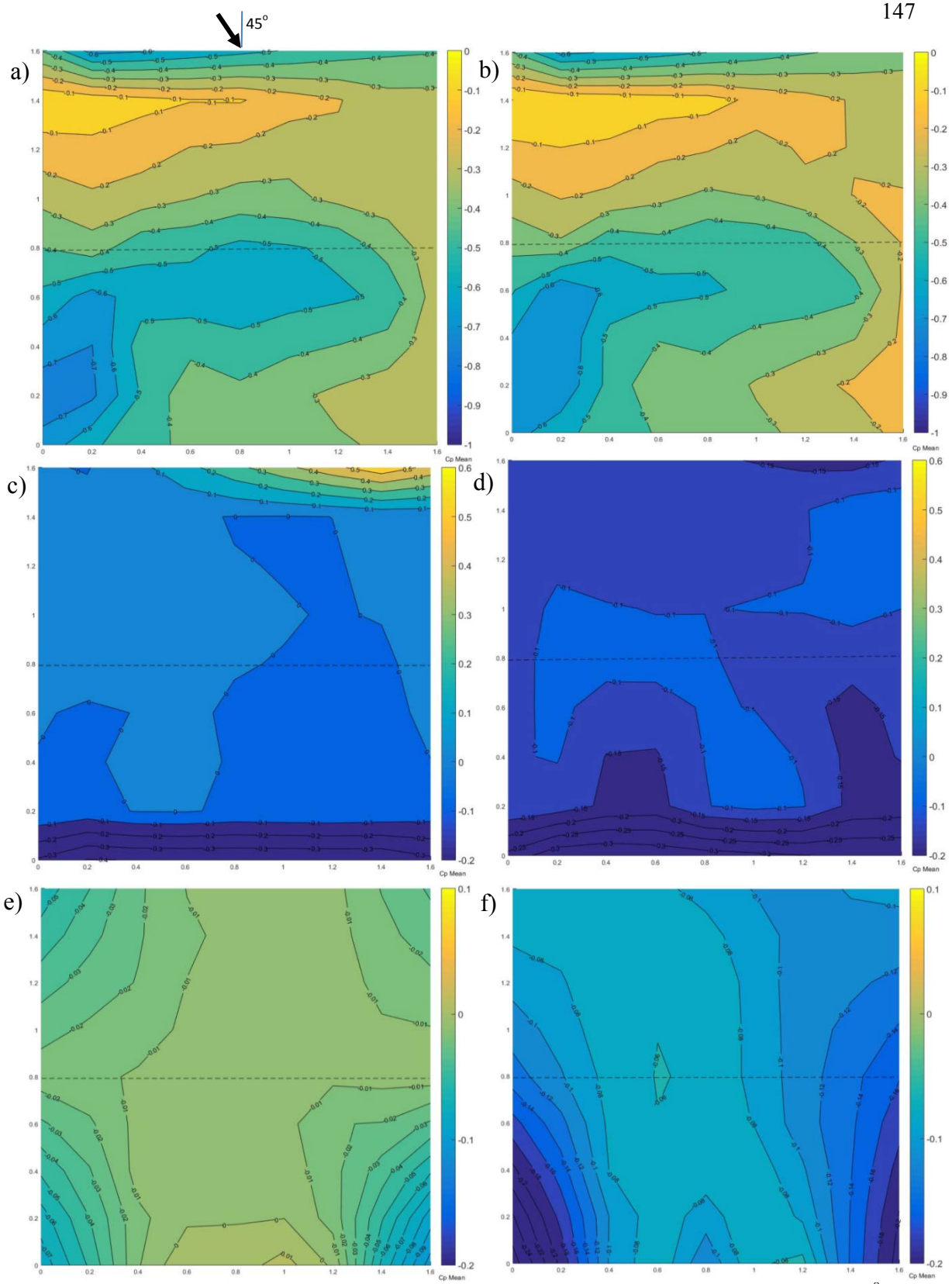

Figure 6-11. Mean pressure coefficients ($C_{p's}$) on the gable roof model for WD = 45°: a) external roof surface without VSVs; b) external roof surface with VSVs; c) internal roof surface without VSVs; d) internal roof surface with VSVs; e) internal attic surface without VSVs; f) internal attic surface with VSVs

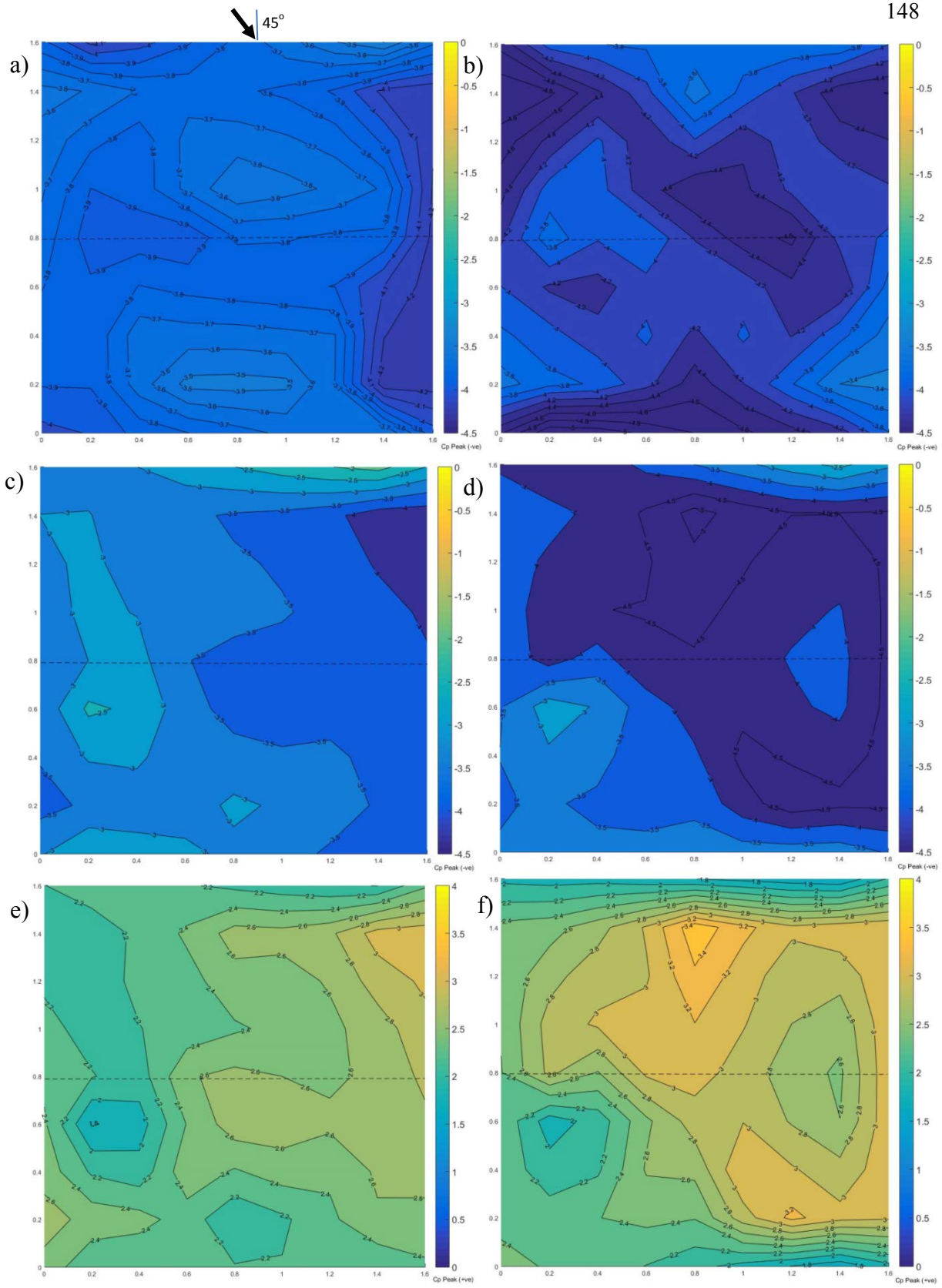

Figure 6-12. Peak pressure coefficients ($C_{p's}$) on the gable roof model for WD = 45°: a) external roof surface without VSVs (-ve); b) external roof surface with VSVs (-ve); c) internal roof surface without VSVs (-ve); d) internal roof surface with VSVs (-ve); e) internal roof surface without VSVs (+ve); f) internal roof surface with VSVs (+ve)

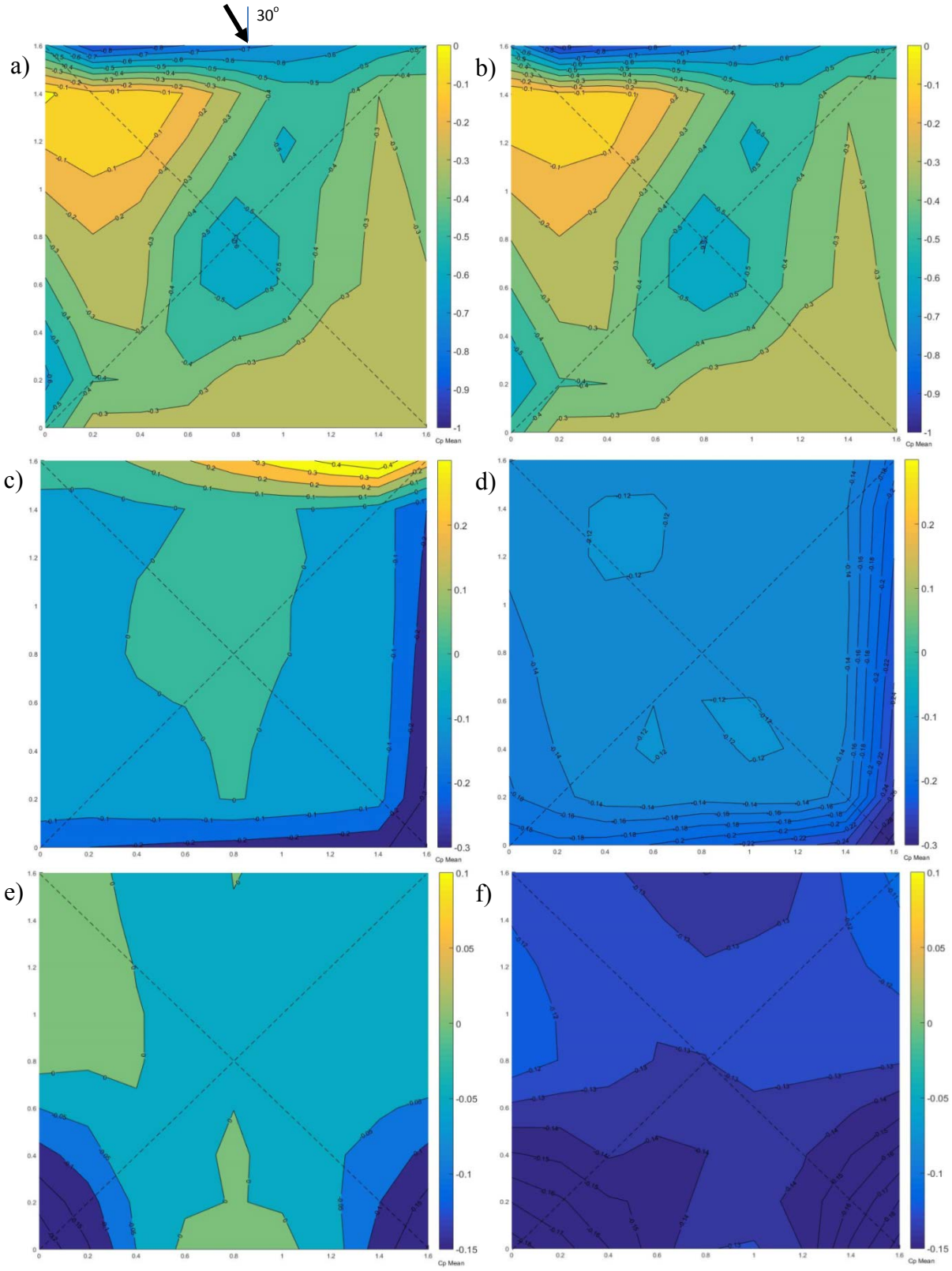

Figure 6-13. Mean pressure coefficients ($C_{p's}$) on the hip roof model for WD = 30°: a) external roof surface without VSVs; b) external roof surface with VSVs; c) internal roof surface without VSVs; d) internal roof surface with VSVs; e) internal attic surface without VSVs; f) internal attic surface with VSVs

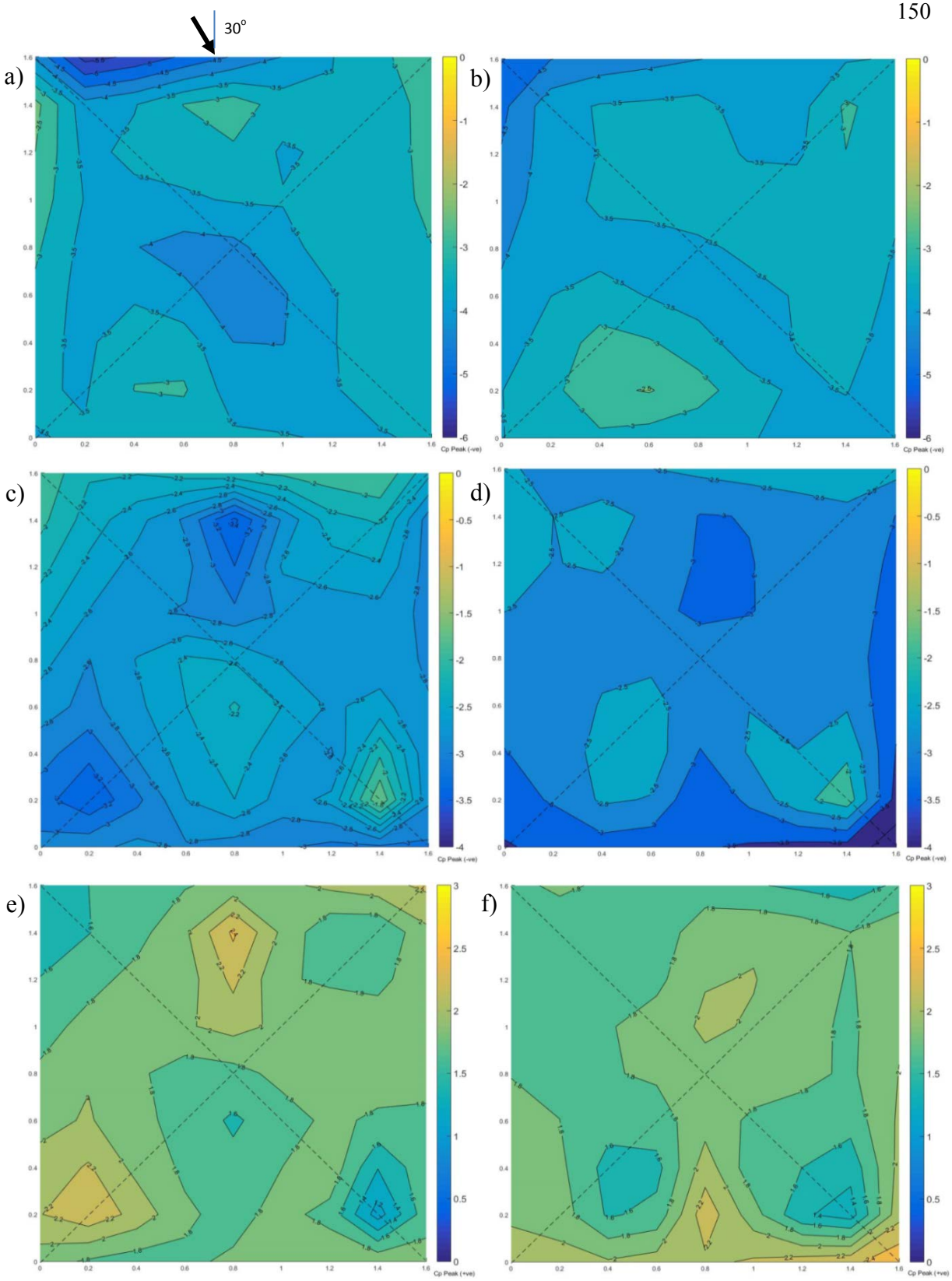

Figure 6-14. Peak pressure coefficients ($C_{p's}$) on the hip roof model for WD = 30°: a) external roof surface without VSVs (-ve); b) external roof surface with VSVs (-ve); c) internal roof surface without VSVs (-ve); d) internal roof surface with VSVs (-ve); e) internal roof surface without VSVs (+ve); f) internal roof surface with VSVs (+ve)

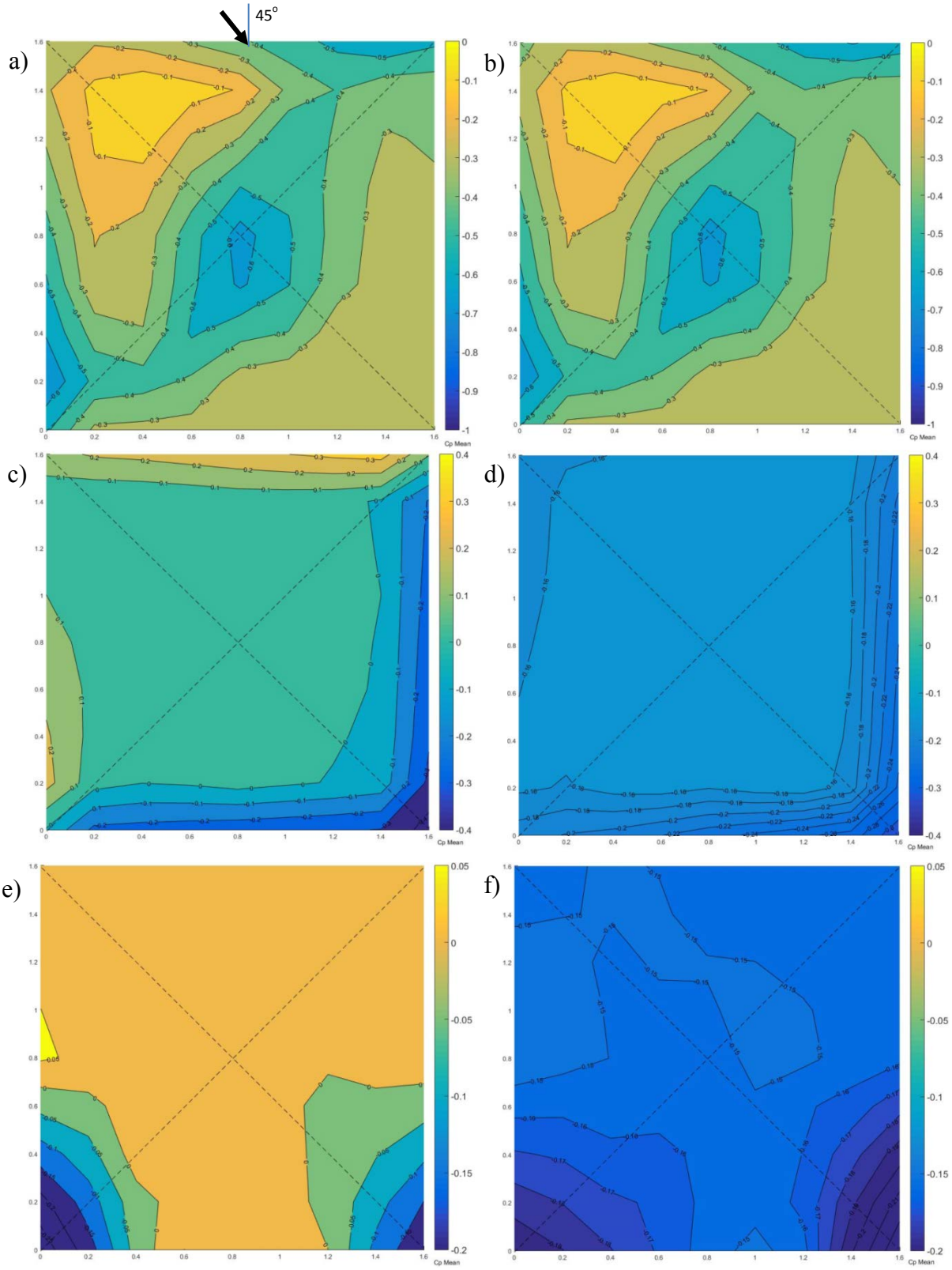

Figure 6-15. Mean pressure coefficients ($C_{p's}$) on the hip roof model for WD = 45°: a) external roof surface without VSVs; b) external roof surface with VSVs; c) internal roof surface without VSVs; d) internal roof surface with VSVs; e) internal attic surface without VSVs; f) internal attic surface with VSVs

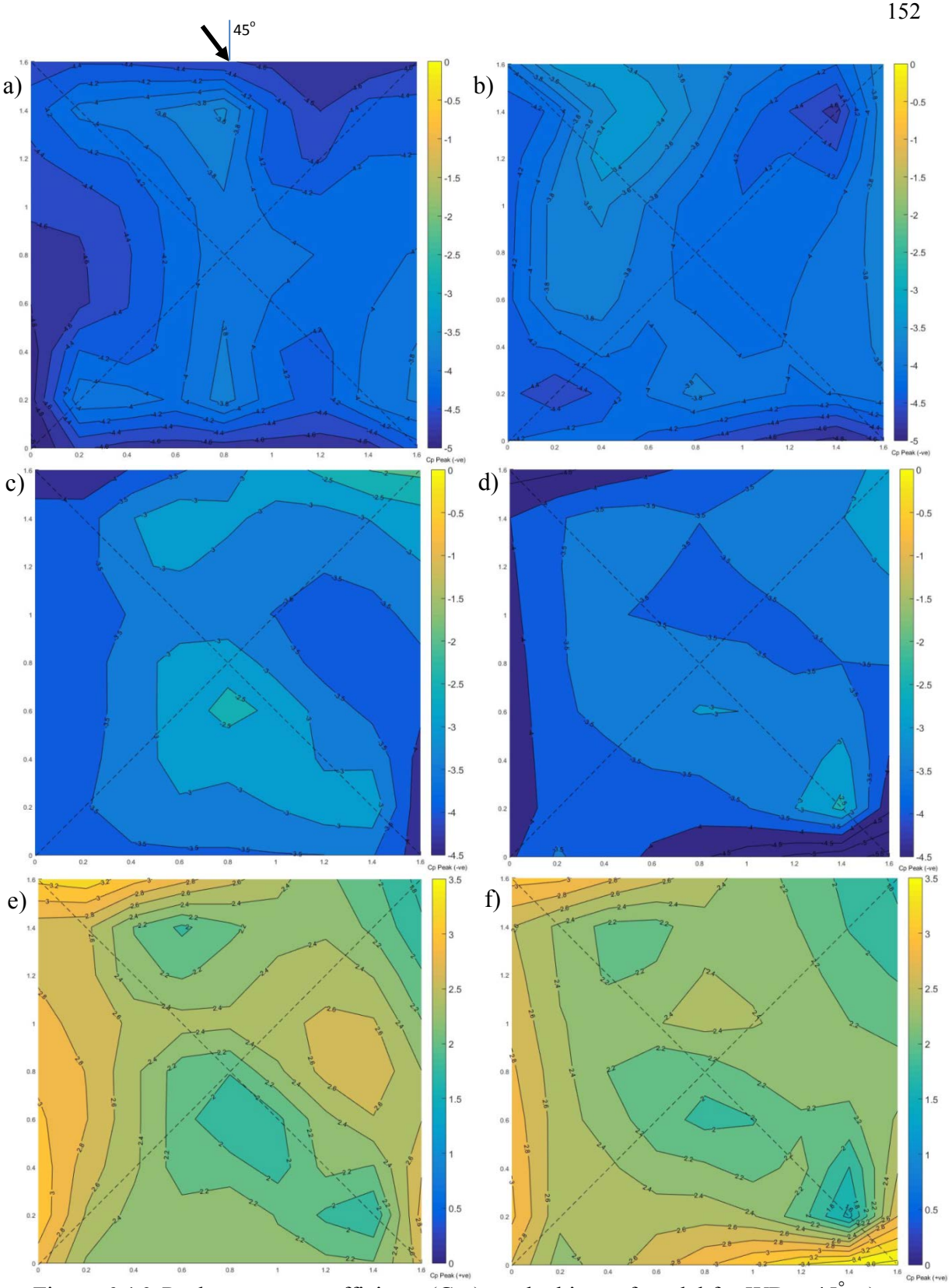

Figure 6-16. Peak pressure coefficients ($C_{p's}$) on the hip roof model for WD = 45°: a) external roof surface without VSVs (-ve); b) external roof surface with VSVs (-ve); c) internal roof surface without VSVs (-ve); d) internal roof surface with VSVs (-ve); e) internal roof surface without VSVs (+ve); f) internal roof surface with VSVs (+ve)

Net Pressure on Roof Envelope

The mean and peak C_p values of the net pressure on the roof envelope are obtained by a summation of the external and internal pressures acting on the surface. Thus, the net pressure coefficients are determined by the following equation:

C_{p_Net} = exterior roof surface $C_{pe(Mean/Peak\ (-ve)}$-interior roof surface $C_{pi(Mean/Peak\ (+ve)}$ (6.3)

The positive pressures are directed toward the surface, while negative pressures are directed away from the surface on which they are acting.

In the absence of valved soffit vents, internal pressures can contribute to the overall wind-induced loading on the roof. For a typical windward soffit opening, the internal pressure will combine with the external suctions on the roof, thus increasing the loading. Therefore, the characteristics of the internal pressure induced through the soffit openings (without and with VSVs) and the extent to which it combines with suction on the roof envelope are important.

Two cases were considered in the analysis of the net pressure on the roof, Case 1 (without VSVs) and Case 2 (with VSVs). The localized areas at the windward vent locations were examined. For the gable roof, this included Vent 1 (V1) and Vent 2 (V2) and for the hip roof, Vent 1, 2, 7 and 8 (V1, V2, V7 and V8). The vent locations are shown on Figures 6-1 and 6-2. For the net pressure to be relevant it is important to select the pressure taps at the location where the net pressures are being investigated. Therefore, in computing the net pressures, specific external roof taps and internal taps at the vent locations were used, which are illustrated in Table 6-3. A total of two pressure taps

located inside the vent openings were used to compute the area average internal pressure at each vent location.

Table 6-3. Pressure taps used for the net pressure analysis

	Gable Roof	
Vent No.	**External Tap No.**	**Internal Tap No.**
V1	25	78 & 79
V2	1*	80 & 81

	Hip Roof	
Vent No.	**External Tap No.**	**Internal Tap No.**
V1	29	114 & 115
V2	6	104 & 105
V7	38	110 & 111
V8	34	112 & 113

* Tap 2 was used for the 30° wind direction for the gable roof due to flawed data recorded at Tap 1.

Tables 6-4 and 6-5 show the results of the net pressure analysis for the mean and peak values for Cases 1 and 2 for the gable and hip roofs with the respective wind directions assuming that the peak external and internal pressure coefficients are simultaneous in time.

Table 6-4. Mean and peak net pressure coefficients for the gable roof

		Wind Direction			
Location/Case	**Cp_Net type**	**0°**	**15°**	**30°**	**45°**
V1_w/out VSVs	Mean	-0.77	-0.82	-0.77	-0.50
	Peak	-6.87	-7.05	-6.00	-6.36
V1_w/VSVs	Mean	-0.62	-0.77	-0.73	-0.44
	Peak	-7.18	-6.09	-5.89	-6.46
V2_w/out VSVs	Mean	-0.92	-0.91	-0.58	-0.63
	Peak	-6.34	-5.75	-5.31	-5.60
V2_w/VSVs	Mean	-0.62	-0.49	-0.16	-0.23
	Peak	-6.46	-5.92	-5.39	-5.87

Table 6-5. Mean and peak net pressure coefficients for the hip roof

		Wind Direction			
Location/Case	**Cp_Net type**	**0°**	**15°**	**30°**	**45°**
V1_w/out VSVs	Mean	-0.96	-1.00	-0.78	-0.28
	Peak	-6.51	-7.00	-7.37	-7.18
V1_w/VSVs	Mean	-0.92	-0.93	-0.73	-0.02
	Peak	-6.47	-7.36	-6.52	-5.98
V2_w/out VSVs	Mean	-1.14	-1.00	-0.8	-0.75
	Peak	-6.11	-6.66	-4.97	-7.01
V2_w/VSVs	Mean	-0.90	-0.64	-0.42	-0.44
	Peak	-6.77	-7.19	-5.25	-6.44
V7_w/out VSVs	Mean	0.03	-0.13	-0.54	-0.68
	Peak	-6.02	-7.45	-5.60	-7.53
V7_w/VSVs	Mean	0.05	-0.08	-0.46	-0.44
	Peak	-6.53	-7.52	-5.41	-7.05
V8_w/out VSVs	Mean	0.00	0.50	0.03	-0.13
	Peak	-5.16	-6.88	-4.3	-6.5
V8_w/VSVs	Mean	0.00	0.47	0.12	-0.06
	Peak	-6.49	-6.99	-6.28	-6.64

The results show that for the gable and hip roofs, the net mean pressure coefficients consistently increased when the VSVs were installed; thus, confirming the suggestion that the VSVs can be utilized to reduce suction on the roof. The highest reductions in suction (increased net mean C_p values) were recorded at the 30° and 45° wind directions for both the gable and hip roofs. For the gable roof, suction on the roof envelope decreased by 72% for WD = 30° and by 63 % for WD = 45°, at V2. The hip roof with VSVs produced reductions in suction on the roof envelope by 75% for WD = 30°, at V8 and by 93% for WD = 45° at V1. The VSVs clearly have an effect on the differential pressure acting on the roof envelope, which help reduce suctions on the external roof sheathing thereby preventing possible roof fly off due to the wind.

As can be observed in Tables 6-4 and 6-5, the increase in net peak C_p values (less suction on the external roof sheathing) was not as consistent as for the net mean C_p values. This could be related to the size and location of the vents. Each vent opening provided a 2.2% open area ratio, which is relatively small. Previous studies have shown that peak internal pressures increase with higher dominant opening areas. The intensity of internal pressure is highly correlated to the size of the opening (Kopp et al. 2008, Tecle et al. 2012). In the present study, the vent openings were located at the roof corners and were small compared with windward soffit area.

The 45° wind direction for the hip roof generated the most consistent reduction in suction on the roof surface, with vents V1, V2 and V7 all providing an increase to net peak C_p between 6-17%.

Figure 6-17 shows the net mean pressure coefficients for the gable and hip roofs. The mean internal pressure was measured at each individual internal pressure tap and numerically averaged. This value was then subtracted from the numerically averaged mean external pressure on the roof.

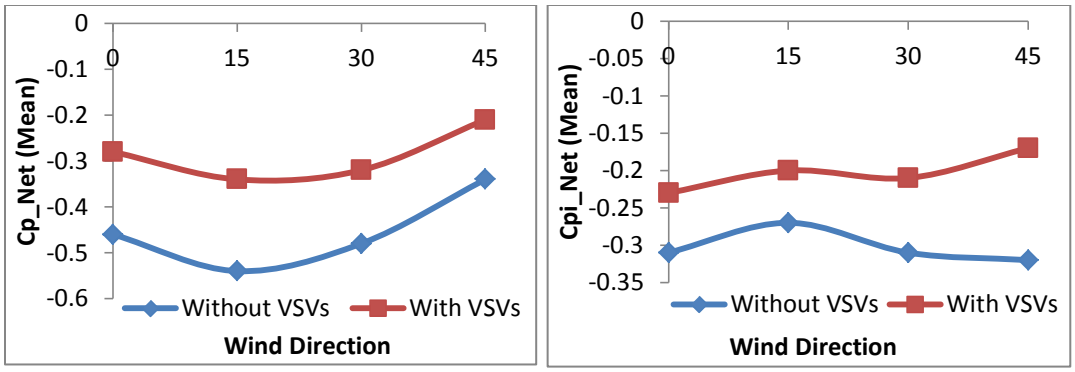

a) b)

Figure 6-17. Net mean pressure coefficients: a) gable roof; b) hip roof

The net mean $C_{p's}$ increased for the gable and hip roofs for the 0 to 45 and 60 degree wind directions. There were increases between 26-39% for the gable roof, with the highest increase being 39% for the 0° wind direction. For the hip roof, there were increases of 26-47%, with the 45° wind direction producing the highest increase (47%).

Comparison of Results: 1:6 Model Scale and Full-Scale BPA Safety Vents

There were two 1:6 model scale roofs that were used for this study ('small gable' and 'small hip') in addition to the 'large gable' and 'large hip' roofs that were used in the study from Chapter 5 to accommodate the full-scale *BPA Safety Vents*. Tables 6-6 and 6-7 include the details of each roof and corresponding areas of the soffit vent openings for the 0 and 30 degree wind directions respectively.

Table 6-6. Roof type and corresponding soffit vent details, 0° wind direction

Description	Large Gable	Small Gable	Large Hip	Small Hip
Vent Type	BPA Safety Vents	1:6 Scale VSVs	BPA Safety Vents	1:6 Scale VSVs
No. of Vents	4	4	8	8
Vent Opening Area	0.72 ft^2/vent	0.04 ft^2/vent	0.72 ft^2/vent	0.04 ft^2/vent
Area of Windward Vents, Aw	1.44 ft^2	0.08 ft^2	1.44 ft^2	0.08 ft^2
Area of Leeward Vents, Al	1.44 ft^2	0.08 ft^2	4.32 ft^2	0.24 ft^2
Ratio of Aw/Al	1	1	0.33	0.33
Windward Soffit Area	8.22 ft^2	1.79 ft^2	8.22 ft^2	1.79 ft^2
Percentage of Aw/Windward Soffit Area	17.50%	4.50%	17.50%	4.50%

Table 6-7. Roof type and corresponding soffit vent details, 30° wind direction

Description	Large Gable	Small Gable	Large Hip	Small Hip
Vent Type	BPA Safety Vents	1:6 Scale VSVs	BPA Safety Vents	1:6 Scale VSVs
No. of Vents	4	4	8	8
Vent Opening Area	0.72 ft^2/vent	0.04 ft^2/vent	0.72 ft^2/vent	0.04 ft^2/vent
Area of Windward Vents, Aw	1.44 ft^2	0.08 ft^2	2.16 ft^2	0.12 ft^2
Area of Leeward Vents, Al	1.44 ft^2	0.08 ft^2	3.6 ft^2	0.20 ft^2
Ratio of Aw/Al	1	1	0.6	0.6
Windward Soffit Area	16.44 ft^2	3.58 ft^2	16.44 ft^2	3.58 ft^2
Percentage of Aw/Windward Soffit Area	8.76%	2.23%	13.10%	3.35%

An investigation of the change in mean internal pressure coefficients (ΔC_{pi}) for the four roofs with respect to the ratio of the windward soffit vent openings to the leeward soffit vent openings (A_w/A_l) and relative soffit vent opening size to the windward soffit area (windward vent porosity) was conducted for 0 to 45 degree wind directions (Tables 6-8 and 6-9).

Table 6-8. Comparison of results between the large gable and large hip roof models

	Large Gable			Large Hip		
Wind Direction	**Aw/Al**	**Windward Vent Porosity**	**ΔCpi**	**Aw/Al**	**Windward Vent Porosity**	**ΔCpi**
0°	1.00	17.50%	0.31	0.33	17.50%	0.15
15°	1.00	17.50%	0.31	0.33	17.50%	0.13
30°	1.00	8.76%	0.27	0.60	13.10%	0.19
45°	1.00	8.76%	0.21	1.00	17.50%	0.21

Table 6-9. Comparison of results between the small gable and small hip roof models

	Small Gable			Small Hip		
Wind Direction	**Aw/Al**	**Windward Vent Porosity**	**ΔCpi**	**Aw/Al**	**Windward Vent Porosity**	**ΔCpi**
0°	1.00	4.50%	0.21	0.33	4.50%	0.08
15°	1.00	4.50%	0.20	0.33	4.50%	0.06
30°	1.00	2.23%	0.14	0.60	3.35%	0.10
45°	1.00	2.23%	0.10	1.00	4.50%	0.15

The results revealed that the reduction in mean internal pressure coefficients increased as the ratio of the windward soffit vent openings to the leeward soffit vent openings increased with respect to wind direction for the hip roofs with VSVs installed. In addition, the reduction in mean internal pressure coefficients increased as the windward vent porosity increased for both the gable and hip roofs with VSVs.

In order to determine how strongly the change in mean internal pressure coefficients (mean pressure drop) is correlated to the windward vent porosity and the A_w/A_l ratio, the correlation coefficients were calculated. The strength of the linear relationship between two random variables x and y with expected values μ_x and μ_y and standard deviations σ_x and σ_y was measured using the correlation coefficient, $\rho_{x,y} = COV_{x,y}/\sigma_x\sigma_y$; where $COV_{x,y} = E[(x-\mu_x)(y-\mu_y)]$ is the covariance, the measure of how much two variables change together. Data results with a correlation coefficient near to 0 are considered uncorrelated, whereas strongly correlated data have a correlation coefficient closer to 1.

For the gable roofs, the correlation coefficient for the windward vent porosity and the change in mean internal pressure was 0.91. The gable roofs had an A_w/A_l ratio of 1.0 for all wind directions as a result of the soffit vents being placed at the front and rear of the gable roofs. There were no vents located at the gable ends. However, the hip roofs had soffit vents at all sides; therefore, the A_w/A_l ratio changed with wind direction. The correlation coefficient for the A_w/A_l ratio and the change in mean internal pressure for the hip roofs was 0.69. In addition, the correlation coefficient for the windward vent porosity and the change in mean internal pressure for the hip roofs was 0.64.

As shown in Figure 6-18, regression lines and corresponding equations for the gable and hip roofs respectively can be estimated to determine the approximate change in mean internal pressure coefficients with VSVs installed.

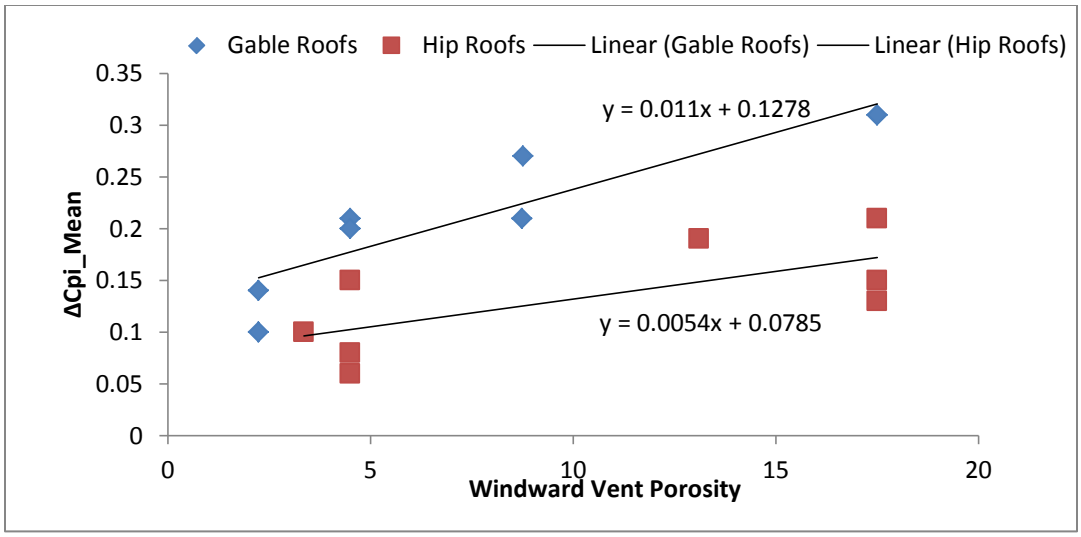

Figure 6-18. Regression lines and equations to estimate the change in mean $C_{pi's}$ with VSVs installed

The equations for the regression lines can be used to predict the reduction in the mean internal pressure coefficient for the attic space once the VSVs are installed. For the gable roofs, y = 0.011x + 0.1278 and for the hip roofs, y = 0.0054x + 0.0785, where x is the windward vent porosity between 2.0-17.5%. The margin of error for the equations is ±0.047.

Immediate Practical Recommendations

The windward vent porosity (soffit vent opening area relative to the windward soffit area) can be used as the characteristic value to predict the performance of the roof with VSVs installed. Reference tables can be developed using selected wind speeds at a specific reference height in order to estimate the mean internal pressure within the attic space without and with VSVs with respect to windward vent porosity. Tables 6-10 and 6-11 show the predicted mean internal pressures without and with VSVs for various

windward vent porosities for a wind speed of 150 mph at a reference height of 10 m (33 ft). The values in Tables 6-10 and 6-11 were calculated using the results from the testing. The internal pressure coefficients that were estimated in the testing were multiplied by the velocity pressure as defined in *ASCE 7-10*, $q_z = 0.00256K_zK_{zt}K_dV^2$; where V^2 is the 3- second gust wind speed at 10 m (33 ft) in an open terrain; K_z is the velocity pressure exposure coefficient, which is 1.0 for Exposure C; K_{zt} is the topographic factor of 1.0; and K_d is the wind directionality factor, which is also 1.0.

Table 6-10. Estimated mean internal pressures without and with VSVs for gable roofs

Wind Speed = 150 mph at 33 ft reference height

Windward Vent Porosity (%)	Mean Internal Pressure without VSVs, psf	Mean Internal Pressure with VSVs, psf
2.00	2.02	-4.90
4.50	5.76	-6.05
9.00	2.02	-11.81
17.50	10.66	-7.20

Table 6-11. Estimated mean internal pressures without and with VSVs for hip roofs

Wind Speed = 150 mph at 33 ft reference height

Windward Vent Porosity (%)	Mean Internal Pressure without VSVs, psf	Mean Internal Pressure with VSVs, psf
3.50	-2.30	-8.06
4.50	-0.58	-9.22
13.00	1.73	-9.22
17.50	3.46	-8.64

Tables 6-10 and 6-11 illustrate that there is negative internal pressure (suction) on the underside of the roof during high velocity winds with VSVs installed for both gable and hip roofs for various windward vent porosities. The values in the tables demonstrate

that the roof performance improves with the VSVs installed as the depressurization of the attic space helps keep the roof sheathing on.

In addition to the internal pressure tables (Tables 6-10 and 6-11), a VSVs design guide can be created as shown in Tables 6-12 and 6-13.

Table 6-12. Number of VSVs required per roof side for a 3.5% windward vent porosity

Area of Soffit, ft^2	Attic Area, ft^2	Soffit Vent Area Req'd by Code, ft^2	Soffit Vent Opening Area, ft^2 (3.5% Porosity)	No. of VSVs
20	100	0.67	0.70	**2**
30	225	1.50	1.05	**2**
40	400	2.67	1.40	**2**
50	625	4.17	1.75	**4**

Table 6-13. Number of VSVs required per roof side for 4.5% and 9% windward vent porosities

Area of Soffit, ft^2	Soffit Vent Opening Area, ft^2 (4.5% Porosity)	No. of VSVs	Soffit Vent Opening Area, ft^2 (9% Porosity)	No. of VSVs
20	0.90	**2**	1.80	**4**
30	1.35	**2**	2.70	**4**
40	1.80	**4**	3.60	**6**
50	2.25	**4**	4.50	**6**

Each VSV has a net opening area of 0.72 ft^2. Therefore, the required soffit vent opening area is divided by 0.72 to determine the number of VSVs that would be needed per roof side. The VSVs are required on all sides of the hip roof; however, they are only required on two sides (front and rear) of the gable roof. As a result, the hip roofs require twice the number of VSVs compared with the gable roofs. The VSVs should be placed near the building corners. In addition, the total area of the VSVs should be greater than 1/150 of the attic area in order to be ventilated as per the International Residential Code.

Conclusions

This study investigated the mean and peak internal pressure coefficients on a hip and a gable roof building without and with valved soffit vents (VSVs). The experimental study was carried out at the Wall of Wind (WOW) facility at FIU for wind directions 0 to 90 degrees for the gable roof building and 0 to 45 degrees for the hip roof building. Two different cases were considered: Case 1, soffit openings without VSVs and Case 2, soffit openings with VSVs. The VSVs prevented air entry into the attic space at higher wind speeds by allowing the wind-induced positive pressure to shut the vent, thereby closing the opening. The mean and peak pressure coefficients were measured on the external and internal roof surfaces, including on the floor of the building attic.

Results revealed that the mean external pressure coefficients did not change markedly for both of the cases on the exterior roof locations. However, the mean pressure coefficients were consistently reduced in magnitude (greater suction) in the interior locations with the VSVs installed. The net mean $C_{p's}$ increased for the gable and hip roofs for the 0 to 45 and 60 degree wind directions. For the gable roof, the highest increase was 39% for the 0° wind direction and for the hip roof, the 45° wind direction produced the highest increase (47%). In addition, net mean C_p values increased by 63-93% for both roofs at the windward vent locations for the case with VSVs, thereby, producing less suction on the roof sheathing.

An evaluation of internal pressure with leakage and an opening in the attic floor with VSVs installed was also conducted. The effect of background leakage was found to be of little consequence for the roofs with VSVs.

The peak pressure coefficients decreased by as much as 33% at localized areas, specifically at the vent locations with VSVs installed. However, net peak C_p values on the roof were not significantly influenced by the VSVs, which indicates that the vent opening areas may need to be larger and positioned at alternate locations.

The results from this present study show the efficacy of the installed VSVs in reducing mean pressure within the attic space, thus, mitigating the possibility of wind-induced damage to the roof.

CHAPTER VII

CONCLUSIONS AND RECOMMENDATIONS FOR FUTURE RESEARCH

This dissertation presents a new technique for reducing internal pressures and eliminating wind-driven rain into the roof attic space of low-rise buildings with gable and hip roofs. A system of valved soffit vents (VSVs) was installed on the roof soffits of the test buildings. The VSVs were equipped with a mechanism of hanging louvers that shut tight by the wind-induced positive pressures and remained open in the wind separation zones. Two main experimental studies were conducted. The first study was a performance evaluation of full-scale VSVs on a gable and a hip roof. External and internal pressures were measured and a wind-driven rain test was performed. The second study used a 1:6 scale model of a low-rise building with interchangeable gable and hip roofs to investigate the effects of valved soffit vents on external and internal pressures. Both studies were conducted at the Wall of Wind (WOW) research facility at Florida International University (FIU) in Miami, Florida.

The main achievement of this research is demonstrating that valved soffit vents are effective in reducing mean pressure within the attic space, increasing mean net pressures on the entire roof envelope and at the leading edge of the roof, reducing peak positive internal pressure at the windward soffit vent locations and disallowing wind-driven rain from entering the building. The VSVs can be retrofitted into existing buildings or installed on new buildings to improve the roof performance in high wind events.

Based on the experimental wind tunnel studies on the effects of valved soffit vents on low-rise buildings with hip and gable roofs, the following conclusions have been drawn:

1) The valved soffit vents (VSVs) used for Study 1 (*BPA Safety Vents*) engage for 3-second gust wind speeds of 15.8 m/s (35 mph) and greater. A wind speed of 39 m/s (87 mph) referenced at the roof eave height, 4'-2" (1.27 m), was found to activate the VSVs at all wind directions.
2) The VSV system operated as hypothesized, where the windward VSVs shut under wind-induced positive pressure, disallowing air flow into the attic space, while the VSVs in the wind separation zones remained open.
3) The VSVs displayed their ability to practically eliminate wind-driven rain from entering the attic space.
4) The effect of VSVs on internal pressures is dependent on the location, size and quantity with respect to wind direction.
5) Results from these studies indicated that there was a correlation between the mean external and internal pressure coefficients at the vent locations. The VSVs maintained this correlation for the VSVs located in the wind separation zones. However, the mean internal pressure coefficients within the attic space at the windward VSV locations were similar in value to the mean external pressure at the leeward VSV locations.
6) Removing the exterior screen from the VSVs had a negligible effect on mean internal pressures for the roofs with VSVs.

7) The effect of background leakage was found to be of little consequence on mean internal pressures for the roofs with VSVs.
8) With regard to the ratio of area of windward soffit vent openings to the area of leeward soffit vent openings (A_w/A_l), it was observed that as the A_w/A_l ratio increases for the hip roofs, the pressure drop in the attic space with VSVs installed also increases. The A_w/A_l ratio was 1.0 for the gable roofs for wind directions 0 to 45 degrees; however, the A_w/A_l ratio varied between 0.33 and 1.0 for the hip roofs.
9) The mean internal pressures increased as the area of windward soffit openings to the area of windward soffit (windward vent porosity ration) increased for the hip and gable roofs. Therefore, the higher the windward vent porosity ratio, the greater the pressure drop inside the attic with VSVs installed according to each roof type. A strong correlation was observed between windward vent porosity and mean internal pressure drop for the gable roofs.
10) The mean internal pressure coefficients decreased for the gable and hip roofs for the various wind directions with VSVs installed.
11) The net mean pressure coefficients on the entire roof surface increased on the gable and hip roofs, thereby providing less suction on the roof when VSVs are utilized. For the roofs in Study 1, the greatest increase was 91% for the gable roof and 65% for the hip roof. There was a 26-39% increase in net mean pressure for the gable roof and a 26-47% increase for the hip roof with respect to the wind direction recorded in Study 2.

12) The net mean pressure coefficients also increased at the leading edge of the roof covering the area at the windward vent locations. The net mean values changed from positive to negative for the gable roof and increased by as much as 98% for the hip roof in Study 1. The results from Study 2 showed that the highest increase was 72% for the gable roof and 93% for the hip roof.
13) The peak positive pressure coefficients were reduced by as much as 33% at localized areas, specifically at the vent locations with VSVs installed.
14) The net peak pressures on the roof surface did not markedly change overall. However, there was an increase in net peak pressure coefficients (reduced suction) for the leading edge of the hip roofs, with a maximum increase of 21% observed in Study 1.
15) The results determined that the VSVs do not have an effect on the internal pressure values for the gable roofs for the 75 and 90 degree wind directions, i.e. wind flow normal to the gable ends. This suggests that further investigation is required as to the possibility of introducing valved vents specifically for the gable ends.
16) CFD simulations validated the decrease in mean internal pressures for roofs with VSVs, although the mean C_{pi} values were lower than the experimental results.
17) Overall, the valved soffit vents showed promise in the area of wind-induced pressure and wind-driven rain damage mitigation.

Recommendations for Future Research

1) Future research is needed to investigate the effects of size, quantity and location of the valved soffits vents on the pressure coefficients.
2) More experimental study is required to examine the valved soffit vent concept with respect to other roof types in low-rise buildings, e.g. mono-slope and complex roofs.
3) Further study is also needed to determine the effects of VSVs on internal pressures for other terrain conditions and with neighboring buildings.
4) More advanced CFD simulations can be developed to further investigate and verify the effects of VSVs on low-rise buildings. The experimental results of this research can be compared with results from a CFD sensitivity analysis.
5) More detailed research is necessary to investigate the effects of combining VSVs with other devices, e.g. roof parapets and soffit trellises, to mitigate net pressure loads on the roof envelope and damage caused by wind-driven rain. The results could be used to develop a database of various mitigation techniques for low-rise buildings that would improve the overall performance of roofs during hurricanes and other high velocity wind events.

APPENDIX A
COMPARISON OF MEAN AND PEAK PRESSURE COEFFICIENTS

This appendix contains tables of the mean and peak pressure coefficients ($C_{p's}$) recorded for the gable and hip roof models for each test conducted within Chapter 5. However, Figure A-1 shows the wind profiles for the WOW used for the variable speed tests.

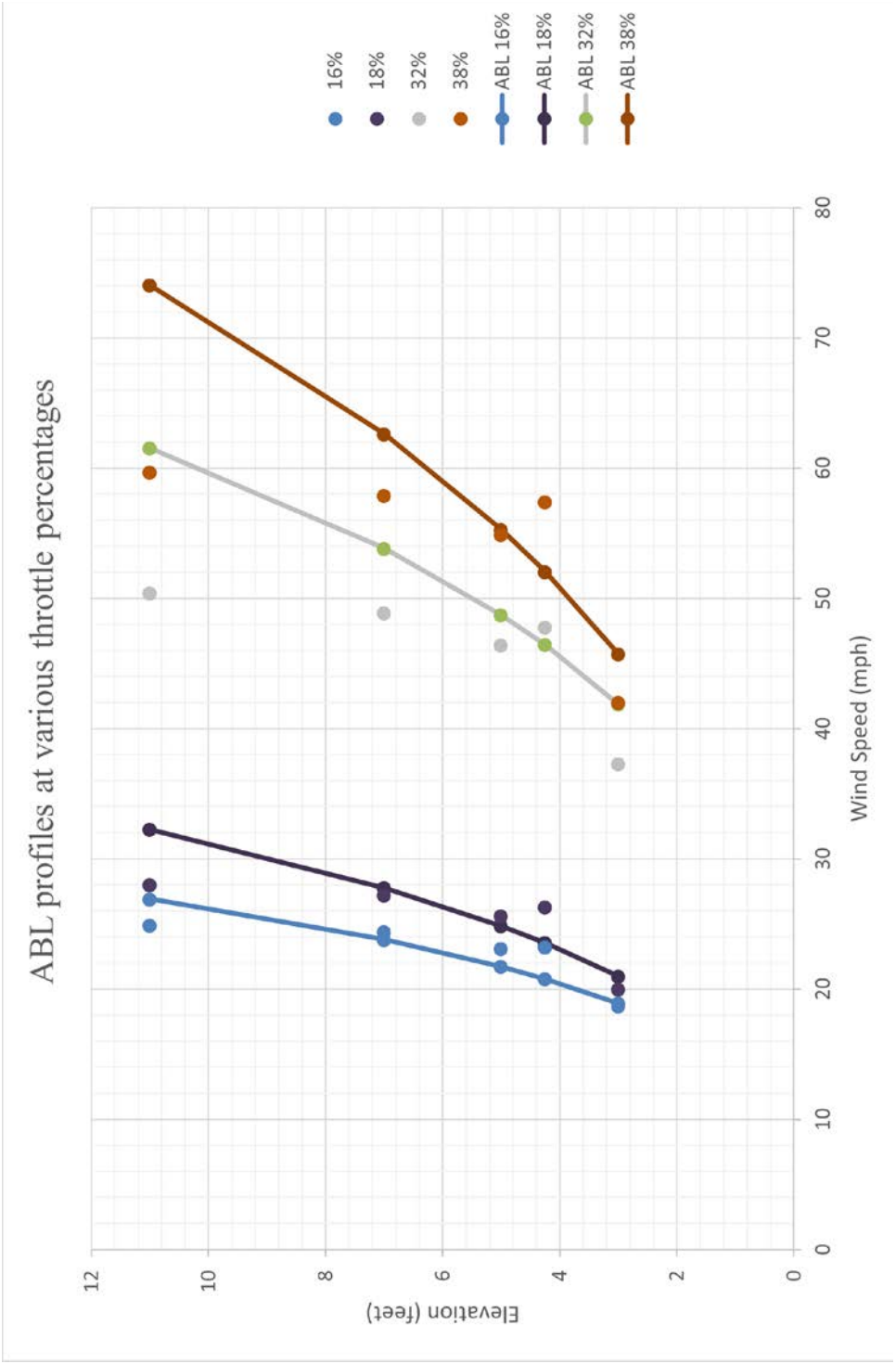

Figure A-1. Atmospheric boundary layer (ABL) velocity profiles at various throttle percentages for the WOW variable speed testing

Table A-1. Comparison of external and internal pressure coefficients without and with VSVs for the large gable roof model at 0° wind direction

	Without VSVs			With VSVs			With VSVs w/out Screen		
Tap No.	Cp Max	Cp Min	Cp Mean	Cp Max	Cp Min	Cp Mean	Cp Max	Cp Min	Cp Mean
1	2.52	-3.22	0.08	2.75	-4.02	0.06	2.92	-3.64	0.06
2	2.81	-3.79	0.04	2.92	-4.02	0.07	2.84	-3.89	0.08
3	2.87	-4.41	-0.28	3.01	-4.57	-0.21	2.58	-3.63	-0.20
4	2.88	-4.24	-0.55	3.14	-4.31	-0.41	2.92	-4.31	-0.38
5	2.07	-3.95	-0.53	2.96	-4.50	-0.45	2.57	-3.83	-0.43
6	2.53	-4.26	-0.37	3.38	-4.73	-0.35	2.64	-3.93	-0.34
7	3.41	-4.22	0.09	3.41	-4.63	0.03	2.58	-3.41	0.03
8	2.50	-3.39	0.07	3.12	-4.12	0.08	2.82	-3.91	0.09
9	2.53	-3.76	-0.27	2.99	-4.43	-0.21	2.26	-3.10	-0.20
10	2.49	-4.01	-0.48	3.45	-5.25	-0.38	2.81	-4.21	-0.36
11	2.35	-3.94	-0.56	3.36	-5.30	-0.47	2.34	-4.19	-0.45
12	3.08	-4.44	-0.36	3.26	-4.91	-0.36	2.46	-3.65	-0.34
13	3.19	-4.02	0.10	3.10	-4.47	0.08	2.60	-2.94	0.09
14	3.83	-5.08	0.07	3.69	-4.90	0.10	2.89	-3.71	0.09
15	2.86	-4.15	-0.22	2.89	-4.24	-0.16	2.61	-3.68	-0.16
16	2.65	-4.30	-0.54	3.14	-4.79	-0.43	2.17	-3.78	-0.40
17	2.67	-4.54	-0.58	2.61	-4.38	-0.48	2.53	-3.93	-0.46
18	3.13	-4.45	-0.40	3.07	-4.41	-0.37	2.72	-4.43	-0.37
19	2.92	-4.31	-0.12	3.15	-4.50	-0.11	2.50	-3.60	-0.11
20	2.95	-4.57	-0.18	2.91	-4.15	-0.16	2.72	-3.91	-0.17
21	3.46	-3.83	0.57	3.01	-3.52	0.50	2.98	-3.42	0.49
22	3.19	-3.71	0.74	3.64	-3.66	0.77	3.66	-3.88	0.79
23	3.78	-4.29	0.72	3.46	-3.98	0.73	3.22	-3.70	0.75
24	2.86	-4.16	-0.31	3.38	-4.83	-0.29	2.69	-3.72	-0.31
25	2.96	-4.02	-0.15	3.50	-4.90	-0.13	2.62	-3.74	-0.12
26	3.07	-4.52	-0.31	3.07	-4.78	-0.33	3.03	-4.48	-0.35
27	3.02	-4.16	0.54	3.49	-4.81	-0.09	2.19	-3.10	-0.08
28	3.26	-4.22	0.18	3.23	-4.45	-0.08	2.81	-3.93	-0.08
29	3.01	-3.80	0.19	3.18	-4.42	-0.08	2.45	-3.30	-0.07
30	3.40	-4.34	0.23	3.64	-5.25	-0.08	2.54	-3.73	-0.08
31	3.31	-5.07	-0.22	2.70	-4.06	-0.12	2.86	-4.09	-0.12
32	3.32	-4.09	0.18	3.31	-5.02	-0.09	3.17	-4.76	-0.08
33	3.21	-4.19	0.18	3.08	-4.20	-0.08	2.85	-4.02	-0.07
34	3.47	-4.43	0.21	3.07	-4.46	-0.08	2.92	-4.12	-0.08
35	3.42	-4.37	0.24	3.26	-4.48	-0.09	2.84	-4.07	-0.08
36	4.03	-5.13	0.23	3.58	-4.88	-0.08	2.82	-3.88	-0.07
37	3.03	-4.12	0.38	3.43	-4.77	-0.09	2.66	-3.91	-0.07
38	3.59	-4.68	0.18	3.62	-5.11	-0.08	2.55	-3.61	-0.09
39	3.19	-4.13	0.22	3.42	-4.57	-0.08	2.73	-3.80	-0.08
40	2.76	-3.26	0.25	2.98	-4.32	-0.08	3.56	-5.03	-0.07
41	2.67	-4.06	-0.18	3.10	-4.46	-0.10	2.94	-4.13	-0.10
42	3.48	-3.66	0.71	3.75	-5.20	-0.07	2.65	-3.75	-0.05
43	3.16	-4.00	0.30	3.27	-4.58	-0.09	3.05	-4.16	-0.09
44	3.38	-4.25	0.21	3.45	-4.82	-0.08	2.73	-3.88	-0.07
45	3.10	-4.17	0.09	3.28	-4.83	-0.09	2.56	-3.66	-0.09
46	3.63	-4.66	0.26	4.36	-5.97	-0.08	2.54	-3.47	-0.07
47	3.02	-3.81	0.20	2.90	-4.02	-0.08	2.55	-3.54	-0.08

48	3.36	-4.68	0.22	3.10	-4.64	-0.09	2.89	-4.14	-0.08
49	2.71	-3.66	0.09	3.03	-4.22	-0.09	2.52	-3.56	-0.09
50	3.45	-4.04	0.73	3.31	-4.72	-0.06	3.08	-4.08	-0.06
51	3.42	-4.30	0.32	3.23	-4.67	-0.08	3.44	-4.75	-0.09
52	3.31	-4.07	0.20	3.14	-4.46	-0.07	2.76	-3.89	-0.08
53	3.29	-4.51	0.02	3.01	-4.36	-0.09	2.58	-3.38	-0.09
54	3.75	-5.01	-0.11	3.08	-4.22	-0.10	3.02	-4.33	-0.08
55	2.98	-4.27	-0.06	3.08	-4.07	-0.09	2.39	-3.41	-0.08
56	3.54	-3.59	0.54	3.71	-4.88	-0.08	2.59	-3.51	-0.09
57	3.11	-3.87	0.42	2.94	-4.20	-0.10	2.92	-4.13	-0.08
58	3.18	-4.63	-0.14	3.66	-4.89	-0.10	2.78	-3.78	-0.10
59	2.97	-4.21	-0.16	3.33	-4.59	-0.10	2.65	-4.00	-0.11
60	3.69	-3.98	0.54	3.64	-4.93	-0.08	2.59	-3.58	-0.08
61	3.53	-3.89	0.52	2.91	-4.07	-0.10	2.44	-3.58	-0.09

Table A-2. Comparison of external and internal pressure coefficients without and with VSVs for the large gable roof model at 15° wind direction

	Without VSVs			With VSVs			With VSVs w/out Screen		
Tap No.	Cp Max	Cp Min	Cp Mean	Cp Max	Cp Min	Cp Mean	Cp Max	Cp Min	Cp Mean
1	3.52	-4.45	-0.03	3.25	-4.40	-0.07	2.44	-3.58	-0.08
2	3.04	-4.14	-0.01	3.29	-4.56	0.01	2.78	-3.86	0.01
3	3.03	-4.63	-0.37	2.73	-4.28	-0.35	2.37	-3.62	-0.36
4	3.12	-4.87	-0.69	2.33	-3.71	-0.68	2.40	-4.21	-0.68
5	2.65	-4.02	-0.55	2.79	-4.57	-0.52	2.65	-4.23	-0.52
6	3.20	-4.80	-0.35	2.72	-4.17	-0.32	2.48	-3.88	-0.34
7	3.42	-4.19	0.12	3.27	-4.72	0.04	2.82	-3.72	0.01
8	3.32	-4.59	0.03	1.94	-2.59	0.04	2.77	-3.52	0.03
9	2.85	-4.35	-0.38	2.76	-4.22	-0.37	2.62	-4.19	-0.38
10	3.26	-5.55	-0.74	2.43	-4.29	-0.71	2.63	-4.43	-0.72
11	2.62	-4.57	-0.62	2.22	-3.93	-0.60	1.91	-3.59	-0.61
12	2.74	-4.25	-0.29	2.79	-4.07	-0.28	2.79	-4.02	-0.29
13	3.32	-4.26	0.11	3.20	-4.46	0.12	2.77	-3.56	0.10
14	3.37	-4.68	0.04	3.42	-4.61	0.06	3.32	-4.52	0.04
15	3.06	-4.80	-0.37	2.65	-4.07	-0.36	1.93	-3.25	-0.37
16	2.64	-4.85	-0.94	1.99	-3.76	-0.92	2.36	-4.49	-0.92
17	2.67	-4.40	-0.55	2.67	-4.51	-0.53	2.19	-3.62	-0.54
18	3.29	-4.73	-0.34	3.35	-4.87	-0.30	2.49	-3.81	-0.31
19	3.95	-5.71	-0.25	2.78	-3.98	-0.19	2.77	-4.07	-0.20
20	3.65	-5.16	-0.24	2.31	-3.48	-0.21	2.81	-4.31	-0.21
21	3.54	-3.93	0.65	3.61	-3.81	0.64	3.10	-3.46	0.62
22	3.40	-3.85	0.69	3.47	-3.83	0.69	2.82	-2.98	0.68
23	4.02	-4.73	0.68	3.25	-3.52	0.70	2.69	-2.89	0.70
24	3.36	-4.29	-0.26	2.60	-3.64	-0.28	2.67	-3.93	-0.30
25	2.42	-3.60	-0.23	3.14	-4.54	-0.22	2.35	-3.56	-0.22
26	4.02	-5.64	-0.20	3.73	-5.19	-0.20	3.27	-4.77	-0.20
27	3.34	-4.07	0.44	2.85	-4.21	-0.16	3.03	-4.31	-0.16
28	3.29	-4.15	0.13	2.19	-3.07	-0.17	2.81	-4.05	-0.17
29	3.77	-4.88	0.15	3.29	-4.86	-0.16	2.57	-3.69	-0.16
30	3.50	-4.63	0.18	3.59	-5.09	-0.16	2.91	-4.14	-0.17
31	3.56	-5.38	-0.30	3.22	-4.55	-0.18	2.47	-3.43	-0.20
32	3.65	-4.88	0.14	2.95	-4.29	-0.16	2.56	-3.77	-0.17
33	2.91	-3.86	0.12	3.49	-4.97	-0.16	2.88	-4.25	-0.16
34	4.20	-5.43	0.13	3.49	-4.82	-0.14	3.23	-4.41	-0.16
35	3.76	-5.00	0.18	2.96	-4.22	-0.15	3.24	-4.60	-0.16
36	3.76	-4.74	0.20	3.12	-4.53	-0.16	3.21	-4.40	-0.16
37	3.66	-4.96	0.31	2.96	-4.27	-0.16	3.01	-4.51	-0.15
38	3.42	-4.47	0.14	3.22	-4.69	-0.17	3.34	-4.69	-0.18
39	3.44	-4.38	0.16	3.06	-4.29	-0.16	2.49	-3.47	-0.17
40	3.38	-4.53	0.17	2.28	-3.31	-0.15	2.45	-3.62	-0.15
41	3.16	-4.81	-0.26	2.93	-4.28	-0.19	2.33	-3.44	-0.20
42	4.21	-4.06	0.63	3.53	-5.09	-0.14	2.41	-3.60	-0.14
43	3.68	-4.95	0.22	2.79	-3.92	-0.15	2.65	-3.84	-0.17
44	2.90	-3.72	0.16	2.54	-3.86	-0.15	2.90	-4.26	-0.16
45	3.83	-5.00	0.01	3.52	-4.97	-0.16	3.01	-4.35	-0.17
46	3.75	-5.03	0.17	3.88	-5.66	-0.15	3.69	-5.47	-0.15
47	3.13	-4.08	0.14	3.30	-4.86	-0.16	3.12	-4.35	-0.17

48	3.88	-5.04	0.16	2.41	-3.82	-0.16	2.63	-3.94	-0.16
49	2.90	-4.02	0.00	3.51	-5.08	-0.17	2.29	-3.26	-0.18
50	4.02	-4.56	0.70	3.38	-4.92	-0.13	3.17	-4.54	-0.14
51	3.87	-4.61	0.28	2.81	-4.00	-0.15	2.82	-4.03	-0.17
52	3.60	-4.73	0.14	2.63	-3.63	-0.15	3.10	-4.47	-0.17
53	3.27	-4.62	-0.04	2.90	-4.21	-0.19	2.69	-3.96	-0.19
54	3.81	-5.41	-0.21	2.72	-4.06	-0.18	3.08	-4.75	-0.18
55	3.38	-5.00	-0.18	2.74	-3.93	-0.19	2.62	-3.72	-0.21
56	3.41	-4.46	0.23	2.98	-4.20	-0.15	2.91	-4.28	-0.17
57	3.65	-4.37	0.56	3.25	-4.76	-0.17	3.04	-4.42	-0.18
58	3.14	-4.69	-0.22	3.57	-5.32	-0.18	2.62	-3.80	-0.18
59	2.74	-4.10	-0.23	2.60	-3.79	-0.19	2.29	-3.42	-0.20
60	3.85	-4.49	0.54	2.27	-3.37	-0.15	2.75	-3.93	-0.17
61	3.33	-3.65	0.47	3.45	-4.85	-0.17	2.83	-4.09	-0.18

Table A-3. Comparison of external and internal pressure coefficients without and with VSVs for the large gable roof model at 30° wind direction

	Without VSVs			With VSVs			With VSVs w/out Screen		
Tap No.	Cp Max	Cp Min	Cp Mean	Cp Max	Cp Min	Cp Mean	Cp Max	Cp Min	Cp Mean
1	2.21	-3.36	-0.10	2.39	-3.41	-0.10	1.86	-2.47	-0.14
2	2.92	-4.08	-0.02	2.63	-3.71	0.01	2.50	-3.69	-0.01
3	2.89	-4.61	-0.34	2.70	-4.08	-0.32	2.44	-3.84	-0.36
4	2.28	-3.99	-0.65	2.28	-3.99	-0.64	1.92	-3.26	-0.65
5	1.44	-2.48	-0.44	2.36	-3.90	-0.42	1.75	-3.08	-0.44
6	2.76	-4.10	-0.31	2.77	-4.08	-0.29	2.25	-3.38	-0.31
7	1.88	-2.34	0.15	2.79	-3.58	0.09	1.66	-2.26	0.04
8	2.65	-3.71	0.02	1.90	-2.69	0.03	2.20	-3.16	0.01
9	2.36	-3.84	-0.39	1.64	-2.90	-0.37	2.05	-3.56	-0.40
10	2.53	-4.75	-0.86	1.73	-3.48	-0.84	1.95	-3.69	-0.87
11	2.37	-3.65	-0.48	2.24	-3.38	-0.46	1.97	-3.49	-0.48
12	3.21	-4.75	-0.24	2.85	-4.19	-0.21	2.35	-3.57	-0.23
13	2.81	-3.62	0.10	2.12	-2.64	0.13	2.04	-2.76	0.09
14	3.28	-4.66	0.03	3.15	-4.41	0.05	2.75	-3.84	0.02
15	2.09	-3.48	-0.39	2.54	-4.23	-0.38	1.91	-3.31	-0.40
16	1.78	-4.10	-1.18	1.80	-4.15	-1.16	1.97	-4.25	-1.19
17	1.96	-3.53	-0.42	2.12	-3.55	-0.40	1.98	-3.33	-0.41
18	2.74	-4.39	-0.34	2.48	-4.02	-0.30	2.41	-3.87	-0.33
19	2.83	-4.12	-0.26	2.81	-4.24	-0.19	2.35	-3.40	-0.23
20	2.56	-4.02	-0.28	3.18	-4.76	-0.21	2.11	-3.20	-0.23
21	2.40	-2.48	0.70	2.41	-2.47	0.74	3.08	-3.43	0.72
22	2.96	-3.37	0.61	3.13	-3.57	0.54	2.92	-3.57	0.54
23	3.17	-3.76	0.55	2.30	-2.60	0.57	2.84	-3.38	0.55
24	2.62	-3.39	0.18	2.09	-2.82	0.20	2.62	-3.62	0.18
25	2.34	-3.70	-0.24	2.00	-3.20	-0.23	1.95	-3.07	-0.25
26	2.57	-3.86	-0.19	2.76	-4.18	-0.18	2.58	-3.84	-0.20
27	2.78	-3.64	0.20	2.77	-4.20	-0.17	1.94	-2.83	-0.17
28	3.16	-4.47	0.09	2.57	-3.87	-0.18	2.52	-3.69	-0.16
29	2.45	-3.40	0.08	2.38	-3.48	-0.18	2.00	-3.01	-0.18
30	2.72	-3.64	0.12	2.70	-3.93	-0.17	2.80	-4.15	-0.17
31	2.28	-3.73	-0.31	2.65	-3.94	-0.20	2.40	-3.43	-0.23
32	2.98	-4.08	0.08	2.67	-4.06	-0.17	2.76	-3.89	-0.17
33	2.39	-3.27	0.07	2.32	-3.53	-0.16	2.34	-3.55	-0.17
34	2.93	-3.96	0.09	3.19	-4.76	-0.15	2.69	-4.09	-0.18
35	2.50	-3.41	0.16	2.32	-3.53	-0.15	1.80	-2.89	-0.20
36	2.67	-3.47	0.21	2.86	-4.30	-0.17	2.67	-3.95	-0.16
37	2.38	-2.33	0.38	2.73	-3.96	-0.17	1.72	-2.57	-0.17
38	2.82	-4.05	0.09	2.52	-3.74	-0.18	1.81	-2.76	-0.17
39	2.24	-2.92	0.10	3.02	-4.30	-0.16	1.82	-2.83	-0.18
40	2.83	-3.83	0.11	2.36	-3.52	-0.15	2.52	-3.70	-0.17
41	2.85	-4.18	-0.23	1.93	-2.99	-0.19	2.64	-3.91	-0.20
42	3.26	-3.79	0.44	2.87	-4.27	-0.15	2.77	-4.03	-0.15
43	3.25	-4.57	0.08	2.45	-3.69	-0.15	2.50	-3.82	-0.21
44	3.59	-4.91	0.09	3.09	-4.49	-0.15	2.85	-4.20	-0.19
45	2.62	-3.54	-0.04	2.89	-4.31	-0.17	2.54	-3.93	-0.20

46	3.41	-4.67	0.10	2.78	-4.13	-0.15	2.91	-4.20	-0.18
47	2.80	-3.83	0.08	2.64	-4.01	-0.16	2.31	-3.51	-0.17
48	3.27	-4.31	0.10	3.28	-4.85	-0.16	2.56	-3.95	-0.19
49	2.35	-3.23	-0.05	2.72	-4.21	-0.17	2.73	-4.13	-0.19
50	2.79	-3.26	0.65	3.00	-4.38	-0.13	3.09	-4.41	-0.16
51	2.39	-3.29	0.28	2.29	-3.45	-0.15	1.88	-3.00	-0.20
52	3.01	-4.33	0.09	2.94	-4.26	-0.16	3.06	-4.49	-0.17
53	2.18	-3.15	-0.06	2.31	-3.63	-0.19	2.47	-3.70	-0.18
54	2.47	-3.90	-0.24	3.11	-4.61	-0.19	2.42	-3.58	-0.20
55	1.95	-3.23	-0.26	2.32	-3.50	-0.20	2.28	-3.31	-0.19
56	3.37	-4.54	-0.02	2.48	-3.73	-0.16	2.05	-3.31	-0.19
57	2.57	-2.41	0.65	2.70	-3.98	-0.18	2.25	-3.51	-0.18
58	2.62	-4.04	-0.24	2.54	-3.83	-0.19	2.55	-3.60	-0.20
59	2.83	-4.29	-0.21	2.37	-3.68	-0.19	1.98	-3.20	-0.21
60	2.96	-3.60	0.53	2.38	-3.54	-0.16	2.28	-3.43	-0.20
61	2.17	-3.22	0.30	2.47	-3.71	-0.17	2.39	-3.58	-0.20

Table A-4. Comparison of external and internal pressure coefficients without and with VSVs for the large gable roof model at 45° wind direction

	Without VSVs			With VSVs			With VSVs w/out Screen		
Tap No.	Cp Max	Cp Min	Cp Mean	Cp Max	Cp Min	Cp Mean	Cp Max	Cp Min	Cp Mean
1	2.06	-3.32	-0.12	2.73	-4.09	-0.14	2.34	-3.65	-0.14
2	2.58	-3.80	-0.06	3.11	-4.20	-0.03	2.41	-3.15	-0.04
3	2.40	-3.85	-0.35	3.07	-4.63	-0.34	2.64	-3.90	-0.35
4	2.31	-3.95	-0.70	2.72	-4.37	-0.69	2.13	-3.99	-0.70
5	2.27	-3.49	-0.27	2.67	-3.97	-0.26	2.49	-3.65	-0.26
6	2.54	-3.78	-0.33	2.96	-4.31	-0.32	2.62	-3.76	-0.33
7	3.00	-4.14	0.09	2.76	-3.85	0.02	2.62	-3.56	-0.01
8	2.58	-3.60	-0.01	2.75	-3.96	-0.03	2.81	-3.90	-0.03
9	2.45	-3.82	-0.37	2.37	-3.98	-0.37	2.21	-3.65	-0.38
10	2.46	-4.55	-0.98	2.65	-4.86	-0.97	2.27	-4.33	-0.99
11	2.44	-3.94	-0.44	2.52	-4.04	-0.43	2.44	-4.09	-0.44
12	2.47	-3.62	-0.24	2.91	-4.18	-0.23	2.32	-3.58	-0.23
13	2.91	-3.75	0.03	2.89	-3.67	0.05	2.40	-3.26	0.04
14	2.77	-3.89	-0.03	2.97	-4.09	-0.01	2.54	-3.48	-0.03
15	2.43	-3.78	-0.36	2.73	-4.31	-0.36	2.28	-3.56	-0.38
16	1.82	-4.35	-1.20	2.11	-4.44	-1.19	2.34	-4.93	-1.21
17	2.17	-3.55	-0.40	2.80	-4.31	-0.39	2.64	-4.24	-0.40
18	2.31	-3.96	-0.35	2.66	-4.13	-0.33	2.63	-3.97	-0.35
19	2.56	-3.82	-0.32	2.87	-4.45	-0.28	2.72	-4.09	-0.30
20	2.30	-3.59	-0.35	3.08	-4.75	-0.31	2.31	-3.30	-0.31
21	2.71	-2.97	0.53	3.15	-3.52	0.58	3.09	-3.40	0.57
22	3.07	-3.59	0.46	3.45	-4.16	0.33	3.24	-3.77	0.31
23	2.65	-3.14	0.32	2.81	-3.32	0.33	2.83	-3.53	0.32
24	2.77	-3.47	0.38	2.71	-3.16	0.39	2.50	-2.76	0.38
25	2.64	-4.07	-0.31	2.75	-4.23	-0.31	2.05	-3.07	-0.32
26	3.17	-4.50	-0.21	3.32	-5.05	-0.21	3.05	-4.37	-0.22
27	2.74	-3.67	0.01	2.55	-3.77	-0.23	2.71	-4.06	-0.23
28	2.68	-3.69	-0.02	2.71	-3.95	-0.21	2.95	-4.12	-0.22
29	2.93	-4.01	-0.04	2.65	-3.98	-0.25	2.39	-3.55	-0.25
30	2.84	-3.88	-0.05	2.98	-4.24	-0.22	3.10	-4.66	-0.23
31	2.40	-4.03	-0.36	2.58	-3.96	-0.27	2.85	-4.18	-0.29
32	2.88	-3.96	-0.06	3.33	-4.91	-0.23	2.72	-4.10	-0.23
33	2.69	-3.81	-0.04	2.82	-4.18	-0.23	2.67	-4.23	-0.23
34	2.87	-3.88	-0.03	3.17	-4.60	-0.23	2.64	-4.04	-0.24
35	3.11	-4.22	0.01	3.17	-4.71	-0.24	2.94	-4.32	-0.26
36	3.19	-4.16	0.09	2.98	-4.45	-0.23	2.54	-3.82	-0.23
37	2.74	-3.42	0.12	2.75	-4.18	-0.23	2.32	-3.42	-0.24
38	2.75	-3.74	-0.03	3.39	-4.95	-0.23	2.67	-3.98	-0.23
39	2.75	-3.98	-0.02	2.45	-3.83	-0.23	2.47	-3.66	-0.24
40	2.66	-3.83	-0.01	3.09	-4.73	-0.23	2.88	-4.29	-0.24
41	2.84	-4.15	-0.28	2.75	-4.18	-0.26	2.91	-4.23	-0.26
42	3.11	-3.88	0.17	3.02	-4.52	-0.21	2.53	-3.76	-0.21
43	2.86	-3.87	-0.07	3.11	-4.66	-0.24	2.67	-3.80	-0.26
44	3.33	-4.68	-0.05	2.96	-4.46	-0.23	2.41	-3.64	-0.24
45	2.88	-4.16	-0.15	2.76	-3.97	-0.24	2.17	-3.48	-0.25
46	3.11	-4.30	-0.04	2.97	-4.56	-0.23	2.71	-4.09	-0.24
47	2.66	-3.64	-0.04	3.21	-4.81	-0.22	2.90	-4.32	-0.23

48	2.74	-3.91	-0.04	2.78	-4.10	-0.24	2.54	-3.91	-0.25
49	2.83	-3.97	-0.15	2.48	-3.71	-0.24	2.50	-3.73	-0.25
50	3.17	-3.72	0.48	3.34	-4.93	-0.22	2.59	-3.93	-0.23
51	2.96	-3.98	0.02	2.99	-4.52	-0.23	2.77	-4.14	-0.25
52	3.02	-4.13	-0.02	2.93	-4.34	-0.22	2.88	-4.17	-0.23
53	2.18	-3.24	-0.17	2.46	-3.70	-0.24	2.83	-4.16	-0.24
54	2.25	-3.84	-0.33	2.90	-4.27	-0.27	2.67	-4.01	-0.26
55	2.43	-3.79	-0.34	2.43	-3.58	-0.25	2.21	-3.36	-0.23
56	2.53	-3.45	-0.16	2.81	-4.13	-0.22	3.13	-4.68	-0.25
57	3.10	-3.44	0.72	2.33	-3.38	-0.24	3.12	-4.43	-0.24
58	2.79	-4.09	-0.29	2.68	-3.90	-0.25	2.68	-3.92	-0.26
59	3.03	-4.32	-0.25	2.89	-4.38	-0.27	3.10	-4.52	-0.28
60	2.89	-3.75	0.21	3.03	-4.58	-0.22	3.26	-4.72	-0.26
61	2.74	-3.61	0.07	2.14	-3.45	-0.24	2.91	-4.27	-0.25

Table A-5. Comparison of external and internal pressure coefficients without and with VSVs for the large gable roof model at 60° wind direction

	Without VSVs			With VSVs			With VSVs w/out Screen		
Tap No.	Cp Max	Cp Min	Cp Mean	Cp Max	Cp Min	Cp Mean	Cp Max	Cp Min	Cp Mean
1	2.32	-3.37	-0.07	2.34	-3.33	-0.08	2.46	-3.45	-0.11
2	2.51	-3.61	-0.07	2.84	-4.00	-0.05	2.47	-3.57	-0.06
3	2.08	-3.10	-0.28	2.70	-4.11	-0.28	2.46	-3.87	-0.30
4	2.66	-3.94	-0.63	2.22	-3.84	-0.64	2.44	-4.33	-0.65
5	2.25	-3.34	-0.24	2.75	-4.14	-0.23	2.71	-4.01	-0.24
6	2.91	-4.14	-0.31	2.86	-4.27	-0.30	2.53	-3.98	-0.32
7	2.68	-3.58	-0.01	2.60	-3.46	-0.05	2.74	-3.86	-0.09
8	2.28	-3.20	-0.03	2.21	-3.19	-0.04	2.56	-3.63	-0.05
9	2.17	-3.31	-0.25	2.42	-3.63	-0.26	2.53	-3.77	-0.27
10	2.17	-3.79	-0.56	2.99	-4.68	-0.56	2.87	-4.44	-0.58
11	2.43	-3.95	-0.38	2.37	-3.80	-0.38	2.44	-3.92	-0.39
12	2.19	-3.30	-0.25	2.64	-3.72	-0.26	2.55	-3.91	-0.27
13	2.45	-3.38	-0.04	2.48	-3.44	-0.02	2.33	-3.20	-0.04
14	2.99	-4.25	-0.06	2.60	-3.68	-0.04	2.69	-3.82	-0.07
15	2.14	-3.18	-0.22	2.50	-3.74	-0.23	2.47	-3.40	-0.25
16	2.47	-3.77	-0.44	2.51	-4.03	-0.44	2.59	-3.83	-0.45
17	2.02	-3.35	-0.39	2.63	-4.00	-0.40	2.03	-3.12	-0.40
18	2.32	-3.66	-0.49	2.75	-4.27	-0.47	2.24	-3.83	-0.49
19	2.30	-3.48	-0.37	2.53	-4.02	-0.30	2.44	-3.94	-0.33
20	2.18	-3.49	-0.38	2.65	-3.94	-0.32	2.44	-3.75	-0.34
21	2.69	-3.60	0.13	2.54	-3.49	0.14	2.43	-3.09	0.10
22	3.06	-3.78	0.28	2.66	-3.61	0.13	2.67	-3.39	0.09
23	2.59	-3.42	0.10	2.48	-3.12	0.11	2.33	-3.12	0.09
24	2.42	-2.50	0.58	3.33	-3.92	0.60	2.92	-3.17	0.56
25	2.12	-3.43	-0.34	2.88	-4.44	-0.33	2.28	-3.77	-0.36
26	3.09	-4.54	-0.20	3.27	-4.66	-0.20	2.77	-4.12	-0.22
27	2.96	-4.29	-0.12	2.76	-3.99	-0.24	2.06	-3.19	-0.27
28	2.42	-3.45	-0.12	2.79	-3.87	-0.22	2.31	-3.56	-0.25
29	2.11	-3.28	-0.15	2.47	-3.64	-0.25	2.82	-4.17	-0.30
30	2.49	-3.45	-0.15	2.98	-4.37	-0.23	2.98	-4.36	-0.26
31	2.30	-3.74	-0.36	2.88	-4.54	-0.29	2.51	-3.90	-0.32
32	2.39	-3.38	-0.14	2.46	-3.73	-0.25	3.14	-4.76	-0.27
33	1.75	-2.62	-0.15	2.63	-4.02	-0.24	2.40	-3.81	-0.26
34	2.64	-3.80	-0.15	2.65	-3.79	-0.24	2.63	-4.09	-0.28
35	1.92	-2.81	-0.14	2.87	-4.23	-0.26	2.65	-4.31	-0.30
36	2.91	-4.08	-0.09	2.95	-4.27	-0.25	2.89	-4.36	-0.27
37	2.31	-3.21	-0.15	2.31	-3.54	-0.25	2.75	-4.08	-0.28
38	2.91	-4.09	-0.13	2.45	-3.62	-0.23	2.98	-4.57	-0.26
39	3.09	-4.33	-0.14	2.76	-4.06	-0.24	2.93	-4.32	-0.28
40	2.55	-3.81	-0.14	2.51	-3.89	-0.25	2.76	-4.34	-0.28
41	2.83	-4.34	-0.29	2.94	-4.43	-0.27	2.05	-3.20	-0.30
42	2.94	-4.10	-0.07	3.01	-4.57	-0.23	2.98	-4.45	-0.25
43	2.43	-3.66	-0.19	2.57	-3.81	-0.26	2.68	-4.05	-0.30
44	3.07	-4.37	-0.17	2.67	-4.24	-0.25	2.77	-4.14	-0.29
45	2.41	-3.57	-0.23	2.56	-3.95	-0.26	2.38	-3.66	-0.29

46	2.73	-3.95	-0.14	2.95	-4.19	-0.25	3.51	-5.11	-0.28
47	2.78	-4.05	-0.13	2.37	-3.58	-0.23	2.45	-3.94	-0.26
48	2.36	-3.48	-0.16	2.80	-4.10	-0.26	2.26	-3.66	-0.29
49	2.57	-3.68	-0.21	2.67	-4.14	-0.25	2.49	-3.90	-0.29
50	2.84	-3.82	-0.04	2.99	-4.52	-0.24	2.29	-3.57	-0.28
51	2.41	-3.46	-0.15	2.64	-3.76	-0.25	2.52	-3.91	-0.29
52	3.16	-4.28	-0.14	2.44	-3.45	-0.20	2.72	-3.97	-0.26
53	2.43	-3.52	-0.22	2.50	-3.81	-0.24	2.47	-3.81	-0.27
54	2.92	-4.67	-0.31	2.34	-3.62	-0.28	2.81	-4.15	-0.29
55	2.44	-3.85	-0.33	2.41	-3.78	-0.27	2.31	-3.59	-0.30
56	2.71	-3.85	-0.17	2.47	-3.86	-0.23	2.57	-3.64	-0.22
57	2.47	-3.04	0.65	2.81	-4.27	-0.25	2.41	-3.65	-0.26
58	1.84	-3.17	-0.31	2.65	-4.05	-0.27	2.95	-4.51	-0.29
59	2.02	-3.07	-0.29	2.57	-3.85	-0.29	3.00	-4.39	-0.31
60	2.43	-3.72	-0.18	2.59	-3.84	-0.24	2.66	-4.00	-0.30
61	2.36	-3.61	-0.11	2.70	-3.89	-0.26	2.96	-4.58	-0.29

Table A-6. Comparison of external and internal pressure coefficients without and with VSVs for the large gable roof model at 75° wind direction

	Without VSVs			With VSVs			With VSVs w/out Screen		
Tap No.	Cp Max	Cp Min	Cp Mean	Cp Max	Cp Min	Cp Mean	Cp Max	Cp Min	Cp Mean
1	2.62	-3.57	-0.04	2.50	-3.45	-0.03	2.58	-3.55	-0.05
2	2.94	-4.03	-0.06	2.91	-4.16	-0.04	2.68	-3.82	-0.05
3	2.38	-3.53	-0.15	3.15	-4.50	-0.14	2.52	-3.49	-0.16
4	2.92	-4.04	-0.16	3.23	-4.67	-0.16	2.46	-3.45	-0.17
5	2.88	-4.23	-0.15	2.83	-4.28	-0.14	1.93	-3.04	-0.15
6	2.94	-4.55	-0.22	3.03	-4.49	-0.21	2.42	-3.59	-0.23
7	2.91	-4.20	-0.12	2.78	-3.95	-0.08	2.59	-3.55	-0.10
8	2.80	-3.99	-0.04	2.81	-4.06	-0.05	2.71	-3.88	-0.05
9	2.62	-3.79	-0.10	3.18	-4.48	-0.10	2.85	-3.97	-0.12
10	3.23	-4.61	-0.19	3.34	-4.72	-0.18	2.97	-4.19	-0.20
11	3.09	-5.10	-0.26	2.86	-4.03	-0.25	2.46	-3.88	-0.27
12	2.80	-4.08	-0.23	2.95	-4.33	-0.23	2.48	-3.82	-0.24
13	2.94	-4.41	-0.10	2.98	-4.21	-0.08	2.38	-3.48	-0.09
14	3.21	-4.53	-0.07	3.48	-5.02	-0.05	2.77	-3.99	-0.08
15	2.91	-4.01	-0.09	3.25	-4.45	-0.09	2.46	-4.03	-0.11
16	2.44	-3.59	-0.31	2.97	-4.23	-0.31	2.81	-3.87	-0.31
17	2.64	-4.21	-0.39	2.58	-4.07	-0.38	2.73	-3.90	-0.39
18	2.75	-4.94	-0.34	2.59	-4.20	-0.32	2.63	-4.16	-0.34
19	2.86	-4.36	-0.33	3.14	-4.87	-0.30	2.78	-4.32	-0.31
20	2.58	-3.82	-0.33	3.15	-4.59	-0.32	2.30	-3.35	-0.32
21	1.89	-3.36	-0.45	2.28	-4.11	-0.52	2.19	-3.80	-0.52
22	2.56	-3.62	-0.34	2.95	-4.41	-0.31	2.60	-3.89	-0.31
23	2.26	-3.67	-0.35	2.85	-3.94	-0.32	2.47	-4.02	-0.32
24	3.28	-3.58	0.72	2.96	-3.39	0.73	2.67	-2.68	0.71
25	2.68	-4.09	-0.33	2.42	-3.74	-0.30	2.10	-3.33	-0.31
26	3.56	-5.35	-0.14	3.01	-4.29	-0.14	2.68	-3.79	-0.15
27	2.53	-4.23	-0.30	2.98	-4.22	-0.28	2.58	-3.86	-0.29
28	2.93	-4.32	-0.29	3.23	-4.91	-0.28	2.75	-4.13	-0.30
29	3.14	-4.77	-0.31	2.90	-4.59	-0.30	2.20	-3.44	-0.36
30	3.07	-4.81	-0.30	3.57	-5.29	-0.28	2.70	-4.22	-0.31
31	2.43	-3.87	-0.34	3.57	-5.28	-0.31	3.00	-4.49	-0.33
32	2.83	-4.38	-0.30	2.91	-4.41	-0.31	2.68	-4.01	-0.32
33	3.10	-4.70	-0.32	3.03	-4.55	-0.30	2.76	-4.08	-0.31
34	3.18	-4.93	-0.32	3.30	-5.00	-0.28	2.86	-4.37	-0.31
35	2.67	-4.27	-0.33	2.53	-4.02	-0.30	2.82	-4.13	-0.33
36	2.83	-4.41	-0.30	3.58	-5.45	-0.29	2.92	-4.66	-0.30
37	2.67	-4.72	-0.48	2.52	-4.02	-0.41	2.29	-3.49	-0.43
38	2.90	-4.49	-0.31	3.93	-5.92	-0.29	2.63	-4.02	-0.30
39	2.79	-4.29	-0.31	3.09	-4.57	-0.29	2.50	-3.74	-0.31
40	3.34	-5.23	-0.32	3.11	-4.50	-0.29	2.40	-3.68	-0.30
41	3.06	-4.64	-0.29	2.88	-4.35	-0.27	2.31	-3.56	-0.29
42	2.97	-4.86	-0.26	3.54	-5.16	-0.24	3.15	-4.61	-0.27
43	3.52	-5.17	-0.33	3.06	-4.56	-0.29	3.19	-4.76	-0.32
44	3.24	-4.84	-0.33	3.16	-4.60	-0.29	2.81	-4.41	-0.31
45	2.88	-4.46	-0.32	3.28	-4.82	-0.29	2.25	-3.39	-0.31
46	3.20	-4.94	-0.34	3.27	-4.94	-0.30	3.18	-4.69	-0.31
47	3.15	-4.75	-0.31	3.45	-5.13	-0.28	2.94	-4.37	-0.30

48	2.94	-4.75	-0.32	2.40	-3.72	-0.30	2.20	-3.42	-0.31
49	3.00	-4.51	-0.31	2.95	-4.51	-0.29	2.07	-3.22	-0.31
50	2.91	-4.85	-0.38	3.73	-5.58	-0.33	2.79	-4.18	-0.35
51	2.90	-4.67	-0.33	2.86	-4.23	-0.29	2.57	-3.95	-0.31
52	2.66	-3.90	-0.30	3.18	-4.88	-0.28	2.89	-4.17	-0.30
53	2.78	-4.21	-0.27	2.72	-3.91	-0.27	2.50	-3.81	-0.27
54	2.81	-4.37	-0.32	3.00	-4.56	-0.31	2.47	-3.93	-0.31
55	2.06	-3.43	-0.32	2.91	-4.23	-0.27	1.93	-2.83	-0.28
56	2.79	-4.35	-0.36	2.97	-4.39	-0.38	2.82	-4.63	-0.42
57	3.25	-4.06	-0.07	3.44	-4.97	-0.32	3.01	-4.34	-0.33
58	3.00	-4.66	-0.33	3.11	-4.61	-0.30	2.63	-3.82	-0.31
59	2.84	-4.55	-0.30	2.86	-4.30	-0.28	1.83	-3.06	-0.30
60	3.27	-4.88	-0.47	2.88	-4.56	-0.40	2.78	-4.21	-0.43
61	2.78	-4.04	-0.32	3.14	-4.58	-0.31	2.57	-4.11	-0.32

Table A-7. Comparison of external and internal pressure coefficients without and with VSVs for the large gable roof model at 90° wind direction

	Without VSVs			With VSVs			With VSVs w/out Screen		
Tap No.	Cp Max	Cp Min	Cp Mean	Cp Max	Cp Min	Cp Mean	Cp Max	Cp Min	Cp Mean
1	2.36	-3.44	-0.13	2.82	-4.20	-0.11	2.39	-3.42	-0.11
2	2.76	-3.89	-0.09	2.48	-3.61	-0.07	2.65	-3.78	-0.06
3	2.00	-3.02	-0.11	2.32	-3.49	-0.09	2.34	-3.53	-0.09
4	2.84	-4.10	-0.07	2.54	-3.58	-0.06	2.49	-3.18	-0.05
5	2.51	-3.58	-0.11	1.99	-3.06	-0.10	1.89	-2.77	-0.08
6	2.35	-3.78	-0.20	2.55	-3.76	-0.19	2.75	-4.02	-0.19
7	2.18	-3.31	-0.18	2.64	-3.91	-0.15	2.53	-3.69	-0.16
8	2.51	-3.56	-0.07	2.82	-4.25	-0.07	2.05	-3.14	-0.08
9	2.60	-3.87	-0.10	2.40	-3.16	-0.10	2.87	-4.12	-0.10
10	2.32	-3.30	-0.12	3.32	-4.44	-0.10	2.49	-3.27	-0.10
11	2.41	-3.62	-0.19	2.12	-3.49	-0.17	2.43	-3.59	-0.17
12	2.53	-3.75	-0.14	2.91	-4.12	-0.14	3.22	-4.62	-0.13
13	2.15	-3.16	-0.19	2.03	-2.89	-0.16	1.76	-2.75	-0.17
14	2.16	-3.73	-0.23	2.39	-3.72	-0.20	2.02	-3.22	-0.21
15	2.36	-3.05	-0.27	2.12	-2.72	-0.28	2.39	-3.89	-0.29
16	2.34	-3.26	-0.31	3.05	-4.16	-0.31	2.78	-3.71	-0.30
17	2.26	-3.65	-0.27	2.30	-3.02	-0.27	2.81	-3.67	-0.26
18	2.71	-4.04	-0.21	2.49	-4.13	-0.19	2.62	-3.72	-0.19
19	2.52	-4.32	-0.42	2.97	-4.52	-0.37	2.38	-3.77	-0.38
20	2.44	-3.75	-0.40	1.83	-3.08	-0.37	2.39	-4.17	-0.38
21	1.79	-2.88	-0.35	1.91	-3.51	-0.34	1.69	-3.09	-0.35
22	2.43	-3.69	-0.34	2.17	-3.42	-0.33	2.03	-3.38	-0.35
23	1.87	-2.99	-0.35	2.13	-3.47	-0.35	2.41	-3.68	-0.36
24	2.75	-2.86	0.75	3.14	-3.63	0.76	2.40	-2.53	0.75
25	1.68	-2.93	-0.39	2.88	-4.27	-0.35	1.96	-3.34	-0.37
26	3.16	-4.30	-0.13	2.84	-4.25	-0.13	3.03	-4.28	-0.12
27	2.89	-4.43	-0.35	2.77	-4.24	-0.32	2.04	-3.45	-0.32
28	2.82	-4.25	-0.28	3.10	-4.70	-0.28	3.22	-4.88	-0.31
29	2.58	-3.96	-0.31	2.99	-4.46	-0.31	2.52	-4.07	-0.36
30	2.69	-3.96	-0.30	2.68	-4.07	-0.29	2.47	-3.98	-0.32
31	2.32	-3.69	-0.37	2.33	-3.70	-0.34	2.91	-4.72	-0.37
32	2.68	-4.34	-0.30	2.58	-3.98	-0.31	2.12	-3.58	-0.32
33	2.35	-3.76	-0.33	2.50	-3.79	-0.31	2.38	-3.68	-0.32
34	2.36	-3.65	-0.33	2.27	-3.63	-0.31	2.56	-3.86	-0.32
35	2.43	-3.88	-0.36	2.47	-3.83	-0.33	3.02	-4.80	-0.35
36	3.32	-5.08	-0.31	3.25	-4.79	-0.31	2.79	-4.37	-0.31
37	2.64	-4.37	-0.33	2.33	-3.79	-0.32	2.68	-4.21	-0.33
38	2.84	-4.32	-0.30	2.85	-4.38	-0.30	2.57	-4.16	-0.32
39	2.46	-3.80	-0.32	3.09	-4.58	-0.30	2.47	-3.87	-0.32
40	2.43	-3.99	-0.33	2.72	-4.13	-0.31	2.22	-3.51	-0.32
41	2.57	-4.06	-0.32	1.86	-3.13	-0.30	2.35	-3.82	-0.32
42	2.85	-4.50	-0.32	2.72	-4.28	-0.30	2.47	-3.79	-0.30
43	2.53	-3.98	-0.36	3.18	-4.87	-0.32	2.57	-4.09	-0.33
44	3.00	-4.59	-0.35	3.31	-4.95	-0.31	3.00	-4.54	-0.32
45	2.59	-4.00	-0.34	2.32	-3.67	-0.31	3.11	-4.81	-0.33

46	2.68	-4.28	-0.35	3.10	-4.74	-0.32	3.36	-5.03	-0.32
47	3.30	-4.98	-0.31	2.90	-4.14	-0.29	2.46	-3.91	-0.31
48	2.52	-4.07	-0.35	2.73	-4.28	-0.32	2.80	-4.40	-0.32
49	2.60	-4.11	-0.33	2.72	-4.15	-0.31	2.05	-3.33	-0.33
50	2.57	-4.06	-0.33	2.96	-4.36	-0.31	2.44	-3.95	-0.32
51	2.54	-4.21	-0.34	2.70	-4.20	-0.31	2.76	-4.20	-0.33
52	2.39	-3.74	-0.29	2.77	-4.19	-0.27	2.89	-4.47	-0.32
53	1.82	-3.00	-0.29	1.96	-3.10	-0.28	2.47	-3.84	-0.31
54	2.47	-3.67	-0.36	2.44	-3.79	-0.34	2.88	-4.50	-0.37
55	1.88	-3.17	-0.35	1.62	-2.68	-0.30	1.87	-2.94	-0.31
56	2.87	-4.58	-0.25	3.14	-4.89	-0.31	2.25	-3.65	-0.34
57	2.43	-3.89	-0.29	2.52	-3.93	-0.33	3.10	-4.65	-0.35
58	2.71	-4.05	-0.35	2.29	-3.63	-0.32	2.16	-3.41	-0.35
59	2.34	-3.63	-0.34	3.21	-4.77	-0.32	1.92	-3.11	-0.33
60	2.57	-4.11	-0.34	2.69	-4.22	-0.31	2.91	-4.60	-0.34
61	2.64	-4.13	-0.36	2.54	-4.04	-0.34	2.48	-3.98	-0.34

Table A-8. Comparison of external and internal pressure coefficients without and with VSVs for the large hip roof model at 0° wind direction

	Without VSVs			With VSVs			With VSVs w/out Screen		
Tap No.	Cp Max	Cp Min	Cp Mean	Cp Max	Cp Min	Cp Mean	Cp Max	Cp Min	Cp Mean
1	3.16	-4.20	-0.18	2.64	-3.39	-0.24	2.15	-3.06	-0.25
2	3.33	-4.18	0.51	3.24	-3.85	0.47	1.35	-1.47	0.49
3	3.15	-4.72	-0.28	2.24	-3.68	-0.35	1.71	-2.72	-0.36
4	2.92	-4.62	-0.26	2.59	-4.01	-0.33	2.01	-3.26	-0.35
5	2.94	-3.06	0.69	3.12	-3.22	0.71	1.14	-0.24	0.73
6	2.08	-3.18	-0.25	2.46	-3.97	-0.25	0.89	-1.75	-0.23
7	1.92	-2.90	-0.13	2.48	-3.82	-0.13	0.83	-1.69	-0.11
8	2.25	-3.34	-0.21	2.37	-3.54	-0.22	1.09	-1.58	-0.20
9	2.59	-4.01	-0.26	2.72	-4.11	-0.28	0.39	-0.80	-0.27
10	3.02	-4.88	-0.45	2.22	-3.74	-0.45	0.46	-1.14	-0.43
11	3.06	-4.86	-0.39	2.59	-4.29	-0.40	0.60	-1.33	-0.38
12	2.86	-4.65	-0.45	2.47	-4.09	-0.44	0.44	-1.34	-0.42
13	2.20	-3.42	-0.29	2.34	-3.81	-0.30	0.37	-1.06	-0.28
14	2.98	-3.83	0.03	2.86	-4.81	-0.30	0.90	-1.73	-0.26
15	1.80	-3.40	-0.67	2.48	-4.27	-0.66	0.24	-1.11	-0.66
16	2.13	-3.26	-0.36	2.17	-3.49	-0.33	0.48	-0.82	-0.35
17	2.04	-3.22	-0.27	2.45	-3.96	-0.28	0.34	-0.69	-0.28
18	2.41	-3.91	-0.44	2.74	-4.50	-0.43	0.36	-1.11	-0.42
19	3.10	-4.96	-0.41	2.18	-3.48	-0.41	0.30	-0.88	-0.38
20	3.32	-5.52	-0.66	2.11	-3.86	-0.67	0.30	-1.12	-0.65
21	2.95	-5.13	-0.82	2.33	-4.46	-0.81	0.24	-1.29	-0.80
22	2.66	-4.09	-0.46	2.88	-4.60	-0.46	0.24	-0.99	-0.47
23	2.45	-3.78	-0.42	2.68	-4.30	-0.41	0.37	-1.11	-0.41
24	1.90	-3.10	-0.36	2.21	-3.60	-0.36	0.42	-0.95	-0.36
25	1.36	-3.04	-0.77	1.93	-3.87	-0.77	0.15	-1.08	-0.75
26	2.29	-3.59	-0.30	3.39	-5.21	-0.29	0.36	-0.79	-0.29
27	2.08	-3.47	-0.46	2.74	-4.28	-0.45	0.22	-0.77	-0.44
28	3.02	-4.76	-0.39	2.26	-3.77	-0.40	0.27	-0.86	-0.42
29	3.03	-4.79	-0.39	2.33	-3.56	-0.38	0.24	-0.72	-0.37
30	3.16	-4.81	-0.27	3.29	-4.84	-0.27	0.37	-0.68	-0.28
31	2.40	-4.35	-0.40	1.96	-3.17	-0.40	0.74	-1.32	-0.35
32	2.66	-4.21	-0.40	2.28	-3.77	-0.42	0.30	-0.82	-0.40
33	1.98	-3.14	-0.35	3.07	-4.62	-0.35	0.31	-0.77	-0.35
34	2.10	-3.53	-0.39	2.42	-3.63	-0.38	0.25	-0.74	-0.37
35	2.07	-3.24	-0.29	2.52	-3.59	-0.33	0.80	-1.76	-0.32
36	2.54	-3.91	-0.28	2.77	-4.21	-0.28	0.34	-0.74	-0.28
37	3.12	-4.72	-0.23	3.11	-4.75	-0.17	0.37	-0.61	-0.17
38	3.51	-5.24	-0.27	2.81	-4.49	-0.27	0.26	-0.81	-0.28
39	3.24	-4.84	-0.26	2.41	-3.75	-0.26	0.32	-0.62	-0.26
40	2.67	-3.95	-0.17	2.91	-4.30	-0.18	0.46	-0.67	-0.17
41	1.84	-3.04	-0.31	2.92	-4.28	-0.36	0.40	-0.91	-0.33
42	2.26	-3.21	-0.18	2.83	-4.32	-0.16	0.34	-0.53	-0.17
43	2.10	-3.33	-0.39	2.39	-4.14	-0.40	0.39	-0.88	-0.38
44	3.10	-3.54	0.69	4.11	-5.03	0.67	1.20	-0.45	0.71
45	2.16	-3.44	-0.28	2.77	-4.13	-0.24	0.32	-0.60	-0.23
46	3.69	-4.24	0.27	2.74	-4.31	-0.25	0.30	-0.65	-0.23
47	3.43	-4.41	0.18	3.11	-4.72	-0.24	0.31	-0.55	-0.25

48	3.20	-4.46	-0.08	2.02	-3.12	-0.25	0.36	-0.67	-0.25
49	3.12	-4.82	-0.27	2.21	-3.38	-0.30	0.33	-0.84	-0.28
50	2.78	-4.00	-0.10	3.16	-4.73	-0.25	0.33	-0.58	-0.23
51	2.28	-3.70	-0.35	2.21	-3.51	-0.33	0.33	-0.72	-0.33
52	2.40	-3.41	-0.19	2.88	-4.34	-0.23	0.35	-0.63	-0.25
53	2.07	-2.88	-0.10	2.34	-3.60	-0.22	0.29	-0.57	-0.24
54	2.24	-3.14	-0.13	3.44	-5.19	-0.25	0.33	-0.51	-0.23
55	2.95	-4.35	-0.15	2.34	-3.64	-0.25	0.30	-0.56	-0.23
56	3.08	-4.46	-0.09	2.60	-3.81	-0.21	0.30	-0.60	-0.24
57	2.72	-4.00	-0.09	2.48	-3.71	-0.23	0.28	-0.57	-0.24
58	2.50	-3.63	-0.19	3.20	-4.86	-0.25	0.28	-0.58	-0.25
59	2.37	-3.65	-0.33	2.44	-3.79	-0.31	0.46	-0.93	-0.29
60	2.79	-4.07	-0.20	2.40	-3.68	-0.24	0.38	-0.68	-0.24
61	1.84	-2.96	-0.40	2.81	-4.22	-0.33	0.38	-0.85	-0.32
62	2.49	-3.74	-0.19	2.90	-4.26	-0.24	0.27	-0.56	-0.23
63	2.55	-3.82	-0.18	2.23	-3.35	-0.24	0.33	-0.59	-0.23
64	2.93	-4.34	-0.22	2.69	-4.05	-0.23	0.51	-0.79	-0.23
65	3.09	-4.49	-0.05	2.31	-3.50	-0.25	0.00	-4.73	-0.26
66	2.93	-3.68	0.48	2.51	-3.74	-0.22	0.29	-0.60	-0.22
67	3.35	-3.99	0.44	2.02	-3.00	-0.22	0.27	-0.53	-0.22
68	2.59	-3.39	-0.21	2.01	-3.07	-0.24	0.31	-0.60	-0.23
69	2.03	-2.92	-0.14	2.43	-3.59	-0.23	0.26	-0.53	-0.21
70	2.41	-2.72	-0.18	2.09	-3.28	-0.25	0.25	-0.58	-0.25
71	1.92	-2.73	-0.14	2.58	-3.88	-0.24	0.23	-0.56	-0.24
72	1.77	-2.70	-0.13	1.44	-2.49	-0.24	0.35	-0.59	-0.23
73	2.69	-4.02	-0.11	2.87	-4.26	-0.23	0.27	-0.50	-0.23
74	3.27	-4.72	-0.13	2.41	-3.73	-0.25	0.30	-0.56	-0.23
75	3.18	-4.40	-0.16	2.70	-4.00	-0.25	0.26	-0.57	-0.24
76	2.32	-3.53	-0.09	2.01	-3.19	-0.26	0.27	-0.57	-0.22
77	2.39	-3.44	-0.11	2.64	-3.83	-0.26	0.30	-0.59	-0.25
78	2.33	-3.35	-0.08	2.69	-4.02	-0.24	0.26	-0.57	-0.23
79	2.19	-3.34	-0.12	2.58	-3.89	-0.25	0.29	-0.59	-0.25
80	1.43	-2.25	-0.10	1.60	-2.81	-0.18	0.39	-0.52	-0.17
81	2.07	-3.01	-0.10	2.81	-4.28	-0.20	0.31	-0.54	-0.20
82	2.70	-3.53	0.37	3.06	-4.53	-0.23	0.32	-0.56	-0.21
83	3.23	-4.55	-0.37	2.59	-4.07	-0.24	0.31	-0.61	-0.23
84	2.75	-4.34	0.38	1.79	-2.98	-0.25	0.29	-0.66	-0.29
85	3.72	-4.05	0.43	1.83	-2.92	-0.25	0.38	-0.67	-0.24
86	2.30	-3.74	-0.31	2.29	-3.54	-0.33	0.29	-0.84	-0.36
87	2.41	-3.65	-0.27	2.48	-3.88	-0.35	0.37	-0.96	-0.37
88	1.46	-2.56	-0.37	1.68	-3.07	-0.33	0.44	-0.90	-0.34
89	2.07	-3.49	-0.28	2.73	-4.33	-0.35	0.45	-0.95	-0.32
90	2.51	-3.69	-0.14	2.37	-3.92	-0.25	0.28	-0.73	-0.24
91	3.01	-4.31	-0.18	3.05	-4.72	-0.24	0.32	-0.58	-0.24
92	2.39	-3.57	-0.14	1.62	-2.65	-0.24	0.34	-0.60	-0.24
93	2.82	-4.04	-0.15	2.49	-3.59	-0.24	0.27	-0.58	-0.24
94	2.57	-3.64	-0.24	2.31	-3.81	-0.32	0.50	-1.08	-0.31
95	2.10	-3.30	-0.29	2.01	-3.11	-0.31	0.42	-0.80	-0.29
96	1.57	-2.73	-0.24	2.04	-3.21	-0.32	0.45	-0.92	-0.29
97	1.71	-2.81	-0.28	3.15	-4.72	-0.30	0.27	-0.78	-0.28

Table A-9. Comparison of external and internal pressure coefficients without and with VSVs for the large hip roof model at 15° wind direction

	Without VSVs			With VSVs			With VSVs w/out Screen		
Tap No.	Cp Max	Cp Min	Cp Mean	Cp Max	Cp Min	Cp Mean	Cp Max	Cp Min	Cp Mean
1	2.86	-4.26	-0.11	2.74	-3.46	-0.11	2.02	-2.77	-0.12
2	3.29	-3.80	0.59	3.52	-4.12	0.63	3.38	-4.04	0.62
3	2.95	-4.72	-0.34	2.58	-4.53	-0.39	2.31	-3.97	-0.38
4	2.71	-4.39	-0.39	3.23	-4.58	-0.46	2.66	-4.46	-0.47
5	3.18	-3.50	0.59	3.23	-3.58	0.63	3.35	-3.84	0.64
6	2.83	-4.41	-0.18	3.77	-5.42	-0.15	2.87	-4.27	-0.16
7	2.63	-3.71	-0.14	3.12	-4.68	-0.11	2.65	-3.71	-0.11
8	2.86	-4.41	-0.31	3.12	-4.43	-0.30	2.27	-3.68	-0.27
9	2.68	-3.88	-0.17	2.88	-4.37	-0.16	2.06	-3.26	-0.17
10	3.12	-5.00	-0.34	3.47	-5.21	-0.30	2.89	-4.39	-0.31
11	2.65	-4.25	-0.41	3.13	-4.77	-0.38	2.45	-3.93	-0.38
12	2.41	-4.11	-0.52	2.56	-4.50	-0.48	3.16	-4.86	-0.48
13	2.74	-4.29	-0.32	2.55	-3.90	-0.30	2.48	-3.81	-0.29
14	2.94	-3.99	0.11	2.83	-4.31	-0.26	3.00	-4.64	-0.28
15	2.56	-4.26	-0.68	1.92	-3.64	-0.65	2.47	-4.46	-0.66
16	2.80	-4.22	-0.29	2.46	-3.76	-0.24	3.34	-5.02	-0.25
17	2.50	-3.69	-0.19	3.58	-5.31	-0.17	2.81	-4.31	-0.18
18	2.58	-4.09	-0.41	3.25	-4.98	-0.36	2.89	-4.57	-0.37
19	2.84	-4.38	-0.39	3.36	-5.21	-0.33	2.78	-4.37	-0.34
20	2.98	-4.90	-0.64	3.02	-5.05	-0.62	2.81	-4.90	-0.62
21	2.62	-4.92	-0.85	3.01	-5.35	-0.82	2.37	-4.26	-0.82
22	2.56	-4.12	-0.47	3.06	-5.02	-0.49	2.82	-4.49	-0.48
23	3.23	-5.09	-0.43	2.98	-4.80	-0.41	2.75	-4.39	-0.42
24	2.99	-4.62	-0.35	3.40	-5.38	-0.33	2.32	-3.70	-0.33
25	2.49	-4.75	-0.78	2.67	-4.65	-0.75	2.46	-4.58	-0.75
26	3.23	-4.80	-0.29	3.19	-4.68	-0.26	3.62	-5.43	-0.27
27	3.25	-5.19	-0.50	2.72	-4.59	-0.48	2.61	-4.28	-0.48
28	2.88	-4.36	-0.37	3.20	-5.13	-0.42	2.89	-4.82	-0.42
29	3.11	-4.66	-0.33	3.10	-4.64	-0.30	2.47	-4.02	-0.31
30	2.62	-3.98	-0.27	3.53	-5.30	-0.28	2.98	-4.57	-0.28
31	2.68	-3.92	-0.22	2.68	-4.20	-0.26	2.91	-4.45	-0.29
32	2.93	-4.67	-0.47	2.66	-4.51	-0.48	3.06	-5.00	-0.47
33	2.60	-3.81	-0.36	2.85	-4.49	-0.33	2.64	-4.11	-0.35
34	2.95	-4.41	-0.33	3.14	-4.91	-0.28	3.11	-4.75	-0.30
35	3.43	-5.21	-0.28	3.28	-4.92	-0.24	2.73	-4.31	-0.24
36	3.06	-4.47	-0.32	3.44	-5.23	-0.30	3.32	-5.29	-0.31
37	2.98	-4.33	-0.19	2.59	-3.79	-0.13	2.80	-4.14	-0.17
38	3.04	-4.42	-0.28	2.99	-4.68	-0.29	3.48	-5.21	-0.30
39	2.57	-3.63	-0.24	3.57	-5.30	-0.22	2.56	-4.12	-0.23
40	2.95	-4.38	-0.19	3.41	-5.09	-0.18	2.65	-4.00	-0.18
41	2.81	-3.87	-0.17	2.76	-4.42	-0.25	1.89	-3.02	-0.27
42	2.72	-4.26	-0.19	3.20	-4.67	-0.17	2.79	-4.23	-0.20
43	2.80	-4.21	-0.29	3.61	-5.28	-0.25	2.58	-3.85	-0.24
44	3.14	-3.74	0.61	3.36	-3.54	0.66	4.06	-4.93	0.65
45	2.83	-4.41	-0.23	2.99	-4.56	-0.18	3.23	-4.78	-0.19
46	3.91	-4.44	0.30	3.87	-5.63	-0.17	3.69	-5.49	-0.19
47	3.00	-4.09	0.00	3.14	-4.62	-0.19	3.29	-4.84	-0.20

48	2.64	-3.72	-0.08	3.21	-4.79	-0.18	3.13	-4.85	-0.21
49	2.18	-3.74	-0.28	2.86	-4.16	-0.33	2.55	-3.94	-0.35
50	3.14	-4.47	-0.09	3.47	-5.26	-0.18	3.45	-4.97	-0.19
51	3.19	-4.87	-0.26	3.51	-5.13	-0.22	3.30	-5.05	-0.22
52	3.25	-4.68	-0.12	3.35	-5.02	-0.18	3.32	-5.10	-0.20
53	3.22	-4.71	-0.06	3.25	-4.83	-0.19	2.52	-3.72	-0.20
54	3.09	-4.29	-0.13	3.45	-5.17	-0.18	3.27	-4.91	-0.19
55	2.86	-4.19	-0.11	2.83	-4.32	-0.19	2.94	-4.42	-0.19
56	2.96	-4.29	-0.04	3.23	-4.74	-0.19	2.67	-4.19	-0.20
57	2.68	-3.97	-0.05	3.30	-4.80	-0.20	2.90	-4.45	-0.20
58	2.58	-3.62	-0.14	3.34	-5.03	-0.19	3.53	-5.26	-0.20
59	2.56	-3.69	-0.18	3.08	-4.59	-0.19	3.25	-4.87	-0.19
60	3.06	-4.54	-0.16	3.17	-4.76	-0.18	3.22	-4.79	-0.20
61	2.72	-3.93	-0.33	3.41	-5.21	-0.24	2.84	-4.29	-0.23
62	3.20	-4.87	-0.15	3.18	-4.75	-0.18	3.42	-5.02	-0.20
63	3.06	-4.30	-0.18	2.94	-4.43	-0.19	2.97	-4.39	-0.19
64	3.09	-4.74	-0.23	3.17	-4.95	-0.17	3.00	-4.59	-0.19
65	2.81	-3.98	-0.03	2.82	-4.16	-0.20	2.22	-3.47	-0.20
66	2.97	-3.40	0.60	2.95	-4.32	-0.17	2.63	-4.08	-0.18
67	3.19	-4.08	0.34	2.87	-4.27	-0.16	2.77	-4.17	-0.19
68	2.11	-3.28	-0.12	2.43	-3.78	-0.19	2.33	-3.63	-0.20
69	2.66	-3.84	-0.10	2.79	-3.98	-0.18	2.75	-4.14	-0.19
70	2.45	-3.55	-0.08	3.17	-4.74	-0.19	2.83	-4.19	-0.20
71	2.69	-3.57	-0.11	3.16	-4.85	-0.19	2.82	-4.22	-0.19
72	1.76	-2.77	-0.09	2.17	-3.55	-0.19	2.22	-3.42	-0.18
73	2.76	-3.81	-0.09	2.85	-4.33	-0.19	2.69	-4.05	-0.19
74	3.09	-4.45	-0.09	3.38	-4.92	-0.20	3.23	-4.97	-0.18
75	2.70	-3.81	-0.10	3.15	-4.64	-0.20	3.05	-4.59	-0.20
76	2.06	-2.97	-0.07	2.53	-3.86	-0.20	2.28	-3.39	-0.16
77	3.24	-4.58	-0.07	3.12	-4.57	-0.19	2.53	-3.92	-0.18
78	2.76	-3.87	-0.05	3.13	-4.65	-0.18	2.45	-3.77	-0.19
79	2.81	-3.87	-0.08	2.66	-3.95	-0.19	2.85	-4.30	-0.19
80	2.25	-3.31	-0.06	1.51	-2.30	-0.13	1.99	-3.18	-0.18
81	2.80	-3.97	-0.08	3.11	-4.55	-0.17	2.99	-4.40	-0.18
82	3.42	-3.87	0.46	2.41	-3.71	-0.16	2.80	-4.13	-0.19
83	3.02	-4.12	-0.12	2.77	-4.24	-0.18	2.96	-4.52	-0.20
84	2.69	-3.22	0.33	2.59	-3.90	-0.22	2.43	-3.87	-0.24
85	3.04	-3.67	0.51	2.06	-3.34	-0.20	2.41	-3.50	-0.19
86	2.37	-3.50	-0.20	3.01	-4.48	-0.23	3.00	-4.34	-0.24
87	3.09	-4.50	-0.19	2.75	-4.22	-0.25	3.09	-4.65	-0.22
88	2.13	-3.40	-0.29	2.18	-3.56	-0.25	1.78	-2.49	-0.24
89	2.80	-4.08	-0.21	2.65	-4.18	-0.27	2.44	-3.75	-0.22
90	2.92	-4.25	-0.16	3.69	-5.65	-0.20	2.60	-3.90	-0.19
91	3.24	-4.73	-0.18	3.11	-4.57	-0.20	2.89	-4.44	-0.19
92	2.16	-3.16	-0.16	1.81	-2.77	-0.16	1.89	-2.85	-0.21
93	3.02	-4.28	-0.15	3.39	-4.93	-0.19	2.46	-3.82	-0.20
94	2.36	-3.46	-0.11	2.77	-4.16	-0.19	2.72	-4.22	-0.21
95	2.73	-4.01	-0.13	2.45	-3.66	-0.20	3.09	-4.42	-0.22
96	1.68	-2.83	-0.23	2.47	-4.15	-0.34	2.50	-3.92	-0.37
97	2.42	-3.74	-0.26	3.18	-4.78	-0.40	2.45	-4.26	-0.39

Table A-10. Comparison of external and internal pressure coefficients without and with VSVs for the large hip roof model at 30° wind direction

	Without VSVs			With VSVs			With VSVs w/out Screen		
Tap No.	Cp Max	Cp Min	Cp Mean	Cp Max	Cp Min	Cp Mean	Cp Max	Cp Min	Cp Mean
1	2.46	-3.39	-0.09	2.46	-3.18	-0.10	1.89	-2.77	-0.12
2	3.30	-3.90	0.65	2.88	-3.33	0.69	2.90	-2.94	0.67
3	2.16	-3.49	-0.35	2.14	-3.55	-0.40	1.69	-2.60	-0.42
4	2.45	-3.66	-0.48	2.35	-3.74	-0.52	1.90	-3.52	-0.55
5	3.26	-3.86	0.48	2.47	-2.91	0.45	2.70	-3.36	0.42
6	2.64	-3.88	-0.11	2.73	-4.04	-0.11	2.84	-4.10	-0.13
7	2.13	-3.26	-0.15	2.52	-3.80	-0.14	2.64	-3.84	-0.16
8	2.19	-3.49	-0.39	2.53	-4.31	-0.40	2.47	-4.05	-0.39
9	2.41	-3.42	-0.06	2.39	-3.49	-0.07	2.19	-3.18	-0.08
10	2.57	-3.98	-0.21	2.65	-4.11	-0.21	2.71	-4.01	-0.23
11	2.17	-3.66	-0.44	2.28	-3.86	-0.44	1.90	-3.33	-0.45
12	3.00	-4.98	-0.58	2.73	-4.60	-0.58	1.69	-3.23	-0.60
13	2.37	-3.80	-0.34	1.86	-3.11	-0.36	2.01	-3.42	-0.37
14	3.40	-4.66	0.40	2.39	-3.33	0.19	2.60	-3.58	0.12
15	0.00	-4.24	-0.68	0.00	-4.32	-0.68	1.60	-3.22	-0.69
16	2.43	-3.94	-0.27	2.85	-4.48	-0.26	2.06	-3.30	-0.31
17	2.55	-3.61	-0.12	2.17	-3.15	-0.12	2.13	-3.16	-0.13
18	2.19	-3.51	-0.36	2.34	-3.78	-0.34	2.65	-4.30	-0.36
19	1.84	-3.15	-0.33	2.58	-4.06	-0.33	2.48	-4.23	-0.35
20	2.73	-4.62	-0.61	2.71	-4.70	-0.62	2.37	-4.39	-0.63
21	2.07	-3.92	-0.85	1.93	-3.82	-0.85	1.70	-3.50	-0.86
22	2.04	-3.59	-0.50	2.34	-3.92	-0.50	1.75	-3.26	-0.50
23	2.40	-3.89	-0.44	2.31	-3.68	-0.43	2.43	-3.98	-0.45
24	2.12	-3.37	-0.36	2.75	-4.30	-0.35	2.45	-3.94	-0.37
25	1.99	-3.97	-0.80	1.95	-3.97	-0.80	1.66	-3.55	-0.81
26	2.48	-3.93	-0.32	2.33	-3.59	-0.30	2.61	-3.87	-0.32
27	2.17	-3.81	-0.53	2.06	-3.78	-0.51	1.74	-3.17	-0.52
28	2.06	-3.48	-0.40	2.21	-3.64	-0.41	2.17	-3.52	-0.41
29	1.85	-3.03	-0.28	1.79	-2.90	-0.27	1.71	-2.78	-0.28
30	2.77	-4.24	-0.30	2.36	-3.70	-0.31	2.45	-3.91	-0.31
31	2.51	-3.05	0.33	2.64	-3.61	0.04	2.41	-3.41	0.01
32	3.01	-4.96	-0.54	2.05	-3.79	-0.55	1.48	-2.73	-0.54
33	2.08	-3.42	-0.37	2.63	-4.18	-0.35	1.72	-2.97	-0.37
34	3.29	-4.98	-0.26	3.18	-4.83	-0.25	2.55	-4.02	-0.27
35	2.68	-4.23	-0.29	3.01	-4.79	-0.30	1.94	-3.24	-0.32
36	3.25	-4.91	-0.34	3.27	-5.11	-0.33	2.61	-4.05	-0.33
37	2.42	-3.81	-0.13	2.66	-3.95	-0.10	1.98	-3.07	-0.13
38	3.31	-4.94	-0.31	2.54	-3.81	-0.31	3.25	-4.90	-0.30
39	2.73	-4.16	-0.22	2.40	-3.71	-0.21	2.47	-3.83	-0.22
40	2.50	-3.73	-0.16	3.27	-5.05	-0.18	3.24	-4.65	-0.18
41	2.79	-3.90	0.09	2.24	-3.17	0.07	2.25	-3.29	0.07
42	2.74	-4.18	-0.17	2.60	-3.95	-0.17	3.56	-5.12	-0.18
43	3.06	-4.56	-0.30	2.21	-3.60	-0.31	2.34	-3.87	-0.34
44	3.85	-4.70	0.49	3.51	-4.29	0.48	3.46	-4.04	0.46
45	3.10	-4.34	-0.03	2.90	-4.38	-0.14	2.26	-3.35	-0.15
46	3.27	-4.53	0.27	2.65	-3.93	-0.15	2.61	-3.81	-0.17
47	2.69	-3.87	0.03	2.48	-3.81	-0.15	2.76	-3.97	-0.15

48	3.11	-4.39	0.03	2.59	-3.95	-0.16	2.28	-3.56	-0.18
49	2.53	-3.54	-0.02	2.37	-3.54	-0.14	2.12	-3.24	-0.15
50	2.78	-4.01	0.01	2.50	-3.65	-0.16	2.68	-4.01	-0.15
51	2.95	-4.48	-0.32	2.84	-4.36	-0.24	2.03	-3.31	-0.27
52	2.80	-4.04	-0.01	3.06	-4.58	-0.14	2.79	-4.11	-0.16
53	2.66	-3.82	0.01	2.38	-3.62	-0.14	2.22	-3.27	-0.13
54	3.12	-4.38	0.03	3.21	-4.73	-0.14	2.81	-4.25	-0.15
55	2.64	-3.74	0.00	2.46	-3.71	-0.16	2.18	-3.35	-0.15
56	3.09	-4.40	0.04	2.66	-4.11	-0.13	2.04	-3.08	-0.11
57	2.98	-4.31	0.03	2.67	-3.99	-0.14	2.11	-3.02	-0.11
58	2.73	-4.10	-0.01	2.24	-3.49	-0.15	2.26	-3.40	-0.14
59	2.82	-4.02	0.01	2.51	-3.76	-0.15	2.62	-4.03	-0.16
60	3.12	-4.51	-0.01	2.31	-3.61	-0.14	2.23	-3.52	-0.15
61	1.97	-3.06	-0.32	2.12	-3.47	-0.26	2.38	-3.80	-0.28
62	2.97	-4.29	0.01	3.04	-4.35	-0.14	2.25	-3.41	-0.14
63	2.38	-3.61	-0.14	2.31	-3.42	-0.15	2.67	-4.06	-0.14
64	2.53	-3.88	-0.24	3.10	-4.59	-0.17	1.89	-3.00	-0.19
65	2.38	-3.46	0.02	2.26	-3.50	-0.16	2.06	-3.15	-0.15
66	2.44	-2.50	0.69	1.70	-2.50	-0.12	2.50	-3.74	-0.12
67	1.99	-2.51	0.19	1.93	-2.99	-0.13	1.94	-2.95	-0.11
68	2.13	-3.12	0.02	1.84	-2.76	-0.15	1.68	-2.51	-0.09
69	2.58	-3.64	0.05	2.12	-3.25	-0.13	1.98	-2.91	-0.10
70	2.36	-3.11	-0.02	2.35	-3.62	-0.16	2.09	-3.15	-0.14
71	2.39	-3.38	0.02	2.56	-3.86	-0.16	2.41	-3.52	-0.14
72	1.76	-2.21	0.02	1.87	-2.69	-0.15	1.77	-2.40	-0.12
73	2.56	-3.54	0.03	2.60	-3.91	-0.14	2.23	-3.38	-0.13
74	2.58	-3.48	-0.03	2.41	-3.67	-0.15	2.81	-4.21	-0.13
75	2.30	-3.29	-0.01	2.62	-4.00	-0.16	2.38	-3.51	-0.14
76	2.56	-3.56	0.00	2.36	-3.57	-0.17	1.71	-2.62	-0.13
77	2.68	-3.74	0.03	2.19	-3.22	-0.15	2.28	-3.53	-0.14
78	3.06	-4.39	0.03	2.07	-3.15	-0.15	2.31	-3.51	-0.14
79	2.68	-3.74	-0.03	2.47	-3.95	-0.16	2.13	-3.29	-0.16
80	1.64	-2.30	0.03	1.96	-2.83	-0.12	1.31	-1.92	-0.11
81	2.73	-3.88	0.00	2.14	-3.36	-0.14	2.21	-3.34	-0.14
82	1.99	-2.15	0.45	1.92	-3.02	-0.14	2.50	-3.79	-0.12
83	1.85	-2.15	0.33	2.19	-3.21	-0.14	2.48	-3.60	-0.10
84	2.37	-2.96	0.15	2.21	-3.43	-0.18	2.10	-3.27	-0.18
85	2.29	-2.79	0.53	2.12	-3.10	-0.16	2.10	-3.11	-0.15
86	2.13	-3.03	-0.20	2.19	-3.59	-0.25	1.98	-3.27	-0.27
87	2.66	-3.91	-0.09	2.35	-3.67	-0.27	2.94	-4.77	-0.28
88	1.73	-2.59	-0.29	2.04	-2.96	-0.26	1.84	-2.94	-0.29
89	2.33	-3.70	-0.20	2.20	-3.76	-0.30	2.21	-3.60	-0.29
90	2.27	-3.25	-0.09	2.24	-3.44	-0.18	2.32	-3.50	-0.17
91	2.36	-3.48	-0.19	2.50	-3.69	-0.19	2.25	-3.38	-0.19
92	2.23	-3.26	-0.14	1.87	-2.62	-0.14	1.49	-2.09	-0.15
93	2.40	-3.58	-0.13	2.42	-3.65	-0.15	2.03	-2.99	-0.15
94	2.62	-3.62	0.40	2.22	-3.44	-0.14	2.60	-3.92	-0.14
95	2.28	-3.29	0.02	2.78	-4.12	-0.14	2.11	-3.27	-0.15
96	2.18	-1.30	0.65	2.55	-3.90	-0.14	1.91	-2.92	-0.13
97	1.74	-2.64	-0.04	2.17	-3.56	-0.15	2.48	-3.71	-0.15

Table A-11. Comparison of external and internal pressure coefficients without and with VSVs for the large hip roof model at 45° wind direction

	Without VSVs			With VSVs			With VSVs w/out Screen		
Tap No.	Cp Max	Cp Min	Cp Mean	Cp Max	Cp Min	Cp Mean	Cp Max	Cp Min	Cp Mean
1	2.51	-3.85	-0.12	2.95	-4.24	-0.12	3.07	-4.48	-0.13
2	3.27	-3.65	0.60	3.73	-4.48	0.54	3.49	-3.98	0.53
3	2.42	-3.58	-0.28	2.88	-4.25	-0.32	2.31	-3.64	-0.34
4	2.85	-3.97	-0.50	2.79	-4.29	-0.51	2.44	-4.09	-0.53
5	3.00	-3.59	0.35	3.03	-3.93	0.25	2.39	-3.37	0.22
6	2.80	-4.12	-0.11	3.18	-4.67	-0.10	2.54	-3.58	-0.11
7	2.82	-4.10	-0.17	3.04	-4.58	-0.17	2.74	-4.20	-0.17
8	2.24	-3.67	-0.44	2.89	-4.66	-0.45	2.60	-4.15	-0.44
9	2.33	-3.16	-0.02	2.88	-3.98	-0.01	2.76	-3.68	-0.03
10	2.38	-3.58	-0.14	3.41	-5.12	-0.13	3.14	-4.54	-0.14
11	2.20	-3.72	-0.47	2.85	-4.79	-0.47	2.68	-4.29	-0.48
12	3.00	-5.21	-0.57	2.62	-4.22	-0.55	2.76	-4.51	-0.57
13	2.55	-3.99	-0.33	2.63	-4.24	-0.33	2.79	-4.26	-0.33
14	3.62	-4.18	0.60	3.53	-4.32	0.58	3.18	-3.94	0.51
15	2.58	-4.65	-0.70	2.25	-4.22	-0.68	2.52	-4.42	-0.70
16	2.53	-3.79	-0.22	2.68	-4.00	-0.20	2.10	-3.59	-0.22
17	2.44	-3.30	-0.10	2.54	-3.66	-0.10	2.45	-3.63	-0.11
18	2.65	-4.00	-0.34	2.85	-4.32	-0.33	2.45	-3.71	-0.35
19	2.66	-4.00	-0.30	3.07	-4.72	-0.30	2.43	-3.84	-0.31
20	2.96	-4.86	-0.58	3.24	-5.37	-0.59	2.50	-4.27	-0.60
21	2.18	-4.16	-0.84	2.49	-4.66	-0.82	2.05	-4.23	-0.83
22	2.43	-4.12	-0.49	3.07	-5.01	-0.48	2.84	-4.72	-0.49
23	2.55	-3.85	-0.41	2.98	-4.64	-0.39	2.49	-4.09	-0.40
24	2.75	-4.26	-0.31	3.36	-5.03	-0.30	2.41	-4.05	-0.30
25	1.82	-3.58	-0.83	2.14	-4.27	-0.83	1.59	-3.58	-0.84
26	2.99	-4.69	-0.35	3.26	-5.26	-0.34	2.83	-4.42	-0.36
27	2.78	-4.38	-0.51	3.14	-5.10	-0.49	2.03	-3.47	-0.50
28	2.18	-3.63	-0.43	3.04	-4.74	-0.42	2.80	-4.31	-0.43
29	2.35	-3.55	-0.25	2.59	-4.06	-0.23	2.56	-3.98	-0.24
30	2.38	-3.47	-0.28	3.25	-4.97	-0.27	3.37	-4.99	-0.28
31	3.46	-4.28	0.47	3.23	-4.19	0.29	2.91	-3.64	0.27
32	3.12	-5.19	-0.58	2.48	-4.21	-0.58	2.88	-5.12	-0.59
33	2.19	-3.61	-0.38	2.84	-4.49	-0.36	2.89	-4.55	-0.38
34	2.81	-4.09	-0.24	3.66	-5.40	-0.22	3.10	-4.73	-0.24
35	3.11	-4.72	-0.26	3.13	-4.84	-0.26	2.62	-4.02	-0.26
36	2.55	-4.01	-0.38	3.40	-5.22	-0.37	2.74	-4.34	-0.38
37	3.00	-4.27	-0.15	3.33	-4.81	-0.13	2.59	-4.10	-0.16
38	2.87	-4.31	-0.34	3.32	-5.07	-0.33	3.16	-4.91	-0.34
39	3.06	-4.55	-0.21	3.04	-4.57	-0.21	2.15	-3.24	-0.21
40	2.76	-4.00	-0.18	3.07	-4.55	-0.20	2.88	-4.17	-0.20
41	2.70	-3.28	0.31	3.15	-3.97	0.31	3.21	-4.05	0.30
42	2.42	-3.51	-0.20	3.47	-5.11	-0.19	3.17	-4.86	-0.21
43	2.79	-4.12	-0.24	3.23	-4.96	-0.24	2.64	-3.88	-0.25
44	3.31	-4.24	0.28	3.74	-5.13	0.28	3.35	-4.22	0.27
45	2.95	-3.98	0.01	2.84	-4.22	-0.14	2.41	-3.64	-0.14
46	3.15	-4.28	0.08	3.26	-4.81	-0.15	3.18	-4.50	-0.15
47	2.82	-3.79	0.06	3.29	-4.81	-0.14	3.14	-4.54	-0.15

48	3.05	-4.24	0.05	3.33	-5.05	-0.15	2.77	-4.30	-0.16
49	2.82	-3.69	0.18	3.31	-4.77	-0.15	2.53	-3.60	-0.17
50	2.87	-3.92	0.04	3.70	-5.40	-0.15	3.61	-5.22	-0.14
51	3.05	-4.24	-0.26	3.14	-4.57	-0.18	2.76	-4.00	-0.19
52	3.40	-4.56	0.01	3.10	-4.50	-0.14	3.38	-5.08	-0.16
53	2.79	-3.66	0.02	3.17	-4.49	-0.14	2.48	-3.63	-0.14
54	3.12	-4.18	0.05	3.81	-5.51	-0.14	3.06	-4.52	-0.12
55	3.37	-4.64	0.05	2.85	-4.34	-0.15	2.86	-4.11	-0.15
56	2.42	-3.13	0.07	3.29	-4.91	-0.13	2.42	-3.67	-0.12
57	2.69	-3.60	0.06	3.07	-4.53	-0.14	2.39	-3.40	-0.13
58	3.17	-4.19	0.04	3.55	-5.11	-0.15	2.56	-3.76	-0.14
59	3.15	-3.99	0.07	3.33	-4.92	-0.14	2.30	-3.45	-0.14
60	3.04	-4.08	0.02	3.51	-5.01	-0.14	3.08	-4.29	-0.15
61	2.59	-3.65	-0.26	2.98	-4.71	-0.21	2.99	-4.31	-0.21
62	3.06	-4.02	0.08	3.22	-4.79	-0.14	2.88	-4.24	-0.14
63	2.92	-4.23	-0.17	3.25	-4.89	-0.16	3.01	-4.32	-0.17
64	2.98	-4.37	-0.25	3.70	-5.50	-0.18	2.86	-4.23	-0.21
65	2.49	-3.41	0.04	2.94	-4.37	-0.16	2.89	-4.37	-0.15
66	2.99	-3.42	0.45	2.89	-4.16	-0.13	2.91	-4.22	-0.13
67	2.61	-3.39	0.14	3.06	-4.44	-0.12	2.48	-3.51	-0.12
68	2.25	-2.59	0.34	2.56	-3.64	-0.14	2.24	-3.26	-0.06
69	2.57	-3.46	0.11	2.90	-4.25	-0.13	2.50	-3.51	-0.11
70	2.85	-3.70	0.09	2.75	-4.15	-0.15	2.50	-3.68	-0.14
71	2.86	-3.84	0.05	3.36	-4.74	-0.15	2.78	-4.16	-0.14
72	1.79	-2.47	0.07	2.13	-3.24	-0.15	1.85	-3.01	-0.14
73	2.63	-3.54	0.06	3.09	-4.49	-0.14	2.90	-4.26	-0.14
74	2.85	-3.85	-0.02	3.42	-4.94	-0.15	2.96	-4.20	-0.13
75	2.83	-3.87	-0.01	3.07	-4.65	-0.15	2.96	-4.23	-0.15
76	2.33	-3.10	0.03	2.58	-3.83	-0.16	2.18	-3.26	-0.13
77	2.27	-3.25	0.06	3.14	-4.62	-0.15	3.08	-4.47	-0.15
78	2.56	-3.57	0.02	3.35	-4.82	-0.14	2.64	-3.80	-0.14
79	2.61	-3.71	-0.04	3.18	-4.80	-0.15	2.86	-4.19	-0.15
80	1.58	-2.36	0.07	1.37	-1.91	-0.10	1.63	-2.66	-0.13
81	2.26	-3.35	0.00	2.45	-3.67	-0.14	2.63	-3.94	-0.14
82	2.56	-3.37	0.27	2.21	-3.37	-0.12	2.20	-3.37	-0.13
83	3.13	-3.17	0.66	3.19	-4.67	-0.13	2.89	-4.23	-0.11
84	2.53	-3.30	0.07	2.64	-4.16	-0.17	2.19	-3.37	-0.18
85	3.04	-3.20	0.64	1.97	-3.14	-0.15	1.75	-2.84	-0.15
86	2.62	-3.88	-0.17	2.82	-4.46	-0.18	2.91	-4.42	-0.20
87	2.72	-3.80	-0.11	3.19	-4.85	-0.20	2.94	-4.42	-0.20
88	1.80	-3.02	-0.27	2.36	-3.73	-0.22	1.73	-2.98	-0.21
89	2.12	-3.20	-0.12	3.07	-4.69	-0.23	2.16	-3.37	-0.22
90	2.69	-3.89	-0.10	3.41	-5.20	-0.19	2.74	-4.21	-0.20
91	2.66	-3.88	-0.22	3.51	-5.17	-0.20	2.53	-3.80	-0.20
92	2.02	-2.84	-0.11	1.95	-2.89	-0.13	1.70	-2.73	-0.18
93	2.39	-3.44	-0.14	2.76	-4.17	-0.17	2.15	-3.52	-0.17
94	2.79	-2.75	0.72	3.15	-4.62	-0.13	2.67	-3.88	-0.13
95	2.89	-3.93	0.09	3.03	-4.41	-0.13	2.23	-3.34	-0.13
96	2.23	-2.49	0.55	2.74	-4.07	-0.15	2.41	-3.56	-0.24
97	2.60	-3.12	0.15	3.07	-4.50	-0.15	2.95	-4.32	-0.20

APPENDIX B
COMPARISON OF MEAN AND PEAK PRESSURE COEFFICIENTS

This appendix contains tables of the mean and peak pressure coefficients ($C_{p's}$) recorded for the gable and hip roof models for each test conducted within Chapter 6.

Table B-1. Comparison of external and internal pressure coefficients without and with VSVs for the small gable roof model at 0° wind direction

	Without VSVs			With VSVs			With VSVs and Leakage			With VSVs, Leakage and Opening		
Tap No.	**Cp Max**	**Cp Min**	**Cp Mean**	**Cp Max**	**Cp Min**	**Cp Mean**	**Cp Max**	**Cp Min**	**Cp Mean**	**Cp Max**	**Cp Min**	**Cp Mean**
1	2.36	-4.13	-0.74	2.50	-4.36	-0.73	2.05	-3.38	-0.72	2.07	-3.88	-0.74
2	2.42	-3.58	-0.18	2.60	-3.52	-0.19	2.59	-3.93	-0.19	2.22	-3.50	-0.20
3	2.53	-4.04	-0.25	2.62	-4.11	-0.25	2.34	-3.61	-0.25	2.49	-3.95	-0.28
4	2.31	-4.34	-0.57	2.72	-4.47	-0.61	2.58	-4.36	-0.60	2.73	-4.45	-0.65
5	2.27	-3.75	-0.30	3.03	-4.54	-0.27	2.33	-3.72	-0.29	2.23	-3.40	-0.31
6	2.60	-3.96	-0.24	2.81	-4.01	-0.20	2.99	-4.16	-0.21	3.10	-4.27	-0.22
7	2.43	-3.56	-0.59	2.66	-3.77	-0.60	2.53	-3.85	-0.59	2.49	-3.84	-0.64
8	2.49	-3.59	-0.34	2.40	-4.02	-0.36	2.54	-3.92	-0.33	2.54	-4.06	-0.38
9	2.54	-3.60	-0.23	2.79	-4.12	-0.23	2.21	-3.32	-0.23	2.38	-3.34	-0.25
10	2.81	-4.66	-0.52	2.56	-4.48	-0.54	2.29	-3.92	-0.55	2.93	-4.40	-0.61
11	2.80	-4.20	-0.34	2.69	-3.95	-0.32	2.32	-3.54	-0.34	2.47	-4.16	-0.36
12	3.04	-4.29	-0.30	2.90	-4.50	-0.28	2.49	-3.95	-0.28	2.84	-4.24	-0.30
13	2.48	-3.67	-0.61	2.39	-3.78	-0.61	3.07	-3.67	-0.60	2.51	-3.70	-0.64
14	2.75	-4.43	-0.38	2.88	-4.73	-0.39	2.26	-3.97	-0.37	2.70	-4.12	-0.41
15	2.67	-4.05	-0.21	2.49	-4.01	-0.22	2.62	-3.73	-0.23	2.71	-3.89	-0.25
16	2.26	-4.04	-0.51	2.85	-4.78	-0.52	2.62	-4.22	-0.54	2.91	-4.09	-0.58
17	2.41	-3.50	-0.36	2.43	-3.80	-0.35	2.71	-3.90	-0.37	2.30	-4.07	-0.38
18	2.57	-4.13	-0.32	3.01	-4.19	-0.29	2.46	-3.49	-0.31	2.63	-3.79	-0.33
19	2.56	-3.84	-0.66	2.64	-4.05	-0.65	2.61	-4.37	-0.65	2.65	-3.83	-0.70
20	3.03	-4.47	-0.31	2.81	-3.72	-0.32	2.88	-3.88	-0.31	2.60	-4.01	-0.35
21	2.64	-4.04	-0.18	2.32	-3.68	-0.17	2.37	-3.73	-0.17	2.40	-3.68	-0.20
22	2.61	-4.28	-0.48	2.60	-4.03	-0.51	2.59	-4.41	-0.49	2.97	-4.51	-0.53
23	2.97	-4.35	-0.35	2.62	-4.15	-0.34	2.66	-4.21	-0.35	2.59	-3.83	-0.36
24	2.64	-4.20	-0.32	2.94	-4.30	-0.31	2.31	-3.58	-0.31	2.65	-3.85	-0.32
25	2.59	-4.30	-0.74	3.01	-4.51	-0.73	2.46	-3.86	-0.73	2.17	-3.74	-0.75
26	2.88	-4.68	-0.13	3.09	-4.29	-0.16	3.12	-4.58	-0.15	3.08	-4.43	-0.16
27	2.59	-3.58	-0.16	3.04	-4.30	-0.15	2.60	-4.01	-0.15	2.70	-3.90	-0.18
28	2.75	-4.36	-0.52	2.49	-4.05	-0.54	2.37	-3.84	-0.53	2.37	-3.95	-0.59
29	2.38	-3.52	-0.34	2.34	-3.90	-0.34	2.61	-4.12	-0.34	2.86	-4.22	-0.34
30	3.07	-4.65	-0.29	3.10	-4.53	-0.28	2.75	-4.29	-0.27	2.27	-4.23	-0.24
31	3.05	-4.34	-0.10	2.97	-4.31	-0.10	2.95	-4.07	-0.12	3.17	-4.43	-0.13
32	2.77	-3.99	-0.06	2.26	-3.15	-0.13	2.82	-4.19	-0.10	2.69	-3.85	-0.12
33	2.67	-3.47	0.07	3.34	-4.00	0.61	2.75	-3.28	0.60	3.06	-3.69	0.60
34	3.13	-3.79	0.50	3.28	-3.78	0.61	3.04	-3.09	0.60	3.22	-3.53	0.60
35	3.33	-3.64	0.73	3.46	-3.87	0.76	3.12	-3.28	0.73	3.44	-3.82	0.71
36	2.68	-4.52	-0.49	2.82	-4.48	-0.52	2.44	-4.18	-0.48	2.71	-4.45	-0.49
37	2.74	-3.82	-0.15	2.76	-4.10	-0.13	3.05	-4.44	-0.15	2.44	-3.61	-0.14
38	2.76	-4.22	-0.54	2.48	-4.44	-0.52	2.31	-4.12	-0.51	3.23	-4.62	-0.51
39	3.23	-4.71	0.13	2.84	-4.20	-0.10	2.92	-4.20	-0.10	2.81	-3.95	-0.11
40	2.95	-4.14	0.09	2.72	-4.03	-0.10	2.46	-3.53	-0.09	3.09	-4.51	-0.12
41	3.17	-4.23	0.06	2.90	-4.27	-0.10	2.42	-3.32	-0.10	2.83	-4.04	-0.10
42	3.24	-4.41	0.10	3.45	-4.92	-0.10	2.77	-3.91	-0.09	3.01	-4.48	-0.11
43	2.74	-3.70	0.10	2.93	-4.18	-0.08	2.63	-3.97	-0.09	3.14	-4.57	-0.12
44	2.88	-3.89	0.11	3.39	-4.92	-0.07	2.88	-4.17	-0.10	3.06	-4.46	-0.11

45	3.04	-4.24	0.10	2.80	-4.16	-0.08	2.82	-4.19	-0.09	3.09	-4.45	-0.11
46	3.44	-4.69	0.10	3.41	-4.64	-0.08	3.36	-4.77	-0.10	3.63	-5.08	-0.11
47	3.37	-4.62	0.11	2.66	-3.80	-0.09	2.72	-3.96	-0.09	3.11	-4.33	-0.10
48	2.64	-3.63	0.10	3.12	-4.55	-0.08	3.26	-4.72	-0.11	3.04	-4.40	-0.12
49	2.57	-3.52	0.10	2.92	-4.18	-0.10	2.27	-3.31	-0.10	2.59	-3.63	-0.12
50	2.91	-3.93	0.11	2.72	-3.86	-0.08	2.88	-4.15	-0.09	3.42	-4.76	-0.11
51	2.58	-3.54	0.14	2.96	-4.14	-0.08	2.65	-3.92	-0.09	2.89	-4.19	-0.12
52	2.51	-3.45	0.09	2.86	-4.04	-0.10	2.79	-4.03	-0.10	2.94	-4.17	-0.11
53	3.24	-4.19	0.06	2.53	-3.56	-0.10	2.94	-4.20	-0.11	2.51	-3.52	-0.10
54	3.21	-4.50	0.21	2.87	-4.01	-0.08	2.65	-3.68	-0.10	2.75	-3.97	-0.12
55	3.11	-4.10	0.10	2.54	-3.62	-0.09	2.41	-3.66	-0.10	2.68	-4.02	-0.12
56	2.85	-3.87	0.10	2.58	-3.82	-0.12	2.63	-3.73	-0.09	2.92	-4.19	-0.10
57	3.05	-4.07	0.10	2.83	-4.04	-0.11	2.39	-3.43	-0.10	2.69	-3.87	-0.10
58	3.12	-4.16	0.10	3.33	-4.58	-0.10	2.93	-4.22	-0.10	2.74	-4.01	-0.11
59	2.76	-3.84	0.11	3.13	-4.63	-0.08	2.49	-3.67	-0.10	2.92	-3.99	-0.11
60	2.94	-3.93	0.10	3.18	-4.41	-0.09	2.65	-3.72	-0.09	2.86	-4.02	-0.12
61	2.84	-3.84	0.11	3.36	-4.78	-0.08	3.05	-4.30	-0.10	3.01	-4.24	-0.12
62	2.73	-3.66	0.11	3.32	-4.71	-0.09	2.62	-3.96	-0.10	3.05	-4.53	-0.10
63	2.72	-3.58	0.11	2.66	-3.63	-0.09	3.02	-4.41	-0.09	3.07	-4.39	-0.11
64	2.88	-4.09	0.11	3.28	-4.82	-0.09	2.38	-3.58	-0.09	2.78	-3.96	-0.10
65	2.44	-3.39	0.10	2.73	-3.81	-0.09	1.84	-2.79	-0.10	2.50	-3.53	-0.11
66	2.18	-2.74	0.10	2.13	-3.03	-0.12	2.17	-3.34	-0.11	2.41	-3.48	-0.11
67	2.62	-3.31	0.11	2.58	-3.68	-0.12	2.15	-3.12	-0.10	2.57	-3.64	-0.10
68	1.92	-2.49	0.11	2.14	-2.94	-0.10	2.04	-2.92	-0.10	1.88	-2.74	-0.09
69	2.13	-2.80	0.11	2.80	-4.14	-0.14	2.15	-3.25	-0.10	1.89	-2.76	-0.10
70	2.31	-3.27	0.16	2.68	-3.87	-0.11	2.48	-3.58	-0.10	2.28	-3.21	-0.10
71	2.31	-3.03	0.12	2.81	-3.98	-0.07	2.31	-3.50	-0.11	2.19	-3.20	-0.10
72	1.58	-2.03	0.10	1.60	-2.39	-0.10	1.91	-2.79	-0.09	1.52	-2.16	-0.10
73	2.42	-3.19	0.10	2.77	-3.86	-0.08	2.52	-3.60	-0.10	2.24	-3.18	-0.10
74	2.81	-4.09	-0.14	2.67	-3.78	-0.12	2.59	-3.80	-0.14	2.53	-3.87	-0.15
75	2.41	-4.00	-0.22	2.60	-3.78	-0.16	2.51	-3.37	-0.16	2.52	-3.58	-0.17
76	2.13	-3.23	-0.17	2.07	-2.96	-0.16	1.69	-2.68	-0.12	1.89	-2.68	-0.14
77	2.66	-3.61	-0.18	2.44	-3.40	-0.13	2.04	-3.03	-0.15	2.20	-3.38	-0.15
78	2.36	-3.80	-0.18	2.73	-3.84	-0.12	1.89	-2.57	-0.09	2.61	-3.61	-0.10
79	2.77	-3.40	0.25	2.63	-3.72	-0.10	2.30	-3.32	-0.10	2.45	-3.60	-0.11
80	1.99	-2.30	0.18	1.65	-2.63	-0.13	1.56	-2.61	-0.15	1.84	-2.77	-0.11
81	2.43	-2.97	0.19	2.56	-3.60	-0.08	2.70	-3.70	-0.10	2.38	-3.51	-0.10

Table B-2. Comparison of external and internal pressure coefficients without and with VSVs for the small gable roof model at 15° wind direction

	Without VSVs			With VSVs			With VSVs and Leakage			With VSVs, Leakage and Opening		
Tap No.	**Cp Max**	**Cp Min**	**Cp Mean**	**Cp Max**	**Cp Min**	**Cp Mean**	**Cp Max**	**Cp Min**	**Cp Mean**	**Cp Max**	**Cp Min**	**Cp Mean**
1	2.17	-3.45	-0.65	2.04	-3.73	-0.61	2.36	-3.96	-0.65	1.90	-3.80	-0.63
2	2.54	-3.91	-0.31	2.31	-3.97	-0.27	2.16	-3.88	-0.32	2.30	-3.80	-0.30
3	2.59	-4.26	-0.35	2.55	-3.68	-0.30	2.78	-4.19	-0.35	2.89	-4.36	-0.34
4	2.19	-3.98	-0.71	2.37	-4.34	-0.69	2.32	-4.05	-0.72	2.46	-4.41	-0.71
5	2.35	-3.78	-0.31	2.91	-4.25	-0.27	2.37	-3.76	-0.31	2.44	-4.17	-0.30
6	2.55	-3.86	-0.29	3.00	-4.49	-0.25	3.38	-4.92	-0.27	2.50	-3.56	-0.26
7	2.18	-2.83	-0.58	2.22	-3.79	-0.55	2.45	-4.11	-0.60	2.34	-3.87	-0.59
8	2.64	-3.87	-0.40	2.11	-3.42	-0.39	2.25	-3.48	-0.41	2.13	-3.62	-0.41
9	2.89	-4.48	-0.36	2.72	-4.14	-0.33	2.42	-3.49	-0.36	2.42	-3.81	-0.35
10	2.51	-4.80	-0.87	2.42	-4.44	-0.81	2.70	-4.72	-0.88	1.84	-3.83	-0.86
11	2.98	-4.45	-0.35	2.41	-4.12	-0.32	3.09	-4.93	-0.36	2.39	-3.61	-0.34
12	2.74	-4.24	-0.31	2.81	-4.27	-0.28	2.88	-4.12	-0.29	2.78	-4.05	-0.29
13	2.38	-3.85	-0.66	3.12	-4.56	-0.61	2.54	-3.81	-0.66	2.46	-3.90	-0.64
14	2.46	-3.90	-0.44	2.76	-4.30	-0.40	2.81	-4.31	-0.43	2.84	-4.00	-0.43
15	2.56	-4.13	-0.38	2.13	-3.31	-0.36	2.69	-4.14	-0.39	1.92	-3.26	-0.37
16	2.07	-3.81	-0.96	2.21	-4.79	-0.91	1.96	-3.97	-0.98	1.79	-3.93	-0.94
17	2.42	-3.86	-0.39	2.66	-4.48	-0.36	2.47	-3.87	-0.37	2.37	-3.92	-0.37
18	3.03	-4.72	-0.32	2.88	-3.98	-0.28	2.92	-4.71	-0.31	2.18	-3.66	-0.31
19	2.52	-4.47	-0.76	2.56	-4.33	-0.71	2.74	-3.99	-0.77	2.29	-3.90	-0.77
20	3.13	-4.40	-0.22	2.05	-3.67	-0.20	2.96	-4.29	-0.23	2.68	-4.51	-0.24
21	2.77	-4.17	-0.34	2.23	-3.54	-0.32	2.61	-4.25	-0.34	2.72	-4.33	-0.33
22	2.40	-4.89	-0.98	1.65	-3.85	-1.01	2.11	-4.25	-1.00	1.83	-3.98	-0.98
23	2.67	-4.29	-0.37	2.94	-4.64	-0.34	2.55	-4.11	-0.35	2.35	-3.83	-0.35
24	2.41	-3.93	-0.28	1.99	-3.34	-0.25	2.31	-3.94	-0.26	2.25	-3.59	-0.25
25	2.93	-4.86	-0.93	2.67	-3.90	-0.91	3.20	-5.20	-0.95	2.15	-4.06	-0.94
26	2.65	-3.78	0.01	2.90	-3.84	0.04	2.81	-4.00	0.01	3.28	-4.19	0.02
27	2.52	-3.88	-0.29	2.48	-3.69	-0.28	2.83	-4.33	-0.29	2.49	-3.89	-0.29
28	2.05	-4.45	-1.18	2.29	-4.74	-1.21	2.18	-5.20	-1.15	2.27	-5.10	-1.15
29	2.87	-4.31	-0.37	2.37	-3.85	-0.36	2.54	-4.01	-0.37	2.50	-4.03	-0.36
30	2.95	-4.68	-0.32	2.86	-4.39	-0.31	2.75	-4.41	-0.30	2.71	-4.23	-0.30
31	2.44	-3.56	-0.18	2.94	-4.15	-0.17	3.01	-4.52	-0.20	3.08	-4.49	-0.20
32	3.26	-4.70	-0.11	3.24	-4.77	-0.19	3.20	-4.88	-0.16	2.66	-3.90	-0.18
33	3.15	-4.17	0.19	3.54	-4.06	0.77	3.67	-4.14	0.76	2.94	-3.41	0.76
34	3.83	-4.73	0.43	3.20	-4.07	0.44	3.21	-3.87	0.41	3.42	-4.07	0.41
35	3.17	-3.68	0.69	3.08	-3.53	0.73	3.30	-3.98	0.66	3.15	-3.40	0.66
36	2.41	-3.71	-0.16	3.26	-4.99	-0.13	3.00	-4.46	-0.14	2.85	-3.82	-0.14
37	2.26	-3.52	-0.25	2.63	-3.93	-0.23	2.83	-4.20	-0.26	2.53	-4.04	-0.25
38	2.64	-4.07	-0.24	2.78	-4.43	-0.25	2.81	-4.22	-0.24	2.77	-4.17	-0.23
39	2.25	-3.14	0.13	3.00	-4.40	-0.11	2.81	-4.14	-0.11	2.86	-4.25	-0.11
40	3.04	-4.10	0.07	3.06	-4.49	-0.11	3.31	-4.77	-0.12	3.11	-4.70	-0.11
41	3.08	-4.23	0.03	2.99	-4.37	-0.13	2.66	-3.88	-0.12	2.73	-3.96	-0.11
42	3.53	-4.70	0.08	3.42	-4.86	-0.11	2.82	-4.17	-0.10	3.23	-4.71	-0.11
43	2.90	-3.93	0.08	2.60	-3.86	-0.08	2.84	-4.14	-0.13	2.75	-4.03	-0.12
44	3.33	-4.53	0.08	3.00	-4.14	-0.07	3.18	-4.55	-0.13	2.85	-4.19	-0.11
45	3.69	-4.95	0.08	2.76	-4.05	-0.09	3.14	-4.66	-0.12	2.77	-4.07	-0.11
46	3.40	-4.66	0.08	2.79	-4.00	-0.08	3.33	-4.90	-0.13	2.78	-3.93	-0.11

47	3.29	-4.33	0.09	2.51	-3.71	-0.11	3.07	-4.45	-0.10	2.93	-4.18	-0.10
48	3.08	-4.36	0.07	2.46	-3.47	-0.09	2.53	-3.75	-0.12	2.56	-3.83	-0.10
49	2.62	-3.62	0.08	2.42	-3.50	-0.11	3.42	-4.93	-0.11	2.43	-3.51	-0.11
50	3.06	-4.27	0.08	3.28	-4.76	-0.08	2.94	-4.28	-0.12	2.71	-4.06	-0.10
51	2.36	-3.35	0.09	2.49	-3.47	-0.08	2.17	-3.26	-0.12	2.31	-3.41	-0.11
52	2.90	-3.92	0.08	3.43	-4.96	-0.13	2.92	-4.28	-0.10	2.46	-3.59	-0.11
53	2.82	-3.88	0.04	3.15	-4.59	-0.14	3.17	-4.56	-0.12	2.47	-3.51	-0.12
54	2.83	-3.99	0.11	3.39	-4.80	-0.09	3.25	-4.48	-0.12	3.19	-4.76	-0.12
55	3.13	-4.12	0.08	2.79	-4.06	-0.10	3.14	-4.51	-0.12	2.51	-3.74	-0.11
56	2.90	-3.96	0.09	2.45	-3.69	-0.15	3.05	-4.46	-0.08	2.65	-3.94	-0.09
57	3.39	-4.50	0.09	2.15	-3.25	-0.14	2.94	-4.18	-0.09	2.91	-4.31	-0.10
58	3.26	-4.51	0.08	2.85	-4.15	-0.12	2.53	-3.63	-0.10	2.64	-3.70	-0.10
59	2.92	-3.90	0.08	2.91	-4.34	-0.09	2.98	-4.28	-0.12	3.09	-4.53	-0.11
60	3.26	-4.43	0.07	3.07	-4.54	-0.10	3.08	-4.44	-0.10	2.72	-4.05	-0.11
61	3.28	-4.49	0.08	3.07	-4.33	-0.09	3.20	-4.77	-0.12	2.70	-3.94	-0.11
62	3.11	-4.33	0.09	2.96	-4.35	-0.11	2.98	-4.42	-0.11	2.99	-4.34	-0.10
63	3.54	-4.75	0.09	2.69	-3.92	-0.10	2.89	-4.18	-0.10	2.68	-4.04	-0.11
64	2.71	-3.82	0.09	2.81	-4.17	-0.11	3.22	-4.74	-0.10	3.29	-4.63	-0.09
65	2.20	-2.91	0.08	1.96	-2.83	-0.11	2.42	-3.73	-0.11	2.51	-3.70	-0.11
66	2.77	-3.72	0.07	2.04	-3.00	-0.13	2.18	-3.06	-0.11	2.30	-3.43	-0.11
67	2.58	-3.53	0.07	2.20	-3.23	-0.13	2.56	-3.76	-0.09	2.53	-3.54	-0.09
68	2.30	-3.09	0.09	2.03	-2.99	-0.12	2.02	-2.90	-0.11	1.84	-2.82	-0.11
69	2.19	-3.08	0.07	2.60	-3.94	-0.15	2.31	-3.45	-0.09	2.32	-3.61	-0.10
70	2.30	-3.29	0.24	2.44	-3.60	-0.13	3.09	-4.36	-0.11	2.24	-3.24	-0.10
71	2.20	-3.15	0.12	2.09	-3.14	-0.09	3.10	-4.47	-0.12	2.56	-3.73	-0.10
72	1.66	-2.09	0.10	1.65	-2.33	-0.12	1.74	-2.57	-0.11	1.53	-2.15	-0.10
73	2.46	-3.34	0.09	2.26	-3.45	-0.11	2.41	-3.63	-0.11	2.36	-3.40	-0.10
74	2.50	-3.86	-0.20	2.67	-4.08	-0.20	2.57	-3.95	-0.21	2.28	-3.50	-0.21
75	2.52	-3.59	-0.26	2.26	-3.79	-0.23	2.98	-4.70	-0.23	2.01	-3.36	-0.23
76	2.04	-3.19	-0.28	2.01	-3.03	-0.23	2.19	-3.19	-0.22	1.87	-2.99	-0.22
77	2.39	-3.63	-0.23	3.09	-4.65	-0.20	2.41	-3.65	-0.22	2.46	-3.73	-0.22
78	2.00	-3.47	-0.40	2.44	-3.66	-0.14	2.47	-3.70	-0.10	2.40	-3.51	-0.10
79	2.38	-3.24	0.17	1.94	-2.84	-0.13	3.11	-4.34	-0.11	2.01	-2.91	-0.10
80	2.05	-2.13	0.34	1.59	-2.37	-0.14	1.42	-2.28	-0.15	1.94	-2.95	-0.10
81	2.55	-3.21	0.17	2.80	-3.99	-0.10	3.07	-4.38	-0.11	2.63	-3.89	-0.10

Table B-3. Comparison of external and internal pressure coefficients without and with VSVs for the small gable roof model at 30° wind direction

	Without VSVs			With VSVs			With VSVs and Leakage			With VSVs, Leakage and Opening		
Tap No.	Cp Max	Cp Min	Cp Mean	Cp Max	Cp Min	Cp Mean	Cp Max	Cp Min	Cp Mean	Cp Max	Cp Min	Cp Mean
1	7.57	-11.58	-0.47	1.79	-3.37	-0.44	2.24	-3.85	-0.45	1.75	-2.99	-0.45
2	1.73	-3.12	-0.30	2.41	-3.82	-0.27	2.05	-3.32	-0.28	1.70	-2.61	-0.28
3	2.34	-3.49	-0.28	2.54	-4.12	-0.24	1.70	-2.75	-0.25	1.97	-3.14	-0.27
4	2.00	-4.08	-0.71	1.96	-3.46	-0.68	1.90	-3.67	-0.70	2.01	-3.83	-0.69
5	2.17	-3.70	-0.30	1.90	-3.39	-0.27	1.86	-3.08	-0.28	1.76	-2.92	-0.29
6	2.37	-3.64	-0.26	2.21	-3.69	-0.23	1.91	-3.24	-0.23	1.91	-3.23	-0.24
7	2.22	-3.46	-0.52	1.99	-3.36	-0.49	1.73	-2.81	-0.51	1.38	-2.47	-0.52
8	1.82	-2.71	-0.34	2.50	-3.62	-0.32	2.17	-2.85	-0.31	2.15	-3.06	-0.32
9	1.70	-2.83	-0.31	1.87	-3.12	-0.28	1.89	-3.05	-0.29	2.49	-4.02	-0.29
10	2.25	-4.02	-0.78	1.72	-3.33	-0.73	1.57	-3.30	-0.76	1.95	-3.78	-0.77
11	1.93	-3.16	-0.36	2.01	-3.41	-0.33	1.51	-2.87	-0.35	1.86	-3.13	-0.35
12	2.21	-3.57	-0.27	2.22	-3.64	-0.25	2.33	-3.72	-0.24	2.29	-3.74	-0.25
13	2.15	-3.23	-0.59	2.08	-3.21	-0.55	1.83	-3.20	-0.57	2.29	-3.08	-0.55
14	2.30	-2.97	-0.23	2.25	-3.49	-0.22	2.18	-2.70	-0.22	2.18	-3.17	-0.21
15	2.23	-3.59	-0.37	2.05	-3.59	-0.35	1.74	-2.96	-0.36	1.75	-3.03	-0.36
16	2.52	-4.38	-0.96	2.27	-4.04	-0.92	2.04	-3.90	-0.95	1.66	-3.49	-0.94
17	2.27	-3.64	-0.37	1.49	-2.72	-0.35	1.67	-2.77	-0.36	1.66	-2.91	-0.37
18	2.04	-3.21	-0.28	2.76	-4.35	-0.25	2.02	-3.11	-0.26	2.38	-3.65	-0.28
19	2.65	-4.19	-0.55	2.68	-3.77	-0.54	2.67	-4.06	-0.56	2.05	-3.34	-0.55
20	2.18	-3.07	-0.02	2.37	-3.27	0.01	2.27	-2.98	0.00	2.41	-3.34	-0.01
21	1.72	-2.87	-0.38	2.14	-3.49	-0.36	2.46	-3.88	-0.36	2.13	-3.66	-0.36
22	1.21	-3.02	-1.26	1.75	-3.98	-1.27	1.44	-3.52	-1.26	1.74	-3.73	-1.25
23	2.22	-3.56	-0.29	2.04	-3.23	-0.28	1.78	-2.90	-0.29	1.74	-2.85	-0.29
24	2.42	-3.61	-0.24	2.39	-3.81	-0.23	1.92	-3.06	-0.23	1.78	-2.92	-0.22
25	2.58	-4.17	-0.85	2.81	-3.79	-0.85	3.43	-4.19	-0.88	3.72	-4.42	-0.86
26	2.88	-3.83	0.03	2.83	-4.11	0.04	2.31	-3.17	0.03	2.19	-3.13	0.04
27	2.67	-4.14	-0.33	2.65	-4.44	-0.32	1.71	-2.91	-0.32	1.87	-3.19	-0.33
28	2.17	-3.52	-0.76	2.24	-4.12	-0.76	1.69	-3.36	-0.74	1.69	-3.36	-0.73
29	2.18	-3.42	-0.55	2.19	-3.47	-0.56	2.28	-3.59	-0.55	2.13	-3.41	-0.55
30	2.29	-3.80	-0.60	2.68	-4.08	-0.61	2.15	-3.44	-0.59	2.64	-4.08	-0.58
31	2.41	-3.63	-0.21	2.03	-3.18	-0.20	1.83	-2.98	-0.21	1.87	-2.99	-0.22
32	2.68	-4.02	-0.14	2.57	-4.10	-0.20	2.53	-3.78	-0.17	1.86	-2.97	-0.17
33	2.15	-2.94	0.21	2.44	-2.62	0.77	1.98	0.00	0.78	2.38	-2.30	0.77
34	2.72	-3.50	0.29	2.82	-3.95	0.22	2.81	-3.86	0.22	2.44	-3.02	0.22
35	2.85	-3.42	0.54	2.97	-3.54	0.56	2.37	-2.73	0.55	2.54	-2.90	0.52
36	2.87	-3.79	0.15	3.34	-4.47	0.16	2.91	-3.84	0.17	2.22	-2.93	0.17
37	1.84	-2.98	-0.28	2.12	-3.42	-0.27	2.31	-3.60	-0.28	2.00	-3.20	-0.27
38	2.87	-4.46	-0.23	2.39	-3.76	-0.23	2.41	-3.74	-0.24	1.66	-2.75	-0.22
39	1.70	-2.50	0.05	2.51	-3.79	-0.10	1.84	-2.65	-0.08	1.73	-2.60	-0.07
40	2.71	-3.92	0.05	2.70	-3.98	-0.10	2.27	-3.34	-0.08	2.91	-4.28	-0.07
41	2.69	-3.86	0.01	2.57	-3.83	-0.12	2.08	-3.18	-0.12	1.66	-2.59	-0.10
42	2.91	-4.03	0.06	2.62	-3.93	-0.10	1.94	-2.92	-0.08	2.74	-3.93	-0.07
43	1.86	-2.67	0.06	2.66	-4.05	-0.08	2.16	-3.27	-0.08	2.22	-3.38	-0.08
44	3.17	-4.46	0.07	3.17	-4.54	-0.07	2.70	-3.98	-0.08	2.59	-3.92	-0.07
45	2.81	-3.96	0.06	2.83	-4.28	-0.09	1.78	-2.73	-0.08	2.10	-3.04	-0.07
46	3.01	-4.16	0.06	2.88	-4.22	-0.08	2.56	-3.72	-0.09	2.67	-3.71	-0.07

47	2.57	-3.59	0.07	2.82	-4.09	-0.09	2.44	-3.67	-0.08	2.03	-3.02	-0.06
48	2.73	-3.76	0.05	2.45	-3.63	-0.09	2.64	-3.80	-0.10	2.54	-3.82	-0.08
49	2.51	-3.47	0.06	2.35	-3.50	-0.10	2.48	-3.53	-0.09	2.07	-3.06	-0.08
50	2.74	-3.67	0.06	3.04	-4.41	-0.08	3.07	-4.47	-0.08	2.65	-3.83	-0.06
51	2.47	-3.45	0.00	2.71	-3.91	-0.08	1.96	-2.91	-0.08	2.50	-3.70	-0.07
52	2.56	-3.54	0.07	2.53	-3.81	-0.10	2.36	-3.55	-0.09	2.06	-3.19	-0.08
53	2.05	-2.92	0.03	2.09	-3.08	-0.13	2.06	-3.05	-0.12	2.45	-3.66	-0.09
54	2.54	-3.41	0.07	2.39	-3.53	-0.08	2.74	-3.87	-0.08	2.88	-4.27	-0.08
55	2.42	-3.44	0.06	2.40	-3.55	-0.09	1.74	-2.74	-0.09	2.25	-3.34	-0.07
56	2.25	-3.19	0.07	2.97	-4.35	-0.13	1.93	-2.82	-0.08	2.09	-3.22	-0.06
57	1.94	-2.66	0.07	3.04	-4.64	-0.12	2.10	-3.13	-0.09	1.94	-2.87	-0.07
58	2.49	-3.58	0.06	2.82	-4.17	-0.11	2.41	-3.51	-0.08	2.34	-3.41	-0.07
59	2.44	-3.35	0.07	2.77	-4.06	-0.09	2.05	-3.02	-0.09	2.02	-3.01	-0.07
60	3.00	-4.09	0.06	2.88	-4.25	-0.09	2.50	-3.66	-0.07	2.77	-4.06	-0.08
61	2.45	-3.29	0.06	2.66	-3.93	-0.08	2.41	-3.44	-0.08	2.35	-3.53	-0.08
62	2.40	-3.27	0.06	2.92	-4.38	-0.09	2.25	-3.21	-0.09	2.22	-3.24	-0.06
63	2.70	-3.54	0.07	2.77	-4.03	-0.09	2.43	-3.58	-0.08	1.90	-2.76	-0.07
64	2.66	-3.79	0.06	2.62	-3.86	-0.09	2.44	-3.54	-0.07	2.29	-3.18	-0.06
65	7.94	-10.46	0.07	1.80	-2.70	-0.09	2.01	-3.00	-0.08	1.71	-2.51	-0.07
66	1.76	-2.43	0.06	2.16	-3.25	-0.13	1.84	-2.75	-0.10	1.61	-2.39	-0.08
67	2.14	-2.96	0.06	2.26	-3.47	-0.15	1.55	-2.30	-0.10	1.97	-2.94	-0.08
68	2.00	-2.80	0.07	1.75	-2.66	-0.11	1.75	-2.69	-0.09	2.02	-3.00	-0.07
69	2.18	-3.03	0.05	1.77	-2.81	-0.16	1.76	-2.58	-0.10	1.97	-2.96	-0.08
70	2.06	-2.62	0.23	2.12	-3.19	-0.11	1.65	-2.52	-0.09	1.96	-2.95	-0.07
71	2.45	-3.36	0.10	2.53	-3.72	-0.07	1.89	-2.78	-0.09	1.65	-2.49	-0.06
72	1.35	-1.72	0.06	1.95	-2.89	-0.11	1.36	-1.96	-0.08	1.36	-1.79	-0.04
73	1.90	-2.62	0.07	1.95	-2.93	-0.09	2.28	-3.38	-0.09	1.95	-2.95	-0.06
74	2.19	-3.53	-0.24	1.98	-3.13	-0.23	1.81	-2.85	-0.25	1.51	-2.47	-0.24
75	1.73	-3.05	-0.30	1.90	-3.16	-0.28	1.85	-3.08	-0.28	1.40	-2.31	-0.28
76	1.63	-2.72	-0.29	1.87	-3.14	-0.27	1.38	-2.37	-0.23	1.75	-2.87	-0.24
77	1.91	-2.99	-0.26	2.28	-3.63	-0.21	1.43	-2.34	-0.24	1.66	-2.76	-0.23
78	1.61	-2.56	-0.26	2.08	-3.17	-0.13	1.22	-1.87	-0.08	1.82	-2.68	-0.07
79	2.05	-2.47	0.09	2.12	-3.18	-0.11	1.30	-2.02	-0.08	1.91	-2.86	-0.06
80	2.00	-1.94	0.48	1.39	-2.16	-0.14	1.27	-1.89	-0.13	1.16	-1.50	-0.08
81	2.38	-3.09	0.07	1.74	-2.60	-0.07	1.67	-2.48	-0.08	1.72	-2.60	-0.06

Table B-4. Comparison of external and internal pressure coefficients without and with VSVs for the small gable roof model at 45° wind direction

	Without VSVs			With VSVs			With VSVs and Leakage			With VSVs, Leakage and Opening		
Tap No.	Cp Max	Cp Min	Cp Mean	Cp Max	Cp Min	Cp Mean	Cp Max	Cp Min	Cp Mean	Cp Max	Cp Min	Cp Mean
1	2.22	-3.44	-0.40	2.33	-3.68	-0.36	1.84	-2.95	-0.38	2.50	-3.77	-0.38
2	2.92	-4.16	-0.26	3.18	-4.59	-0.21	2.49	-3.77	-0.24	2.83	-3.73	-0.23
3	2.35	-3.63	-0.25	2.55	-3.93	-0.20	2.14	-3.35	-0.23	2.13	-3.35	-0.24
4	2.29	-4.04	-0.56	3.16	-4.68	-0.51	2.38	-4.07	-0.56	2.20	-3.75	-0.54
5	2.83	-4.29	-0.23	2.20	-3.36	-0.18	2.44	-3.56	-0.22	2.25	-3.54	-0.22
6	2.56	-3.74	-0.27	2.51	-4.09	-0.23	2.23	-3.48	-0.24	2.71	-4.03	-0.23
7	2.19	-3.36	-0.48	2.26	-3.82	-0.42	2.26	-4.23	-0.46	2.07	-3.20	-0.46
8	2.29	-3.87	-0.17	2.33	-4.08	-0.15	2.52	-3.81	-0.14	2.44	-3.60	-0.15
9	2.36	-3.67	-0.33	2.57	-4.02	-0.29	1.73	-2.76	-0.31	2.57	-3.98	-0.31
10	2.49	-4.47	-0.72	2.60	-4.29	-0.65	2.40	-3.99	-0.70	2.60	-4.54	-0.70
11	2.31	-3.49	-0.29	2.64	-3.97	-0.25	2.30	-3.72	-0.29	2.93	-4.35	-0.28
12	2.51	-3.65	-0.25	3.05	-4.66	-0.22	2.36	-3.57	-0.22	2.65	-3.99	-0.23
13	2.72	-3.86	-0.32	2.44	-3.65	-0.28	2.04	-3.04	-0.31	2.26	-3.86	-0.30
14	2.71	-3.81	-0.07	2.21	-3.32	-0.04	2.58	-3.79	-0.06	2.73	-3.86	-0.06
15	2.12	-3.46	-0.39	2.91	-4.74	-0.37	2.39	-3.88	-0.38	2.25	-3.83	-0.37
16	2.36	-3.98	-0.63	2.42	-3.92	-0.56	2.28	-4.11	-0.61	2.59	-4.65	-0.60
17	2.26	-3.45	-0.37	2.92	-4.51	-0.35	2.23	-3.55	-0.36	2.39	-3.79	-0.36
18	3.09	-4.61	-0.30	3.10	-4.82	-0.26	2.28	-3.44	-0.29	2.92	-4.28	-0.30
19	2.59	-3.50	-0.23	2.68	-3.49	-0.18	2.49	-3.81	-0.23	2.24	-3.30	-0.23
20	2.56	-3.75	-0.08	2.90	-4.23	-0.03	2.55	-3.60	-0.05	2.43	-3.62	-0.06
21	2.45	-4.00	-0.36	2.95	-4.43	-0.33	2.82	-4.35	-0.35	2.52	-3.89	-0.34
22	2.15	-4.09	-0.64	2.03	-3.96	-0.65	2.02	-3.85	-0.62	2.41	-4.42	-0.60
23	2.44	-3.46	-0.30	2.91	-3.95	-0.30	2.68	-4.12	-0.31	2.21	-4.07	-0.31
24	2.19	-3.64	-0.30	2.66	-4.88	-0.30	2.32	-3.47	-0.29	2.15	-3.20	-0.30
25	3.09	-4.10	-0.59	2.65	-3.92	-0.57	2.46	-4.20	-0.61	2.63	-4.00	-0.58
26	2.66	-3.59	-0.03	3.45	-4.89	-0.01	2.86	-4.20	-0.03	2.81	-4.16	-0.02
27	2.72	-4.00	-0.25	2.34	-3.61	-0.22	2.61	-3.75	-0.23	2.50	-3.93	-0.22
28	2.05	-3.87	-0.62	2.42	-4.49	-0.69	2.36	-4.18	-0.63	2.06	-3.95	-0.63
29	2.04	-3.89	-0.75	1.86	-3.61	-0.70	2.13	-3.58	-0.71	1.93	-4.06	-0.66
30	2.43	-3.90	-0.51	3.02	-4.82	-0.52	2.56	-4.25	-0.49	2.47	-4.22	-0.47
31	2.47	-3.58	-0.25	2.95	-4.36	-0.21	2.35	-3.63	-0.24	2.46	-3.81	-0.23
32	2.76	-4.06	-0.19	3.36	-4.97	-0.22	2.59	-3.61	-0.19	3.16	-4.56	-0.18
33	3.16	-4.12	0.17	3.27	-3.92	0.53	3.16	-3.54	0.51	3.01	-3.50	0.51
34	2.49	-3.28	0.14	2.96	-4.07	0.04	2.82	-3.81	0.01	3.04	-4.31	0.02
35	2.97	-3.71	0.32	3.42	-4.39	0.38	3.17	-3.81	0.32	3.02	-3.52	0.30
36	3.51	-4.59	0.36	3.38	-4.33	0.41	3.14	-3.74	0.38	3.10	-3.70	0.39
37	2.61	-3.99	-0.33	2.04	-3.43	-0.30	2.29	-3.49	-0.32	2.16	-3.23	-0.30
38	2.77	-4.10	-0.23	2.56	-3.93	-0.25	2.71	-3.79	-0.23	2.52	-3.84	-0.22
39	2.66	-3.60	-0.02	2.45	-3.70	-0.10	2.52	-3.63	-0.09	2.31	-3.23	-0.06
40	2.37	-3.18	-0.01	3.34	-4.82	-0.09	2.30	-3.32	-0.08	2.66	-4.08	-0.06
41	2.69	-3.89	-0.05	2.46	-3.69	-0.14	2.21	-3.23	-0.13	2.62	-3.91	-0.09
42	2.98	-4.23	0.00	3.67	-5.28	-0.11	2.70	-3.84	-0.09	3.03	-4.41	-0.07
43	2.86	-4.05	-0.01	3.69	-5.22	-0.06	2.55	-3.58	-0.09	2.82	-4.13	-0.07
44	2.92	-3.88	0.00	3.38	-4.68	-0.05	2.81	-3.98	-0.09	2.79	-4.08	-0.07
45	3.06	-4.28	-0.01	3.11	-4.41	-0.08	2.49	-3.48	-0.09	2.76	-3.96	-0.07
46	3.18	-4.32	-0.01	3.25	-4.63	-0.06	3.10	-4.48	-0.10	3.07	-4.27	-0.06

47	2.74	-3.84	0.00	3.21	-4.63	-0.10	2.84	-4.00	-0.09	3.08	-4.33	-0.06
48	2.90	-3.99	-0.01	3.28	-4.69	-0.07	2.48	-3.62	-0.10	2.35	-3.35	-0.07
49	2.64	-3.74	-0.01	2.90	-4.33	-0.10	2.41	-3.54	-0.10	2.80	-3.95	-0.07
50	2.17	-2.94	0.00	3.11	-4.47	-0.07	3.09	-4.37	-0.09	2.89	-4.17	-0.06
51	2.65	-3.60	-0.03	3.00	-4.29	-0.07	2.67	-3.85	-0.09	3.22	-4.58	-0.07
52	2.89	-4.20	-0.01	3.42	-4.97	-0.13	2.64	-3.67	-0.09	2.87	-4.11	-0.07
53	2.83	-4.05	-0.04	2.56	-3.80	-0.16	1.97	-2.88	-0.13	2.46	-3.47	-0.09
54	3.12	-4.36	0.02	3.15	-4.55	-0.07	2.64	-4.00	-0.09	2.81	-4.13	-0.07
55	2.62	-3.70	0.00	2.57	-3.85	-0.09	2.93	-4.16	-0.09	2.27	-3.36	-0.07
56	2.69	-3.77	-0.01	2.44	-3.65	-0.18	2.53	-3.62	-0.09	2.50	-3.48	-0.06
57	2.59	-3.54	0.00	3.12	-4.66	-0.16	2.38	-3.45	-0.10	2.67	-3.81	-0.07
58	2.66	-3.71	-0.01	3.06	-4.56	-0.12	2.62	-3.79	-0.09	2.96	-4.23	-0.06
59	3.12	-4.32	0.00	3.06	-4.53	-0.08	2.46	-3.53	-0.09	2.82	-4.08	-0.06
60	2.08	-2.88	0.00	3.47	-5.03	-0.10	2.83	-3.87	-0.08	2.65	-3.75	-0.07
61	2.27	-3.18	0.00	3.34	-4.86	-0.07	2.63	-3.88	-0.09	3.08	-4.40	-0.07
62	2.73	-3.59	0.00	3.61	-5.27	-0.10	2.97	-4.35	-0.09	3.09	-4.38	-0.06
63	2.33	-3.32	0.00	3.18	-4.57	-0.10	2.55	-3.74	-0.08	2.97	-4.21	-0.06
64	2.89	-3.89	0.00	3.04	-4.40	-0.09	2.68	-3.93	-0.08	3.05	-4.39	-0.05
65	2.02	-2.90	-0.01	2.41	-3.61	-0.10	2.18	-3.00	-0.10	2.18	-3.03	-0.05
66	2.35	-3.35	0.01	2.83	-4.34	-0.16	2.20	-3.12	-0.10	2.33	-3.23	-0.09
67	2.03	-2.78	0.03	2.25	-3.32	-0.18	1.97	-2.94	-0.09	1.98	-2.85	-0.09
68	1.79	-2.47	0.01	2.78	-4.17	-0.11	1.89	-2.99	-0.10	2.03	-2.86	-0.06
69	2.43	-3.40	0.03	2.47	-3.80	-0.20	2.27	-3.21	-0.09	2.44	-3.43	-0.10
70	2.09	-2.99	0.03	2.49	-3.78	-0.13	2.07	-3.05	-0.10	2.41	-3.54	-0.06
71	2.12	-2.85	0.03	3.04	-4.51	-0.08	2.63	-3.92	-0.10	2.43	-3.40	-0.05
72	1.47	-1.99	-0.01	1.70	-2.43	-0.09	1.97	-3.01	-0.09	1.46	-2.04	-0.04
73	2.56	-3.49	-0.01	2.29	-3.43	-0.10	1.94	-2.65	-0.10	2.31	-3.27	-0.05
74	2.29	-3.71	-0.29	2.32	-3.59	-0.26	2.69	-4.10	-0.29	2.12	-3.35	-0.25
75	2.31	-3.47	-0.34	2.03	-3.25	-0.32	2.40	-3.92	-0.31	1.98	-3.07	-0.30
76	1.67	-2.75	-0.30	2.14	-3.38	-0.29	1.56	-2.37	-0.25	1.77	-2.74	-0.26
77	2.30	-3.60	-0.31	2.39	-3.94	-0.23	1.79	-2.85	-0.27	2.28	-3.56	-0.24
78	2.31	-3.46	-0.17	2.01	-3.00	-0.15	2.12	-2.98	-0.09	2.41	-3.44	-0.07
79	2.22	-3.17	0.00	3.06	-4.49	-0.11	2.11	-3.09	-0.09	2.29	-3.30	-0.05
80	2.06	-1.99	0.52	1.75	-2.54	-0.16	1.48	-2.18	-0.11	1.64	-2.61	-0.08
81	2.24	-3.15	-0.06	2.62	-3.86	-0.08	2.59	-3.67	-0.09	2.37	-3.24	-0.04

Table B-5. Comparison of external and internal pressure coefficients without and with VSVs for the small gable roof model at 60° wind direction

	Without VSVs			With VSVs			With VSVs and Leakage			With VSVs, Leakage and Opening		
Tap No.	Cp Max	Cp Min	Cp Mean	Cp Max	Cp Min	Cp Mean	Cp Max	Cp Min	Cp Mean	Cp Max	Cp Min	Cp Mean
1	2.26	-3.52	-0.28	1.71	-2.92	-0.27	2.07	-3.10	-0.29	1.71	-2.83	-0.26
2	2.45	-3.40	-0.15	2.49	-3.80	-0.13	2.63	-3.74	-0.15	2.48	-3.59	-0.13
3	3.02	-4.35	-0.21	1.98	-2.96	-0.18	2.10	-3.18	-0.21	2.46	-3.63	-0.20
4	2.33	-3.72	-0.38	2.32	-3.58	-0.36	2.30	-3.76	-0.38	2.63	-4.46	-0.37
5	2.42	-3.62	-0.23	2.20	-3.08	-0.21	2.26	-3.48	-0.24	2.54	-3.89	-0.22
6	2.12	-2.97	-0.30	2.30	-3.70	-0.29	2.23	-3.37	-0.30	2.86	-4.07	-0.28
7	2.74	-3.84	-0.20	2.24	-3.22	-0.18	1.91	-2.83	-0.21	2.53	-3.70	-0.19
8	2.26	-3.28	-0.08	2.42	-3.86	-0.08	1.85	-2.48	-0.07	2.26	-3.38	-0.07
9	2.30	-3.47	-0.25	2.09	-3.20	-0.24	2.15	-3.27	-0.25	1.71	-2.54	-0.24
10	2.10	-3.60	-0.43	2.18	-3.37	-0.40	2.70	-4.26	-0.44	1.78	-3.10	-0.42
11	2.92	-4.37	-0.31	2.46	-4.05	-0.29	2.32	-3.79	-0.32	2.05	-3.56	-0.31
12	2.42	-3.57	-0.32	2.08	-3.04	-0.29	2.59	-3.95	-0.31	2.28	-3.36	-0.29
13	2.35	-3.50	-0.11	1.77	-2.59	-0.10	2.53	-3.80	-0.13	2.16	-3.12	-0.11
14	2.20	-3.32	-0.09	2.95	-4.25	-0.08	2.62	-3.67	-0.09	2.74	-3.93	-0.08
15	2.75	-4.18	-0.28	1.65	-2.79	-0.27	1.99	-3.10	-0.28	2.27	-3.33	-0.27
16	2.17	-3.23	-0.45	2.03	-3.46	-0.42	2.00	-3.31	-0.47	2.52	-3.83	-0.43
17	1.64	-2.82	-0.41	1.92	-3.11	-0.39	1.95	-3.38	-0.40	2.10	-3.24	-0.40
18	1.68	-2.92	-0.41	2.00	-3.70	-0.39	2.03	-3.37	-0.42	2.14	-3.26	-0.40
19	2.71	-3.91	-0.15	2.56	-3.72	-0.13	2.63	-3.89	-0.16	1.89	-3.00	-0.15
20	2.26	-3.28	-0.09	2.33	-3.28	-0.08	2.66	-3.85	-0.10	2.81	-4.00	-0.09
21	2.49	-3.82	-0.23	2.46	-3.61	-0.21	2.30	-3.56	-0.21	2.48	-3.71	-0.21
22	2.01	-3.30	-0.52	2.24	-3.73	-0.53	2.44	-3.62	-0.50	2.71	-4.10	-0.51
23	2.94	-4.37	-0.47	1.94	-3.49	-0.46	2.05	-3.39	-0.47	2.36	-3.69	-0.46
24	2.00	-3.40	-0.50	1.76	-3.02	-0.50	2.14	-3.97	-0.49	2.28	-3.91	-0.48
25	2.03	-3.50	-0.24	2.71	-4.33	-0.23	2.24	-3.23	-0.26	1.92	-3.18	-0.24
26	2.08	-2.99	-0.08	2.39	-3.30	-0.08	2.55	-3.57	-0.09	2.64	-3.68	-0.07
27	2.28	-4.55	-0.69	2.11	-3.13	-0.71	2.12	-3.88	-0.70	2.06	-3.16	-0.71
28	2.27	-3.65	-0.63	2.20	-4.00	-0.66	2.30	-3.83	-0.59	1.93	-3.29	-0.62
29	1.91	-3.55	-0.62	2.13	-3.63	-0.63	2.12	-3.35	-0.62	1.83	-3.10	-0.61
30	2.60	-4.16	-0.66	2.35	-3.71	-0.68	2.50	-4.47	-0.66	2.28	-4.41	-0.65
31	3.00	-4.21	-0.26	2.30	-3.56	-0.25	2.42	-3.60	-0.27	2.45	-3.75	-0.25
32	2.64	-3.86	-0.21	2.24	-3.37	-0.23	2.78	-4.13	-0.19	2.58	-4.21	-0.19
33	2.57	-3.55	0.08	2.44	-3.82	-0.06	2.57	-4.27	-0.08	2.79	-4.66	-0.08
34	2.32	-3.27	0.01	2.25	-3.28	-0.10	1.99	-3.08	-0.12	2.92	-4.20	-0.09
35	3.17	-4.31	0.11	2.30	-3.12	0.13	2.09	-2.85	0.08	2.75	-3.79	0.10
36	3.01	-3.34	0.58	3.45	-3.93	0.58	3.14	-3.66	0.60	3.01	-3.42	0.59
37	2.01	-3.27	-0.33	1.84	-3.00	-0.32	2.07	-3.20	-0.33	1.79	-3.01	-0.32
38	2.00	-2.95	-0.20	2.44	-3.60	-0.22	2.32	-3.62	-0.19	2.10	-3.07	-0.20
39	3.26	-4.60	-0.09	2.79	-3.98	-0.13	2.24	-3.25	-0.10	2.48	-3.45	-0.05
40	2.57	-3.77	-0.09	2.18	-3.10	-0.13	2.25	-3.23	-0.11	2.64	-3.93	-0.06
41	2.51	-3.56	-0.12	2.19	-3.11	-0.16	2.38	-3.43	-0.13	2.60	-3.85	-0.10
42	2.75	-3.95	-0.08	3.00	-4.47	-0.13	2.83	-4.10	-0.09	3.16	-4.39	-0.06
43	3.35	-4.70	-0.08	2.33	-3.46	-0.10	2.13	-3.15	-0.12	3.06	-4.31	-0.06
44	3.01	-4.19	-0.07	2.47	-3.50	-0.09	2.68	-3.91	-0.12	2.37	-3.30	-0.04
45	2.53	-3.73	-0.08	1.88	-2.96	-0.11	2.47	-3.61	-0.11	1.85	-2.82	-0.05
46	2.64	-3.74	-0.09	2.10	-3.10	-0.11	2.71	-3.87	-0.12	2.10	-3.05	-0.05

47	3.04	-4.36	-0.08	2.27	-3.43	-0.12	2.66	-3.90	-0.09	1.71	-2.54	-0.05
48	2.19	-3.02	-0.08	2.00	-2.99	-0.11	2.80	-4.11	-0.12	2.74	-4.02	-0.05
49	1.79	-2.67	-0.08	2.18	-3.12	-0.13	2.41	-3.61	-0.11	2.38	-3.33	-0.06
50	2.22	-3.08	-0.08	3.29	-4.76	-0.11	2.84	-4.15	-0.11	2.94	-4.30	-0.05
51	2.81	-3.91	-0.08	2.23	-3.15	-0.11	2.41	-3.51	-0.11	2.83	-4.06	-0.05
52	2.24	-3.05	-0.09	2.92	-4.02	-0.14	2.63	-3.63	-0.09	2.84	-4.00	-0.06
53	2.46	-3.60	-0.11	2.55	-3.77	-0.16	2.14	-3.21	-0.12	2.60	-3.73	-0.10
54	2.36	-3.40	-0.06	2.51	-3.50	-0.10	2.40	-3.38	-0.11	1.94	-2.87	-0.06
55	3.26	-4.65	-0.08	2.41	-3.58	-0.12	2.19	-3.30	-0.11	1.90	-2.62	-0.06
56	2.56	-3.57	-0.09	2.40	-3.72	-0.16	2.17	-3.20	-0.07	2.29	-3.21	-0.06
57	2.50	-3.51	-0.08	1.94	-2.90	-0.15	2.19	-3.09	-0.08	2.07	-2.96	-0.07
58	2.04	-2.86	-0.09	3.05	-4.40	-0.13	2.64	-3.81	-0.09	2.80	-4.06	-0.06
59	3.20	-4.47	-0.07	2.26	-3.32	-0.11	2.58	-3.63	-0.11	2.49	-3.56	-0.05
60	2.52	-3.47	-0.08	2.57	-3.76	-0.12	2.52	-3.64	-0.09	2.52	-3.58	-0.06
61	2.68	-3.60	-0.07	2.69	-3.95	-0.11	2.53	-3.62	-0.11	2.74	-4.06	-0.06
62	2.34	-3.36	-0.08	2.44	-3.57	-0.12	2.47	-3.67	-0.10	2.50	-3.54	-0.05
63	3.26	-4.49	-0.07	2.29	-3.30	-0.12	1.93	-2.78	-0.09	2.55	-3.69	-0.06
64	2.59	-3.74	-0.08	3.05	-4.37	-0.11	2.09	-3.10	-0.09	2.21	-3.27	-0.04
65	2.10	-3.06	-0.09	1.74	-2.58	-0.13	2.17	-3.22	-0.10	1.73	-2.41	-0.05
66	1.84	-2.75	-0.09	2.08	-3.06	-0.15	2.20	-3.19	-0.09	2.13	-2.99	-0.07
67	2.76	-3.82	-0.08	1.73	-2.47	-0.15	1.83	-2.74	-0.08	2.28	-3.23	-0.06
68	1.74	-2.60	-0.08	1.66	-2.64	-0.13	1.76	-2.53	-0.08	2.03	-3.05	-0.06
69	2.16	-3.06	-0.08	2.04	-2.90	-0.16	1.88	-2.68	-0.08	2.49	-3.40	-0.07
70	1.73	-2.48	-0.09	1.93	-2.86	-0.14	1.67	-2.45	-0.09	2.30	-3.31	-0.06
71	2.84	-3.91	-0.07	1.93	-2.93	-0.11	1.72	-2.60	-0.11	2.42	-3.44	-0.05
72	1.24	-1.94	-0.09	1.49	-2.21	-0.13	1.28	-1.81	-0.10	1.49	-1.95	-0.06
73	2.25	-3.32	-0.08	2.08	-3.09	-0.12	2.12	-2.99	-0.11	1.57	-2.30	-0.05
74	1.85	-2.89	-0.30	1.69	-2.73	-0.30	2.50	-3.66	-0.31	1.65	-2.60	-0.30
75	2.63	-4.02	-0.36	2.36	-3.79	-0.36	2.15	-3.52	-0.35	2.06	-3.32	-0.35
76	1.57	-2.54	-0.28	1.36	-2.17	-0.27	1.79	-2.93	-0.26	1.75	-2.89	-0.26
77	2.45	-3.63	-0.27	1.97	-3.22	-0.25	2.63	-3.95	-0.27	2.30	-3.71	-0.26
78	2.11	-2.95	-0.14	2.66	-3.81	-0.14	2.22	-3.21	-0.09	2.61	-3.73	-0.05
79	2.61	-3.59	-0.14	2.00	-2.89	-0.13	1.94	-2.93	-0.10	2.43	-3.42	-0.05
80	1.69	-1.88	0.37	1.09	-1.58	-0.13	1.50	-2.17	-0.11	1.63	-2.41	-0.04
81	1.84	-2.79	-0.11	1.75	-2.65	-0.11	1.92	-2.91	-0.10	1.61	-2.33	-0.04

Table B-6. Comparison of external and internal pressure coefficients without and with VSVs for the small gable roof model at 75° wind direction

	Without VSVs			With VSVs			With VSVs and Leakage			With VSVs, Leakage and Opening		
Tap No.	**Cp Max**	**Cp Min**	**Cp Mean**	**Cp Max**	**Cp Min**	**Cp Mean**	**Cp Max**	**Cp Min**	**Cp Mean**	**Cp Max**	**Cp Min**	**Cp Mean**
1	1.93	-2.96	-0.11	2.45	-3.43	-0.10	2.49	-3.50	-0.08	2.44	-3.60	-0.09
2	2.63	-3.98	-0.12	2.54	-3.69	-0.11	3.02	-4.46	-0.10	2.51	-3.61	-0.11
3	2.92	-4.09	-0.12	2.50	-3.65	-0.09	3.36	-4.72	-0.10	2.99	-4.29	-0.10
4	2.86	-4.30	-0.20	2.58	-3.64	-0.18	2.50	-3.53	-0.18	2.88	-4.19	-0.18
5	2.52	-3.70	-0.23	2.39	-3.80	-0.21	2.43	-4.04	-0.20	1.82	-2.82	-0.21
6	2.46	-3.90	-0.32	2.44	-3.59	-0.31	2.82	-4.35	-0.30	1.97	-3.26	-0.29
7	2.81	-3.80	-0.10	2.69	-3.79	-0.09	2.80	-4.04	-0.10	2.82	-4.20	-0.10
8	2.10	-3.07	-0.07	2.54	-3.65	-0.07	2.93	-4.10	-0.06	2.99	-4.50	-0.06
9	2.50	-3.50	-0.12	2.34	-3.24	-0.11	2.43	-3.82	-0.10	2.36	-3.32	-0.10
10	2.28	-3.68	-0.25	2.21	-3.63	-0.23	2.94	-4.58	-0.24	2.55	-4.21	-0.25
11	2.53	-3.92	-0.30	1.76	-2.72	-0.28	2.45	-4.06	-0.27	2.89	-4.14	-0.28
12	2.86	-4.45	-0.32	2.48	-3.80	-0.31	2.45	-3.78	-0.29	2.66	-4.28	-0.30
13	2.43	-3.52	-0.10	2.89	-4.01	-0.09	3.10	-4.26	-0.08	1.86	-2.77	-0.09
14	2.71	-3.89	-0.11	2.69	-3.88	-0.09	3.19	-4.63	-0.09	2.86	-4.23	-0.09
15	2.68	-3.72	-0.19	1.99	-3.57	-0.18	2.76	-4.11	-0.18	2.41	-3.52	-0.19
16	2.59	-3.78	-0.38	2.41	-3.67	-0.36	2.45	-3.63	-0.34	2.85	-4.07	-0.36
17	2.20	-3.65	-0.38	2.39	-3.79	-0.37	2.53	-4.05	-0.36	2.31	-3.36	-0.36
18	2.64	-4.07	-0.40	2.25	-3.78	-0.39	2.71	-4.13	-0.37	2.32	-3.66	-0.38
19	2.66	-4.07	-0.22	2.34	-3.39	-0.21	3.06	-4.71	-0.21	3.00	-4.46	-0.23
20	2.88	-4.24	-0.16	2.58	-3.94	-0.15	2.53	-3.55	-0.15	2.61	-3.85	-0.16
21	2.39	-4.03	-0.45	2.83	-4.15	-0.44	2.19	-3.95	-0.43	2.41	-3.74	-0.45
22	2.16	-3.56	-0.55	2.02	-3.45	-0.56	2.36	-3.83	-0.53	2.46	-3.16	-0.52
23	2.36	-4.34	-0.49	2.36	-3.88	-0.49	2.59	-4.46	-0.48	2.88	-4.40	-0.47
24	2.20	-4.00	-0.48	2.77	-5.08	-0.49	1.72	-3.41	-0.44	2.38	-3.99	-0.45
25	2.45	-3.81	-0.42	1.79	-2.80	-0.42	2.34	-3.74	-0.42	2.02	-3.56	-0.43
26	3.00	-4.44	-0.67	2.60	-4.18	-0.69	2.45	-4.28	-0.70	3.13	-4.15	-0.73
27	2.29	-4.23	-0.76	2.09	-3.81	-0.77	2.12	-4.12	-0.75	2.53	-4.36	-0.75
28	2.00	-3.89	-0.68	2.19	-3.94	-0.71	2.80	-4.51	-0.70	2.63	-4.44	-0.67
29	2.10	-3.77	-0.76	2.09	-3.20	-0.77	2.29	-4.32	-0.77	1.75	-3.71	-0.77
30	2.26	-4.05	-0.64	2.60	-4.06	-0.65	2.42	-4.67	-0.61	2.39	-4.70	-0.59
31	2.11	-3.48	-0.32	2.08	-3.61	-0.31	2.71	-3.96	-0.31	2.35	-3.70	-0.29
32	2.50	-3.91	-0.26	2.82	-4.32	-0.28	3.42	-5.14	-0.25	2.98	-4.47	-0.21
33	2.68	-4.17	-0.12	2.41	-3.42	-0.08	2.81	-4.20	-0.12	2.40	-3.35	-0.07
34	2.75	-4.02	-0.07	2.67	-3.68	-0.18	2.66	-4.10	-0.19	1.99	-3.02	-0.17
35	2.79	-4.39	-0.23	2.43	-3.54	-0.22	2.84	-4.41	-0.25	2.93	-4.46	-0.26
36	3.48	-3.89	0.70	3.49	-3.72	0.71	3.44	-3.83	0.69	3.24	-3.65	0.72
37	2.67	-4.14	-0.32	2.34	-3.71	-0.33	2.23	-3.63	-0.32	1.91	-3.01	-0.30
38	3.01	-4.38	-0.15	2.70	-4.02	-0.16	2.84	-4.20	-0.14	2.56	-3.56	-0.15
39	2.39	-3.64	-0.21	2.30	-3.53	-0.25	2.77	-4.31	-0.20	2.68	-4.04	-0.12
40	2.59	-3.99	-0.22	2.61	-3.93	-0.25	2.66	-4.13	-0.19	2.82	-4.30	-0.13
41	2.93	-4.20	-0.23	2.88	-4.13	-0.26	2.79	-4.03	-0.22	2.58	-3.96	-0.16
42	2.83	-4.36	-0.21	2.93	-4.36	-0.24	2.89	-4.13	-0.19	2.92	-4.38	-0.13
43	2.62	-3.72	-0.21	2.30	-3.45	-0.23	3.28	-4.85	-0.18	3.06	-4.48	-0.13
44	3.13	-4.72	-0.20	2.93	-4.38	-0.22	3.29	-4.87	-0.18	3.03	-4.35	-0.13

45	2.60	-3.85	-0.21	2.56	-3.87	-0.23	2.60	-4.02	-0.19	2.87	-4.14	-0.12
46	2.75	-3.97	-0.21	2.64	-3.99	-0.23	3.41	-5.00	-0.19	3.13	-4.41	-0.13
47	2.71	-4.17	-0.20	2.47	-3.85	-0.24	3.11	-4.58	-0.19	3.26	-4.64	-0.12
48	3.42	-4.78	-0.22	2.09	-3.08	-0.23	2.94	-4.47	-0.18	2.80	-3.95	-0.13
49	2.38	-3.70	-0.21	2.57	-3.78	-0.24	2.66	-3.84	-0.19	2.24	-3.37	-0.13
50	2.79	-4.23	-0.21	2.58	-3.91	-0.23	2.93	-4.26	-0.19	2.35	-3.41	-0.12
51	2.37	-3.62	-0.28	2.32	-3.53	-0.30	2.48	-3.87	-0.27	2.83	-4.51	-0.22
52	2.38	-3.58	-0.21	2.68	-4.02	-0.25	2.38	-3.56	-0.18	2.84	-4.27	-0.13
53	2.42	-3.63	-0.21	2.36	-3.71	-0.25	2.86	-4.23	-0.21	2.18	-3.30	-0.14
54	2.82	-4.33	-0.20	2.77	-4.12	-0.23	3.21	-4.89	-0.19	2.96	-4.31	-0.13
55	2.59	-3.99	-0.21	2.69	-4.06	-0.24	2.81	-4.31	-0.18	2.94	-4.16	-0.13
56	2.27	-3.64	-0.21	2.77	-4.28	-0.27	2.35	-3.48	-0.18	2.34	-3.50	-0.12
57	2.12	-3.27	-0.21	2.27	-3.58	-0.26	2.59	-3.77	-0.19	2.37	-3.54	-0.13
58	2.38	-3.54	-0.21	2.85	-4.34	-0.25	2.38	-3.57	-0.20	2.34	-3.54	-0.13
59	2.34	-3.60	-0.20	2.39	-3.73	-0.23	2.05	-3.13	-0.18	3.30	-4.69	-0.12
60	2.58	-3.97	-0.21	2.44	-3.73	-0.24	2.56	-3.72	-0.17	2.46	-3.49	-0.13
61	2.51	-3.96	-0.20	2.36	-3.63	-0.23	3.04	-4.68	-0.19	2.16	-3.10	-0.13
62	2.72	-3.99	-0.21	2.69	-4.05	-0.24	2.85	-4.23	-0.19	2.82	-3.99	-0.12
63	2.46	-3.65	-0.20	2.57	-3.99	-0.24	2.68	-3.89	-0.18	3.30	-4.79	-0.12
64	2.92	-4.38	-0.21	2.53	-3.82	-0.24	2.65	-4.11	-0.21	2.15	-3.22	-0.11
65	1.87	-2.96	-0.22	1.96	-3.12	-0.24	2.11	-3.25	-0.19	2.13	-3.12	-0.12
66	2.09	-3.18	-0.21	1.94	-3.14	-0.25	2.36	-3.44	-0.20	2.19	-3.20	-0.14
67	2.23	-3.41	-0.20	2.02	-3.20	-0.25	2.67	-4.05	-0.20	2.65	-3.73	-0.14
68	2.13	-3.36	-0.20	1.81	-2.83	-0.25	1.90	-3.00	-0.21	2.05	-3.22	-0.13
69	2.26	-3.43	-0.20	2.08	-3.19	-0.26	2.33	-3.62	-0.20	1.84	-2.69	-0.14
70	2.31	-3.38	-0.22	2.14	-3.40	-0.26	2.47	-3.88	-0.21	2.13	-3.21	-0.14
71	2.33	-3.42	-0.21	2.36	-3.63	-0.23	2.88	-4.13	-0.20	3.35	-4.82	-0.12
72	1.37	-2.16	-0.22	1.45	-2.39	-0.25	1.55	-2.63	-0.22	1.72	-2.55	-0.10
73	2.17	-3.29	-0.21	2.22	-3.31	-0.24	2.40	-3.51	-0.20	1.52	-2.41	-0.11
74	2.11	-3.30	-0.36	2.15	-3.61	-0.36	2.40	-3.93	-0.37	2.00	-3.12	-0.34
75	2.06	-3.94	-0.40	1.83	-2.58	-0.41	2.56	-4.30	-0.40	2.36	-3.78	-0.39
76	1.93	-3.02	-0.27	1.68	-2.66	-0.28	1.74	-2.74	-0.27	1.65	-2.68	-0.25
77	2.55	-3.87	-0.27	2.71	-3.92	-0.27	2.72	-3.90	-0.26	1.79	-2.74	-0.24
78	1.93	-3.77	-0.65	2.00	-3.54	-0.65	2.42	-4.40	-0.65	2.20	-3.66	-0.66
79	2.17	-3.76	-0.64	1.83	-3.53	-0.64	2.51	-4.21	-0.64	1.92	-3.61	-0.63
80	1.90	-2.19	0.00	1.46	-2.46	-0.26	1.40	-2.41	-0.20	1.56	-2.31	-0.14
81	2.20	-3.40	-0.24	2.66	-3.88	-0.23	2.27	-3.52	-0.19	2.07	-3.20	-0.11

Table B-7. Comparison of external and internal pressure coefficients without and with VSVs for the small gable roof model at 90° wind direction

	Without VSVs			With VSVs			With VSVs and Leakage			With VSVs, Leakage and Opening		
Tap No.	**Cp Max**	**Cp Min**	**Cp Mean**	**Cp Max**	**Cp Min**	**Cp Mean**	**Cp Max**	**Cp Min**	**Cp Mean**	**Cp Max**	**Cp Min**	**Cp Mean**
1	1.88	-2.81	-0.21	1.79	-2.59	-0.20	1.81	-3.15	-0.20	1.73	-2.60	-0.20
2	1.81	-2.73	-0.16	1.90	-2.84	-0.13	1.85	-2.77	-0.14	2.03	-3.08	-0.14
3	2.16	-2.89	-0.11	2.07	-2.85	-0.08	2.42	-3.41	-0.11	2.01	-3.09	-0.10
4	2.43	-3.74	-0.11	2.14	-3.32	-0.09	2.55	-3.89	-0.11	1.81	-2.98	-0.11
5	2.26	-3.40	-0.13	1.98	-2.73	-0.09	2.26	-3.07	-0.11	2.24	-3.65	-0.11
6	2.47	-3.81	-0.20	2.09	-2.98	-0.17	2.30	-3.83	-0.18	2.03	-3.04	-0.17
7	2.58	-3.45	-0.23	1.78	-3.11	-0.21	2.05	-3.34	-0.24	1.81	-3.05	-0.23
8	1.99	-3.31	-0.18	2.33	-3.60	-0.18	1.98	-3.32	-0.18	1.91	-3.08	-0.18
9	2.22	-3.69	-0.18	1.83	-2.99	-0.17	2.09	-3.20	-0.17	1.97	-2.96	-0.17
10	2.55	-3.48	-0.17	2.28	-3.61	-0.14	2.46	-4.08	-0.17	2.24	-3.24	-0.17
11	2.56	-3.61	-0.20	2.37	-3.60	-0.16	1.53	-3.01	-0.18	1.44	-2.35	-0.19
12	2.59	-4.00	-0.22	1.86	-3.00	-0.18	2.20	-3.05	-0.19	2.10	-3.37	-0.20
13	1.97	-3.44	-0.34	1.98	-3.14	-0.31	2.08	-3.46	-0.33	1.71	-3.13	-0.33
14	2.42	-4.09	-0.30	2.18	-2.87	-0.27	1.80	-2.89	-0.28	1.90	-3.15	-0.28
15	2.56	-4.09	-0.33	1.95	-3.06	-0.32	2.65	-4.03	-0.33	1.87	-2.79	-0.33
16	2.50	-3.70	-0.35	2.31	-3.50	-0.31	2.53	-3.43	-0.33	2.14	-3.24	-0.32
17	2.30	-4.05	-0.30	2.09	-3.50	-0.28	1.66	-3.48	-0.29	1.86	-3.21	-0.29
18	2.14	-3.79	-0.34	1.91	-3.42	-0.31	2.55	-3.48	-0.33	2.05	-3.53	-0.34
19	1.89	-3.42	-0.50	1.88	-3.84	-0.47	1.69	-3.56	-0.47	2.07	-3.41	-0.48
20	2.78	-4.47	-0.50	1.97	-3.67	-0.47	2.00	-3.33	-0.46	1.90	-3.20	-0.47
21	1.80	-3.08	-0.62	2.01	-3.70	-0.61	2.07	-2.90	-0.60	2.28	-3.62	-0.61
22	2.04	-3.81	-0.60	2.41	-3.83	-0.62	2.41	-3.47	-0.60	1.83	-3.33	-0.59
23	2.19	-3.45	-0.47	2.11	-3.47	-0.45	2.37	-2.91	-0.48	1.89	-3.39	-0.46
24	1.86	-3.23	-0.44	2.24	-4.26	-0.42	2.51	-4.06	-0.41	2.18	-3.74	-0.41
25	2.02	-3.32	-0.58	2.07	-3.27	-0.53	1.82	-3.61	-0.53	1.49	-3.53	-0.53
26	1.78	-3.71	-0.97	2.15	-3.70	-0.97	1.86	-3.63	-0.98	2.09	-3.87	-0.96
27	1.93	-3.43	-0.81	1.72	-3.34	-0.80	2.29	-4.15	-0.79	1.27	-2.78	-0.79
28	2.64	-5.09	-0.84	2.07	-4.35	-0.87	1.75	-3.21	-0.82	1.89	-3.92	-0.83
29	2.12	-4.06	-1.03	1.89	-3.68	-1.03	2.12	-3.61	-1.01	2.42	-3.57	-1.01
30	2.65	-4.26	-0.60	1.82	-3.36	-0.61	1.71	-3.35	-0.60	2.18	-4.32	-0.58
31	1.77	-3.18	-0.37	1.71	-3.26	-0.33	1.98	-3.39	-0.36	2.02	-3.67	-0.35
32	2.11	-3.53	-0.37	2.05	-3.57	-0.37	2.01	-3.37	-0.36	1.99	-3.30	-0.34
33	1.75	-2.75	-0.26	2.31	-3.56	-0.17	1.90	-2.95	-0.15	1.93	-2.95	-0.12
34	2.56	-4.14	-0.37	2.45	-3.98	-0.33	1.94	-3.09	-0.26	2.32	-3.65	-0.27
35	2.25	-4.00	-0.51	1.74	-3.27	-0.46	2.45	-4.22	-0.47	1.92	-3.49	-0.48
36	3.52	-4.15	0.73	3.10	-3.36	0.75	3.12	-3.36	0.73	3.26	-3.61	0.74
37	2.43	-4.35	-0.50	2.45	-3.97	-0.47	1.86	-3.47	-0.51	2.08	-3.51	-0.49
38	2.98	-4.27	-0.13	2.84	-4.26	-0.14	2.24	-3.41	-0.12	2.17	-3.20	-0.13
39	2.62	-4.14	-0.30	2.49	-3.82	-0.28	1.87	-3.02	-0.25	2.24	-3.44	-0.20
40	2.72	-4.21	-0.30	2.50	-3.97	-0.26	2.30	-3.60	-0.22	2.46	-3.66	-0.18
41	2.14	-3.42	-0.29	2.20	-3.45	-0.27	2.17	-3.41	-0.24	2.01	-3.13	-0.20
42	2.93	-4.53	-0.28	2.71	-4.33	-0.26	2.54	-3.97	-0.22	2.18	-3.27	-0.17
43	2.45	-3.86	-0.29	2.31	-3.51	-0.24	2.30	-3.72	-0.22	2.16	-3.35	-0.18
44	3.23	-4.94	-0.29	2.68	-3.99	-0.22	2.61	-4.08	-0.22	3.04	-4.52	-0.17

45	2.47	-3.89	-0.29	2.16	-3.48	-0.25	2.20	-3.46	-0.22	2.41	-3.67	-0.17
46	3.08	-4.76	-0.29	2.65	-4.03	-0.24	2.89	-4.42	-0.22	2.85	-4.22	-0.17
47	2.75	-4.33	-0.28	1.76	-2.79	-0.26	2.22	-3.60	-0.22	2.31	-3.52	-0.17
48	2.81	-4.39	-0.30	2.23	-3.53	-0.25	2.66	-3.93	-0.22	2.16	-3.37	-0.18
49	2.34	-3.60	-0.29	2.19	-3.34	-0.26	2.25	-3.41	-0.22	2.15	-3.30	-0.18
50	2.99	-4.59	-0.29	2.77	-4.36	-0.24	2.51	-3.81	-0.23	2.28	-3.45	-0.17
51	2.25	-3.51	-0.32	2.52	-3.90	-0.27	2.05	-3.30	-0.25	1.86	-2.93	-0.21
52	2.48	-3.89	-0.28	2.23	-3.51	-0.27	2.47	-3.84	-0.20	2.35	-3.54	-0.18
53	2.17	-3.55	-0.28	2.38	-3.76	-0.29	1.51	-2.48	-0.25	1.85	-2.88	-0.21
54	2.43	-3.80	-0.28	2.84	-4.34	-0.24	2.37	-3.75	-0.22	2.23	-3.47	-0.18
55	3.25	-5.03	-0.29	2.36	-3.67	-0.25	1.85	-2.90	-0.21	2.33	-3.57	-0.18
56	2.39	-3.73	-0.27	1.69	-2.84	-0.30	2.61	-4.04	-0.20	1.91	-2.95	-0.17
57	2.44	-3.73	-0.27	2.30	-3.70	-0.28	2.01	-3.11	-0.21	1.59	-2.49	-0.18
58	2.47	-3.95	-0.29	2.20	-3.56	-0.27	2.42	-3.67	-0.22	2.25	-3.45	-0.18
59	2.88	-4.61	-0.28	1.91	-3.09	-0.25	2.02	-3.22	-0.22	1.88	-2.79	-0.17
60	2.40	-3.74	-0.29	3.05	-4.70	-0.26	2.58	-4.01	-0.21	2.51	-3.83	-0.18
61	2.28	-3.71	-0.29	2.15	-3.40	-0.24	2.04	-3.18	-0.22	1.95	-3.13	-0.18
62	2.66	-4.12	-0.28	2.48	-3.83	-0.25	2.75	-4.22	-0.22	2.56	-3.81	-0.17
63	2.51	-3.95	-0.28	2.60	-4.05	-0.25	2.14	-3.44	-0.21	1.89	-3.04	-0.17
64	2.63	-4.12	-0.28	2.40	-3.71	-0.25	2.18	-3.31	-0.23	2.46	-3.73	-0.17
65	2.28	-3.65	-0.29	1.67	-2.77	-0.27	1.88	-2.98	-0.22	1.73	-2.68	-0.18
66	1.73	-2.88	-0.28	1.47	-2.55	-0.27	1.49	-2.48	-0.23	1.55	-2.40	-0.18
67	2.06	-3.35	-0.28	1.78	-2.96	-0.27	2.13	-3.31	-0.23	1.76	-2.69	-0.17
68	1.68	-2.65	-0.25	1.62	-2.70	-0.27	1.99	-3.13	-0.24	1.54	-2.39	-0.19
69	1.81	-2.87	-0.28	1.64	-2.81	-0.28	1.87	-2.96	-0.24	1.93	-3.02	-0.17
70	1.93	-3.06	-0.29	1.50	-2.49	-0.28	1.93	-3.10	-0.23	1.55	-2.36	-0.18
71	1.74	-2.88	-0.27	1.86	-2.97	-0.25	2.24	-3.62	-0.22	1.81	-2.83	-0.19
72	1.53	-2.21	-0.29	1.35	-2.05	-0.27	1.37	-2.00	-0.25	1.45	-1.94	-0.19
73	2.28	-3.58	-0.28	2.08	-3.32	-0.26	2.01	-3.07	-0.22	1.74	-2.61	-0.17
74	2.05	-3.11	-0.36	1.94	-3.43	-0.34	2.13	-3.36	-0.36	2.03	-2.85	-0.36
75	2.09	-3.49	-0.38	2.03	-3.67	-0.37	1.29	-2.23	-0.36	1.61	-2.43	-0.36
76	1.70	-2.89	-0.41	1.50	-2.77	-0.40	1.47	-2.75	-0.43	1.33	-2.48	-0.40
77	1.81	-2.94	-0.38	1.99	-3.48	-0.38	1.96	-3.05	-0.39	1.63	-3.02	-0.39
78	2.05	-3.52	-0.41	1.90	-3.23	-0.39	1.44	-2.74	-0.37	1.71	-2.82	-0.37
79	2.30	-3.88	-0.43	2.32	-3.79	-0.41	2.28	-4.08	-0.38	1.38	-2.45	-0.39
80	1.35	-1.97	-0.39	1.28	-2.06	-0.38	1.37	-2.27	-0.37	1.36	-1.87	-0.34
81	2.25	-3.51	-0.36	1.66	-2.81	-0.37	1.54	-2.96	-0.35	1.29	-2.19	-0.35

Table B-8. Comparison of external and internal pressure coefficients without and with VSVs for the small hip roof model at 0° wind direction

	Without VSVs			With VSVs			With VSVs and Leakage			With VSVs, Leakage and Opening		
Tap No.	**Cp Max**	**Cp Min**	**Cp Mean**	**Cp Max**	**Cp Min**	**Cp Mean**	**Cp Max**	**Cp Min**	**Cp Mean**	**Cp Max**	**Cp Min**	**Cp Mean**
1	2.55	-3.84	-0.40	2.22	-3.64	-0.39	2.01	-3.20	-0.40	2.32	-4.20	-0.40
2	2.01	-3.37	-0.38	2.75	-4.54	-0.36	2.04	-3.06	-0.38	3.02	-4.69	-0.38
3	2.75	-4.31	-0.41	2.74	-4.18	-0.40	2.53	-3.86	-0.44	2.69	-4.07	-0.42
4	2.38	-3.59	-0.28	3.25	-4.81	-0.28	2.60	-3.94	-0.30	2.82	-4.28	-0.29
5	1.78	-2.76	-0.25	2.53	-3.89	-0.22	2.70	-4.18	-0.27	2.61	-3.78	-0.25
6	2.03	-3.93	-1.12	2.26	-4.57	-1.10	3.08	-4.93	-1.12	2.37	-4.99	-1.12
7	2.29	-3.98	-0.39	2.64	-4.03	-0.37	2.57	-3.89	-0.39	2.40	-3.78	-0.38
8	2.66	-4.18	-0.35	2.96	-4.68	-0.34	2.92	-4.49	-0.36	3.28	-4.97	-0.36
9	2.25	-3.40	-0.32	2.56	-3.95	-0.32	2.47	-3.70	-0.33	2.54	-3.82	-0.32
10	1.90	-2.99	-0.20	2.92	-4.61	-0.17	3.01	-4.17	-0.21	2.62	-3.76	-0.18
11	2.38	-4.07	-0.98	2.35	-4.08	-0.98	2.44	-4.44	-0.99	2.66	-4.59	-1.00
12	2.79	-4.47	-0.72	2.38	-4.10	-0.70	3.51	-4.86	-0.74	3.03	-5.08	-0.76
13	1.79	-3.18	-0.53	2.23	-3.88	-0.51	2.46	-3.99	-0.53	2.37	-4.13	-0.51
14	2.60	-4.02	-0.25	2.42	-3.67	-0.23	2.56	-3.70	-0.25	2.98	-4.52	-0.24
15	2.57	-3.66	-0.22	2.02	-3.22	-0.21	2.40	-3.70	-0.23	2.72	-4.12	-0.22
16	3.30	-4.88	-0.99	3.10	-4.71	-0.98	2.92	-4.00	-1.00	2.31	-4.23	-1.01
17	2.32	-3.72	-0.62	3.01	-4.24	-0.61	3.14	-4.09	-0.63	2.46	-4.14	-0.65
18	2.24	-3.42	-0.25	3.14	-4.64	-0.23	2.99	-4.22	-0.26	3.16	-4.57	-0.24
19	2.41	-3.98	-0.53	2.89	-4.77	-0.53	2.13	-3.62	-0.55	2.91	-4.80	-0.52
20	2.41	-4.07	-0.65	2.28	-3.99	-0.64	2.21	-3.99	-0.65	2.83	-4.71	-0.63
21	2.04	-3.45	-0.39	2.56	-3.95	-0.38	2.35	-3.96	-0.40	2.72	-4.35	-0.39
22	1.94	-3.05	-0.21	3.00	-4.24	-0.20	2.27	-3.31	-0.20	2.56	-3.82	-0.21
23	2.90	-4.06	-0.17	2.72	-3.95	-0.16	2.80	-4.18	-0.19	2.90	-4.13	-0.18
24	2.59	-4.58	-0.97	2.19	-4.81	-0.96	2.67	-4.60	-0.96	2.54	-4.03	-0.98
25	2.75	-3.32	-0.68	3.20	-4.56	-0.67	2.65	-3.83	-0.71	3.35	-5.07	-0.71
26	2.49	-3.96	-0.42	3.13	-4.65	-0.42	2.95	-4.59	-0.44	2.70	-4.47	-0.43
27	2.84	-4.35	-0.29	3.14	-4.71	-0.28	2.66	-4.00	-0.30	3.23	-4.79	-0.28
28	2.51	-3.97	-0.21	2.78	-3.83	-0.22	2.67	-4.05	-0.21	2.24	-3.46	-0.22
29	2.17	-4.25	-1.13	2.42	-4.06	-1.13	2.18	-4.08	-1.15	1.93	-5.12	-1.15
30	2.70	-4.24	-0.37	2.50	-4.08	-0.38	2.85	-4.35	-0.38	3.00	-4.73	-0.38
31	2.76	-3.96	-0.32	2.70	-4.23	-0.32	2.66	-4.00	-0.34	2.39	-3.50	-0.31
32	3.37	-5.13	-0.37	2.55	-4.00	-0.36	2.27	-3.62	-0.39	3.15	-4.90	-0.39
33	2.44	-3.70	-0.17	2.81	-3.84	-0.18	2.60	-3.82	-0.21	3.38	-4.69	-0.19
34	2.10	-3.26	-0.38	3.19	-4.75	-0.38	2.20	-3.75	-0.43	2.80	-4.05	-0.39
35	2.80	-4.28	-0.39	2.86	-4.61	-0.39	2.01	-3.29	-0.42	3.22	-4.94	-0.39
36	2.98	-4.50	-0.32	3.30	-4.72	-0.31	2.39	-3.69	-0.32	3.00	-4.62	-0.31
37	2.13	-3.11	-0.28	2.88	-4.31	-0.29	2.48	-3.85	-0.31	3.00	-4.29	-0.29
38	2.53	-3.76	-0.24	2.57	-3.93	-0.24	2.99	-4.23	-0.23	3.29	-4.65	-0.24
39	2.34	-3.97	-0.66	2.85	-4.81	-0.66	2.48	-4.36	-0.67	3.28	-5.09	-0.67
40	2.55	-4.57	-0.67	3.45	-5.44	-0.66	2.25	-4.01	-0.68	2.82	-4.76	-0.66
41	2.18	-3.36	-0.20	2.68	-3.88	-0.17	2.20	-3.32	-0.19	3.08	-4.43	-0.16
42	2.87	-3.98	-0.11	2.96	-4.38	-0.12	2.74	-3.89	-0.14	3.34	-4.75	-0.12
43	2.63	-4.10	-0.34	2.63	-3.96	-0.34	3.02	-4.54	-0.40	3.00	-4.54	-0.33
44	2.98	-4.59	-0.40	2.51	-4.53	-0.40	2.80	-4.30	-0.47	3.23	-4.96	-0.39
45	2.36	-2.57	0.68	2.81	-2.90	0.63	3.27	-3.47	0.59	3.01	-3.34	0.62
46	2.66	-3.70	0.08	3.22	-3.34	0.63	3.17	-3.60	0.59	3.93	-4.55	0.62

47	2.53	-4.20	-0.42	2.38	-3.91	-0.40	2.54	-3.84	-0.39	3.08	-4.61	-0.39
48	3.08	-4.65	-0.38	2.13	-3.46	-0.34	2.82	-4.03	-0.35	2.90	-4.36	-0.34
49	2.41	-2.28	0.71	3.79	-4.19	0.73	2.98	-3.44	0.71	2.82	-2.80	0.73
50	2.26	-3.74	-0.44	2.78	-4.39	-0.45	2.86	-4.49	-0.52	2.80	-4.51	-0.45
51	2.34	-3.68	-0.31	2.81	-4.40	-0.31	2.95	-4.62	-0.34	2.17	-3.48	-0.31
52	2.63	-3.85	-0.13	2.58	-3.87	-0.21	2.09	-3.06	-0.20	2.78	-3.99	-0.19
53	2.20	-3.29	-0.12	2.86	-4.17	-0.21	2.52	-3.78	-0.20	2.80	-4.04	-0.20
54	2.58	-3.92	-0.11	3.22	-4.82	-0.20	2.80	-4.11	-0.23	3.05	-4.35	-0.20
55	2.84	-4.12	-0.21	2.52	-3.62	-0.24	2.63	-3.84	-0.26	2.82	-4.22	-0.24
56	2.77	-3.98	-0.09	2.30	-3.60	-0.22	3.04	-4.50	-0.18	2.83	-4.12	-0.20
57	2.09	-3.01	-0.12	2.71	-3.97	-0.18	2.22	-3.26	-0.17	2.69	-4.00	-0.18
58	2.28	-3.28	-0.12	2.49	-3.52	-0.20	2.56	-3.78	-0.21	2.98	-4.45	-0.20
59	2.78	-4.04	-0.12	2.49	-3.75	-0.21	2.45	-3.60	-0.23	2.78	-4.08	-0.20
60	3.10	-4.48	-0.12	2.94	-4.33	-0.21	2.46	-3.68	-0.23	2.75	-3.93	-0.19
61	2.50	-3.62	-0.12	3.01	-4.30	-0.20	2.88	-4.25	-0.23	2.95	-4.28	-0.19
62	2.64	-3.79	-0.12	2.87	-4.31	-0.20	2.95	-4.22	-0.22	2.95	-4.29	-0.20
63	2.61	-3.98	-0.12	3.06	-4.30	-0.20	2.58	-3.64	-0.21	2.45	-3.60	-0.18
64	2.88	-4.32	-0.10	2.78	-4.18	-0.19	2.40	-3.58	-0.22	3.33	-4.72	-0.20
65	2.12	-2.91	-0.12	2.27	-3.32	-0.22	1.98	-3.08	-0.22	2.02	-2.93	-0.20
66	1.52	-2.32	-0.13	2.50	-3.63	-0.20	1.90	-2.90	-0.21	2.42	-3.56	-0.19
67	2.44	-3.47	-0.10	2.48	-3.79	-0.19	2.35	-3.41	-0.22	2.13	-3.29	-0.19
68	1.94	-2.91	-0.11	2.29	-3.46	-0.21	1.59	-2.42	-0.20	1.98	-3.11	-0.21
69	1.75	-2.42	-0.05	2.28	-3.40	-0.18	1.87	-2.73	-0.22	2.32	-3.49	-0.20
70	2.09	-2.99	-0.12	2.18	-3.27	-0.20	2.23	-3.23	-0.21	2.33	-3.44	-0.20
71	2.33	-3.68	-0.29	2.60	-4.06	-0.32	2.11	-3.22	-0.33	2.34	-3.74	-0.30
72	1.66	-2.60	-0.12	1.75	-2.94	-0.21	1.84	-2.82	-0.22	1.80	-2.81	-0.21
73	1.97	-2.93	-0.11	2.36	-3.40	-0.21	2.15	-3.26	-0.22	2.32	-3.52	-0.20
74	1.75	-2.70	-0.12	2.78	-4.12	-0.21	2.39	-3.44	-0.22	2.29	-3.38	-0.20
75	2.18	-3.28	-0.21	2.14	-3.63	-0.25	2.18	-3.18	-0.27	2.46	-3.62	-0.25
76	1.92	-2.72	-0.19	1.67	-2.69	-0.20	1.70	-2.75	-0.24	1.72	-2.63	-0.23
77	1.88	-2.75	-0.12	2.48	-3.79	-0.22	2.43	-3.54	-0.21	2.52	-3.86	-0.20
78	2.23	-3.24	-0.11	2.40	-3.49	-0.20	2.12	-3.08	-0.22	2.60	-3.86	-0.20
79	2.30	-3.27	-0.12	2.23	-3.25	-0.21	2.26	-3.36	-0.22	2.21	-3.48	-0.20
80	1.48	-2.37	-0.11	1.64	-2.70	-0.18	1.43	-2.04	-0.22	1.53	-2.42	-0.20
81	2.31	-3.26	-0.12	2.20	-3.22	-0.21	2.62	-3.86	-0.21	2.34	-3.56	-0.20
82	2.12	-2.92	-0.10	2.29	-3.17	-0.18	2.13	-3.18	-0.22	2.61	-3.73	-0.19
83	2.27	-3.46	-0.10	2.12	-3.26	-0.19	1.93	-2.92	-0.22	2.77	-4.05	-0.19
84	1.90	-2.65	-0.10	1.99	-2.79	-0.21	1.82	-2.71	-0.21	2.32	-3.37	-0.19
85	1.63	-2.42	-0.12	2.64	-4.03	-0.21	2.39	-3.53	-0.21	2.66	-3.99	-0.19
86	1.56	-2.38	-0.11	2.28	-3.38	-0.20	2.10	-3.12	-0.21	2.29	-3.38	-0.20
87	2.44	-3.32	-0.12	2.45	-3.62	-0.21	2.28	-3.57	-0.22	2.47	-3.82	-0.20
88	1.89	-2.72	-0.13	1.48	-2.35	-0.22	1.48	-2.32	-0.21	1.52	-2.53	-0.20
89	2.15	-2.98	-0.13	2.39	-3.62	-0.22	2.09	-3.16	-0.21	2.63	-3.99	-0.20
90	1.93	-2.69	-0.12	2.63	-3.79	-0.22	2.56	-3.82	-0.21	2.39	-3.49	-0.20
91	2.56	-3.68	-0.13	2.76	-4.24	-0.22	2.22	-3.45	-0.20	2.89	-4.20	-0.19
92	1.87	-2.87	-0.16	2.17	-3.18	-0.24	1.97	-3.06	-0.22	1.95	-2.88	-0.20
93	2.09	-3.06	-0.12	2.21	-3.21	-0.22	2.23	-3.31	-0.21	2.44	-3.73	-0.19
94	2.14	-3.16	-0.12	2.12	-3.17	-0.20	2.12	-3.11	-0.22	2.66	-4.01	-0.19
95	2.18	-3.06	-0.16	2.45	-3.65	-0.21	2.09	-2.96	-0.23	2.34	-3.59	-0.21
96	1.90	-2.87	-0.12	1.64	-2.59	-0.21	1.34	-2.22	-0.20	1.53	-2.36	-0.16
97	2.29	-3.28	-0.12	2.43	-3.60	-0.21	2.49	-3.74	-0.21	2.49	-3.66	-0.20
98	1.79	-2.48	-0.11	2.38	-3.36	-0.20	2.00	-3.07	-0.22	1.95	-2.90	-0.20
99	2.30	-3.32	-0.12	2.36	-3.52	-0.21	2.33	-3.28	-0.22	2.38	-3.55	-0.20
100	1.92	-3.51	-0.44	2.27	-3.58	-0.40	1.61	-2.48	-0.37	1.94	-3.34	-0.40
101	1.80	-2.95	-0.44	2.32	-3.83	-0.40	1.74	-2.89	-0.39	2.55	-4.40	-0.41
102	2.01	-3.29	-0.33	2.25	-3.43	-0.29	1.94	-2.96	-0.29	2.64	-4.02	-0.30
103	2.58	-3.96	-0.28	3.18	-4.18	-0.30	2.35	-3.43	-0.30	2.87	-4.45	-0.31

104	2.29	-2.52	0.02	2.02	-3.32	-0.20	1.47	-2.37	-0.22	1.80	-2.87	-0.21
105	2.08	-2.82	0.01	2.39	-3.54	-0.21	1.78	-2.66	-0.21	2.83	-4.14	-0.20
106	2.46	-3.62	-0.16	2.68	-3.86	-0.21	2.16	-3.23	-0.22	2.63	-3.92	-0.21
107	2.56	-3.78	-0.18	2.63	-3.99	-0.20	2.81	-4.09	-0.20	2.44	-3.83	-0.18
108	2.36	-3.43	-0.14	2.06	-3.07	-0.18	1.75	-2.80	-0.21	2.24	-3.48	-0.21
109	1.88	-2.82	-0.15	2.72	-3.80	-0.20	2.63	-3.85	-0.19	2.32	-3.47	-0.18
110	2.29	-3.46	-0.25	2.54	-3.69	-0.28	2.23	-3.32	-0.30	2.72	-4.18	-0.29
111	2.24	-3.99	-0.29	2.66	-3.98	-0.29	2.22	-3.49	-0.31	2.91	-4.19	-0.30
112	1.90	-3.33	-0.37	1.31	-2.42	-0.37	1.52	-2.55	-0.43	1.69	-2.62	-0.38
113	1.90	-3.23	-0.38	2.37	-3.43	-0.39	2.52	-4.06	-0.43	2.29	-3.80	-0.38
114	2.01	-3.04	-0.27	2.36	-3.43	-0.22	2.73	-4.13	-0.22	2.86	-4.29	-0.21
115	2.51	-3.29	-0.05	2.45	-3.63	-0.21	2.73	-3.96	-0.23	2.11	-3.08	-0.21
116	1.79	-2.64	-0.12	1.98	-3.04	-0.14	1.85	-2.52	-0.14	2.03	-3.18	-0.13
117	1.86	-3.11	-0.49	2.66	-3.86	-0.47	2.21	-3.86	-0.44	2.44	-4.12	-0.47

Table B-9. Comparison of external and internal pressure coefficients without and with VSVs for the small hip roof model at 15° wind direction

	Without VSVs			With VSVs			With VSVs and Leakage			With VSVs, Leakage and Opening		
Tap No.	**Cp Max**	**Cp Min**	**Cp Mean**	**Cp Max**	**Cp Min**	**Cp Mean**	**Cp Max**	**Cp Min**	**Cp Mean**	**Cp Max**	**Cp Min**	**Cp Mean**
1	2.52	-4.05	-0.36	2.12	-3.55	-0.35	2.58	-3.75	-0.37	2.53	-4.09	-0.38
2	3.11	-4.73	-0.33	2.95	-4.82	-0.32	2.72	-4.64	-0.33	3.01	-4.70	-0.34
3	2.76	-4.62	-0.35	2.90	-4.28	-0.35	2.49	-3.90	-0.38	2.67	-4.48	-0.38
4	2.61	-3.94	-0.29	3.02	-4.62	-0.30	3.25	-4.93	-0.32	2.72	-4.32	-0.32
5	3.09	-4.33	-0.34	2.68	-4.22	-0.33	2.62	-4.17	-0.36	2.84	-4.43	-0.37
6	2.21	-4.33	-0.83	3.02	-4.84	-0.82	2.50	-4.49	-0.81	2.84	-4.87	-0.83
7	3.12	-5.05	-0.35	2.76	-3.96	-0.33	2.54	-3.89	-0.35	2.91	-4.61	-0.35
8	2.42	-3.73	-0.33	2.73	-4.35	-0.31	2.13	-3.68	-0.34	2.17	-3.46	-0.34
9	2.74	-3.78	-0.32	2.61	-4.06	-0.32	2.79	-4.26	-0.32	2.94	-4.51	-0.33
10	3.36	-5.11	-0.24	2.94	-4.63	-0.23	2.91	-4.37	-0.23	3.12	-4.56	-0.25
11	2.37	-4.46	-0.80	2.56	-4.97	-0.78	2.32	-4.34	-0.78	2.67	-4.81	-0.80
12	2.43	-3.90	-0.64	2.50	-4.00	-0.61	2.97	-4.84	-0.63	3.08	-5.15	-0.65
13	2.31	-3.65	-0.44	2.68	-4.45	-0.43	3.28	-5.04	-0.44	3.02	-4.55	-0.45
14	2.82	-4.17	-0.24	3.39	-5.01	-0.23	3.13	-4.56	-0.23	2.84	-3.87	-0.25
15	2.27	-3.48	-0.25	2.90	-4.24	-0.24	3.09	-4.40	-0.25	3.28	-4.61	-0.25
16	2.88	-4.34	-0.86	2.89	-4.23	-0.83	2.43	-3.91	-0.83	2.98	-4.10	-0.85
17	3.17	-3.83	-0.54	2.55	-4.17	-0.50	2.43	-4.22	-0.52	2.43	-4.02	-0.53
18	2.88	-4.32	-0.19	2.80	-4.16	-0.18	3.27	-4.66	-0.19	2.59	-4.02	-0.21
19	2.83	-4.55	-0.49	2.82	-4.83	-0.49	2.93	-4.80	-0.49	2.71	-4.39	-0.51
20	2.76	-4.84	-0.63	3.36	-5.27	-0.61	3.06	-5.19	-0.61	2.97	-5.18	-0.62
21	2.15	-3.61	-0.38	2.58	-4.06	-0.36	3.41	-5.12	-0.38	2.70	-4.42	-0.38
22	3.07	-4.69	-0.23	3.24	-4.72	-0.22	3.31	-4.91	-0.23	3.17	-4.61	-0.22
23	3.23	-4.75	-0.20	3.21	-4.79	-0.19	2.97	-4.31	-0.20	3.37	-5.08	-0.21
24	2.41	-4.71	-0.84	2.25	-4.22	-0.80	2.55	-4.63	-0.81	2.89	-4.92	-0.82
25	2.30	-4.44	-0.46	2.68	-4.59	-0.46	3.18	-4.05	-0.46	2.62	-4.48	-0.47
26	3.16	-4.75	-0.35	3.98	-6.08	-0.35	3.93	-5.94	-0.35	2.87	-4.51	-0.36
27	2.68	-4.07	-0.36	2.71	-4.30	-0.33	3.23	-5.00	-0.34	2.51	-3.75	-0.35
28	3.19	-4.63	-0.30	3.12	-4.57	-0.27	3.20	-4.96	-0.28	2.94	-4.49	-0.28
29	2.48	-5.13	-1.14	3.62	-4.86	-1.12	2.58	-5.28	-1.14	3.18	-5.49	-1.15
30	3.30	-4.90	-0.20	3.51	-5.04	-0.19	3.41	-4.93	-0.20	2.86	-4.36	-0.20
31	2.66	-4.07	-0.18	3.56	-5.31	-0.18	2.54	-3.75	-0.17	3.16	-4.50	-0.18
32	3.33	-5.15	-0.32	2.88	-4.53	-0.31	3.20	-5.10	-0.34	2.50	-4.04	-0.34
33	2.66	-4.36	-0.27	3.08	-4.43	-0.26	3.02	-4.72	-0.27	2.82	-4.26	-0.28
34	3.30	-4.90	-0.23	3.54	-5.10	-0.23	3.07	-4.61	-0.23	2.70	-4.07	-0.24
35	3.05	-4.43	-0.19	3.38	-5.06	-0.20	3.54	-5.30	-0.19	2.57	-3.88	-0.21
36	2.93	-4.30	-0.17	3.67	-5.17	-0.15	4.06	-5.93	-0.15	3.31	-4.87	-0.15
37	3.30	-4.78	-0.21	3.17	-4.79	-0.21	3.72	-5.56	-0.21	2.37	-3.60	-0.22
38	3.14	-4.63	-0.23	3.21	-4.72	-0.22	3.03	-4.67	-0.22	3.36	-5.06	-0.22
39	2.64	-4.27	-0.61	2.96	-4.78	-0.60	3.28	-5.52	-0.61	2.36	-4.13	-0.62
40	2.24	-3.82	-0.63	2.94	-5.18	-0.61	3.42	-5.66	-0.63	2.41	-4.36	-0.64
41	3.03	-4.47	-0.23	3.03	-4.35	-0.03	3.31	-4.74	-0.02	3.71	-5.09	0.04
42	2.85	-4.35	-0.18	3.62	-5.15	-0.15	3.85	-5.46	-0.17	2.85	-4.12	-0.17
43	3.27	-4.56	-0.02	3.95	-5.66	-0.02	3.51	-5.08	-0.07	3.55	-5.32	-0.09
44	2.71	-4.67	-0.56	2.81	-4.81	-0.55	3.37	-5.55	-0.55	2.71	-4.79	-0.56
45	3.43	-3.88	0.79	3.30	-3.59	0.78	3.72	-4.69	0.78	3.01	-3.47	0.76
46	3.36	-4.53	0.11	3.43	-4.27	0.48	3.82	-4.81	0.48	3.13	-3.86	0.46

47	3.22	-4.66	-0.20	3.00	-4.40	-0.20	3.75	-5.55	-0.20	3.03	-4.58	-0.21
48	2.91	-4.73	-0.27	3.38	-5.09	-0.26	3.07	-4.77	-0.26	2.65	-4.18	-0.26
49	3.54	-3.91	0.70	4.08	-4.36	0.71	3.63	-4.28	0.69	2.98	-3.44	0.69
50	2.70	-4.27	-0.17	3.13	-4.59	-0.16	2.65	-4.07	-0.16	3.54	-4.96	-0.17
51	2.53	-3.70	-0.16	2.90	-4.49	-0.19	3.55	-5.18	-0.20	2.72	-4.07	-0.21
52	2.75	-4.11	-0.11	3.26	-4.87	-0.17	3.38	-5.02	-0.17	2.75	-3.98	-0.16
53	2.72	-3.95	-0.10	3.42	-4.95	-0.17	3.29	-5.00	-0.19	3.06	-4.56	-0.16
54	2.85	-4.04	-0.08	3.76	-5.63	-0.16	3.19	-4.74	-0.17	3.26	-4.62	-0.18
55	3.14	-4.70	-0.19	3.10	-4.68	-0.22	3.65	-5.41	-0.23	2.90	-4.41	-0.23
56	3.09	-4.47	-0.06	2.78	-4.18	-0.18	2.89	-4.32	-0.18	2.98	-4.37	-0.15
57	2.19	-3.28	-0.14	2.85	-4.25	-0.17	3.15	-4.62	-0.18	2.54	-3.79	-0.17
58	3.36	-4.81	-0.11	3.59	-5.29	-0.17	3.63	-5.36	-0.18	2.97	-4.30	-0.17
59	3.30	-4.70	-0.10	3.68	-5.35	-0.17	3.20	-4.87	-0.18	3.27	-4.72	-0.17
60	3.26	-4.68	-0.10	3.17	-4.61	-0.17	2.99	-4.48	-0.17	2.96	-4.35	-0.17
61	3.31	-4.76	-0.09	3.21	-4.74	-0.16	2.99	-4.51	-0.17	3.19	-4.67	-0.17
62	3.18	-4.50	-0.09	4.15	-5.99	-0.17	3.20	-4.70	-0.18	3.23	-4.64	-0.17
63	3.31	-4.83	-0.10	3.25	-4.75	-0.17	3.46	-5.15	-0.16	3.04	-4.43	-0.15
64	3.41	-4.89	-0.07	3.14	-4.68	-0.16	3.63	-5.25	-0.18	3.16	-4.73	-0.17
65	2.47	-3.52	-0.10	2.26	-3.44	-0.19	2.49	-3.75	-0.18	2.41	-3.63	-0.17
66	2.74	-3.96	-0.11	2.63	-3.89	-0.17	2.08	-3.20	-0.17	2.76	-4.07	-0.16
67	2.49	-3.51	-0.08	2.70	-3.88	-0.15	2.11	-3.22	-0.17	2.48	-3.62	-0.17
68	1.98	-2.93	-0.09	2.33	-3.52	-0.17	2.39	-3.56	-0.19	2.08	-3.17	-0.17
69	2.68	-3.79	-0.05	2.77	-4.08	-0.15	2.59	-4.00	-0.18	2.65	-3.88	-0.17
70	2.36	-3.41	-0.14	2.89	-4.21	-0.18	2.53	-3.82	-0.19	2.73	-4.11	-0.18
71	2.77	-4.49	-0.47	2.41	-3.85	-0.44	2.23	-3.69	-0.44	2.68	-4.12	-0.43
72	1.53	-2.25	-0.10	1.86	-2.73	-0.17	1.56	-2.45	-0.19	1.61	-2.33	-0.17
73	2.38	-3.48	-0.09	2.58	-3.86	-0.17	2.63	-4.09	-0.18	2.84	-4.27	-0.16
74	3.05	-4.38	-0.10	2.38	-3.53	-0.17	2.34	-3.47	-0.18	2.89	-4.34	-0.16
75	2.70	-3.94	-0.10	3.14	-4.56	-0.18	2.79	-4.19	-0.18	3.12	-4.45	-0.17
76	1.83	-2.48	-0.13	2.27	-3.29	-0.16	2.49	-3.78	-0.20	2.18	-3.30	-0.19
77	2.89	-4.23	-0.11	3.15	-4.61	-0.18	2.87	-4.37	-0.18	3.31	-4.87	-0.16
78	2.51	-3.64	-0.09	3.03	-4.33	-0.16	2.48	-3.82	-0.18	2.34	-3.44	-0.17
79	2.30	-3.33	-0.10	2.99	-4.34	-0.18	2.86	-4.18	-0.18	2.94	-4.38	-0.16
80	1.54	-2.39	-0.08	1.43	-2.09	-0.15	1.68	-2.50	-0.18	1.95	-3.20	-0.16
81	2.23	-3.27	-0.10	2.37	-3.53	-0.17	3.13	-4.57	-0.18	2.58	-3.96	-0.16
82	2.18	-3.13	-0.07	2.12	-3.22	-0.15	2.69	-4.09	-0.17	2.54	-3.92	-0.16
83	2.06	-3.05	-0.08	2.44	-3.68	-0.15	2.80	-4.09	-0.17	2.85	-4.13	-0.16
84	2.35	-3.41	-0.11	2.65	-4.04	-0.18	2.54	-3.72	-0.17	2.13	-3.18	-0.13
85	2.33	-3.46	-0.11	2.19	-3.31	-0.18	3.34	-5.03	-0.17	2.28	-3.48	-0.15
86	2.43	-3.37	-0.10	2.88	-4.22	-0.17	2.67	-4.02	-0.18	2.44	-3.58	-0.16
87	2.70	-4.02	-0.10	3.11	-4.66	-0.18	2.54	-3.76	-0.19	2.69	-4.00	-0.16
88	1.86	-2.83	-0.12	1.29	-2.18	-0.19	1.96	-3.07	-0.18	2.13	-3.12	-0.16
89	2.94	-4.23	-0.12	3.34	-4.86	-0.19	2.94	-4.36	-0.18	2.79	-4.00	-0.16
90	2.46	-3.63	-0.11	3.17	-4.84	-0.19	3.25	-4.84	-0.18	2.54	-3.71	-0.16
91	2.71	-3.96	-0.11	2.72	-4.16	-0.19	2.92	-4.37	-0.17	2.26	-3.30	-0.15
92	2.50	-3.61	-0.15	2.35	-3.55	-0.21	2.79	-4.15	-0.18	2.37	-3.54	-0.17
93	2.77	-3.80	-0.10	3.09	-4.71	-0.19	2.77	-4.19	-0.18	3.03	-4.50	-0.14
94	2.55	-3.71	-0.09	2.57	-3.97	-0.16	2.82	-4.23	-0.17	2.28	-3.35	-0.16
95	2.16	-3.17	-0.17	2.88	-4.29	-0.19	2.23	-3.42	-0.19	2.73	-3.92	-0.18
96	1.79	-2.60	-0.10	1.60	-2.49	-0.18	1.33	-2.10	-0.15	1.59	-2.46	-0.16
97	2.90	-4.12	-0.11	2.89	-4.22	-0.18	2.67	-4.08	-0.18	3.03	-4.47	-0.16
98	2.69	-3.76	-0.09	2.76	-4.14	-0.17	1.99	-3.14	-0.18	2.22	-3.34	-0.17
99	2.57	-3.74	-0.09	2.62	-3.82	-0.18	2.46	-3.60	-0.18	2.31	-3.51	-0.16
100	2.12	-3.23	-0.22	2.32	-3.46	-0.20	2.51	-3.96	-0.22	2.16	-3.25	-0.22
101	2.78	-3.91	-0.23	2.56	-4.14	-0.21	3.27	-4.84	-0.22	2.28	-3.58	-0.23
102	2.18	-3.39	-0.30	2.32	-3.73	-0.27	2.15	-3.46	-0.29	3.00	-4.20	-0.29
103	2.73	-3.69	-0.33	2.83	-4.47	-0.31	3.14	-4.72	-0.33	2.69	-4.19	-0.32

104	2.00	-2.02	0.30	1.97	-2.77	-0.17	1.99	-2.86	-0.19	1.45	-2.25	-0.17
105	2.65	-3.51	0.04	2.72	-3.91	-0.17	2.89	-4.34	-0.18	3.43	-4.87	-0.16
106	2.52	-3.56	-0.20	2.87	-4.25	-0.20	2.76	-4.32	-0.21	2.15	-3.19	-0.21
107	2.91	-4.10	-0.26	3.12	-4.52	-0.21	3.02	-4.75	-0.21	3.57	-5.09	-0.22
108	2.56	-3.82	-0.17	2.51	-3.65	-0.17	2.57	-3.85	-0.21	1.98	-3.00	-0.20
109	2.79	-4.26	-0.19	3.14	-4.72	-0.20	3.26	-4.86	-0.19	2.27	-3.52	-0.19
110	2.67	-3.97	-0.08	2.81	-3.91	-0.08	2.38	-3.69	-0.09	2.38	-3.78	-0.08
111	2.97	-4.48	-0.13	2.79	-4.12	-0.20	2.91	-4.45	-0.20	2.89	-4.08	-0.19
112	1.58	-3.33	-0.78	1.50	-3.40	-0.74	1.14	-3.30	-0.79	1.68	-3.33	-0.77
113	2.36	-4.01	-0.67	2.28	-4.04	-0.64	2.58	-4.25	-0.66	2.56	-3.93	-0.65
114	1.71	-2.71	-0.26	2.75	-4.10	-0.19	2.44	-3.70	-0.20	3.77	-5.38	-0.17
115	2.06	-2.80	-0.02	2.25	-3.39	-0.18	3.12	-4.62	-0.19	3.00	-4.26	-0.17
116	2.15	-3.43	-0.23	2.36	-3.58	-0.22	2.57	-3.91	-0.21	1.73	-2.54	-0.18
117	2.52	-3.89	-0.26	3.09	-4.49	-0.25	3.31	-5.08	-0.26	2.50	-3.83	-0.25

Table B-10. Comparison of external and internal pressure coefficients without and with VSVs for the small hip roof model at 30° wind direction

	Without VSVs			With VSVs			With VSVs and Leakage			With VSVs, Leakage and Opening		
Tap No.	**Cp Max**	**Cp Min**	**Cp Mean**	**Cp Max**	**Cp Min**	**Cp Mean**	**Cp Max**	**Cp Min**	**Cp Mean**	**Cp Max**	**Cp Min**	**Cp Mean**
1	1.84	-2.88	-0.33	1.87	-3.23	-0.35	1.84	-2.90	-0.35	1.55	-2.52	-0.34
2	2.43	-3.86	-0.30	2.21	-3.36	-0.31	1.90	-3.52	-0.31	2.10	-3.36	-0.30
3	2.33	-3.80	-0.32	2.10	-3.16	-0.35	1.86	-2.74	-0.36	1.71	-3.19	-0.34
4	2.70	-4.10	-0.25	2.34	-3.78	-0.27	2.16	-3.60	-0.28	2.89	-4.48	-0.27
5	2.00	-3.14	-0.28	2.23	-3.75	-0.30	1.54	-2.78	-0.30	2.37	-3.64	-0.29
6	1.73	-3.09	-0.56	2.01	-3.55	-0.55	2.13	-3.60	-0.55	2.70	-4.40	-0.54
7	2.02	-3.21	-0.30	1.66	-2.88	-0.31	2.09	-3.19	-0.31	2.65	-4.23	-0.30
8	2.02	-3.09	-0.27	2.08	-3.10	-0.28	1.94	-3.01	-0.29	1.49	-2.99	-0.28
9	2.02	-3.17	-0.26	2.19	-3.44	-0.27	2.26	-3.64	-0.27	1.97	-3.30	-0.26
10	2.25	-3.49	-0.22	2.28	-3.64	-0.22	1.78	-2.93	-0.22	2.22	-3.49	-0.21
11	2.01	-4.00	-0.64	1.60	-3.41	-0.64	2.18	-3.35	-0.65	1.67	-3.10	-0.63
12	2.23	-3.58	-0.53	2.15	-4.01	-0.53	2.30	-3.66	-0.55	2.20	-3.58	-0.53
13	1.57	-2.93	-0.43	2.03	-3.41	-0.44	1.42	-2.46	-0.43	2.04	-3.52	-0.42
14	2.37	-3.70	-0.19	2.44	-3.64	-0.20	2.53	-3.87	-0.20	2.22	-3.23	-0.19
15	1.82	-2.82	-0.23	2.09	-3.20	-0.23	1.85	-2.87	-0.23	1.61	-2.67	-0.23
16	2.21	-3.29	-0.70	2.06	-3.60	-0.72	2.06	-3.83	-0.75	2.40	-3.63	-0.71
17	1.72	-2.62	-0.28	1.99	-3.35	-0.30	2.45	-2.82	-0.32	1.92	-3.02	-0.31
18	1.99	-3.11	-0.19	2.78	-4.06	-0.20	2.09	-3.14	-0.19	2.97	-4.59	-0.18
19	2.12	-3.58	-0.53	1.53	-3.02	-0.55	1.27	-2.49	-0.55	2.03	-3.59	-0.53
20	2.61	-4.51	-0.68	2.33	-4.08	-0.67	1.84	-3.43	-0.66	2.45	-4.30	-0.66
21	2.63	-4.29	-0.40	2.31	-3.75	-0.41	1.92	-3.29	-0.41	2.13	-3.42	-0.40
22	2.50	-3.81	-0.24	1.75	-2.81	-0.24	2.31	-3.62	-0.23	2.26	-3.53	-0.24
23	2.08	-3.32	-0.22	2.34	-3.64	-0.22	2.57	-3.98	-0.22	2.09	-3.29	-0.21
24	1.96	-3.47	-0.47	2.64	-3.95	-0.49	2.48	-3.40	-0.52	2.82	-3.57	-0.51
25	2.04	-3.04	-0.01	2.21	-3.46	-0.03	2.66	-3.45	-0.04	2.27	-2.73	-0.03
26	1.85	-3.09	-0.33	2.50	-4.09	-0.33	2.23	-3.57	-0.33	2.55	-4.01	-0.32
27	1.46	-2.53	-0.42	1.40	-2.29	-0.42	1.36	-2.76	-0.41	2.34	-4.01	-0.41
28	2.49	-3.83	-0.35	1.98	-3.24	-0.33	1.70	-2.74	-0.33	2.26	-3.70	-0.33
29	3.97	-5.61	-0.83	4.07	-4.32	-0.86	3.75	-4.88	-0.94	4.22	-5.97	-0.92
30	2.88	-4.25	-0.09	2.41	-3.44	-0.09	2.55	-3.78	-0.09	2.53	-3.69	-0.09
31	2.52	-3.79	-0.12	2.44	-3.52	-0.12	1.94	-2.96	-0.12	2.37	-3.64	-0.12
32	2.16	-3.61	-0.37	1.90	-3.02	-0.38	1.92	-3.13	-0.37	2.40	-3.81	-0.36
33	2.20	-3.33	-0.29	1.83	-3.01	-0.29	2.00	-3.37	-0.29	2.04	-3.47	-0.28
34	2.09	-2.69	0.00	3.22	-4.40	-0.02	2.26	-2.95	-0.02	2.36	-3.20	-0.02
35	3.00	-4.34	-0.08	2.41	-3.53	-0.09	2.55	-3.80	-0.09	2.92	-4.30	-0.08
36	2.42	-3.71	-0.14	2.79	-4.06	-0.14	1.93	-3.03	-0.12	2.58	-3.70	-0.13
37	2.31	-3.57	-0.25	2.08	-3.16	-0.26	1.33	-2.28	-0.26	2.08	-3.19	-0.26
38	1.96	-3.49	-0.55	1.95	-3.46	-0.53	2.12	-3.55	-0.52	1.70	-3.60	-0.54
39	1.99	-3.64	-0.63	2.17	-3.68	-0.64	1.66	-3.19	-0.64	1.79	-3.13	-0.63
40	2.22	-3.95	-0.65	2.26	-4.01	-0.64	1.98	-3.73	-0.65	2.96	-4.97	-0.64
41	2.34	-3.64	-0.29	2.05	-3.04	-0.07	1.94	-2.80	-0.06	2.50	-3.59	-0.03
42	2.58	-3.80	-0.19	2.63	-3.98	-0.18	2.83	-4.21	-0.17	2.29	-3.45	-0.17
43	2.51	-3.45	0.09	2.46	-3.29	0.07	2.28	-3.32	-0.01	2.62	-3.78	0.01
44	2.91	-3.82	0.23	2.88	-3.69	0.13	2.53	-3.32	0.13	2.42	-3.21	0.17
45	3.04	-3.35	0.75	3.05	-3.45	0.79	2.94	0.00	0.80	2.53	-2.56	0.81
46	3.23	-4.31	0.14	3.25	-4.22	0.29	2.76	-3.62	0.29	2.48	-3.24	0.30

47	2.47	-3.65	-0.18	2.34	-3.51	-0.18	1.96	-2.98	-0.17	1.91	-2.90	-0.17
48	2.44	-3.81	-0.24	2.51	-3.82	-0.23	1.77	-2.85	-0.23	2.61	-4.03	-0.22
49	2.21	-2.37	0.54	2.53	-2.87	0.54	1.69	-1.79	0.56	2.38	-2.46	0.55
50	2.92	-3.91	0.15	3.15	-4.21	0.15	3.29	-4.29	0.14	2.64	-3.51	0.16
51	1.98	-2.95	-0.11	2.19	-3.24	-0.16	1.90	-2.93	-0.17	2.94	-4.30	-0.14
52	3.11	-4.49	-0.01	2.89	-4.19	-0.13	2.51	-3.57	-0.12	2.90	-4.17	-0.09
53	1.80	-2.60	-0.01	2.66	-3.89	-0.13	1.99	-2.95	-0.12	2.41	-3.52	-0.11
54	3.00	-4.30	0.01	3.05	-4.48	-0.13	2.65	-3.81	-0.13	2.46	-3.56	-0.09
55	2.02	-2.93	-0.13	1.82	-2.85	-0.19	1.82	-2.91	-0.18	2.64	-4.02	-0.17
56	2.34	-3.37	-0.01	2.32	-3.43	-0.12	1.98	-2.91	-0.10	1.89	-2.83	-0.10
57	2.43	-3.49	-0.11	2.05	-3.14	-0.16	2.14	-3.34	-0.15	2.02	-3.08	-0.15
58	2.97	-4.17	-0.01	1.91	-2.87	-0.13	2.20	-3.28	-0.12	2.15	-3.26	-0.10
59	2.06	-2.86	0.00	2.43	-3.62	-0.13	2.40	-3.51	-0.12	2.95	-4.32	-0.10
60	2.60	-3.75	-0.01	2.88	-4.24	-0.14	2.44	-3.66	-0.13	2.85	-4.06	-0.10
61	2.11	-3.03	0.00	2.70	-3.98	-0.14	2.14	-3.27	-0.13	2.73	-3.90	-0.10
62	2.96	-4.19	0.00	3.09	-4.56	-0.13	2.49	-3.57	-0.12	2.91	-4.17	-0.10
63	2.48	-3.52	-0.01	2.76	-4.06	-0.13	2.23	-3.31	-0.11	2.67	-3.86	-0.09
64	2.50	-3.33	0.00	3.24	-4.70	-0.14	1.90	-2.77	-0.12	2.58	-3.81	-0.09
65	1.92	-2.76	0.00	1.81	-2.82	-0.13	1.75	-2.70	-0.13	1.45	-2.18	-0.10
66	2.18	-3.15	-0.03	1.75	-2.57	-0.13	1.56	-2.51	-0.12	1.76	-2.58	-0.10
67	2.23	-3.17	-0.02	1.82	-2.76	-0.12	1.64	-2.40	-0.13	1.84	-2.64	-0.10
68	1.97	-2.82	-0.01	1.71	-2.44	-0.15	1.81	-2.74	-0.13	2.05	-3.12	-0.11
69	1.44	-2.18	0.01	1.93	-2.89	-0.13	1.27	-2.11	-0.12	2.30	-3.33	-0.09
70	1.56	-2.38	-0.12	2.04	-3.05	-0.17	1.80	-2.68	-0.16	2.27	-3.40	-0.15
71	1.89	-2.72	-0.01	1.82	-2.66	-0.13	1.64	-2.43	-0.12	2.77	-4.00	-0.10
72	1.28	-1.60	-0.02	1.46	-1.97	-0.13	1.35	-1.83	-0.13	1.14	-1.43	-0.11
73	1.91	-2.72	0.01	2.02	-2.93	-0.12	2.11	-3.13	-0.12	2.13	-3.03	-0.10
74	2.00	-2.71	0.00	1.96	-2.93	-0.13	1.47	-2.37	-0.12	1.82	-2.82	-0.10
75	2.30	-3.25	0.00	1.83	-2.89	-0.13	1.82	-2.70	-0.12	1.97	-2.82	-0.10
76	1.55	-2.07	-0.04	1.80	-2.67	-0.13	1.68	-2.53	-0.15	2.00	-2.91	-0.12
77	1.84	-2.70	0.00	2.11	-3.13	-0.13	1.57	-2.41	-0.12	2.32	-3.58	-0.10
78	1.93	-2.73	-0.01	1.74	-2.71	-0.13	2.27	-3.38	-0.13	1.94	-2.80	-0.10
79	1.48	-2.20	0.00	1.88	-2.79	-0.13	1.87	-2.78	-0.12	1.91	-2.73	-0.10
80	1.02	-1.47	-0.04	1.20	-1.46	-0.14	1.33	-1.65	-0.12	0.92	-1.19	-0.08
81	1.63	-2.28	0.00	1.97	-2.91	-0.13	2.18	-3.31	-0.11	1.38	-2.19	-0.09
82	1.25	-1.89	-0.02	2.17	-3.26	-0.12	1.77	-2.65	-0.12	1.98	-3.06	-0.09
83	1.99	-2.93	-0.03	1.50	-2.38	-0.12	1.33	-2.01	-0.12	1.61	-2.35	-0.09
84	2.20	-3.08	0.00	1.87	-2.79	-0.13	1.34	-2.03	-0.08	1.89	-2.82	-0.09
85	2.51	-3.55	0.00	1.97	-3.07	-0.14	1.25	-1.91	-0.11	2.09	-3.10	-0.09
86	2.26	-3.22	-0.02	1.15	-1.90	-0.13	1.49	-2.31	-0.11	2.04	-3.04	-0.10
87	2.05	-2.91	0.01	2.08	-3.17	-0.13	1.94	-2.93	-0.12	2.17	-3.19	-0.10
88	1.51	-2.09	0.01	1.87	-2.49	-0.12	1.09	-1.54	-0.12	1.45	-1.97	-0.10
89	2.15	-3.10	0.01	2.39	-3.69	-0.14	1.87	-2.81	-0.12	1.59	-2.49	-0.10
90	1.72	-2.38	0.01	2.36	-3.52	-0.13	1.92	-2.81	-0.12	2.05	-3.16	-0.10
91	1.70	-2.54	0.01	1.70	-2.60	-0.13	1.36	-2.19	-0.11	2.28	-3.42	-0.09
92	1.79	-2.62	0.00	1.53	-2.31	-0.11	1.50	-2.21	-0.13	1.85	-2.78	-0.11
93	1.92	-2.72	0.01	1.58	-2.37	-0.13	1.48	-2.23	-0.12	1.96	-2.98	-0.08
94	1.88	-2.69	-0.02	1.34	-2.07	-0.12	1.78	-2.66	-0.12	1.68	-2.61	-0.10
95	1.60	-2.37	-0.05	1.72	-2.59	-0.13	1.75	-2.55	-0.12	2.05	-3.09	-0.10
96	1.38	-1.87	0.00	0.93	-1.38	-0.13	0.99	-1.45	-0.12	1.35	-2.00	-0.10
97	1.95	-2.76	0.00	1.76	-2.62	-0.13	1.92	-2.90	-0.12	2.19	-3.21	-0.10
98	1.51	-2.24	0.00	2.26	-3.46	-0.13	1.65	-2.58	-0.13	1.72	-2.64	-0.10
99	2.49	-3.55	-0.02	1.88	-2.88	-0.14	2.05	-3.22	-0.12	2.63	-3.84	-0.10
100	1.93	-2.87	-0.19	1.92	-2.99	-0.21	1.45	-2.07	-0.18	1.93	-3.01	-0.18
101	2.11	-3.26	-0.22	2.09	-3.12	-0.19	1.31	-2.05	-0.18	1.80	-2.90	-0.19
102	1.78	-2.83	-0.29	1.56	-2.86	-0.25	1.66	-2.59	-0.24	1.74	-2.92	-0.24
103	1.67	-2.67	-0.31	2.03	-3.48	-0.29	2.05	-3.07	-0.28	2.01	-2.96	-0.30

104	2.08	-1.83	0.45	1.54	-2.08	-0.13	1.42	-1.95	-0.13	1.63	-2.28	-0.11
105	1.67	-2.38	0.02	1.86	-2.80	-0.13	1.42	-2.20	-0.12	2.20	-3.24	-0.10
106	1.77	-2.71	-0.21	2.07	-3.19	-0.22	2.05	-3.24	-0.22	1.67	-2.64	-0.23
107	2.14	-3.45	-0.29	1.99	-3.11	-0.25	1.73	-2.68	-0.25	2.11	-3.38	-0.27
108	1.86	-2.90	-0.15	1.95	-3.09	-0.17	1.53	-2.47	-0.19	1.68	-2.60	-0.17
109	2.49	-3.76	-0.19	2.29	-3.37	-0.17	2.38	-3.61	-0.17	2.15	-3.32	-0.17
110	2.02	-3.12	0.01	1.98	-2.94	0.01	1.94	-2.74	0.02	1.88	-2.42	0.03
111	2.20	-3.13	-0.03	1.92	-3.08	-0.16	1.66	-2.63	-0.15	1.89	-2.70	-0.13
112	1.53	-2.04	-0.02	1.66	-2.25	-0.13	1.44	-1.92	-0.11	1.30	-1.70	-0.08
113	1.69	-2.33	-0.04	2.10	-3.07	-0.14	1.62	-2.57	-0.12	1.75	-2.53	-0.10
114	1.89	-3.14	-0.14	2.61	-3.91	-0.13	3.05	-4.44	-0.12	1.84	-2.63	-0.10
115	1.63	-2.26	0.05	1.80	-2.71	-0.13	2.00	-2.99	-0.13	2.23	-3.31	-0.10
116	2.32	-3.47	-0.21	2.20	-3.22	-0.21	1.65	-2.60	-0.18	2.09	-3.14	-0.21
117	1.62	-2.66	-0.22	2.27	-3.57	-0.23	1.80	-2.68	-0.23	2.39	-3.72	-0.23

Table B-11. Comparison of external and internal pressure coefficients without and with VSVs for the small hip roof model at 45° wind direction

	Without VSVs			With VSVs			With VSVs and Leakage			With VSVs, Leakage and Opening		
Tap No.	**Cp Max**	**Cp Min**	**Cp Mean**	**Cp Max**	**Cp Min**	**Cp Mean**	**Cp Max**	**Cp Min**	**Cp Mean**	**Cp Max**	**Cp Min**	**Cp Mean**
1	2.45	-4.28	-0.32	2.40	-3.70	-0.33	2.63	-3.98	-0.35	1.84	-2.82	-0.33
2	2.39	-3.48	-0.32	3.19	-4.54	-0.32	2.76	-4.18	-0.34	2.23	-3.68	-0.32
3	2.57	-3.90	-0.34	2.72	-4.26	-0.36	2.71	-4.36	-0.38	2.55	-3.97	-0.36
4	2.54	-3.59	-0.19	2.56	-3.90	-0.21	2.89	-4.20	-0.22	2.76	-4.05	-0.19
5	2.50	-3.72	-0.23	2.64	-3.77	-0.24	2.61	-3.86	-0.25	2.42	-3.72	-0.23
6	2.80	-4.76	-0.57	2.50	-4.23	-0.59	2.39	-4.17	-0.61	2.82	-4.85	-0.59
7	2.74	-4.30	-0.33	3.01	-4.83	-0.33	2.32	-3.74	-0.35	2.43	-3.83	-0.33
8	2.56	-4.07	-0.25	2.71	-3.96	-0.25	2.76	-4.08	-0.27	2.85	-4.34	-0.26
9	2.47	-3.89	-0.21	2.58	-3.98	-0.22	3.07	-4.62	-0.23	2.53	-3.97	-0.21
10	2.98	-4.52	-0.22	3.15	-4.64	-0.21	2.69	-4.15	-0.22	2.87	-4.28	-0.22
11	2.08	-3.52	-0.65	2.48	-4.69	-0.64	2.41	-4.20	-0.66	2.67	-4.99	-0.62
12	3.04	-4.75	-0.44	2.55	-4.32	-0.43	3.36	-4.50	-0.46	2.91	-4.56	-0.44
13	2.14	-3.51	-0.43	2.70	-4.40	-0.43	2.63	-4.14	-0.44	2.38	-3.88	-0.42
14	2.99	-4.44	-0.20	2.57	-4.00	-0.20	3.03	-4.46	-0.21	3.13	-4.52	-0.20
15	2.27	-3.42	-0.25	2.69	-4.25	-0.25	2.49	-3.75	-0.25	2.63	-3.92	-0.24
16	2.67	-4.16	-0.46	2.44	-3.79	-0.44	2.27	-3.74	-0.46	2.77	-3.75	-0.45
17	2.58	-3.51	-0.08	2.42	-3.63	-0.07	2.36	-3.14	-0.08	2.68	-3.97	-0.08
18	3.10	-4.69	-0.27	2.56	-3.92	-0.27	2.51	-3.78	-0.28	3.13	-4.61	-0.27
19	2.31	-3.88	-0.58	2.57	-4.23	-0.59	2.40	-3.97	-0.60	2.55	-4.40	-0.58
20	2.27	-3.82	-0.71	2.11	-4.11	-0.71	2.53	-4.40	-0.72	2.47	-4.25	-0.70
21	1.80	-2.98	-0.41	2.70	-4.43	-0.41	2.90	-4.55	-0.42	2.55	-3.95	-0.41
22	2.50	-3.68	-0.24	2.51	-3.71	-0.25	2.71	-4.14	-0.23	2.97	-4.37	-0.23
23	2.37	-3.58	-0.23	2.52	-3.93	-0.23	2.67	-4.14	-0.24	2.34	-3.39	-0.22
24	2.50	-3.42	-0.07	2.63	-3.67	-0.07	2.52	-3.62	-0.06	2.80	-3.72	-0.07
25	2.56	-3.82	0.01	2.19	-3.04	0.01	2.79	-3.89	-0.01	2.92	-3.97	0.02
26	2.58	-4.11	-0.30	2.80	-4.40	-0.30	3.08	-4.61	-0.30	3.10	-4.67	-0.29
27	2.76	-4.20	-0.45	2.62	-4.09	-0.45	2.24	-3.72	-0.44	2.17	-3.48	-0.44
28	2.19	-3.59	-0.37	2.59	-4.03	-0.35	2.51	-4.03	-0.33	2.89	-4.17	-0.34
29	3.03	-4.33	-0.18	3.12	-3.27	-0.18	2.76	-3.96	-0.19	2.83	-3.55	-0.19
30	2.50	-3.78	-0.03	2.80	-4.14	-0.02	2.90	-3.95	-0.01	3.01	-4.28	0.00
31	3.06	-4.63	-0.08	2.52	-3.49	-0.07	2.61	-3.98	-0.10	2.56	-3.72	-0.07
32	2.08	-3.41	-0.45	2.98	-4.73	-0.47	2.53	-3.79	-0.46	2.70	-4.10	-0.44
33	2.65	-4.38	-0.32	2.65	-4.17	-0.32	2.57	-4.10	-0.33	2.53	-3.86	-0.31
34	3.31	-4.25	-0.18	3.62	-4.29	-0.22	3.77	-4.61	-0.24	3.23	-4.28	-0.22
35	2.58	-3.74	-0.08	3.08	-4.08	-0.09	2.94	-4.18	-0.11	2.44	-3.79	-0.10
36	2.66	-4.35	-0.36	2.75	-4.04	-0.36	2.99	-4.05	-0.35	2.52	-4.24	-0.35
37	2.44	-4.06	-0.44	2.70	-3.81	-0.44	2.30	-4.20	-0.44	3.04	-4.38	-0.44
38	3.07	-4.70	-0.60	2.53	-4.30	-0.60	2.56	-4.28	-0.57	2.62	-3.99	-0.57
39	2.60	-4.57	-0.71	2.63	-4.92	-0.72	2.54	-4.83	-0.72	2.45	-4.64	-0.70
40	2.66	-4.56	-0.64	3.08	-5.17	-0.63	2.60	-4.54	-0.65	2.64	-4.48	-0.62
41	2.28	-3.74	-0.33	2.96	-4.17	-0.03	2.86	-3.86	-0.03	2.34	-3.24	-0.01
42	3.30	-4.99	-0.22	3.17	-4.68	-0.20	3.04	-4.31	-0.19	3.18	-4.60	-0.19
43	2.49	-3.17	0.24	3.31	-4.63	0.03	3.27	-4.29	-0.01	3.10	-4.08	0.04
44	3.63	-4.30	0.50	3.05	-3.38	0.60	3.70	-4.16	0.58	3.93	-4.37	0.60
45	2.95	-3.40	0.53	3.05	-3.16	0.58	3.13	-3.52	0.57	3.38	-4.08	0.59
46	3.32	-4.56	0.09	3.44	-4.65	0.12	3.18	-4.40	0.10	3.48	-4.66	0.11

47	2.89	-4.18	-0.18	2.89	-4.16	-0.19	3.25	-4.73	-0.19	2.90	-4.15	-0.18
48	2.82	-4.46	-0.24	3.29	-4.80	-0.22	2.55	-4.09	-0.23	2.98	-4.43	-0.22
49	2.86	-3.42	0.32	3.24	-3.92	0.32	2.67	-3.33	0.33	3.33	-4.27	0.32
50	3.40	-4.29	0.35	3.55	-4.55	0.37	2.76	-3.31	0.34	3.19	-3.68	0.36
51	2.54	-3.64	-0.11	2.73	-3.95	-0.17	2.91	-4.15	-0.20	2.89	-4.03	-0.15
52	2.48	-3.48	0.03	2.80	-4.09	-0.15	2.61	-3.84	-0.13	2.96	-4.27	-0.11
53	2.15	-3.09	0.02	2.62	-3.75	-0.15	2.59	-3.58	-0.13	2.70	-3.92	-0.10
54	2.91	-3.92	0.03	3.45	-4.80	-0.15	2.89	-4.28	-0.16	2.79	-4.25	-0.11
55	2.76	-4.02	-0.11	2.55	-3.85	-0.20	3.07	-4.46	-0.20	3.07	-4.35	-0.17
56	2.44	-3.44	0.01	2.54	-3.68	-0.15	2.49	-3.51	-0.11	2.33	-3.49	-0.09
57	3.05	-4.43	-0.09	2.85	-4.13	-0.19	2.35	-3.42	-0.16	3.01	-4.38	-0.15
58	2.77	-3.89	0.02	2.81	-4.21	-0.15	2.76	-4.03	-0.14	3.08	-4.29	-0.10
59	3.26	-4.57	0.02	3.02	-4.45	-0.15	2.89	-4.21	-0.15	2.96	-4.31	-0.11
60	2.65	-3.73	0.02	2.24	-3.35	-0.15	2.99	-4.32	-0.16	2.87	-4.01	-0.12
61	3.58	-4.87	0.02	2.71	-3.87	-0.16	3.02	-4.30	-0.16	2.70	-4.12	-0.11
62	2.50	-3.49	0.02	2.40	-3.59	-0.15	2.79	-4.05	-0.15	3.10	-4.55	-0.11
63	3.18	-4.32	0.02	2.72	-3.96	-0.15	2.81	-4.11	-0.13	2.60	-3.69	-0.10
64	3.07	-4.25	0.03	2.89	-4.46	-0.16	2.74	-4.14	-0.15	2.30	-3.40	-0.09
65	2.58	-3.54	0.03	1.76	-2.71	-0.16	2.18	-3.22	-0.14	1.86	-2.70	-0.11
66	2.01	-2.79	0.00	2.17	-3.17	-0.15	2.36	-3.50	-0.14	2.19	-3.13	-0.11
67	2.49	-3.45	0.01	2.07	-3.11	-0.15	2.48	-3.59	-0.14	2.29	-3.37	-0.11
68	1.98	-2.52	0.02	1.66	-2.51	-0.17	1.92	-2.97	-0.15	1.80	-2.57	-0.08
69	2.68	-3.47	0.00	2.06	-3.14	-0.15	2.32	-3.36	-0.14	1.85	-2.91	-0.11
70	2.67	-3.79	-0.12	2.25	-3.47	-0.18	2.16	-3.25	-0.17	2.38	-3.53	-0.15
71	2.44	-3.60	0.00	2.51	-3.91	-0.16	2.23	-3.21	-0.14	2.16	-3.07	-0.10
72	1.68	-2.38	0.01	1.41	-2.25	-0.15	1.68	-2.56	-0.15	1.66	-2.47	-0.10
73	2.81	-3.79	0.04	2.75	-3.87	-0.15	2.65	-3.96	-0.14	2.19	-3.18	-0.10
74	2.74	-3.70	0.03	2.70	-3.96	-0.16	2.51	-3.82	-0.14	2.51	-3.66	-0.11
75	2.36	-3.32	0.02	2.52	-3.71	-0.16	2.59	-3.85	-0.15	2.77	-4.05	-0.11
76	2.14	-2.93	0.00	1.98	-3.01	-0.16	2.15	-3.25	-0.17	2.02	-2.95	-0.11
77	2.24	-2.85	0.03	2.77	-4.02	-0.15	2.65	-3.78	-0.14	2.42	-3.59	-0.10
78	2.74	-3.83	0.02	2.26	-3.45	-0.15	2.50	-3.68	-0.15	2.57	-3.64	-0.11
79	2.27	-3.11	0.03	2.49	-3.64	-0.15	2.44	-3.49	-0.14	2.61	-3.82	-0.10
80	1.71	-2.45	-0.01	1.36	-2.10	-0.16	1.62	-2.46	-0.14	1.70	-2.44	-0.12
81	2.39	-3.23	0.03	2.25	-3.15	-0.15	2.49	-3.66	-0.14	2.62	-3.89	-0.10
82	2.55	-3.64	0.01	2.11	-3.14	-0.14	2.25	-3.35	-0.14	2.61	-3.73	-0.11
83	2.04	-2.78	0.00	2.31	-3.30	-0.14	2.21	-3.21	-0.14	2.39	-3.54	-0.11
84	2.29	-3.09	0.04	1.62	-2.49	-0.15	1.85	-2.84	-0.10	1.97	-2.81	-0.11
85	2.15	-2.90	0.04	2.35	-3.48	-0.16	2.60	-3.78	-0.13	2.68	-3.79	-0.11
86	2.48	-3.43	0.02	2.16	-3.16	-0.15	2.04	-2.98	-0.13	2.59	-3.70	-0.11
87	2.53	-3.47	0.04	2.52	-3.82	-0.16	2.28	-3.30	-0.14	2.26	-3.25	-0.10
88	1.65	-2.10	0.06	1.76	-2.74	-0.15	1.76	-2.72	-0.14	1.81	-2.56	-0.12
89	2.06	-2.84	0.05	1.95	-2.89	-0.16	2.53	-3.60	-0.14	2.75	-4.02	-0.11
90	2.37	-3.22	0.05	2.53	-3.76	-0.16	2.65	-3.74	-0.14	2.68	-3.95	-0.10
91	2.31	-3.11	0.04	2.48	-3.57	-0.16	2.17	-3.28	-0.13	2.44	-3.56	-0.10
92	1.85	-2.48	0.01	2.01	-3.16	-0.15	1.95	-2.91	-0.15	2.30	-3.48	-0.12
93	2.53	-3.54	0.04	2.40	-3.48	-0.15	2.74	-3.93	-0.14	2.54	-3.79	-0.08
94	2.25	-3.01	0.00	2.52	-3.81	-0.15	2.14	-3.25	-0.14	2.24	-3.38	-0.11
95	2.63	-3.74	0.00	2.28	-3.44	-0.15	2.43	-3.51	-0.14	2.21	-3.29	-0.10
96	1.28	-1.96	0.03	1.51	-2.49	-0.13	1.56	-2.33	-0.14	1.62	-2.50	-0.12
97	2.73	-3.70	0.03	2.34	-3.37	-0.15	2.47	-3.68	-0.14	2.69	-3.97	-0.10
98	2.11	-2.87	0.02	2.06	-2.91	-0.14	2.53	-3.74	-0.15	2.51	-3.77	-0.10
99	2.42	-3.49	0.01	2.28	-3.47	-0.16	2.53	-3.71	-0.14	2.51	-3.67	-0.11
100	1.87	-2.78	-0.20	1.85	-2.72	-0.22	2.00	-2.80	-0.19	1.82	-2.65	-0.16
101	2.48	-4.05	-0.27	2.65	-3.83	-0.20	2.26	-3.51	-0.20	2.35	-3.45	-0.20
102	2.64	-3.91	-0.28	2.19	-3.44	-0.25	2.28	-3.48	-0.23	1.86	-2.92	-0.24
103	2.85	-4.29	-0.31	2.61	-4.10	-0.28	2.54	-3.91	-0.27	2.18	-3.61	-0.28

104	2.06	-2.07	0.32	1.96	-3.17	-0.15	1.45	-2.30	-0.15	1.85	-2.85	-0.09
105	2.44	-3.34	0.03	2.46	-3.56	-0.15	2.52	-3.81	-0.14	2.38	-3.44	-0.10
106	2.77	-4.17	-0.23	2.55	-3.83	-0.24	2.61	-3.92	-0.24	2.68	-4.07	-0.23
107	2.10	-3.23	-0.30	3.06	-4.58	-0.27	2.84	-4.17	-0.26	2.44	-3.66	-0.26
108	2.41	-3.52	-0.17	1.82	-2.63	-0.19	2.21	-3.20	-0.20	2.37	-3.38	-0.17
109	2.36	-3.59	-0.20	2.33	-3.50	-0.19	2.54	-3.86	-0.18	2.74	-3.87	-0.18
110	3.04	-3.70	0.19	2.90	-4.24	-0.16	2.53	-3.74	-0.14	2.82	-4.00	-0.10
111	2.60	-3.78	-0.02	2.60	-3.77	-0.15	3.24	-4.54	-0.14	2.67	-3.88	-0.11
112	1.82	-2.63	-0.13	2.16	-3.45	-0.16	1.70	-2.35	-0.13	1.79	-2.55	-0.11
113	2.69	-3.74	0.02	2.55	-3.89	-0.17	2.59	-3.82	-0.14	2.73	-4.12	-0.11
114	3.18	-4.21	0.19	2.92	-4.43	-0.16	2.58	-3.80	-0.14	2.37	-3.61	-0.10
115	2.53	-3.36	0.02	2.51	-3.67	-0.16	2.83	-4.03	-0.15	2.70	-3.76	-0.11
116	2.24	-3.22	-0.22	2.23	-3.41	-0.24	1.76	-2.76	-0.20	1.99	-3.13	-0.23
117	2.32	-3.80	-0.22	2.55	-3.73	-0.24	2.07	-3.27	-0.23	2.45	-3.73	-0.23

REFERENCES

ASCE No. 67, 1999. Wind tunnel studies of buildings and structures. ASCE Manuals and Reports on Engineering Practice. American Society of Civil Engineers.

ASCE Standard. ASCE/SEI 7-10, 2010. Minimum design loads for buildings and other structures. American Society of Civil Engineers.

ASCE Standard. ASCE/SEI 49-12, 2012. Wind tunnel testing for buildings and other structures. American Society of Civil Engineers.

ASCE, 2012. Wind issues in the design of buildings. Structural Wind Engineering Committee. American Society of Civil Engineers.

Aly, M.A., Gan Chowdhury, A., Bitsuamlak, G., 2011. Wind profile management and blockage assessment for a new 12-fan Wall of Wind facility at FIU. Wind and Structures, Vol. 14, No. 4, 285-300.

Aynsley, R.M., Melbourne, W., Vickery, B.J., 1977. Architectural Aerodynamics. Applied Science Publishers Ltd., London.

Baheru, T., Gan Chowdhury, A., Bitsuamlak, G., Masters, F.J., 2014. Simulation of wind-driven rain associated with tropical storms and hurricanes using the 12-fan Wall of Wind. Building and Environment 76, 18-29.

Bailey, A., 1933. Wind pressures on buildings. The Institution of Civil Engineers. Selected Engineering Paper No. 139, 3-31.

Bailey, A., Vincent, N.D.G., 1943. Wind-pressure on buildings including effects of adjacent buildings. Journal of the Institute of Civil Engineers, Vol. 20, No. 8, 243-275.

Balderrama, J.A., Masters, F.J., Gurley, K.R., Prevatt, D.O., Aponte-Bermúdez, L.D., Reinhold, T.A., Pinelli, J.-P., Subramanian, C.S., Schiff, S.D., Chowdhury, A.G., 2011. The Florida Coastal Monitoring Program (FCMP): A review. Journal of Wind Engineering and Industrial Aerodynamics 99, 979-995.

Banks, D., 2000. The suction induced by conical vortices on low-rise buildings with flat roofs. PhD Thesis, Dept. of Civil Engineering, Colorado State University, Fort Collins, Colorado.

Baskaran, A., Stathopoulos, T., 1988. Roof corner wind loads and parapet configurations. Journal of Wind Engineering and Industrial Aerodynamics 29, 79-88.

Bitsuamlak, G.T., Warsido, W., Ledesma, E., Gan Chowdhury, A., 2013. Aerodynamic mitigation of roof and wall corner suctions using simple architectural elements. Journal of Engineering Mechanics, Vol. 139, No. 3, 396-408.

Blackmore, P.A., 1988. Load reduction on flat roofs – the effect of edge profile. Journal of Wind Engineering and Industrial Aerodynamics 29, 89-98.

Blessings, C., Gan Chowdhury, A., Lin, J., Huang, P., 2009. Full-scale validation of vortex suppression techniques for mitigation of roof uplift. Engineering Structures 31, 2936-2946.

BND, Board of Natural Disasters, 1999. Mitigation emerges as major strategy for reducing losses caused by natural disasters. Science, Vol. 284, 1943-1947.

Borges, A.R.J., 1998. Fundamental aspects of turbulent boundary-layer flow over bluff bodies. Wind Effects on Buildings and Structures, Riera & Davenport. Balkema, Rotterdam, 39-59.

Boulard, T., Baille, A., 1995. Modelling of air exchange rate in a greenhouse equipped with continuous roof vents. Journal of Agricultural Engineering Research, 61, 37-48.

Breeze G., 2003. Aerodynamic and water penetration investigations upon pitched roof vents. Journal of Wind Engineering and Industrial Aerodynamics 91, 1225-1236.

Case, P.C., Isyumov, N., 1998. Wind loads on low buildings with 4:12 gable roofs in open country and suburban exposures. Journal of Wind Engineering and Industrial Aerodynamics 77-78, 107-118.

Cermak, J.E., 1975. Applications of fluid mechanics to wind engineering – A Freeman Scholar Lecture. Journal of Fluids Engineering, 9-37.

Cheung, J.C.K., Holmes, J.D., Melbourne, W.H., Lakshmanan, N., Bowditch, P., 1997. Pressures on a 1/10 scale model of the Texas Tech building. Journal of Wind Engineering and Industrial Aerodynamics 67-71, 529-538.

Cochran, L.S., Cermak, J.E., 1992. Full- and model-scale cladding pressures on the Texas Tech University experimental building. Journal of Wind Engineering and Industrial Aerodynamics 41-44, 1589-1600.

Cook, N.J., 1985. The designer's guide to wind loading of building structures. Part 1: Background, damage survey, wind data and structural classification. Building Research Establishment, Butterworths.

COST., 2007. Best practice guideline for the CFD simulation of flows in the urban environment. COST Action 732.

Curry, J.A., 2007. Dangerous climate change. Statement to the Select Committee on Energy Independence and Global Warming of the United States House of Representatives.

Davenport, A.G., 1982. Engineering meteorology: fundamentals of meteorology and their application to problems in environment and civil engineering. The Interaction of Wind and Structures, 527-537.

Davenport, A.G., Surry, D., 1984. The estimation of external pressures due to wind with application to cladding pressures and infiltration. Proceedings, Wind Pressure Workshop. Brussels, Belgium.

Dixon, C.R., Prevatt, D.O., 2010. What do we learn from wind uplift tests of roof systems? Structures Congress, ASCE, 2405-2416.

Emmanuel, K., 2005. Increasing destruction of tropical cyclones over the past 30 years. Nature, Vol. 436, 686-688.

Engineering Science Data Unit (ESDU) 85020, 2001. Characteristics of atmospheric turbulence near the ground. Part II: single point data for strong winds (neutral atmosphere).

FEMA (2010). Minimizing water intrusion through roof vents in high-wind regions. Technical Fact Sheet No. 7.5, 1-8.

Fu, T.C., Aly, A.M., Gan Chowdhury, A., Bitsuamlak, G., Yeo, D.H, Simiu, E., 2012. A proposed technique for determining aerodynamic pressures on residential homes. Wind and Structures, Vol. 15, No. 1, 27-41.

Fu, T.C., 2012. Development of effective approaches to the large-scale aerodynamic testing of low-rise buildings. Ph.D. Thesis, Florida International University, Miami, Florida.

Gan Chowdhury, A., Simiu, E., Leatherman, S.P., 2009. Destructive testing under simulated hurricane effects to promote hazard mitigation. Natural Hazards Review, Vol. 10, No. 1, 1-10.

Gan Chowdhury, A., Bitsuamlak, G.T., Fu, T.C., Kawade, P., 2010. A study on roof vents subjected to simulated hurricane effects. Natural Hazard Review. American Society of Civil Engineers, 1-33.

Gavanski, E., Kordi, B., Kopp, G. A., Vickery, P.J., 2013. Wind loads on roof sheathing of houses. Journal of Wind Engineering and Industrial Aerodynamics 114, 106-121.

Gerhardt, H.J., Kramer, C., 1992. Effect of building geometry on roof wind loading. Journal of Wind Engineering and Industrial Aerodynamics 41-44, 1765-1773.

Ginger, J.D., Mehta, K.C., Yeatts, B.B., 1997. Internal pressures in a low-rise full-scale building. Journal of Wind Engineering and Industrial Aerodynamics 72, 163-174.

Ginger, J.D., Letchford, C.W., 1999. Net pressures on a low-rise full-scale building. Journal of Wind Engineering and Industrial Aerodynamics 83, 239-250.

Ginger, J.D., Reardon, G.F., Whitbread, B.J., 2000. Wind load effects and equivalent pressures on low-rise house roofs. Engineering Structures 22, 638-646.

Ginger, J.D., Holmes, J.D., 2003. Effect of building length on wind loads on low-rise buildings with steep roof pitch. Journal of Wind Engineering and Industrial Aerodynamics 91, 1377-1400.

Ginger, J.D., Henderson, D., Edwards, M., Holmes, J.D., 2010. Housing damage in windstorms and mitigation for Australia. Available online at: http://www.iawe.org/WRDRR/2010/Ginger.pdf.

Graettinger, A.J., Van de Lindt, J.W., Gupta, R., Pryor, S.E., Skaggs, T.D., Fridley, K.J., 2006. Overview of wind damage to woodframe structure caused by Hurricane Katrina. Structures Congress.

Grant, E.J., Jones, J.R., Vlachos, P.P., 2007. Design and wind tunnel performance testing of a new omnidirectional roof vent. Journal of Architectural Engineering, Vol. 13, No. 1, 18-21.

Ham, H.J., Bienkiewicz, B., 1998. Wind tunnel simulation of TTU flow and building roof pressure. Journal of Wind Engineering and Industrial Aerodynamics 77 & 78, 119-133.

Hillier, R., Cherry, N.J., 1981. The effects of stream turbulence on separation bubbles. Journal of Wind Engineering and Industrial Aerodynamics 8, 49-58.

Holmes, J.D., 1979. Mean and fluctuating internal pressures induced by wind. Proceedings, 5th International Conference on Wind Engineering, Colorado, USA.

Homes, J.D., 1983. Wind loads on low-rise buildings – A Review. CSIRO. Division of Building Research, Highett. Victoria, Australia.

Holmes, J.D., Carpenter, P., 1990. The effects of Jensen number variations on wind loads on a low-rise building. Journal of Wind Engineering and Industrial Aerodynamics 36, 1279-1288.

Holmes, J.D., 1994. Wind pressures on tropical housing. Journal of Wind Engineering and Industrial Aerodynamics 53, 105-123.

Holmes, J.D., 2007. Wind Loading of Structures, 2nd Edition. Taylor & Francis.

Hoxey, R.P., Robertson, A.P., 1994. Pressure coefficients for low-rise building envelopes derived from full-scale experiments. Journal of Wind Engineering and Industrial Aerodynamics 53, 283-297.

Hoxey, R.P., Reynolds, A.M., Richardson, G.M., Robertson, A.P., Short, J.L., 1998. Observations of Reynolds number sensitivity in the separated flow region on a bluff body. Journal of Wind Engineering and Industrial Aerodynamics 73, 231-249.

ICC IRC. 2009. International Residential Code. International Code Council.

Irwin, H.P.A. H., Cooper, K.R., Girard, R., 1979. Correction of distortion effects caused by tubing systems in measurements of fluctuating pressures. Journal of Industrial Aerodynamics, 5, 93-107.

Irwin, P.A., Sifton, V.L., 1998. Risk considerations for internal pressures. Journal of Wind Engineering and Industrial Aerodynamics 77 & 78, 715-723.

Irwin, P.A., 2014. Partial turbulence simulation applied to a PV system. Wall of Wind Technical Notes. Florida International University, Miami, FL.

Irwin, P.A., 2015. Notes on guidelines for partial turbulence simulation (PTS). Wall of Wind Technical Notes. Florida International University, Miami, FL.

Jensen, M., 1958. The model-law for phenomena in natural wind. Ingenioren-International Edition, Vol. 2, No. 4, 121-127.

Jesteadt, J., Reynolds, R., Masters, F., 2007. A preliminary investigation into wind-driven rain intrusion through soffits. Proceedings 12th International Conference on Wind Engineering, Cairns, Australia, 327-334.

Kareem, A., Lu, P.C., 1992. Pressure fluctuations on flat roofs with parapets. Journal of Wind Engineering and Industrial Aerodynamics 41-44, 1775-1786.

Katsoulas, N., Bartzanas, T., Boulard, T., Mermier, M., Kittas, C., 2006. Effect of vent openings and insect screens on greenhouse ventilation. Biosystems Engineering 93 (4), 427-436.

Kawai, H., Nishimura, G., 1996. Characteristics of fluctuating suction and conical vortices on a flat roof in oblique flow. Journal of Wind Engineering and Industrial Aerodynamics 60, 211-225.

Kind, R.J., 1988. Worst suctions near edges of flat rooftops with parapets. Journal of Wind Engineering and Industrial Aerodynamics 31, 251-264.

Kopp, G.A., Mans, C., Surry, D., 2005. Wind effects of parapets on low buildings: Part 4. Mitigation of corner loads with alternative geometries. Journal of Wind Engineering and Industrial Aerodynamics 93, 873-888.

Kopp, G.A., Oh, J.H., Inculet, D.R., 2008. Wind-induced internal pressures in houses. Journal of Structural Engineering, Vol. 134, No. 7, 1129-1138.

Kopp, G.A., Morrison, M.J., Henderson, D.J., 2012. Full-scale testing of low-rise, residential buildings with realistic wind loads. Journal of Wind Engineering and Industrial Aerodynamics 104-106, 25-39.

Kopp, G.A., Banks, D., 2013. Use of the wind tunnel test method for obtaining design wind loads on roof-mounted solar arrays. Journal of Structural Engineering, Vol. 139, No. 2, 284-287.

Krishna, P., 1995. Wind loads on low-rise buildings – A review. Journal of Wind Engineering and Industrial Aerodynamics 54/55, 383-396.

Leatherman, S.P., Gan Chowdhury, A., Robertson, C.J., 2007. Wall of Wind full-scale destructive testing of coastal houses and hurricane damage mitigation. Journal of Coastal Research, 23 (5), 1211-1217.

Leatherman, S., Robertson, C., Chowdhury, A.G., Simiu, E., Bitsuamlak, G., Huang, P. 2008. Full-scale destructive testing of houses to hurricane force wind and rain. Solutions to Coastal Disasters Congress.

Levitan, M.L., Mehta, K.C., 1992a. Texas Tech field experiments for wind loads part 1: building and pressure measuring system. Journal of Wind Engineering and Industrial Aerodynamics 41-44, 1565-1576.

Levitan, M.L., Mehta, K.C., 1992b. Texas Tech field experiments for wind loads part II: building and pressure measuring system. Journal of Wind Engineering and Industrial Aerodynamics 41-44, 1577-1588.

Lim, H.E., Castro, I.P., Hoxey, R.P., 2007. Bluff bodies in deep turbulent boundary layers: Reynolds-number issues. Journal of Fluid Mechanics, vol. 571, 97-118.

Lin, J.X., Surry, D., 1993. Suppressing extreme suction on low buildings by modifying the roof corner geometry. Proceedings of the Seventh United States National Wind Engineering Conference, University of California, Los Angeles, 413-422.

Lin, J.X., Surry, D., Tieleman, 1995. The distribution of pressure near roof corners of flat roof low buildings. Journal of Wind Engineering and Industrial Aerodynamics 56, 235-265.

Lin, J.X., Surry, D., 1998. The variation of peak loads with tributary area near corners on flat low building roofs. Journal of Wind Engineering and Industrial Aerodynamics 77-78, 185-196.

Liu, H., 1978. Building code requirements on internal pressures. Proceedings, the third U.S. National Conference, Wind Engineering Research: February 26-March 1. University of Florida, Gainesville.

Liu, H., Turner, E.J., Gould, P.L., 1989. Strategies for wind damage mitigation-summary. Journal of Aerospace Engineering, Vol. 2, No. 4, 179-185.

Liu, H., 1991. Wind Engineering: A Handbook for Structural Engineers. Prentice Hall, USA.

Lott, N., Ross, T., 2006. Tracking and Evaluating U.S. billion dollar weather disasters, 1980-2005. Available online at: http://www.ncdc.noaa.gov/oa/reports/billionz.html.

Lythe, G., Surry, D., 1983. Wind loading of flat roofs with and without parapets. Journal of Wind Engineering and Industrial Aerodynamics 11, 75-94.

Marshall, R.D., 1975. A study of wind pressures on a single-family dwelling in model and full-scale. Journal of Industrial Aerodynamics 1, 177-199.

Masters, F.J., Kiesling, A.A., 2012. Final report (structural and wind-driven rain resistance of soffits). Fiscal Year 2011/2012, scope of work. Department of Civil and Coastal Engineering, University of Florida, Gainesville, Florida, 1-35.

Meecham, D., Surry, D., Davenport, A.G., 1991. The magnitude and distribution of wind-induced pressures on hip and gable roofs. Journal of Wind Engineering and Industrial Aerodynamics 38, 257-272.

Meecham, D., 1992. The Improved Performance of Hip Roofs in Extreme Winds – A Case Study. Journal of Wind Engineering and Industrial Aerodynamics 41-44, 1717-1726.

Mehta, K.C., Levitan, M.L., Iverson, R.E., McDonald, J.R., 1992. Roof corner pressures measured in the field on a low building. Journal of Wind Engineering and Industrial Aerodynamics 41-44, 181-192.

Melbourne, W.H., 1980. Turbulence effects on maximum surface pressures – A mechanism and possibility of reduction. Wind Engineering. Multi-Science Pub. Co., 541-551.

Melbourne, W.H., 1993. Turbulence and the leading edge phenomenon. Journal of Wind Engineering and Industrial Aerodynamics 49, 45-64.

Meloy, N., Sen, R., Pai, N., Mullins, G., 2007. Roof damage in new homes caused by hurricane Charley. Journal of Performance of Constructed Facilities, Vol. 21, No. 2, 97-107.

Milford, R.V., Goliger, A.M., Waldeck, J.L., 1992. Jan Smuts experiment: comparison of full-scale and wind-tunnel results. Journal of Wind Engineering and Industrial Aerodynamics 41-44, 1705-1716.

Minor, J.E., Mehta, K.C., 1979. Wind damage observations and implications. Journal of the Structural Division. Proceedings of the American Society of Civil Engineers, Vol. 105, 2279-2291.

Minor, J.E., 2005. Lessons learned from failures of the building envelope in windstorms. Journal of Architectural Engineering, Vol. 11, No. 1, 10-13.

Mooneghi, M.A., Irwin, P., Chowdhury, A.G., 2015. Partial turbulence simulation for small structures. Proceedings of the 14th International conference on wind engineering, June 21-26, Porto-alegre, Brazil.

NOAA, 2015. Global Analysis –Annual 2015. National Oceanic and Atmospheric Administration. Available online at: http://www.ncdc.noaa.gov/sotc/global/201513.

NOAA, 2014. Billion-dollar weather and climate disasters. National Oceanic and Atmospheric Administration. Available online at: http://www.ncdc.noaa.gov/billions.

Oh, J.H., Kopp, G.A., Inculet, D.R., 2007. The UWO contribution to the NIST aerodynamic database for wind loads on low buildings: Part 3. Internal pressures. Journal of Wind Engineering and Industrial Aerodynamics 95, 755-779.

Okada, H., Ha, Y.C., 1992. Comparison of wind tunnel and full-scale pressure measurement tests on Texas Tech building. Journal of Wind Engineering and Industrial Aerodynamics 41-44, 1601-1612.

Peterka, J.A., Meroney, R.N., Kothari, K.M., 1985. Wind flow patterns about buildings. Journal of Wind Engineering and Industrial Aerodynamics 21, 21-38.

Pielke Jr., R.A., Gratz, J., Landsea, C.W., Collins, D., Saunders, M.A., Musulin, R., 2008. Natural Hazards Review, Vol. 9, No. 1, 29-42.

Platts, R. E., Woods, T., Davenport, A. G., 2003. Recent advances in hurricane resistance retrofit measures. Presented at the National Building Envelope Council Conference-Vancouver, Canada.

Quarles, S.L., Brown, T.M., Cope, A.D., Lopez, C., Masters, F.J., 2012. Water entry through roof sheathing joints and attic vents: A preliminary study. Insurance Institute for Business & Home Safety (IBHS) Research Center.

Reardon, G., Boughton G., Henderson, D., Ginger, J., (1999). The effects of Tropical Cyclone Vance on Exmouth. Australian Journal of Emergency Management, 31-34.

Richardson, G.M., Surry, D., 1991. Comparisons of wind-tunnel and full-scale surface pressure measurements on low-rise pitched-roof buildings. Journal of Wind Engineering and Industrial Aerodynamics 38, 249-256.

Richardson, G.M., Hoxey, R.P., Robertson, A.P., Short, J.L., 1997. The Silsoe Structures Building: Comparisons of pressures measured at full scale and in two wind tunnels. Journal of Wind Engineering and Industrial Aerodynamics 72, 187-197.

Richards, P.J., Hoxey, R.P., Short, L.J., 2001. Wind pressures on a 6m cube. Journal of Wind Engineering and Industrial Aerodynamics 89, 1553-1564.

Robertson, A.P., 1991. Effect of eaves detail on wind pressures over an industrial building. Journal of Wind Engineering and Industrial Aerodynamics 38, 325-333.

Saathoff, P.J., Liu, H., 1983. Internal pressures of multi-room buildings. Journal of Engineering Mechanics, Vol. 109, No. 3, 908-919.

Saathoff, P.J., Melbourne, W.H., 1989. The generation of peak pressures in separated/reattaching flows. Journal of Wind Engineering and Industrial Aerodynamics 32, 121-134.

Sharma, R.N., Richards, P.J., 2003. The influence of Helmholtz resonance on internal pressures in a low-rise building. Journal of Wind Engineering and Industrial Aerodynamics 91, 807-828.

Sharma, R.N., Richards, P.J., 2005. Net pressures on the roof of a low-rise building with wall openings. Journal of Wind Engineering and Industrial Aerodynamics 93, 267-291.

Sill, B.L., Cook, N.J., Blackmore, P.A., 1989. IAWE Aylesbury comparative experiment – Preliminary results of wind tunnel comparisons. Journal of Wind Engineering and Industrial Aerodynamics 32, 285-302.

Sill, B.L., Cook, N.J., Fang, C., 1992. The Aylesbury comparative experiment: a final report. Journal of Wind Engineering and Industrial Aerodynamics 41-44, 1553-1564.

Simiu, E., Scanlan, R., 1996. Wind Effects on Structures, Fundamentals and Applications to Design, 3rd Edition. John Wiley & Sons, Inc.

Simiu, E., Miyata, T., 2006. Design of Buildings and Bridges for Wind. John Wiley & Sons, Inc.

Smith, A.B., Katz, R.W., (2013). U.S. billion-dollar weather and climate disasters: data sources, trends, accuracy and biases. Journal of Natural Hazards, Vol. 67(2), 387-410. Available online at: http://link.springer.com/article/10.1007/s11069-013-0566-5.

Statholpoulos, T., 1979. Turbulent wind action on low rise buildings. Ph.D. Dissertation, University of Western Ontario, London, Canada.

Stathopoulos, T., Surry, D., 1983. Scale effects in wind tunnel testing of low buildings. Journal of Wind Engineering and Industrial Aerodynamics 13, 313-326.

Stathopoulos, T., Surry, D., Davenport, A.G., 1979. Internal pressure characteristics of low-rise buildings due to wind action. Proceedings, 5th International Conference on Wind Engineering, Fort Collins, Colorado, Pergamon Press, New York.

Stathopoulos, T. 1984. Wind loads on low-rise buildings: a review of the state of the art. Engineering Structures, Vol. 6, 119-135.

Stathopoulos, T., Baskaran, A., 1987. Wind pressures on flat roofs with parapets. Journal of Structural Engineering, Vol. 113, No. 11, 2166-2180.

Stathopoulos, T., Luchian, H.D., 1989. Transient wind-induced internal pressures. Journal of Engineering Mechanics, Vol. 115, No. 7, 1501-1514.

Stathopoulos, T., Marathe, R., Wu, H., 1999. Mean wind pressures on flat roof corners affected by parapets: field and wind tunnel studies. Engineering Structures 21, 629-638.

Stathopoulos, T, Baniotopoulos, C.C., 2007. Wind effects on buildings and design of wind-sensitive structures. CISM Courses and Lectures No. 493, 1-30.

St. Pierre, L.M., Kopp, G.A., Surry, D., and Ho, T.C.E., 2005. The UWO contribution to the NIST aerodynamic database for wind loads on low buildings. 2: comparison of data with wind load provisions. Journal of Wind Engineering and Industrial Aerodynamics 93 (1), 31-59.

Suaris, W., Irwin, P., 2010. Effects of roof-edge parapets on mitigating extreme roof suctions. Journal of Wind Engineering and Industrial Aerodynamics 98, 483-491.

Surry, D., 1991. Pressure measurements on the Texas Tech building: wind tunnel measurements and comparisons with full scale. Journal of Wind Engineering and Industrial Aerodynamics 38, 235-247.

Surry, D., Lin, J.X., 1995. The effect of surroundings and roof corner geometric modifications on roof pressures on low-rise buildings. Journal of Wind Engineering and Industrial Aerodynamics 58, 113-138.

Surry, D., Ho, E.T.C., Kopp, G.A., 2008. Measuring pressures is easy, isn't it? Proceedings, 11th International Conference on Wind Engineering, Lubbock, Texas. 2617-2624.

Surry, D., Kopp, G.A., 2005. Wind load testing of low buildings to failure at model and full scale. Natural Hazards Review, Vol. 6, No. 3, 121-128.

Taher, R., 2007. Design of low-rise buildings for extreme wind events. Journal of Architectural Engineering, Vol. 13, No. 1, 54-62.

Tecle, A.S., Jiru, T.E, Bitsuamlak, G.T., 2010. Computational evaluation and validation of internal and external pressures for low-rise building. Proceedings, Fifth International Symposium on Computational Wind Engineering (CWE2010). Chapel Hill, North Carolina, USA.

Tecle, A.S., Bitsuamlak, G.T., Gan Chowdhury, A., 2012. Opening & compartmentalization effects of internal pressure in low-rise buildings with gable & hip roofs. Journal of Architectural Engineering, Vol. 21, 04014002-1-14.

Tieleman, H.W., Akins, R.E., 1990. Effects of incident turbulence on pressure distributions on rectangular prisms. Journal of Wind Engineering and Industrial Aerodynamics 36, 579-588.

Tieleman, H.W., 1992. Problems associated with flow modeling procedures for low-rise structures. Journal of Wind Engineering and Industrial Aerodynamics 41-44, 923-934.

Tieleman, H.W., Surry, D., Lin, J.X., 1994. Characteristics of mean and fluctuating pressure coefficients under corner (delta wing) vortices. Journal of Wind Engineering and Industrial Aerodynamics 52, 263-275.

Tieleman, H.W., Surry, D., Mehta, K.C., 1996. Full/model-scale comparison of surface pressures on the Texas Tech experimental building. Journal of Wind Engineering and Industrial Aerodynamics 61, 1-23.

Tieleman, H.W., 1996. Model/full scale comparison of pressures on the roof of the TTU experimental building. Journal of Wind Engineering and Industrial Aerodynamics 65, 133-142.

Tieleman, H.W., Reinhold, T.A., Hajj, M.R., 1997. Importance of turbulence for the prediction of surface pressures on low-rise structures. Journal of Wind Engineering and Industrial Aerodynamics 69-71, 519-528.

Tieleman, H.W., Hajj, M.R., Reinhold, T.A., 1998. Wind tunnel simulation requirements to assess wind loads on low-rise buildings. Journal of Wind Engineering and Industrial Aerodynamics 74-76, 675-685.

Trenberth, K., 2005. Uncertainty in hurricanes and global warming. Science, Vol. 308, 1753-1754.

Uematso, Y., Isyumov, N., 1999. Review: wind pressures acting on low-rise buildings. Journal of Wind Engineering and Industrial Aerodynamics 82, 1-25.

Vickery, P.J., Surry, D., 1983. The Aylesbury experiments revisited – Further wind tunnel tests and comparisons. Journal of Wind Engineering and Industrial Aerodynamics 11, 39-62.

Vickery, B.J., Bloxham, C., 1992. Internal pressure dynamics with a dominant opening. Journal of Wind Engineering and Industrial Aerodynamics 41-44, 193-204.

Vickery, B.J., 1994. Internal pressures and interactions with the building envelope. Journal of Wind Engineering and Industrial Aerodynamics 53, 125-144.

Vickery, P.J., 2008. Component and cladding wind loads for soffits. Journal of Structural Engineering, 846-853.

Weather, 2016. 5 things to know about Tropical Cyclone Winston. The Weather Channel. Available online at: https://weather.com/storms/hurricane/news/cyclone-winston-impacts-preps.

Womble, J.A., Yeatts, B.B., Cermak, J.E., Mehta, K.C., 1995. Internal wind pressures in a full- and small-scale building. Proceedings, 9th International Conference on Wind Engineering, New Delhi, India, 1079-1090.

Woods, A.R., Blackmore, P.A., 1995. The effect of dominant openings and porosity on internal pressures. Journal of Wind Engineering and Industrial Aerodynamics 57, 167-177.

Wu, F., 2000. Full scale study of conical vortices and their effects near corners. Ph.D. Thesis, Dept. of Civil Engineering, Texas Tech Univ., Lubbock, Texas.

Wyndham Partners Consulting Limited (WPC), 2004. Hurricane Charley 2004 Damage Survey.

Wyndham Partners Consulting Limited (WPC), 2005. Hurricane Katrina Preliminary Damage Survey.

Xu, Y.L., Reardon, G.F., 1998. Variations of wind pressure on hip roofs with roof pitch. Journal of Wind Engineering and Industrial Aerodynamics 73, 267-284.

Yeatts, B.B., Mehta, K.C., 1993. Field experiments for building aerodynamics. Journal of Wind Engineering and Industrial Aerodynamics 50, 213-224.

Yeo, D., Gan Chowdhury, A., 2013. Simplified wind flow model for the estimation of aerodynamic effects on small structures. Journal of Engineering Mechanics, Vol. 139, No. 3, 367-375.

Yu, B., Gan Chowdhury, A., Masters, F.J., 2008. Hurricane wind power spectra, cospectra, and integral length scales. Boundary-Layer Meteorol 129, 411-430.

VITA

Garth Alexander Arch was born in George Town, Cayman Islands, to Heber and Beryl Arch. After graduating from the John Gray High School in Grand Cayman, Garth moved to Miami, Florida, to attend the University of Miami where he earned a bachelor's degree in civil engineering in 1998. He then earned his master's degree in 2000 from the University of California at Berkeley. Garth remained in California to work with an engineering consulting firm in San Francisco, where he gained valuable engineering experience and obtained his Professional Engineering (P.E.) license for the State of California. In the fall of 2010, he pursued graduate studies for his doctoral degree at the University of Miami. Garth Arch is a member of the American Society of Civil Engineers, the American Society of Wind Engineering, the Institution of Civil Engineers (U.K.), the Institution of Structural Engineers (U.K.) and the Chartered Institute of Building (U.K.). Garth is married to Dana, and they have two daughters, Anasofia and Beryl.